DEVELOPMENT OF A COMPREHENSIVE LINEAR RESPONSE HISTORY ANALYSIS PROCEDURE FOR SEISMIC LOAD ANALYSIS

Adrian Tola

Thesis submitted to the Faculty of the
Virginia Polytechnic Institute and State University
in partial fulfillment of the requirements for the degree of

MASTER OF SCIENCE

in

CIVIL ENGINEERING

Finley A. Charney, Committee Chairman

Carin L. Roberts-Wollmann, Committee Member

Matthew R. Eatherton, Committee Member

November 29, 2010
Blacksburg, Virginia

Keywords: Linear response history analysis, selection and scaling of ground motions, artificial seismograms, diaphragm flexibility, accidental torsion, structural modeling

DEVELOPMENT OF A COMPREHENSIVE LINEAR RESPONSE HISTORY ANALYSIS PROCEDURE FOR SEISMIC LOAD ANALYSIS

Adrian Tola

(ABSTRACT)

This thesis reviews the parameters required to perform linear response history analysis according to Chapter 16 of the American Standard ASCE 7-10. A careful analysis is presented about the selection of ground motions using real records and using artificial records generated such that their response spectrum matches with a defined target spectrum; three different techniques are studied for the generation of these artificial records. Also, this document revises the scaling of ground motion techniques in the American Standard ASCE-7 as well as in other seismic codes. It presents a detailed analysis of the variables influencing the scaling of ground motions, and it suggests a new scaling technique for linear response history analysis. The assumptions made establishing the flexibility of the diaphragms are also analyzed as well as dynamic methods to include accidental torsion when doing a linear response history analysis. Other modeling issues such as the orientation of the ground motion axis, scaling of element forces and displacements, orthogonal loading, solution techniques, P-Delta effects, modeling of the basement, and calculation of drifts are also studied in the context of linear response history analysis. The thesis concludes with suggested code language for linear response history analysis intended to be considered in future editions of the American Standard ASCE 7.

Acknowledgements

I would like to express my gratitude to Dr. Finley Charney for serving as my advisor and committee chairman; Dr. Charney's guidance and support have been a key of my academic and personal development during these two and a half years. Also, I want to thank the rest of the members of my committee, Dr. Carin Roberts-Wollmann and Dr. Matthew Eatherton for taking the time to provide valuable insight for my thesis.

Also, I would like to thank my family, Esperanza, Jaime, Mauricio and Daniela, for providing me all the strength and love to make this dream true. My gratitude goes also for my grandparents Vicente, Leonor, Maria, and Luis, for my aunts, uncles, cousins and other relatives for always giving me their support.

In addition, I want to thank to all my friends with whom I share my best moments in Blacksburg; some of them are Miguel Ortega and his family, Francisco Flores, Richard Lizardi, Juan Pablo y Margarita Sanchez, Andres Ramirez, Veronica de Freitas, Hao Yuan, Fae Garstang, Joseph Dulka, Leonardo Hasburn, Rohan Talwalkar, Chinmay Damle, Maninder Singh Bajwa, Vathana Poev, Lori Koch, Michelle Lee, Andrew Dolan, Chris David, and all the innumerable good friends that I have not been able to mention.

My special gratitude to Jordan Jarrett for her friendship and for helping me reviewing this thesis.

Furthermore, I want to thank to Fulbright Ecuador and LASPAU for all the support, and I will always appreciate the opportunity you gave to me to grow up academically and personally.

Finally, I want to thank God for always being present in my life.

TABLE OF CONTENTS

List of Figures

List of Tables

Chapter 1. INTRODUCTION AND LITERATURE REVIEW

1.1 Introduction

Seismic loading of structures using static procedures such as the equivalent lateral force method, denoted hereafter ELF, and using dynamic procedures such as the response spectrum analysis, denoted hereafter RSA, are the two techniques most used in practice. However, both procedures present limitations and disadvantages, which could be overcome by a rational linear response history analysis, denoted hereafter LRHA. The equivalent lateral force procedure defined in the American standard ASCE 7-10 (ASCE/SEI, 2010) has limitations related with the inclusion of higher mode effects as well as limitations for the case of irregular structures. Also, in a response spectrum analysis, the sign of the element forces is lost, and it causes a lack of clarity in the results (i.e. forces, displacements). Additionally, advanced techniques such as nonlinear response history analysis, denoted NLRHA, requires a significant effort to model inelastic behavior in critical components, and also to overcome the associated uncertainties such as the strain hardening properties of the member, damping and convergence. Therefore, a rational LRHA could overcome the limitations of the ELF and RSA procedures without involving the amount of time required to perform a NLRHA.

Code requirements to perform LRHA are already presented in Chapter 16 of ASCE 7-10, which describes procedures for the modeling of the structure, the number of ground motions required for analysis, the selection and scaling of those ground motions for two dimensional and three dimensional analysis, a brief description of the scaling requirements for sites located close to an active fault, and the procedure to obtain the force and displacement parameters for each ground motion and their respective final combination for design, which depends on the number of earthquakes used in the analysis.

The variables described in Chapter 16 of ASCE 7-10 are not sufficient when actual design is performed; therefore, more detailed information of existent variables as well as definition of new variables is required to adjust to the needs of practicing structural engineers. For instance, two variables that require refinement are the selection and scaling of ground motions and the procedure for selecting earthquakes from a database given the seismic hazard scenario.

The current method for selection and scaling of ground motions is defined differently depending on whether the structure is modeled in two or three dimensions. Refinement is required in this case because the nature of the ground motion that shakes the building is completely independent of how many dimensions the structure is modeled. Also, when using the current scaling procedure of ASCE 7-10, two designers can obtain different scaling factors when using the same suite of ground motions, and this randomness in the scaling factors needs to be corrected so that all designers would get the same scale factors if given the same suite of ground motions. Besides, the range of periods where the scaling of ground motions is done is still arguable; for example, the upper limit of that range is $1.5T$, where T is the fundamental vibration period of the structure, and consideration of periods larger than T is not needed for linear analysis, since the period cannot increase as it is the case for nonlinear analysis. A period higher than T as the upper limit of the period range of interest could be considered appropriate if it is intended to provide a margin of safety to the uncertainty in the computation of T, and it could possibly yield higher scale factors of the ground motions than if considering T as the upper limit.

Also, Chapter 16 of ASCE 7-10 states that the selected earthquakes should have magnitude, fault distance, and source mechanisms similar to the values that control the maximum considered earthquake scenario at the location of interest; however, it is not stated that the soil conditions where the ground motion was recorded should be similar to the ones at the location of interest. Besides, ASCE 7-10 does not mention specific procedures to determine the magnitude and fault distance that controls the seismic hazard at a specific location, and the definition of such procedure is needed. Also, since it is almost impossible to find earthquakes in a database with the desired target magnitude and fault distance, it is necessary to define an acceptable range of magnitudes and fault distances where the target values fit.

Another variable requiring refinement in ASCE 7-10 is the scaling of the results of LRHA when the base shear from the analysis is less than some percentage of the base shear predicted by the ELF procedure. The procedure described in ASCE 7-10 does not specify if such scaling should be done in only one or in the two principal directions of the structure when loading is acting simultaneously in both principal directions. It might be the case that different procedures for scaling should be considered when using real records with two horizontal components or when using artificial seismograms with one or two horizontal components. The clarification of these requirements will affect directly the application of orthogonal loading.

Additionally, the modeling of accidental torsion in ASCE7-10 for linear response history analysis is based on static forces, and dynamic procedures need to be explored; these procedures need to be described for rigid and semirigid assumptions in the flexibility of the diaphragms.

While the definitions of some variables and procedures in ASCE 7-10 need adjustments, other variables that also affect LRHA procedures have not been addressed at all. Some of these variables include an acceptability criterion for artificial seismograms, the treatment of orthogonal loading, modeling of damping when using direct integration procedures instead of modal analysis, and the explicit definition of the load combinations depending on the number of earthquakes used for analysis.

Also, the number of real earthquakes with the desired characteristics of magnitude, fault distance, source mechanism and soil conditions might be less than the number required for analysis. If that is the case, ASCE 7-10 allows the use of artificial seismograms; however, no information is given about an acceptability criterion for these seismograms in terms of duration, maximum peak ground acceleration, respective velocity and displacement records, and respective base shear and interstory drifts.

Another parameter that has not been addressed by ASCE 7-10 is the treatment of the orthogonal loading for LRHA. The appropriateness of using 100 percent of the seismic forces in one direction plus 30 percent of the seismic forces in a perpendicular direction (30% rule), as is used by ELF, is unknown for LRHA. Also, the rule used for RSA to account for orthogonal effects by calculating the square root of the sum of the squares (SRSS) of one hundred percent of the load applied in both directions might or might not be applicable to LRHA; however, its application would result in losing the sign of the element forces and displacement when doing LRHA, and this fact would go against the benefits of using LRHA.

Moreover, ASCE 7-10 does provide information about damping assumptions for LRHA when using modal analysis; however, there are no such specifications when a designer performs LRHA using direct integration procedures. Also, guidelines are needed referring to the appropriateness of using Ritz vectors instead of Eigen vectors for modal analysis.

The treatment of all the variables mentioned above is for specific application to LRHA; however, other variables required for LRHA can also be applied in a broader sense to ELF and RSA procedures. Three of these variables refer to the assumptions used for the modeling of the basement in buildings, the application of accidental torsion using static forces for buildings

modeled using semirigid diaphragms, and the calculation of the drifts at the center of mass and at one of the sides of a building for the case of semirigid diaphragms, all of which need clarification in ASCE 7-10.

ASCE 7-10 does not provide any information about appropriate conditions for analytical modeling of the basement in buildings. This information is very important, because some structures can have many stories below the ground level, and the assumptions in the modeling of these stories can significantly change the results, particularly the base shear used to design the basement walls.

Likewise a procedure to implement static accidental torsion when using semirigid diaphragms is applicable to any type of analysis. The relevance of this procedure for LRHA is due to the complexities associated with moving the center of mass in structures modeled with semirigid diaphragms. It might be the case that accidental torsion could be dictated by a static procedure even if the rest of the analysis uses dynamic loads.

It might not be possible to include in code language the specific treatment and calculation of the distinct variables that influence LRHA; however, it should be recognized that doing so would greatly facilitate the application of LRHA for design purposes.

1.2 Motivation

Several factors motivated this research; the most important was to explore in detail the variables needed to perform LRHA, and provide constructive discussion and criticism of the current procedure of ASCE 7-10 for LRHA so that this document can serve to improve, if needed, code language in the section of LRHA for future editions of ASCE 7. Also, this thesis was motivated by the fact that LRHA could yield more economical designs than ELF or RSA; however, without explicit procedures, LRHA could not be performed properly. Furthermore, it was believed that a rational and well defined procedure for LRHA could serve as the basis to understand NLRHA procedures. Moreover, LRHA can be more accurate than RSA, and given a proper detailed procedure, LRHA could be performed instead of RSA. Finally, ASCE 7-10 has not adopted officially LRHA as a method of analysis in Chapter 12, and this document was motivated to reach that point.

1.3 Purpose and objectives

The following are the objectives pursued by this thesis.

- Identify the variables that need refinement in the current procedure of ASCE 7.
- Identify new variables needed to perform LRHA in the context of ASCE 7.
- Provide detail examples of the selection and scaling of ground motions.
- Develop a proposal of code language and commentary for a new section is ASCE 7 denoted "12.10 Linear Response History Analysis", which could follow the already described procedures of Section 12.8 and 12.9 defined as Equivalent Lateral Force Procedure and Modal Response Spectrum Analysis, respectively.
- Provide procedures in the context of LRHA that can also be applicable for the case of ELF and RSA.

1.4 Overview of thesis

This document has been divided into six chapters and four appendices, in which the remaining part of Chapter 1 presents a literature review regarding procedures for LRHA suggested by other seismic codes.

Chapter 2 provides an analysis of the selection of ground motions for LRHA, and it covers topics such as the definition of the seismic hazard for a site, the selection of appropriate records based on ground motion parameters, the requirements for selecting records stated in other seismic codes, and the selection of records based on matching a response spectrum.

Chapter 3 studies the scaling of ground motions. It describes the variables that influence the scaling of earthquake records, gives a quick review of the scaling procedures used in different seismic codes, provides some guidelines for the scaling of spectral matched acceleration histories, describes a new proposal for the scaling earthquakes, and shows comparison of such proposed method with other approaches.

Although the selection and scaling of ground motions are connected procedures, it was decided to discuss each of these variables in different chapters so that the variables that affect each of these parameters the most can be emphasized.

Chapter 4 has been divided in two parts; the first refers to the assumptions used in the assessment of the flexibility of the diaphragm and its relation with LRHA procedures, while the second part analyzes alternatives to implement accidental torsion using LRHA. Some of the topics covered in this second part are a general explanation of the basics of accidental torsion, the provisions given in different codes, some techniques developed in the last years to improve static procedures of accidental torsion, the application and comparison of static and dynamic

procedures to account for accidental torsion, and the description of procedures to obtain and use rotational records as well as rotational response spectrum.

Chapter 5 analyzes modeling aspects for LRHA not treated in the previous chapters. The variables covered are the orientation of ground motion axis, the use of the vertical component of ground motion, the scaling of design parameters, the procedures for applying orthogonal loading, the combination of results, load combinations, solution techniques for LRHA and its damping assumptions, number of modes required, P-Delta effects, modeling of the basement, and the calculation of drifts when using semirigid diaphragms.

The last chapter of this document, Chapter 6, contains the summary, conclusions, and future recommendations for research.

Regarding the content in the appendixes, Appendix A shows drawings and other details of the buildings analyzed within this document, while Appendix B shows design examples of the scaling of ground motions using different approaches. Appendix C provides information regarding the translational and rotational masses of the buildings of Appendix A, which were used for models using rigid diaphragms. Appendix D states a proposal worded in building code language with new recommendations for LRHA. The intention of this appendix is to provide code language that could be considered for future editions of ASCE 7. A brief commentary section is also provided, when appropriate. Finally, Appendix E provides a list of abbreviations used in this document.

1.5 Literature Review

Regulations in seismic codes of different countries were investigated to establish the variables that influence LRHA procedures as well as to study how these codes define such variables. The codes studied were the American standard (ASCE/SEI, 2010), the National Building Code of Canada (Canadian Commission on Building and Fire Codes, 2005), the New Zealand Standard NZS 1170.5 (Council of Standards New Zealand, 2004), the Eurocode 8 Part 1 (British Standards, 2004), the Chilean standard (Instituto Nacional de Normalizacion, 1996), the Mexican standard (Administracion Publica del Distrito Federal, 2004), FEMA750 (FEMA, 2009), and the American standard for the design of nuclear facilities ASCE 4-98 (ASCE, 2000); these codes are abbreviated hereafter as ASCE 7-10, NBCC, NZS, EC8, CHS, MXS, FEMA750, and ASCE 4-98, respectively.

Because of the recent release of ASCE 7-10,commentaries of the provisions of its Chapter 16 regarding linear response history analysis procedures were not initially found; however, valuable information was obtained from criticism to the provisions of ASCE 7-05 (ASCE/SEI, 2006), since the definition of many of the variables had not changed from ASCE 7-05 to ASCE 7-10. For instance, the analysis of a twelve story building done by Charney et al. (2010b) contains important information about the use of the provisions of Chapter 16 in ASCE 7-05, and it applies at large extent to the provisions of ASCE 7-10.

Due to the vast number of variables influencing linear response history analysis procedures, the documentation regarding the state of each of these variables within and beyond building codes is described within the particular section in this document. For instance, the current procedures suggested for the scaling of ground motions is covered specifically in Chapter 3.

1.6 Nomenclature

For the remainder of this document, there is a difference between the terms "earthquake," "record," and "earthquake component"; the term "earthquake" will refer to different earthquake events like Loma Prieta in 1989, Northridge in 1994 or Tabas in 1978, and the acceleration histories recorded at different stations of an earthquake are denoted as "records" or "earthquake records". For instance, the NGA database (PEER, 1999) contains the information recorded from 84 stations during the Loma Prieta earthquake in 1989; therefore, this event in particular has 84 records (records NGA0731 through NGA0813 and NGA3548). Finally, each record usually has two horizontal and a vertical acceleration history, and each of them is denoted as an "earthquake component."

Additionally, the reader is addressed to the abbreviation list of Appendix E if clarification of the abbreviations used along this document is needed.

Chapter 2. SELECTION OF GROUND MOTIONS USING ACTUAL RECORDS AND ARTIFICIAL RECORDS

The selection and scaling of ground motions for linear response history analysis (LRHA) is one of the most important variables in this type of analysis, because it directly influences the magnitude of the element forces and displacements obtained from the mathematical model. Appropriate records for design purposes can be selected from recorded earthquakes, from records generated by simulation of the source and travel path mechanisms, and from artificial records generated so that their spectrum matches closely with a defined target spectrum (Gomes et al., 2006); these three types of acceleration histories are denoted hereafter as recorded, simulated, and artificial records, respectively. Additionally, artificial records include acceleration histories generated using a seed record, and also acceleration histories generated without a seed record. This chapter will focus on the selection of ground motions for linear response history analysis using recorded and artificial records.

The first part of the chapter discusses the selection of recorded acceleration histories, and it has been divided into four topics. The first of them refers to the definition of the seismic hazard for the site of interest, while the second topic covers the selection of records based on parameters like the magnitude of the seismic event and the fault distance predicted by a seismic hazard analysis. Also, within this second topic the requirements for the selection of ground motions of the American standard, ASCE 7-10 (ASCE/SEI, 2010), have been included. The third topic briefly discusses near-fault and far-field earthquakes, and the last topic lists the requirements provided in other seismic codes but not listed in ASCE 7-10 regarding the selection of ground motions.

The second part of this chapter refers to the selection of artificial records, and it includes the discussion of three different types of software that generate such acceleration histories. Finally, a summary of recommendations given for future editions of ASCE 7-10 based on the content of this chapter is provided.

The reader is referred to Appendix E of this document for explanation of abbreviations not specified within the text.

2.1 Selection of ground motions using recorded earthquakes

2.1.1 Definition of the seismic hazard for the site of interest

Chapter 16 of ASCE 7-10 (ASCE/SEI, 2010) does not provide details on how the seismic hazard analysis for a site should be done. However, the American standard for the Seismic Analysis of Safety-Related Nuclear Structures ASCE 4-98 (ASCE, 2000), denoted hereafter ASCE 4-98, states in its Section 2.1.1 that "Probabilistic estimates of the seismic hazard at the site may be used to determine the principal contributors to the seismic hazard, which are those earthquake magnitudes and distances which govern the spectra." Also, the New Zealand Standard NZS 1170.5 (Council of Standards New Zealand, 2004), denoted hereafter NZS, states that "The seismological characteristics upon which records are to be selected will generally involve a de-aggregation of the design spectra into at least two period bands so as to establish the seismological signature of records appropriate for use within each band." A specific procedure defining the seismic hazard for the site of interest is considered appropriate for future editions of ASCE 7-10, and the use of the deaggregation maps provided by the U.S. Geological Survey (2009) can be an alternative.

The magnitude and fault distance of the earthquake that controls the seismic hazard at a specific location can be estimated using the deaggregation maps provided by the U.S. Geological Survey (2009a) which is denoted hereafter as USGS. Figure 2-1 shows the input required for running the deaggregation model of the USGS, and it can be noticed that the data required are the location of interest (Latitude and Longitude), the probability of exceedence of the design event (Return Period), the fundamental frequency or fundamental period of the structure, and the average shear-wave velocity in the top 30 m (V_s^{30}).

Also, the deaggregation model of the USGS will report the mean and modal values of the magnitude and fault distance that control the seismic hazard at the site of interest. The use of the modal parameters is preferred, because it represents the magnitude and fault distance of the most expected earthquake event for the site of interest, while the mean value could be biased by isolated events. As an example of the use of the deaggregation model of the USGS, Table B- 12 in Appendix B shows the modal magnitude and fault distance that controls the seismic hazard at different periods for a site with Latitude = 38.5, Longitude = -100.0 (near Scott City, Kansas), probability of exceedance of 2% in 50 years, and average shear wave velocity in the top 30 m. equal to 760 m/s (same data of Figure 2-1).

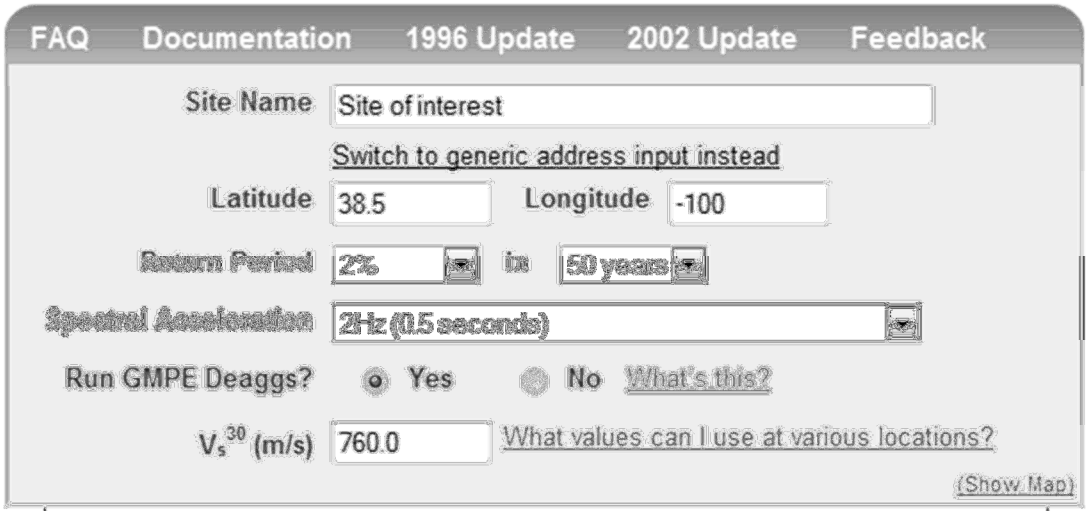

Figure 2-1 Input required for running the 2008 deaggregation model of the USGS (U.S. Geological Survey, 2009a)

Furthermore, the designer has to be aware that the hazard at one location can be given by more than one pair of Magnitude-Distance values, and such information can only be identified by careful observation of the deaggregation plots generated by the USGS. For instance, Figure 2-2 shows the deaggregation model corresponding to the information of Figure 2-1, and it can be seen that the highest contribution to the seismic hazard comes from three pairs of modal magnitude and fault distance identified in Table 2-1.

2.1.2 Selection of records based on the magnitude and fault distance predicted by the seismic hazard of the site of interest

After identifying appropriate parameters of magnitude and fault distance, a list of records with such characteristics can be downloaded from databases such as the NGA database (PEER, 1999), COSMOS database (COSMOS, 2007), or any other applicable database. These databases will include the type of soil where the ground motion was recorded, and such soil classification needs to be compared with the soil type for the site of interest (in an ideal case, the type of soil in the recording station and in the site of interest will be the same). Additionally, the deaggregation model of the USGS does not provide the source mechanism (strike-slip fault, normal fault, or reverse fault) of the predicted earthquake for the site of interest; however, if the source mechanism is known (i.e. when the seismic hazard is given by a deterministic approach) the selection of ground motions from a database can also include this parameter. The set of

parameters magnitude, fault distance, source mechanism, and soil type is denoted hereafter as M-D-SM-ST.

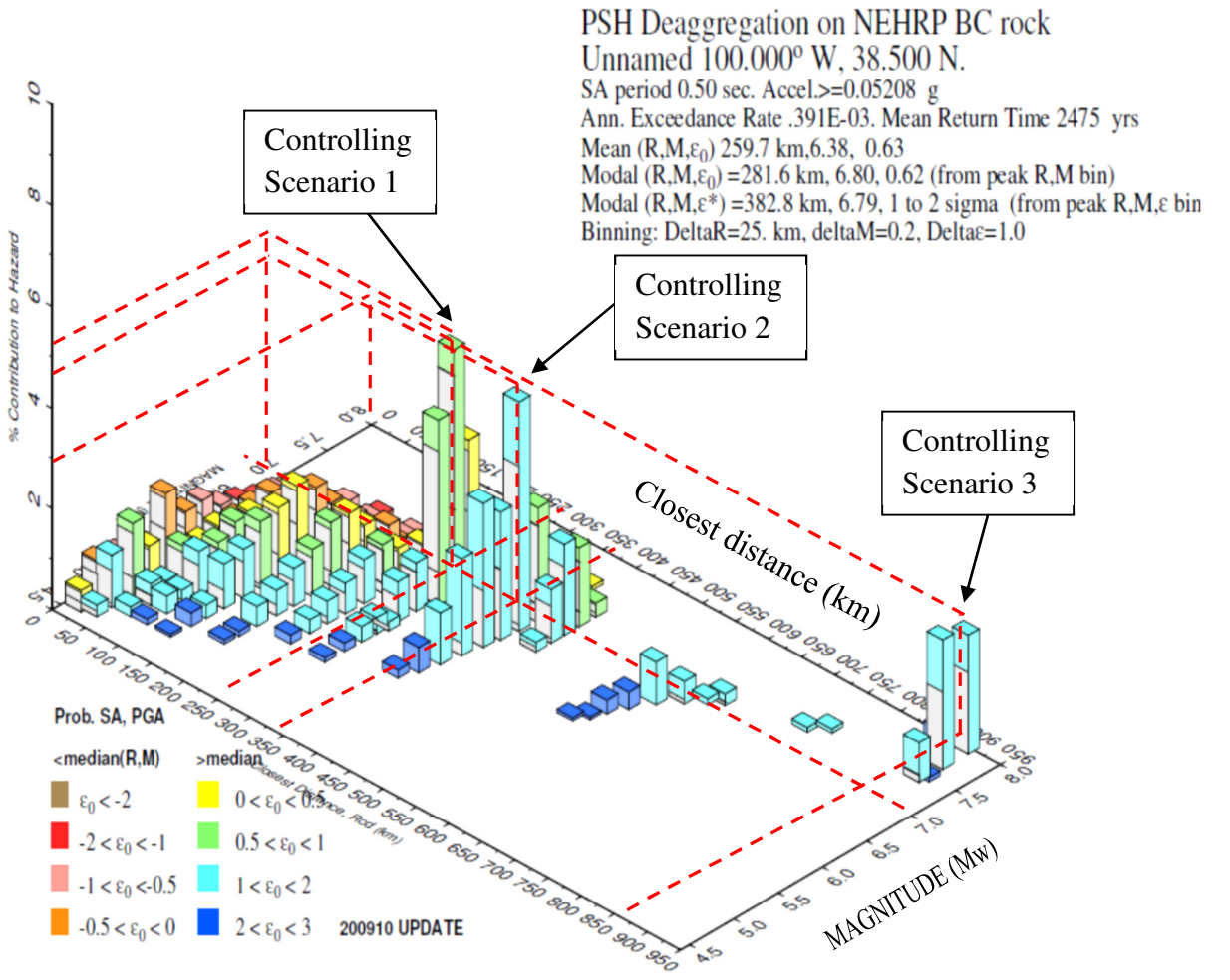

Figure 2-2 Deaggregation model for a site with Latitude = 38.5, Longitude = -100, probability of exceedance of 2% in 50 years, and period equal to 0.5 sec

Table 2-1 Controlling scenarios of Magnitude and Fault distance for a site with Latitude = 38.5, Longitude = -100, probability of exceedance of 2% in 50 years, and period equal to 0.5 sec

Scenario	Fault distance R (km)	Magnitude M
1	260	6.9
2	350	6.9
3	875	8

Earthquakes are usually selected by picking parameters M-D-SM-ST that coincide with the location of interest. The requirements of ASCE 7-10, ASCE 4-98, NZS, the National Building Code of Canada (Canadian Commission on Building and Fire Codes, 2005), denoted hereafter NBCC, and the Eurocode 8 (British Standards, 2004), denoted hereafter EC8, are shown in Table 2-2 where the "x" symbol accounts for a stated requirement. Similar information can be found in Beyer and Bommer (2007).

Table 2-2 Requirements of different codes for the selection of ground motions

Code[c]	Magnitude	Distance	Source Mechanism	Soil Type
ASCE 7-10	x	x	x	
ASCE 4-98	x	x	x[a]	x[a]
NBCC	x	x		
NZS	x	x	x	x
EC8	x[b]	x[b]	x[b]	x

[a] specified by appropriate "geological and seismological environment"

[b] specified by appropriate "seismogenetic features of the sources"

[c] Refer to list of abbreviations in Appendix E

Also, the Mexican specifications for seismic design (Administracion Publica del Distrito Federal, 2004), denoted hereafter MXS (for Mexican standard), states in Section 9.2 that selected records will have intensities according to the seismic criteria of the Mexican standard; however, no further explanation is specified.

The acceptable range of variability of the parameters M-D-SM-ST is not specified in ASCE 7-10; however, definitions of those limits are important to standardizing the selection procedure of ground motions. Stewart et al. (2001) suggest that "It is desirable to use earthquake magnitudes within 0.25 magnitude units of the target magnitude," and such recommendation is based on the definition of moment magnitude and the seismic moment given in Eq. 2-1 (Hanks and Kanamori, 1979) and Eq. 2-2 respectively, as follows:

$$M_w = \frac{2}{3}\log M_0 - 10.7 \qquad \textbf{Eq. 2-1}$$

$$M_0 = \mu AD \qquad \textbf{Eq. 2-2}$$

where M_w is the moment magnitude

M_0 is the seismic moment given in dyne-cm

μ is the shear modulus of the earth's crust in dyne/cm^2.

A is the area of the rupture fault in cm^2

D is the fault displacement in cm

Stewart et al. (2001) stated the importance of having records with magnitude close to the target because this parameter influences the frequency content and the duration of the ground motion. Also, according to Bommer and Acevedo (2004), some flexibility in the criteria of fault distance and soil type can be accepted, as long as these parameters do not differ considerably from those target values.

Also, when the number of records with desired parameters of magnitude, fault distance and soil type, denoted M-D-ST, are not available from recorded events, the appropriate acceleration histories can be generated from records with different parameters M-D-ST. An alternative using this methodology is explained in Carballo and Cornell (1998), and it consists of two steps. First, a target spectrum representative of the ideal conditions M-D-ST is generated by modifying the spectrum of the available record (parameters M-D-ST different than the desired or ideal parameters) by a factor accounting for the difference in magnitude and fault distance, and by a factor accounting for differences in the soil type. The second step of this procedure consists of modifying the available record such that its spectrum matches with the target spectrum generated in the first step.

The factor accounting for the difference in frequency content of the signal from the earthquake representative of the ideal conditions M-D-ST and the signal from the available earthquake can be obtained by creating two response spectra using attenuation laws for the ideal and available parameters M-D-ST, and then obtaining the ratio between these spectra at different periods. Consequently, each period of the original spectrum will be modified by a different factor at this stage. Also, the factor that accounts for the soil conditions can be obtained by attenuation laws that already include soil conditions or by a study of the amplification or de-amplification of a signal through different soil types using appropriate software such as RASCAL (Silva and Lee, 1987), DESRA-2 (Lee and Finn, 1978), WAVES (Hart and Wilson, 1989), EQTools (Charney and Syed, 2004, 2010) or SHAKE2000 (Ordoñez, 2008), where the latter integrates the computer programs SHAKE (Schnabel et al., 1972), SHAKE91 (Idriss and Sun, 1992), and ShakEdit (Ordoñez, 2008). Furthermore, the matching of spectra required in the

second step can be done using RSPMatch (Atik and Abrahamson, 2010) or RASCAL (Silva and Lee, 1987) . It is mentioned in Carballo and Cornell (1998) that one of the disadvantages of this technique is that the duration of the original record could not be modified to be consistent with the duration corresponding to an event with M-D-ST according to the target.

2.1.3 Treatment of earthquakes recorded at near distances and far distances from the source

The designer has to account for the distinction of near and far sources in the selection of ground motions in addition to choosing ground motions with appropriate parameters M-D-SM-ST. The distance delineating near and far source is not consistently defined, so designers will have to follow the definitions of the applicable seismic code. For instance, ASCE 7-10 provides specific guidelines for sites located less than 5 km from the source. Also, Stewart et al. (2001) stated that at distances less than 20 to 60 km from the seismic source, there will be a significant influence of near-fault effects (i.e. rupture directivity). In the case of the New Zealand Standard 1170.5 (NZS) there is a near-fault factor denoted *N(T,D)* that affects structures located less than 20 km from the closer of a specific list of faults provided in this standard; therefore, it can be stated that fault distances less than 20 km would define an earthquake near to the source according to this standard. The factor *N(T,D)*, according to the NZS, is equal to 1.0 for a probability of exceedance ≥ 1/250; however, if that is not the case this factor is calculated as follows:

$$N(T,D)=\begin{cases} N\,max(T) & D \le 2km \\ 1+(N\,max(T)-1)\dfrac{20-D}{18} & 2km < D \le 20km \\ 1.0 & D > 20km \end{cases} \qquad \text{Eq. 3.1(3) of NZS 1170.5}$$

where D is the shortest distance (in km) from the site of interest to the nearest fault

$N\,max\,(T)$ is the maximum near fault factor, and it varies from 1.00, 1.12, 1.36, 1.60, and 1.72 for periods less than 1.5 sec, period equal to 2 sec, 3 sec, 4 sec, and period higher than 5 sec, respectively

T is the fundamental period of the structure

Moreover, the Eurocode 8 (EC8) does not mention the effects of sources located near or far from the site of interest in the chapters describing the seismic actions in the design of

buildings (Chapters 3 and 4 of EC8); however, Chapter 10 of EC8 regarding base isolation systems states that "In buildings of importance class IV, site-specific spectra including near source effects should also be taken into account, if the building is located at a distance less than 15 km from the nearest potentially active fault with a magnitude *M*s ≥6.5."

The distance defining earthquakes near to the source has specific applications; for instance, ASCE 7-10 requires the rotation of the record components in the fault-normal and fault-parallel directions for distances to the source less than 5 km. In the case of the NZS it is stated that "one record in three in each family selected shall have a forward directivity component, while the remainder of the family shall be of near-neutral or backwards directivity" when the near fault factor *N(T,D)*, defined according this standard, is bigger than 1. This way, it could be considered that the NZS has a similar requirement to that of ASCE 7-10 about rotating the original components of the record to the fault-normal and fault-parallel directions except that ASCE 7-10 would require satisfying this criterion in all the selected earthquakes and not just in some of them, as it would be required in the NZS.

The classification of near-fault and far-field earthquakes based on a distance from the source is not easily defined by a simple number according to Professor Martin Chapman of the Geosciences Department of Virginia Tech (2010b), because the change in behavior from near-fault to far-field earthquakes depends on the frequency of interest and on the physical size of the source from where the wavefield is radiated.

2.1.4 Other requirements stated in different codes

Other requirements not covered in ASCE 7-10 but included in other seismic codes are indicated next.

2.1.4.1 Statistical independence between the components of the ground motion

A requirement mentioned in ASCE 4-98 is that when the input of each record consists of two horizontal components and one vertical component then those three components have to be statistically independent. The criteria followed by ASCE 4-98 to satisfy this requirement is that "Two time histories shall be considered statistically independent if the absolute value of the correlation coefficient does not exceed 0.3". The basis of ASCE 4-98 to choose the value of 0.3 can be found in Hadjian (1984) and Lin (1980). The correlation coefficient, denoted *r*, is the Pearson Product-Moment correlation coefficient (or normalized covariance), and it is calculated

as the ratio between the covariance of two vectors divided by the product of their standard deviations (Howell David C., 2007) as it is shown in the equation 2.3 below:

$$r = \frac{covariance(A,B)}{SD(A) * SD(B)} = \frac{\frac{\sum_{i=1}^{n}(A_i - \overline{A})(B_i - \overline{B})}{n}}{\sqrt{\frac{\sum_{i=1}^{n}(A_i - \overline{A})^2}{n}}\sqrt{\frac{\sum_{i=1}^{n}(B_i - \overline{B})^2}{n}}} = \frac{\sum_{i=1}^{n}(A_i - \overline{A})(B_i - \overline{B})}{\sqrt{\sum_{i=1}^{n}(A_i - \overline{A})^2 \sum_{i=1}^{n}(B_i - \overline{B})^2}} \quad \textbf{Eq. 2-3}$$

where	r	is the correlation coefficient
	A and B	are the vectors which correlation coefficient is desired
	n	is the number of rows of vectors A or B
	$\overline{A}$	is the mean value of the vector A
	$\overline{B}$	is the mean value of the vector B
	$covariance(A,B)$	is the covariance of the vectors A and B
	$SD(A)$	is the standard deviation of the vector A
	$SD(B)$	is the standard deviation of the vector B

Beyer and Bommer (2007) criticize the requirements of ASCE 4-98 because it does not specify if the data to be compared corresponds to the acceleration record, velocity record, displacement record, response spectra or the power spectral density spectra of the components of the record. Section C2.3-1 of the commentary of ASCE 4-98 states specifically the formula to calculate the correlation coefficient, and apparently the variables to be compared are time functions; therefore, such statistical independence would not refer to the response spectra or to the power spectral density spectra. However, as criticized by Beyer and Bommer (2007), the correlation coefficient will change if the parameters compared are the acceleration, velocity or displacement records. For instance, Table 2-3 and Table 2-4 show the variation in the correlation coefficients for the horizontal components of acceleration, velocity, and displacement for a set of records recorded at far distances from the source in the case of Table 2-3 and at close distance from the source as shown in Table 2-4.

Table 2-3 Correlation coefficient for horizontal components of acceleration, velocity and displacement, for a sample of 8 earthquakes with Magnitude>6 and Epicenter distance>60km

NGA Record Number	Magnitude	Epicenter distance (km)	Correlation coefficients of horizontal components		
			Acceleration components	Velocity components	Displacements components
280	7.20	76.75	0.003	0.333	0.428
433	6.50	97.70	0.093	0.224	0.185
439	6.88	94.99	0.159	0.274	0.280
785	6.93	137.64	0.437	0.329	0.165
883	7.28	191.54	0.089	0.113	0.282
1103	6.90	196.18	0.134	0.206	0.485
1146	7.51	223.07	0.236	0.443	0.681
1372	7.62	215.47	0.106	0.119	0.349

Table 2-4 Correlation coefficient for horizontal components of acceleration, velocity and displacement, for a sample of 8 earthquakes with Magnitude>5.5 and Epicenter distance<20km

NGA Record Number	Magnitude	Epicenter distance (km)	Correlation coefficients of horizontal components		
			Acceleration components	Velocity components	Displacements components
2	6.00	6.31	0.296	0.205	0.219
6	6.95	12.99	0.13	0.13	0.278
95	6.24	5.68	0.025	0.097	0.216
106	5.89	12.58	0.289	0.138	0.002
214	5.80	17.13	0.346	0.548	0.402
297	6.20	18.89	0.346	0.216	0.121
410	5.77	11.09	0.073	0.218	0.101
502	5.60	15.86	0.054	0.089	0.101

It can be noticed from the two tables above that the correlation coefficient can change considerably depending on if it is calculated using the acceleration, velocity or the displacement components. Also, it can be noticed in Table 2-3 that for most of the cases the correlation coefficients of the velocity and displacements components are higher than those of the acceleration components; however, that is not the case for the earthquake identified as NGA#785 where the opposite occurs. Moreover, the NGA record 785 in Table 2-3 and the NGA records

214 and 297 in Table 2-4 have correlations coefficients in the acceleration components (0.437, 0.346, and 0.346, respectively) that are very different from zero, and it implies a "small" degree of correlation in those components. Additionally, Table 2-4 shows no trends in the correlation coefficients of velocity and displacements relative to the acceleration correlation coefficient, and due to the small size of the sample in both tables, it is not possible to state any conclusion about the trends of the correlation coefficients in the three parameters analyzed (acceleration, velocity and displacement).

The requirement of statistical independence needs to be studied in more detail, because as mentioned by Martin Chapman, Professor of the Geosciences Department of Virginia Tech (2010b), ground motions at low frequencies might be highly correlated.

2.1.4.2 Consistent average value of PGA from the selected records

Another requirement of ASCE 4-98 and EC8 is that the average of the peak ground acceleration, denoted PGA, of the records used in the analysis should equal or exceed the design ground acceleration. The procedure to control this requirement could be different when using artificial records than when using recorded records. For the first case, the PGA could be specified directly in software that generates artificial seismograms like SIMQKE-I (Vanmarcke et al., 1976, 1990) and then this requirement can be accomplished with no difficulties. In the case of using actual records, it is suggested the check of the average PGA using the original selected records (not scaled), because it indirectly indicates consistence with desired magnitude and duration.

Moreover, it should be noticed that when using as a target, the design response spectrum given in Chapter 11 of ASCE 7-10 the PGA is given by $0.4*S_{DS,}$ where S_{DS} is the 5 percent damped design spectral acceleration parameter at short periods. Also, ASCE 7-10 provides in Figure 22-7 through Figure 22-10 maps containing the PGA values (as a percentage of the gravity) for different locations in the U.S. for soil type B, and the corresponding values for other types of soil can be obtained applying the equation 11.8-1 of the same standard. Then, the PGA value provided by these maps could be a better approximation of the PGA for the site of interest than $0.4S_{DS}$.

2.1.4.3 Range of periods of interest within the range of periods usable for the particular earthquake

A particular record with similar parameters M-D-SM-ST to those at the site of interest might not be used in the analysis if the usable range of periods for that particular earthquake, which depends on the filters applied to process the original signal, does not include the range of periods of interest of the structure (Beyer and Bommer, 2007). Chapter 16 of ASCE 7-10 specifies that the average of the scaled ground motions (see Section 3.1.1 for specific guidelines of scaling in ASCE 7-10) has to be above the design spectrum within $0.2T$ and $1.5T$, where T is the fundamental period of vibration in the direction analyzed, and therefore all the periods in this range can be considered as the period range of interest in ASCE 7-10. The lower limit ($0.2T$) accounts for the effect of higher modes, while the upper limit ($1.5T$) accounts for the lengthening of the fundamental period under inelastic response.

The information to identify the usable range of periods for the records from the NGA database (PEER, 1999) is provided in the "Flatfile" available in the PEER database, which gives the lowest usable frequency for the particular record, and therefore, the maximum usable period. Then, this maximum usable period must be compared with the upper limit of the range of periods of interest as defined by the appropriate seismic code (Beyer and Bommer, 2007). For instance, the NGA record 0001 has a high pass filter of 0.2 Hz (PEER, 1999), which indicates that it could be used for structures where the upper limit of the period range of interest does not exceed 1/0.2 = 5 sec. Additionally, the Flatfile of the PEER database website (PEER, 1999) provides the corner frequencies of the low pass filters for each of the horizontal components of the ground motions, and from there it can be obtained the minimum usable period. Furthermore, the minimum usable period could be given by the period corresponding to the Nyquist frequency of the record. This way, the frequency of the minimum usable period corresponds to the smaller of the Nyquist frequency and the frequency of the low pass filter specified in the Flatfile of the NGA database. For example, the NGA record 0001 has a Nyquist frequency of 50 Hz, and a low pass filter of 15 Hz (PEER, 1999); therefore, the minimum usable period is equal to 1/15 = 0.067 sec.

2.2 Selection of earthquakes for linear response history analysis using artificial records

Ground motions for linear response history analysis are usually scaled so that they are compatible with the target spectrum, which is normally the design spectrum for the site of

interest. The matching of recorded earthquakes with the target spectrum can be done usually only within a small range of periods because of the high variability of a spectrum at different periods compared with a usually smoothed target spectrum. This is also because the target spectrum is a uniform risk spectrum that does not represent the response of a particular seismic event, but it represents the envelope of maximum responses at different periods coming from possibly different earthquakes, which causes difficulties in fitting procedures. Therefore, matching the target over several periods using recorded earthquakes is not likely to occur, so artificial seismograms can be created to accomplish this goal.

2.2.1 Specific requirements for the creation of artificial records

ASCE 7-10 does not have any information referring to the process to create artificial records; however, the requirements given in ASCE 4-98 about statistical independence of the record components (as explained in Section 2.1.4.1 of this document) and about average PGA higher than the design ground acceleration (as explained in Section 2.1.4.2 of this document) are also applicable for artificial records. Three additional requirements will be explained in this section: a consistent amplitude and duration of the artificial records according to the magnitude and distance that controls the seismic hazard for the site of interest, zero velocity at the end of the record, and degree of variability of the spectrum from the artificial record compared to the target spectrum.

2.2.1.1 Amplitude and duration according to the magnitude and distance that controls the seismic hazard for the site

ASCE 4-98 requires having records with amplitude and duration according to the magnitude and fault distance that control the seismic hazard for the site, and the same requirement is stated in Section 3.2.3.1.2 of EC8. Useful information to satisfy this requirement can be found in Table 2.3-1 of ASCE 4-98, which provides appropriate values of rise time, strong motion, and decay time based on a trapezoidal envelope of an artificial seismogram for different ranges of magnitudes of the control scenario. Also, EC8 states for artificial seismograms that "… the minimum duration T_s of the stationary part of the accelerograms should be equal to 10 s:" however, specific definition of the "stationary part" is not provided. Complete or selected parts of time series (i.e. acceleration histories) can have properties of strong stationarity or weak stationarity, and conditions to satisfy each type of stationarity can be found

in Madsen (2008) and Kendall and Ord (1990). According to Madsen (2008) "A weakly stationary process is characterized by the fact that both the mean value and the variance are constant, while the autocovariance function depends only on the time difference." Also, if a time series satisfies the requirements of weak stationarity and if the elements of the time series are normally distributed, then it will be guaranteed strong stationarity (Pollock, 1999). This way, the stationary part of an accelerogram could be understood as its part having constant mean and variance.

Also, if artificial accelerograms are created with a trapezoidal envelope as shown in Figure 2-3 and if the duration of the stationary part is the difference between the times TLVL and TRISE shown in the same figure, the minimum requirement of 10 sec for the stationary part required by the Eurocode 8 would apply to the time interval denoted as $t_{strong\ motion}$ in Figure 2-3. Also, Table 2.3-1 of ASCE 4-98 recommends values of $t_{strong\ motion}$ varying between 5 and 13 sec depending on the magnitude of the earthquake that such artificial accelerogram represents. Recommendations for amplitude and duration of a generated earthquake signal are intended to ensure appropriate peak ground acceleration (PGA), as well as to provide reasonable values of the rise, strong motion, and decay time intervals of an earthquake signal. This is necessary because too small values of rise, strong motion or decay time, could yield a signal that is poor in the frequencies of interest. If that is the case, signals with too short duration will have difficulty when trying to match a target spectrum. On the other hand, if the duration of the generated signal is considerably longer that the duration of a real scenario for the location of interest, the time required for solving a particular analysis will increase with respect to the time of analysis for the same structure with a more realistic duration of the generated earthquake signal.

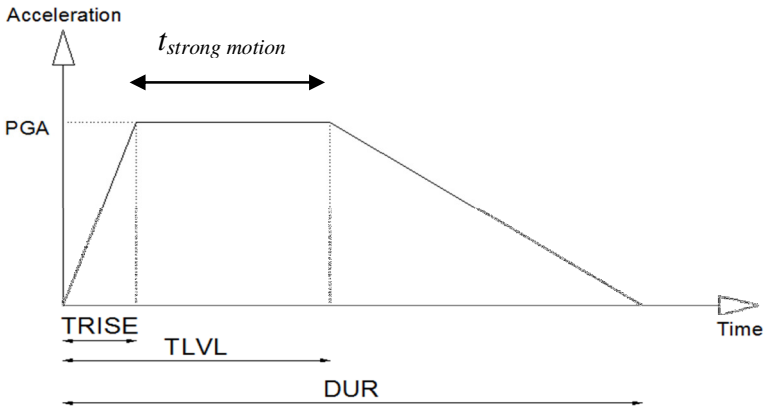

Figure 2-3 Trapezoidal envelope of artificial accelerograms

2.2.1.2 Zero velocity at the end of the record

The movement of the ground stops at the end of an earthquake. This fact indicates that the velocity of a record, which is obtained by numerical integration of the acceleration record, has to be zero at the end of both horizontal record components. However, software that generates artificial seismograms such as SIMQKE-I (Vanmarcke et al., 1976, 1990) , RASCAL (Silva and Lee, 1987) or RSPMatch (Atik and Abrahamson, 2010), might have algorithms that do not guarantee a zero velocity at the end of the generated earthquake signal; therefore, baseline correction would be required in those cases. A common alternative for base line correction consists of obtaining the parabolic curve that adjusts best to the generated acceleration record, and then subtract such polynomial from the generated acceleration record (U.S. Geological Survey, 2006). Another technique to correct artificial records consists of subtracting the mean acceleration from the accelerogram before getting the velocity history, and do the same with the velocity before getting the displacement history (see Section 2.2.2.1 for application of this procedure).

The importance of baseline correction is more significant for structures with long periods because in this case, the displacements of the structure tend to be equal to the ground displacement, and if the later are predicted by non-corrected accelerograms the displacement in the analyzed structure could be unrealistic.

2.2.1.3 Degree of variability of the spectrum from the artificial record compared to the target spectrum.

The shape of the spectrum from artificial earthquakes is not required to perfectly match the target; instead, it is preferable to have variability in the generated spectrum so it will indirectly represent the uncertainty involved in the earthquake signal.

2.2.2 Studying the characteristics of artificial records

Three different types of software were investigated to obtain equivalent acceleration histories that match a target spectrum. These software consists of a) a routine developed by the Professor Martin Chapman from Virginia Tech (2010a), b) the program SIMQKE-I (Vanmarcke et al., 1976, 1990) and c) the stochastic maps generated by the USGS website (U.S. Geological Survey, 2009a). Although the software SIMQKE-I was developed in 1976 and updated in 1990,

it is still currently used in research to create artificial earthquakes (Fahjan and Ozdemir, 2008), and that was the reason for exploring this tool.

An analysis of each of these utilities is presented next, and it will be used to provide preliminary guidelines for an acceptability criterion for artificial seismograms.

2.2.2.1 Routine developed by Martin Chapman

The routine developed by Martin Chapman matches a target response spectrum using phase-invariant Fourier amplitude scaling of a user-selected input accelerogram. Because the phase of the input time-series is preserved, many aspects of the input time domain signal are preserved on output, such as duration and envelope shape. This routine requires as input an initial earthquake signal, preferably from an earthquake with magnitude and distance similar to those that control the hazard scenario, because the original and transformed signals have the same duration. The input of the original record is in the format of Time vs. Acceleration. The routine also asks for the target spectrum and the number of iterations to perform a cyclic procedure as explained later. The format for the input of the target spectrum is Frequency – PSA response, where PSA is the pseudo spectral acceleration.

This software generates a transformed signal with compatible response spectrum to a target spectrum by following the next steps:

1) Fitting of the target response spectrum with a polynomial function.
2) Calculation of the Fourier Amplitude Spectrum of the initial input time series.
3) Calculation of the response spectra of the initial input time series
4) Calculation of the ratio of the target PSA spectrum to that of the input time series.
5) Multiplication of the Fourier amplitude spectrum of the initial input time series by the ratio from step 4.
6) Fourier transformation of the result of step 5 to the time domain.
7) Repeat steps 2 through 6 with the new time series until the spectrum from the generated time series converges to the target spectrum.

This program does not have the capability to ensure zero velocity at the end of the signal; therefore, baseline correction is required. An alternative to solve this issue consists in subtracting the mean of the acceleration record from each acceleration value and integrating this new set of data if the velocity record is desired. This procedure will guarantee having a velocity equal to zero at the end of the record. Also, although it is not required to have a zero

displacement, the same procedure could be applied with the velocity record in order to get a displacement record with zero value at the end of the signal. The use of the negative of the mean velocity as the constant of integration required to obtain displacement is optional: however, if the designer considers this approach not appropriate, then a different constant of integration would still be required in order to avoid undesirable trends in the displacement record. The procedure mentioned above to obtain the velocity and displacement record is shown in the following equations.

$$VelCh = \int (AccCh - \overline{AccCh})\, dt \qquad \textbf{Eq. 2-4}$$

$$DispCh = \int (VelCh - \overline{VelCh})\, dt \qquad \textbf{Eq. 2-5}$$

where $AccCh$ is the acceleration history reported by Chapman's routine.

$\overline{AccCh}$ is the mean value of AccCh.

$VelCh$ is the corrected velocity record.

$\overline{VelCh}$ is the mean value of *VelCh*.

DispCh is the displacement record with zero displacement at the end of the earthquake.

An advantage of this software is that it generates acceleration and velocity records similar to the same parameters in the original input signal, and therefore the characteristics of the original signal are relatively carried over to the new signal. The generated displacement record preserves the characteristics of the original record only to a small degree, as it is explained later. Furthermore, this tool can be used for any type of soil, because the target spectrum will already include this effect. This is an important feature because the stochastic seismograms generated by the USGS website are not capable to account for different types of soil as it will be explained later.

An example is developed next to study the mentioned features of this tool. The target spectrum will be given by the same spectrum used by Charney et al. (2010b) in a design example of a twelve story building. The parameters that define the target spectrum are shown in Table 2-5, and they were based on ASCE 7-05 (ASCE/SEI, 2006); also, the respective plot of the design spectrum (target spectrum) is shown in Figure 2-4.

Table 2-5 Data for target spectrum to match spectra from artificial seismograms

Parameter	Value
Longitude	-121.9
Latitude	37.365
S_S:	1.25
S_1:	0.4
Site class:	C
Fa:	1
Fv:	1.4
S_{MS}:	1.250
S_{M1}:	0.560
S_{DS}:	0.833
S_{D1}:	0.373

where S_S is the mapped MCE, 5% damped, spectral response acceleration parameter at short periods

S_1 is the mapped MCE, 5% damped, spectral response acceleration parameter at a period of 1sec.

Fa is the short-period site coefficient (at 0.2 sec period).

Fv is the long-period site coefficient (at 1.0 sec period).

S_{MS} is the MCE, 5% damped, spectral response acceleration at short periods adjusted for site class effects.

S_{M1} is the MCE, 5% damped, spectral response acceleration at a period of 1 s adjusted for site class effects.

S_{DS} is the design, 5% damped, spectral response acceleration parameter at short periods.

S_{D1} is the design, 5% damped, spectral response acceleration parameter at a period of 1 s.

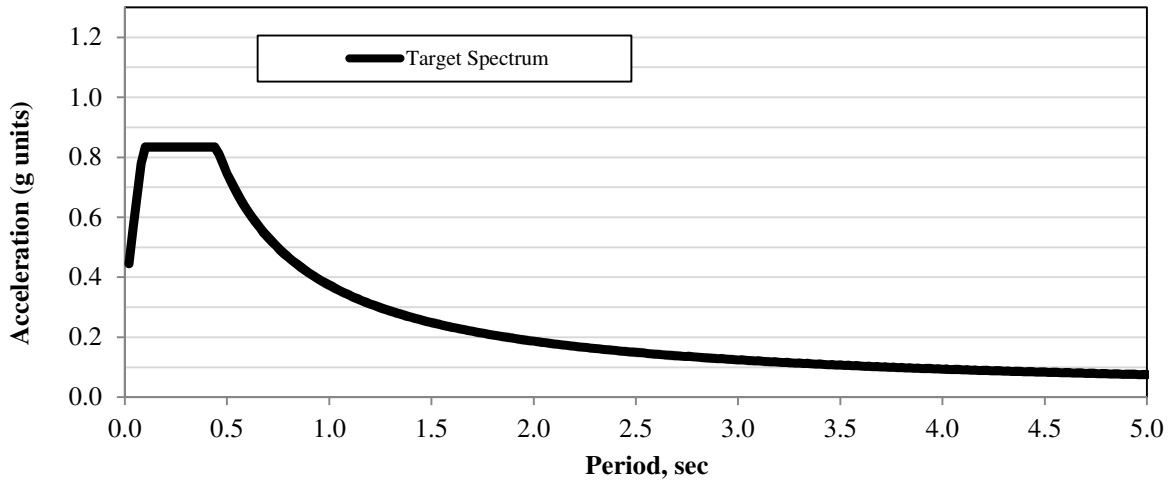

Figure 2-4 Target Spectrum to match spectra from artificial seismograms

The routine developed by Chapman was applied for the three earthquakes used also by Charney et al. (2010b), and they were taken from the NGA database (PEER, 1999). The description of these earthquakes is given in Table 2-6, and only the components with the highest PGA, A90, B00, and C90 were used for each record. Such components will generate acceleration histories denoted hereafter as Ch-1, Ch-2, and Ch-3.

Table 2-6 Suite of ground motions used to evaluate spectra from artificial seismograms

Earthquake	NGA Record Number	Magnitude [Epicenter Distance, km]	Site Class	Number of Points and Digitization Increment	Component Source Motion	PGA (g)	Record Name for Example FEMA
A	879	7.28 [44]	C	9625 @ 0.005 sec	Landers/LCN260	0.73	A00
					Landers/LCN345	0.79	A90
B	725	6.54 [11.2]	D	2230 @ 0.01 sec	SUPERST/B-POE270	0.45	B00
					SUPERST/B-POE360	0.30	B90
C	139	7.35 [21]	C	1192 @ 0.02 sec	TABAS/DAY-LN	0.33	C00
					TABAS/DAY-TR	0.41	C90

Before comparing the generated spectrum for each signal, it was convenient to evaluate the appropriate number of iterations explained in the seventh step of Chapman's routine (see Section 2.2.2.1 of this document) so that the spectrum from the generated signal would converge to the target spectrum. The study of the number of iterations to convergence towards a target

spectrum was needed, because the number of iterations that would guarantee a good match with the target spectrum was unknown. The number of iterations varied between 1 and 5, and the spectra of the acceleration histories generated for the component A90 of the Landers earthquake doing such variations is shown in Figure 2-5. The same plot for periods less than 1 sec only is shown in Figure 2-6.

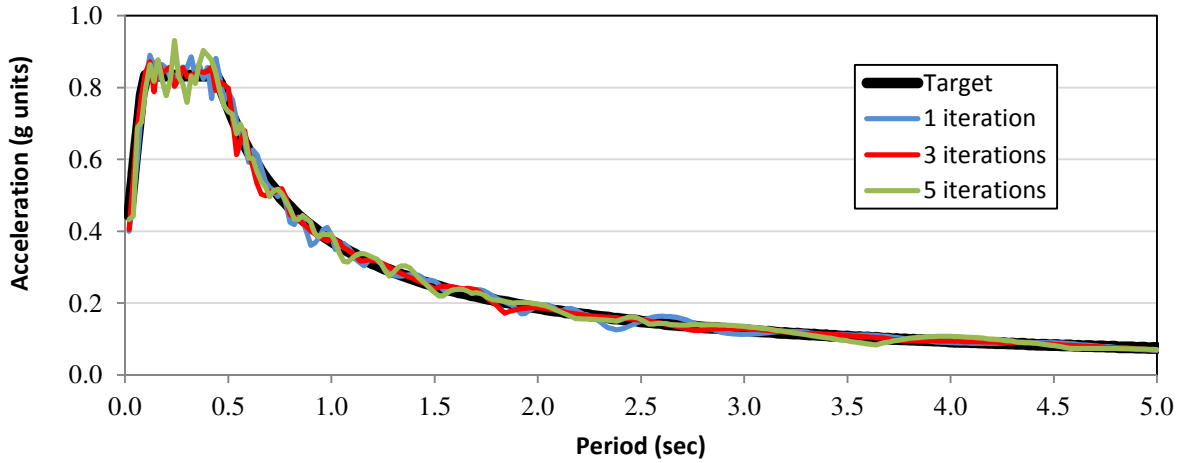

Figure 2-5 Variation of the generated spectra for different number of iterations using Chapman's routine given as the input the component A90 of the Landers earthquake.

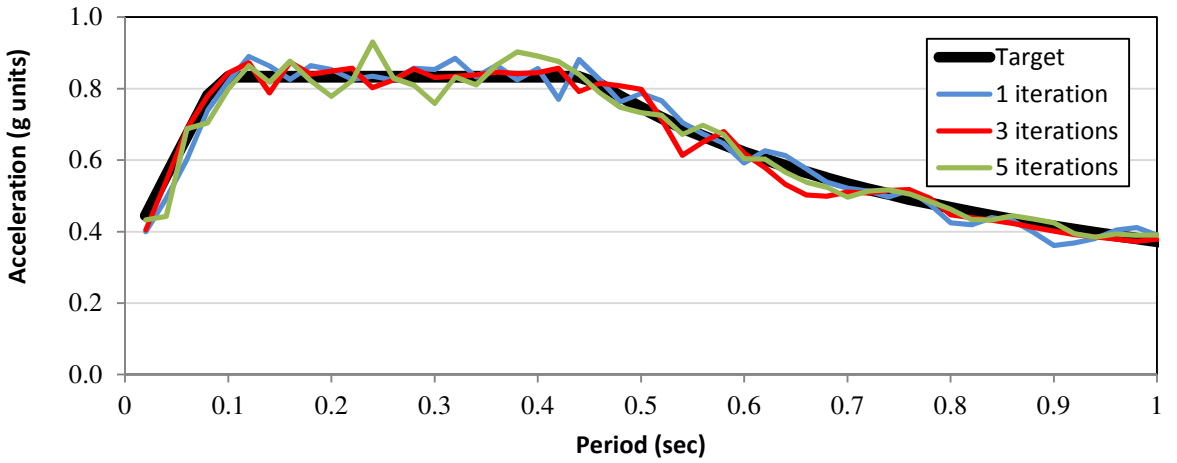

Figure 2-6 Variation of the generated spectra for different number of iterations using Chapman's routine given as the input the component A90 of the Landers earthquake, zoom in the constant acceleration period.

It can be noticed in Figure 2-5 and Figure 2-6 that the first iteration gives a good approximation to the target spectrum, and it has small differences when compared to the spectrum generated using 5 iterations. In fact, in the region of constant acceleration shown in

Figure 2-6, the spectrum of the generated earthquake using one iteration in Chapman's routine is closer to the target spectrum than when using five iterations.

Despite this small difference between the spectral shape obtained with one and five iterations, five iterations were chosen to generate the spectra of each input earthquake using Chapman's routine. The original spectra of the three acceleration histories corresponding to the components A90, B00, and C90 are shown in Figure 2-7, and the spectra from the respective transformed signals using Chapman's routine, Ch-1, Ch-2, Ch-3 are shown in Figure 2-8. Both figures are plotted together with the target spectrum.

It can be noticed from Figure 2-7 and Figure 2-8 that the spectral shape changes drastically between the original spectrum and the spectrum corresponding to the transformed signal, and this fact means that the highly variable frequency content of recorded ground motions has been drastically removed in order to achieve the goal of creating acceleration histories with response spectrum matching the one given by the code. Furthermore, it can be seen in Figure 2-7 that the spectrum of the original earthquake component C90 is the one closer to the target spectrum; however, it is interesting that the spectrum resulting from applying Chapman's routine to the component C90 is the one that diverges most from the target spectrum as shown in Figure 2-8. Also, it can be noticed in Figure 2-8 that regardless of the input acceleration history the generated signals have spectrums very similar to the one given by the code, and that shows the great efficiency of this tool.

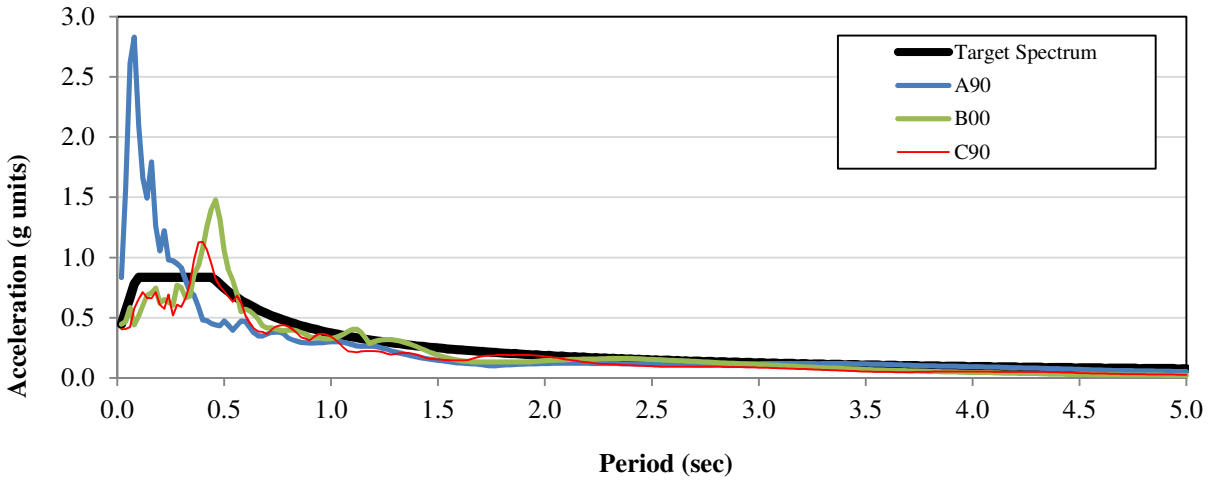

Figure 2-7 Spectra of the original components A90, B00, and C90 compared to the target spectrum

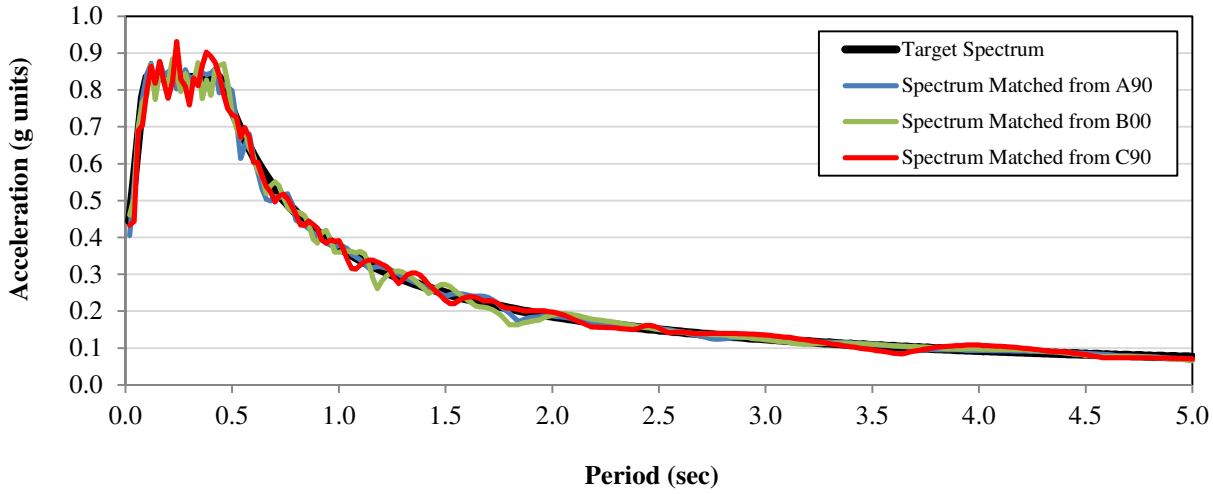

Figure 2-8 Spectra of the transformed signal Ch-1, Ch-2, Ch-3 compared to the target spectrum

Another aspect that requires analysis is the comparison between the acceleration, velocity, and displacement of the original and generated records. Figure 2-9, Figure 2-10, and Figure 2-11 show the plots of acceleration, velocity and displacement of the original record components A90, B00, C90, and their respective generated signals Ch-1, Ch-2, and Ch-3. In those plots the acceleration, velocity, and displacement of the original record component have been calculated without any constant of integration assuming that the NGA records integrated this way produce zero velocity at the end of the record. For the case of the generated signals the equations 2-4, and 2-5 were used.

From Figure 2-9, Figure 2-10, and Figure 2-11 it can be seen that the generated signals preserve at significant degree the characteristics of acceleration, and velocity of the original record component; however, that is not the case for the generated displacement history since it preserves the characteristics of the original signal only at a very small degree. The similarities are expected because the routine developed by Chapman modifies the amplitudes of the Fourier Spectra of the original signal, but it keeps the phase unchanged. Also, the smaller degree of similitude in the displacement records is due to the fact that the displacements obtained from the original seismograms would guarantee a zero velocity but not a zero displacement (from the assumption that the NGA records integrated without any constant of integration would produce a zero velocity at the end of the record); however, when using Equation 2-5 in the generated signals the displacement at the end will be zero as explained before.

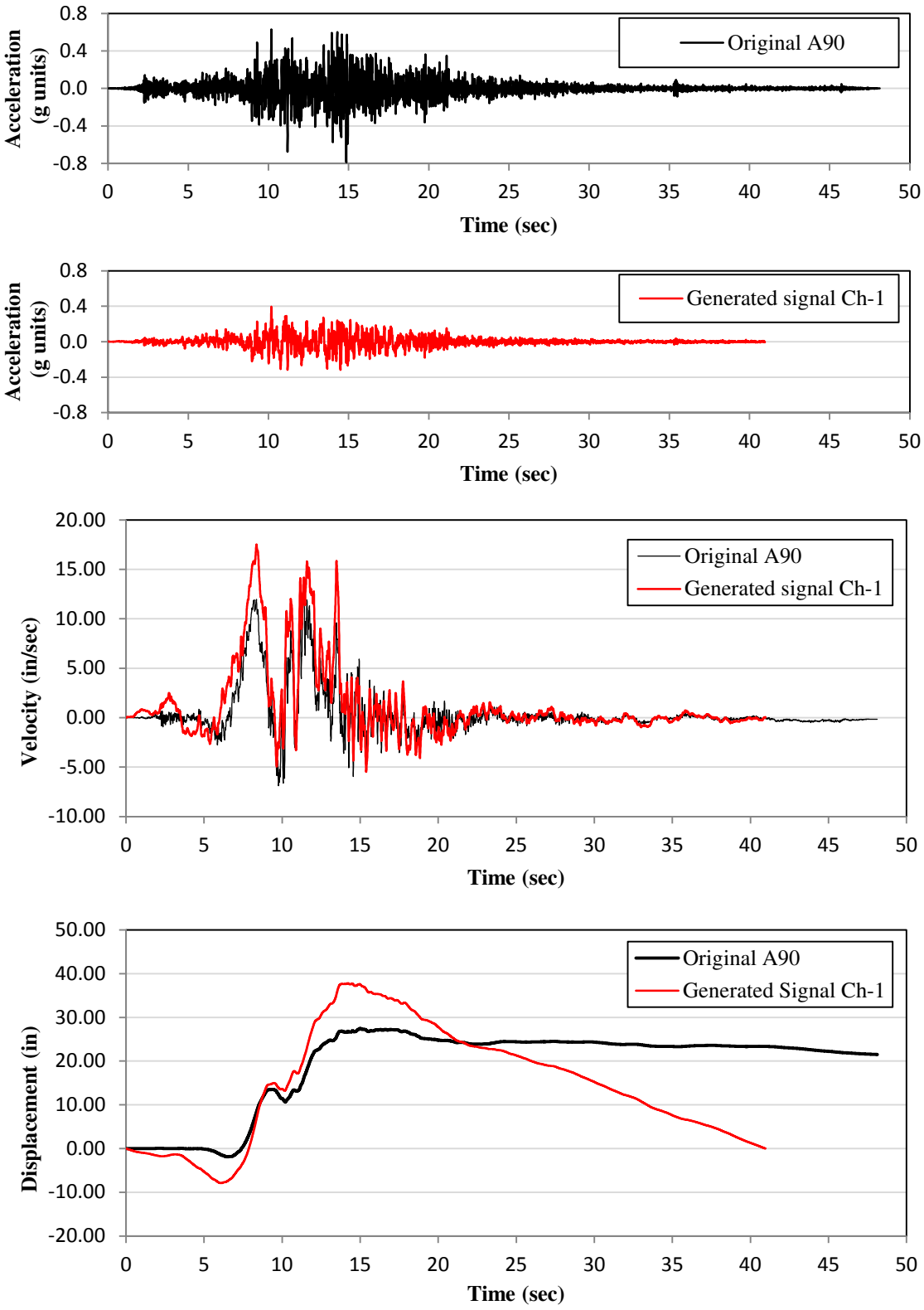

Figure 2-9 Acceleration, Velocity, and Displacement in original signal A90 and its respected transformed signal Ch-1

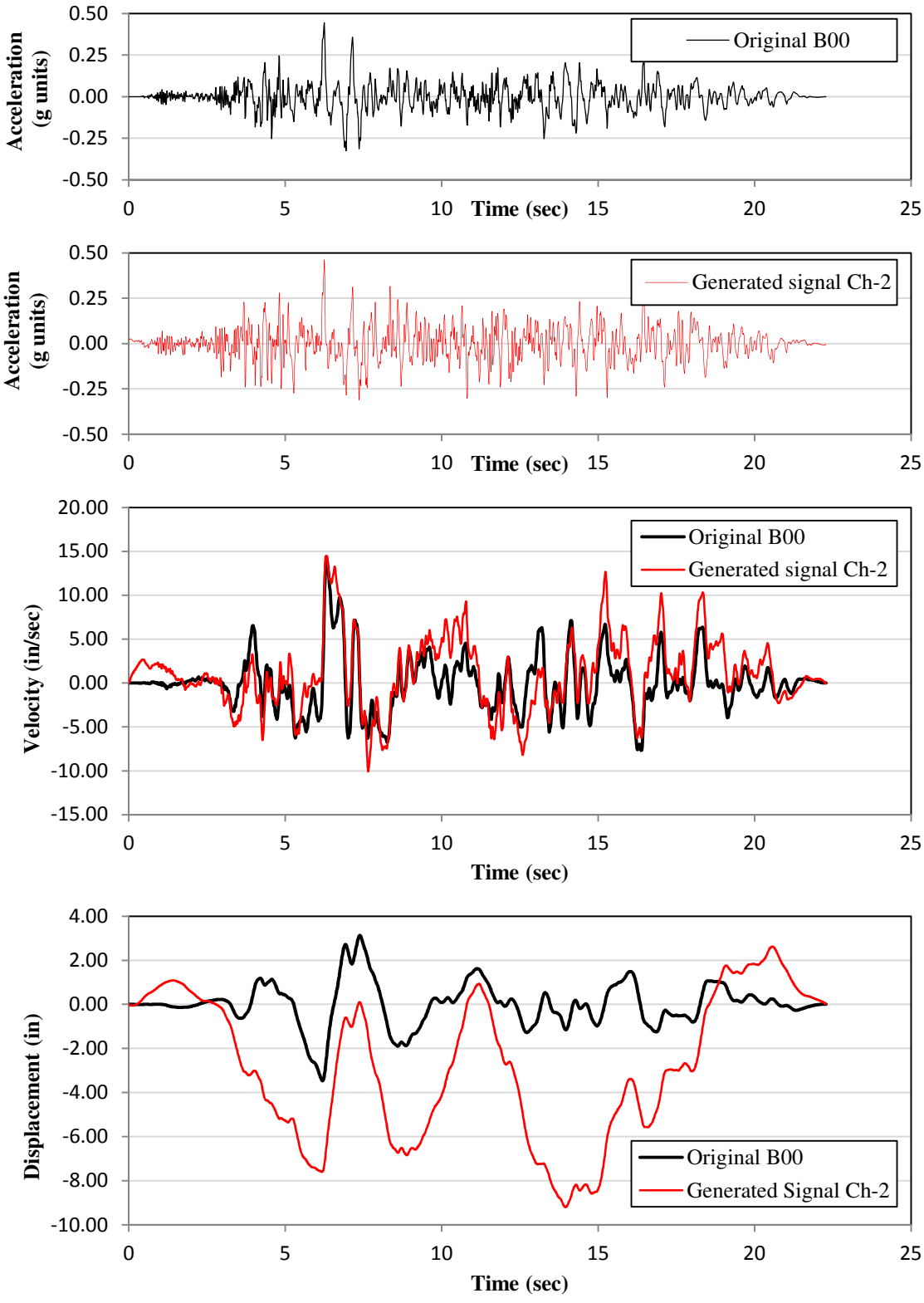

Figure 2-10 Acceleration, Velocity, and Displacement in original signal B00 and its respected transformed signal Ch-2

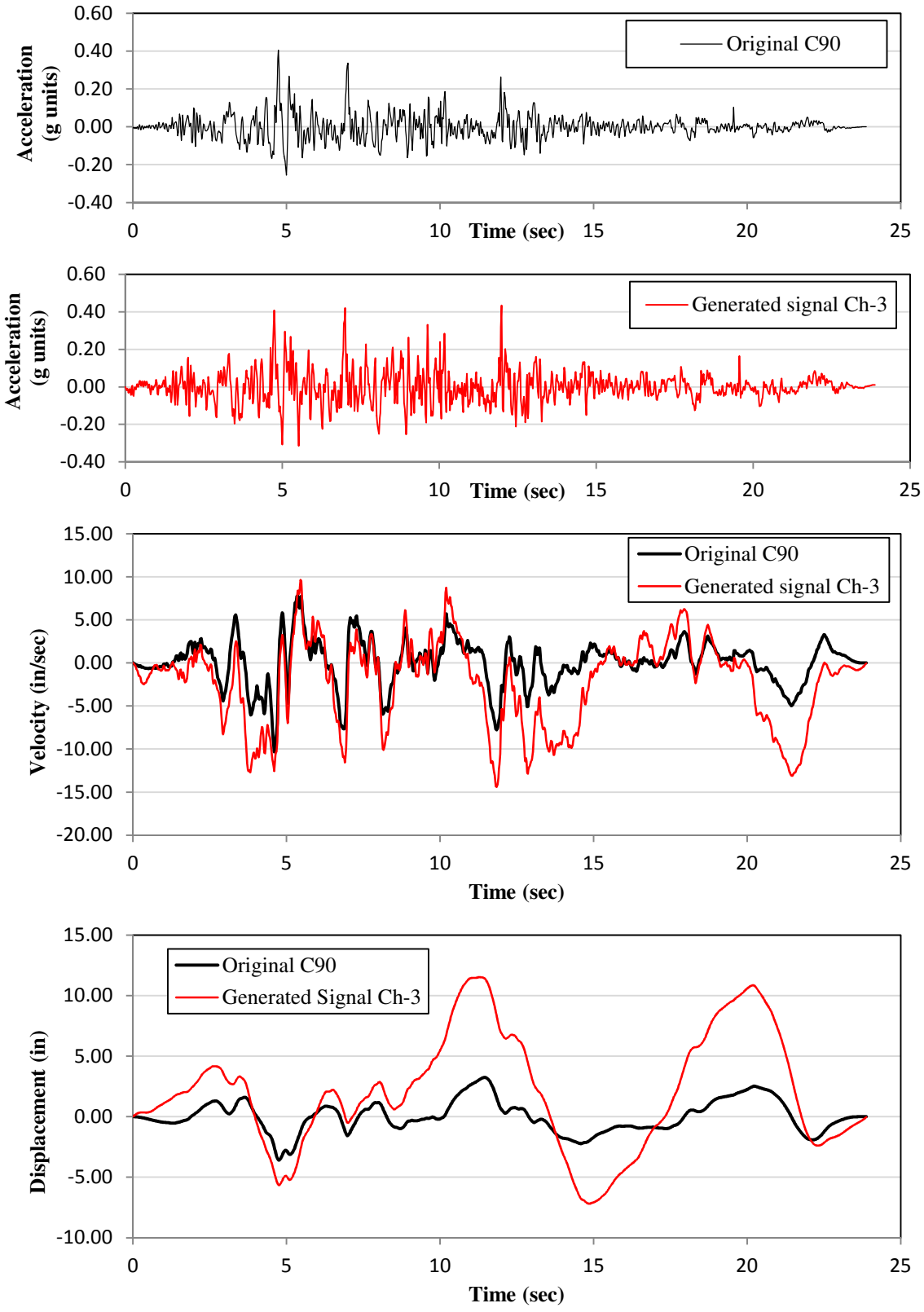

Figure 2-11 Acceleration, Velocity, and Displacement in original signal C90 and its respected transformed signal Ch-3

Also, it can be noticed that Figure 2-9 shows different duration between the original and the generated signal, and this happened because the routine used to generate the new signals allows only a number of data equal to 2^{13} = 8192, and record A90 had 9625 data points (see Table 2-6). However, this limitation of the number of data could be easily changed according to Chapman (2010a).

Some conclusions about the use of the routine developed by Chapman are stated next:

- The routine transforms an acceleration record into a new signal where acceleration response spectrum or velocity response spectrum match with a specified target spectrum.
- The inherent variability of the original spectrum is reduced in this process due to design implications.
- The generated signals appear to preserve the time domain characteristics of acceleration and velocity of the original signal for the sample of ground motions used in this document; however, the generated displacement histories preserve only at a small degree the characteristics of the original displacement history.
- The routine can be applied to any type of soil by giving an appropriate target spectrum.
- The routine can be applied to the two components of the original signal if it is desired to explore orthogonal loading.

2.2.2.2 Artificial earthquake signals created by the software SIMQKE-I

A second procedure to generate artificial seismograms was explored, and it consisted of the program SIMQKE-I (Vanmarcke et al., 1976, 1990). This software can develop acceleration histories such that their spectra can match closely to a defined target spectrum. Documentation about the methodology and characteristics of the input can be found in Vanmarcke and Gasparini (1976), and the software itself can be downloaded from The Earthquake Engineering Online Archive (NISEE Pacific Earthquake Engineering Research (PEER) Center, 2007). This software generates acceleration histories using different types of envelopes such as trapezoidal, exponential, and compound. Also, it can create several acceleration histories that match a target spectrum with only one run. The required input for this software is as shown in Table 2-7.

Table 2-7 Input format for software SIMQKE-I

TS	TL	TMIN1	TMAX1	YMIN	YMAX				
ICASE	TRISE	TLVL	DUR	AO	α0	β0	IPOW		
DELT	Max Acc	IIX	NDAMP	NCYCLE	NPA	NKK	NRES	NGWK	IPCH
Damping									
Period 1	PSV 1								
Period 2	PSV 2								
Period 3	PSV 3								
-	-								
Period i	PSV i								
-	-								
Period n	PSV n								

The definition of these variables is explained next, and they have been taken from Vanmarcke and Gasparini (1976).

TS: Smallest period (sec) of the desired response spectrum.

TL: Largest period (sec) of the desired response spectrum.

TMIN1: Smallest period used to determine the range of frequencies to be represented in the simulation. By default it is equal to TS.

TMAX1: Largest period used to determine the range of frequencies to be represented in the simulation. By default it is equal to TL.

YMIN: Estimated smallest velocity response spectral value (in/sec).

YMAX: Estimated largest velocity response spectral value (in/sec).

ICASE: Equal to 1 for no intensity envelope.
Equal to 2 for trapezoidal intensity envelope.
Equal to 3 for exponential intensity envelope.
Equal to 4 for compound intensity envelope.

TRISE: As defined in Figure 2-12.

TLVL: As defined in Figure 2-12.

DUR: Desired duration of the accelerogram, as defined in Figure 2-12.

A0, α0, β0, and IPOW are variables that apply to envelopes other than the trapezoidal shape.

DELT: Is the time interval of the accelerogram.

AGMX: Desired maximum ground acceleration in g units.

IIX: Arbitrary odd integer that serves as a seed for the random phase angle generator.

NDAMP: Number of damping values desired.

NCYCLE: Number of iterations to smoothen a response spectrum.

NPA: Number of artificial seismograms desired.

NKK: Number of periods at a logarithmic scale < 300.

NRES: Number of points of the target response spectrum.

NGWK: If equal to zero then SIMAKE-I generates its own power spectrum but it different to zero, then a piecewise linear power spectrum is generated.

IPCH: Variable equal to 0 or 1 depending if punched output was done.

Damping: Damping coefficients

Period i: Period in seconds for the i^{th} pair (Period, PSV) of the target spectrum.

PSV i: Pseudo Spectral velocity for the i^{th} pair (Period, PSV) of the target spectrum.

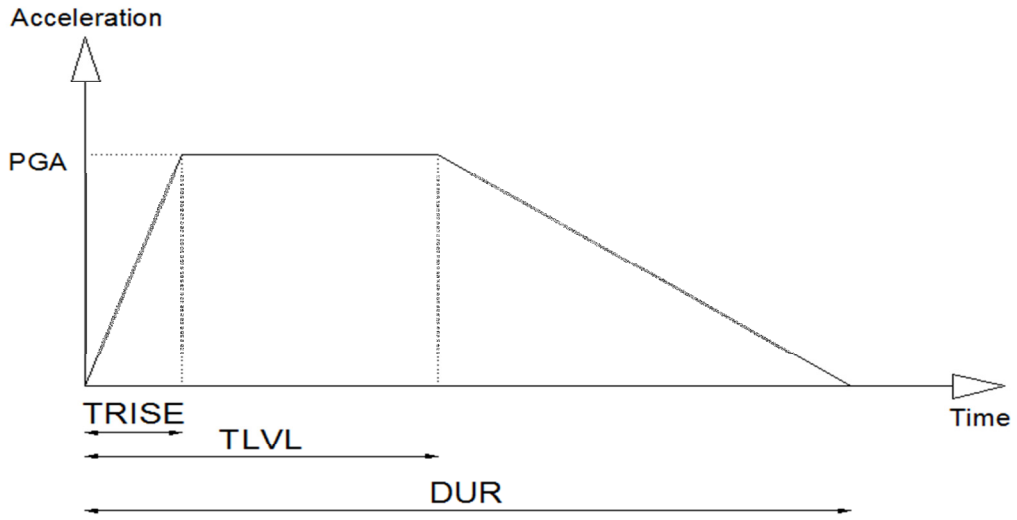

Figure 2-12 Trapezoidal envelope shape for input in SIMQKE-I

Three seismograms were generated using SIMQKE-I in order to study their applicability to LRHA. The input parameters to obtain those seismograms are shown in Table 2-8.

Table 2-8 Input parameters for generation of three artificial seismograms using SIMQKE-I

TS	**TL**	**TMIN1**	**TMAX1**	**YMIN**	**YMAX**				
0.02	5.0	0.02	5.0	0.1	500				
ICASE	**TRISE**	**TLVL**	**DUR**	**AO**	**α0**	**β0**	**IPOW**		
2	1.5	11.5	21.5	0	0	0	0		
DELT	**AGMX**	**IIX**	**NDAMP**	**NCYCLE**	**NPA**	**NKK**	**NRES**	**NGWK**	**IPCH**
0.01	0.43	1235	1	5	3	300	250	0	0
Damping									
0.05									

The target spectrum was the pseudo-velocity values corresponding to the acceleration spectrum shown in Figure 2-4 and which information is given in Table 2-5. This target was chosen so that the results from seismograms generated with SIMQKE-I can be compared with the records generated using the routine developed by Chapman. This way, the values of TS, TL, TMIN1, and TMAX1 were chosen to coincide with the values used to generate the target spectrum when using Chapman's routine. The maximum spectral velocity calculated was 22.96 in/sec; however, the input value for YMAX was chosen arbitrarily as 500 in/sec, and this decision would not make any difference in the results, because such value, as stated in the User's Manual (Gasparine and Vanmarcke, 001976), "is used mainly to determine the maximum ordinate on a plot of the response." The assigned value of 2 to the variable ICASE corresponds to a trapezoidal shape envelope.

Also, the parameters TRISE, TLVL, and DUR were taken from Table 2.3-1 of ASCE 4-98 (ASCE, 2000), which gives recommended values for rise time, duration of strong motion, and decay time based on the magnitude of the ground motion expected. Such magnitude was chosen so that the generated seismograms can represent the seismic hazard for a location that coincides with the one chosen for the building analyzed by Charney et al. (2010b). The average of the fundamental periods of vibration for the two translational directions of the building is 2.74 sec,

and according to a deaggregation model for the site of interest (see Table B- 12), the governing scenario has a magnitude of 8.01. However, a magnitude of reference equal to 7.0 was chosen from Table 2.3-1 of ASCE 4-98 considering that the generated seismograms would have the same spectrum as the ones generated with a different magnitude. Future research might include the generation of earthquakes using SIMQKE-I for a magnitude closer to 8.01.

The values for rise time, duration of strong motion, and decay time recommended by ASCE 4-98 for a trapezoidal shape envelope and for a range of magnitudes varying from 6.5 to 7.0, are 1.5 sec, 10 sec, and 7 sec, which explain why the values of TRISE and TLVL were taken as 1.5 sec and 11.5 sec. The decay time was taken as 10 sec instead of 7 sec, which gives a total duration, DUR, of 21.5 sec.

Furthermore, the parameters A0, $\alpha 0$, $\beta 0$ and IPOW are taken equal to zero, because those variables do not apply when using a trapezoidal envelope shape. The time interval for the points in the generated record was chosen arbitrarily as 0.01 sec. Also, the maximum ground acceleration was assumed as 0.43 g, which corresponds to the spectral acceleration given by the target spectrum shown in Figure 2-4 for a period of 0.02 sec, which is assumed to be close enough to the maximum PGA. The artificial seismograms were generated for only one value of damping, which was chosen as 0.05 as a fraction of the critical damping. Additionally, the specified number of iterations for each ground motion generated, NCYCLE, was chosen as 5, and three signals were generated so that NPA =3. The number of periods reported in logarithm scale, NKW, was taken as 300, and the specified target spectrum had 250 rows with periods specified every 0.02 seconds from 0 sec to 5 sec.

The three time series generated using SIMQKE-I, denoted hereafter SQK-1, SQK-2, and SQK-3, are shown in Figure 2-13 with the specified envelope, and it can be seen that PGA is reached at different times in each record.

Figure 2-14 shows the spectrum for each of the generated acceleration histories, and it can be noticed that it is a good match for all the range of periods. Also, when comparing Figure 2-8 with Figure 2-14, it can be seen that both procedures, the routine developed by Chapman as well as SIMQKE-I, satisfy the objective of generating time histories that have spectrum that match with a defined target.

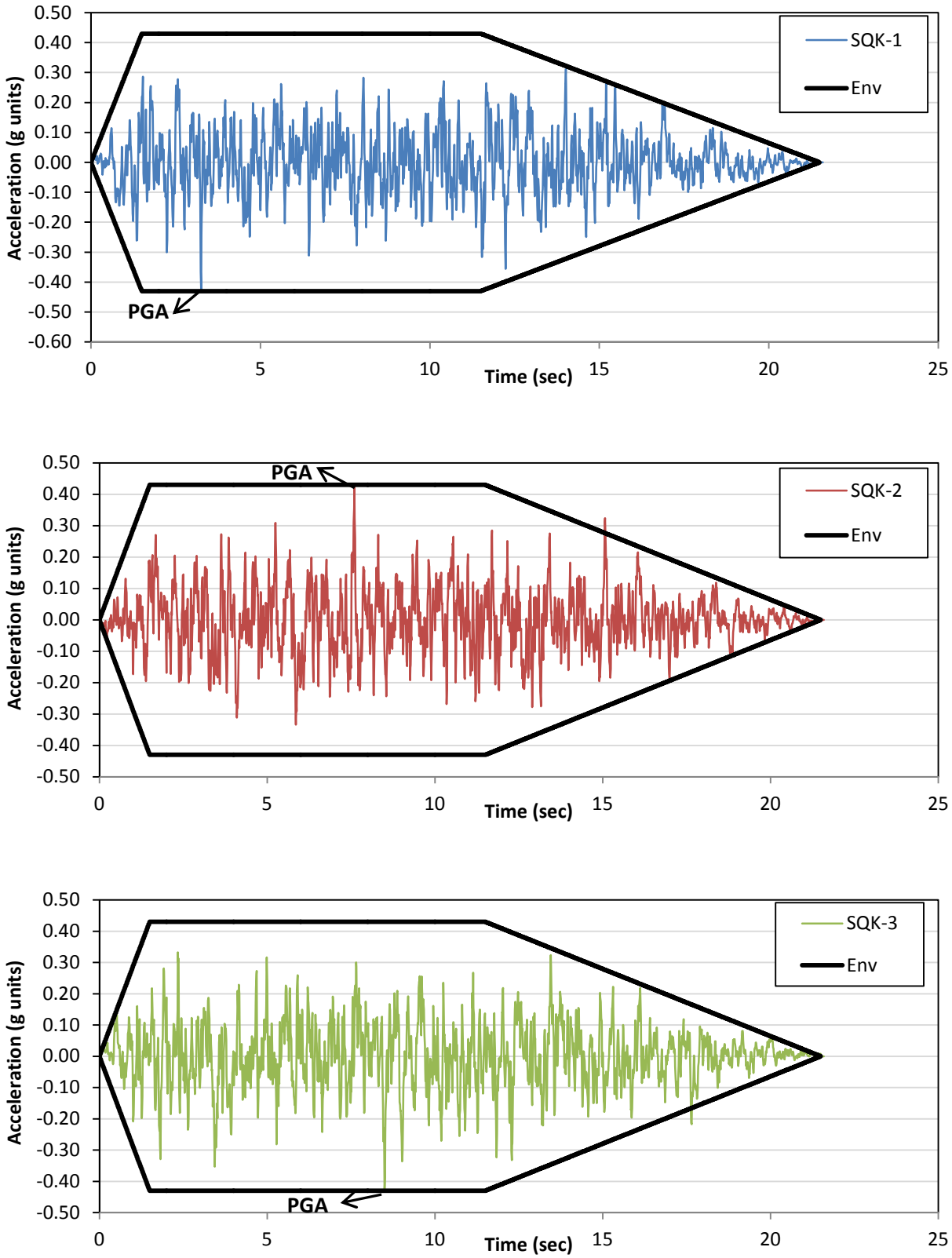

Figure 2-13 Artificial seismograms generated by SIMQKE-I

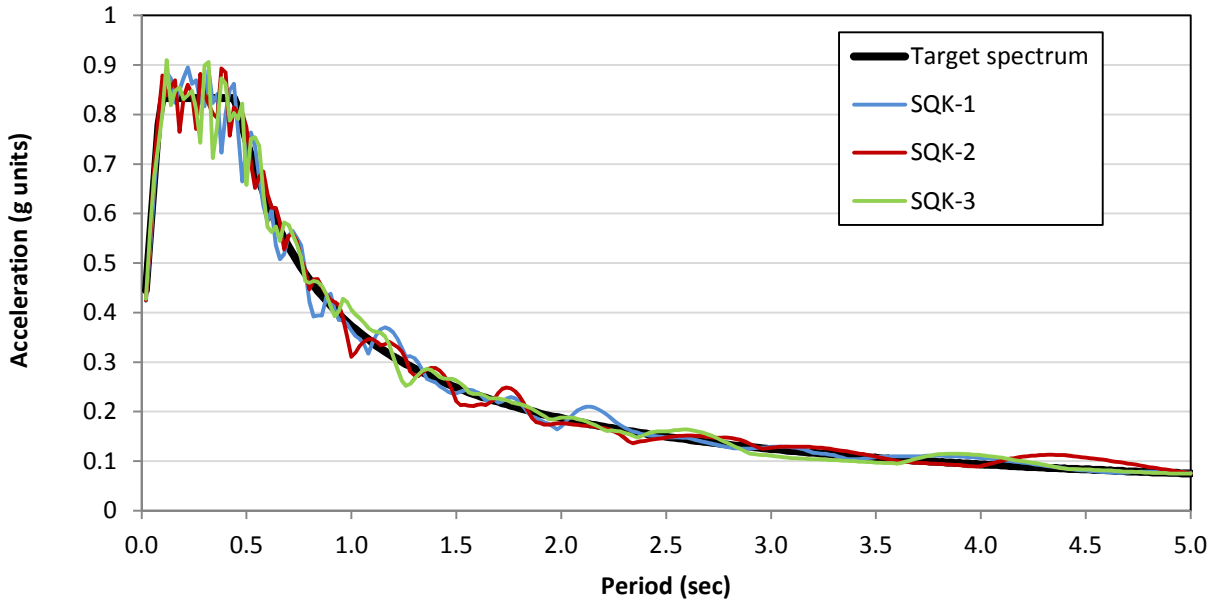

Figure 2-14 Spectrum of three seismograms generated with SIMQKE-I compared with the target spectrum

Figure 2-15, Figure 2-16, and Figure 2-17 show the parameters of acceleration, velocity, and displacement, for each of the three generated signals, after baseline correction using equations 2-4 and 2-5 (when using these equations, the acceleration record *AccCh* and the velocity record *VelCh* were replaced with the corresponding acceleration and velocity records generated using SIMQKE-I). Also, Figure 2-15, Figure 2-16 and Figure 2-17 are not compared against an original record, because SIMQKE-I does not use a seed to generate the spectral matched acceleration history.

Also, it is interesting to analyze the Pearson Product-Moment correlation coefficient *r* (or normalized covariance) between the three generated earthquakes; these values are shown in Table 2-9, and it is noticed that *r* is very close to zero, which means that each seismogram is statistically independent from each other. This property coincides with the description of the program given in the Earthquake Engineering Online Archive (NISEE Pacific Earthquake Engineering Research (PEER) Center, 2007), which states that "SIMQKE-1 generates statistically independent accelerograms."

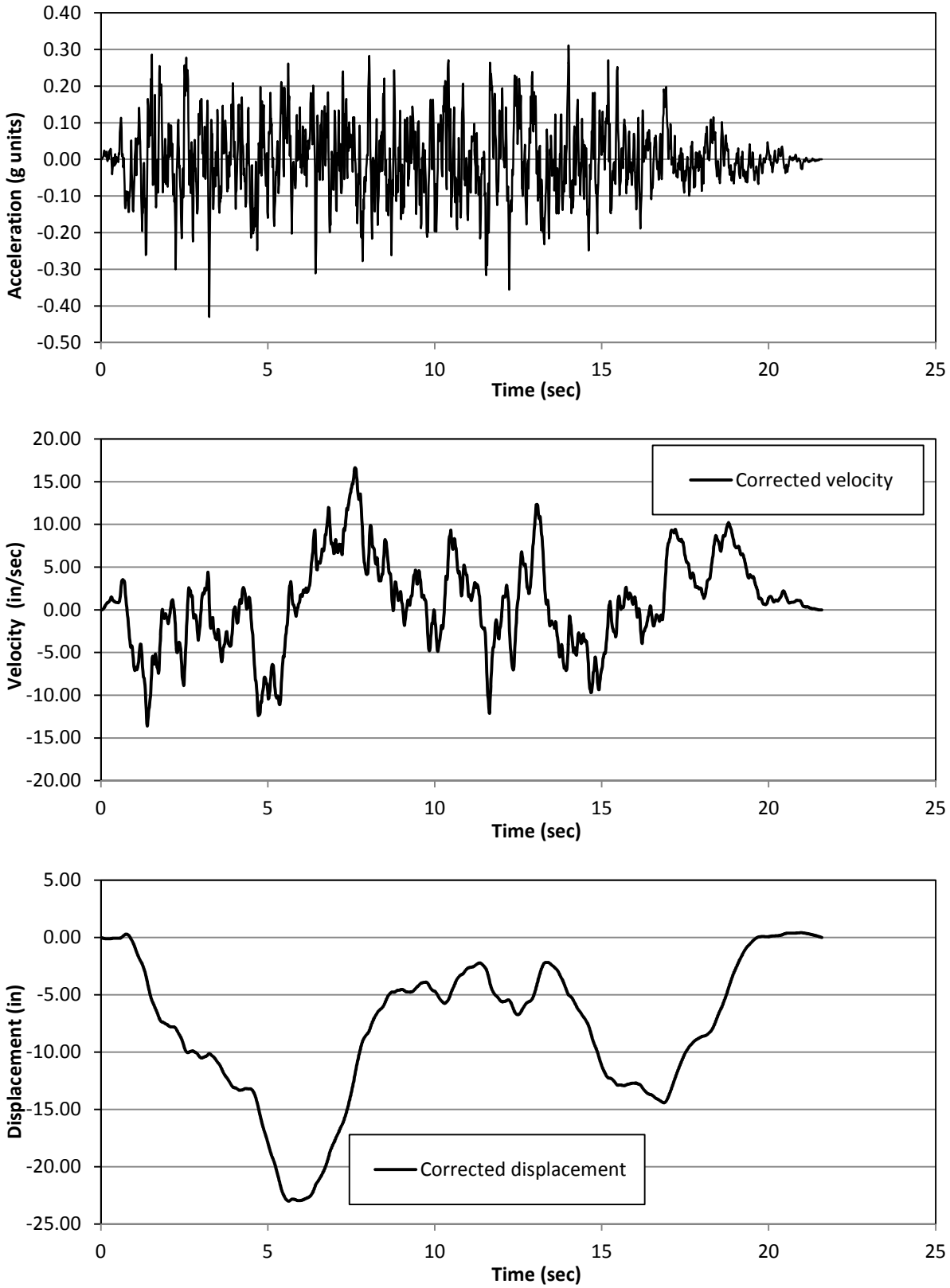

Figure 2-15 Acceleration, velocity and displacement record for seismogram SQK-1

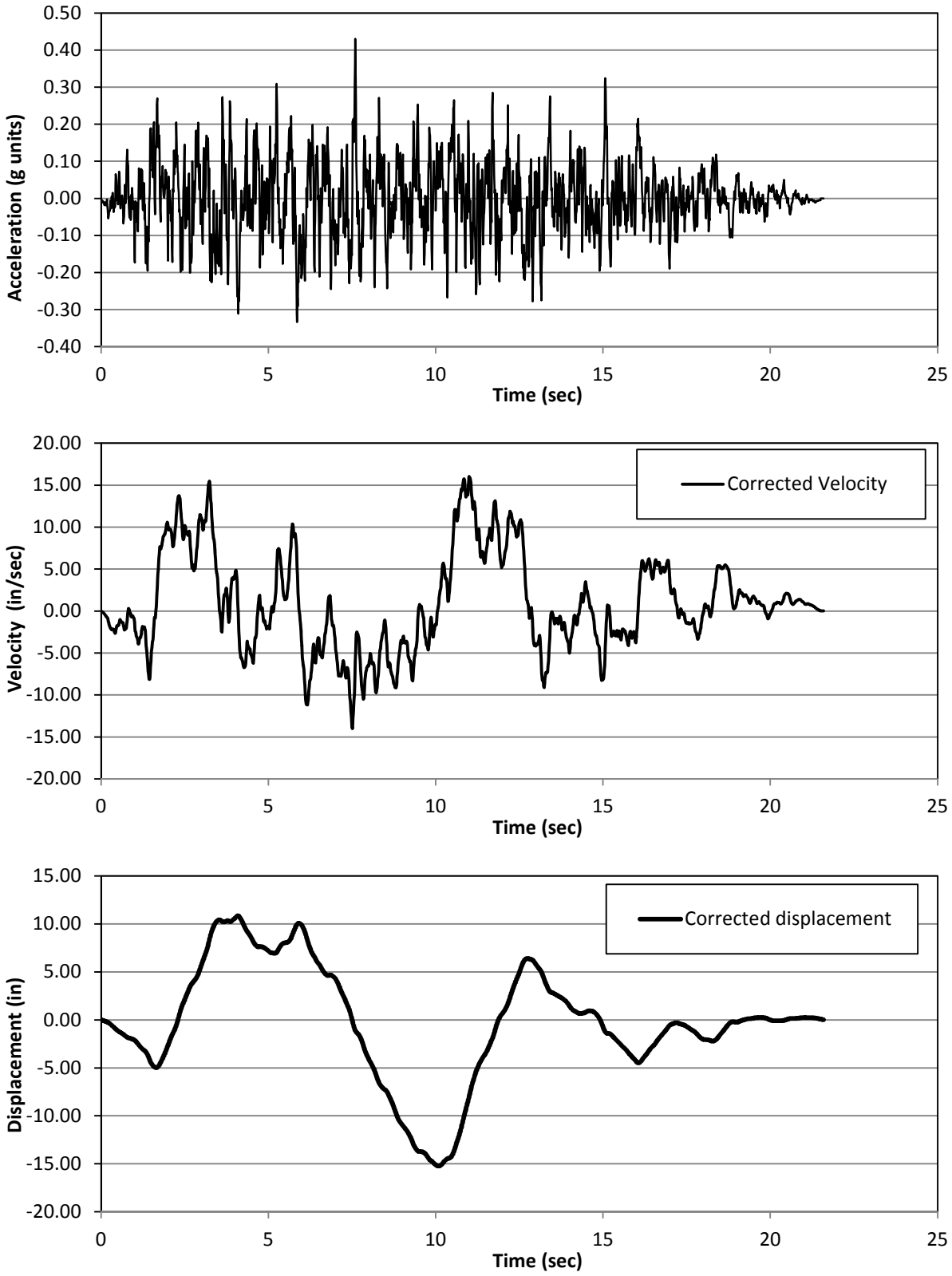

Figure 2-16 Acceleration, velocity and displacement record for seismogram SQK-2

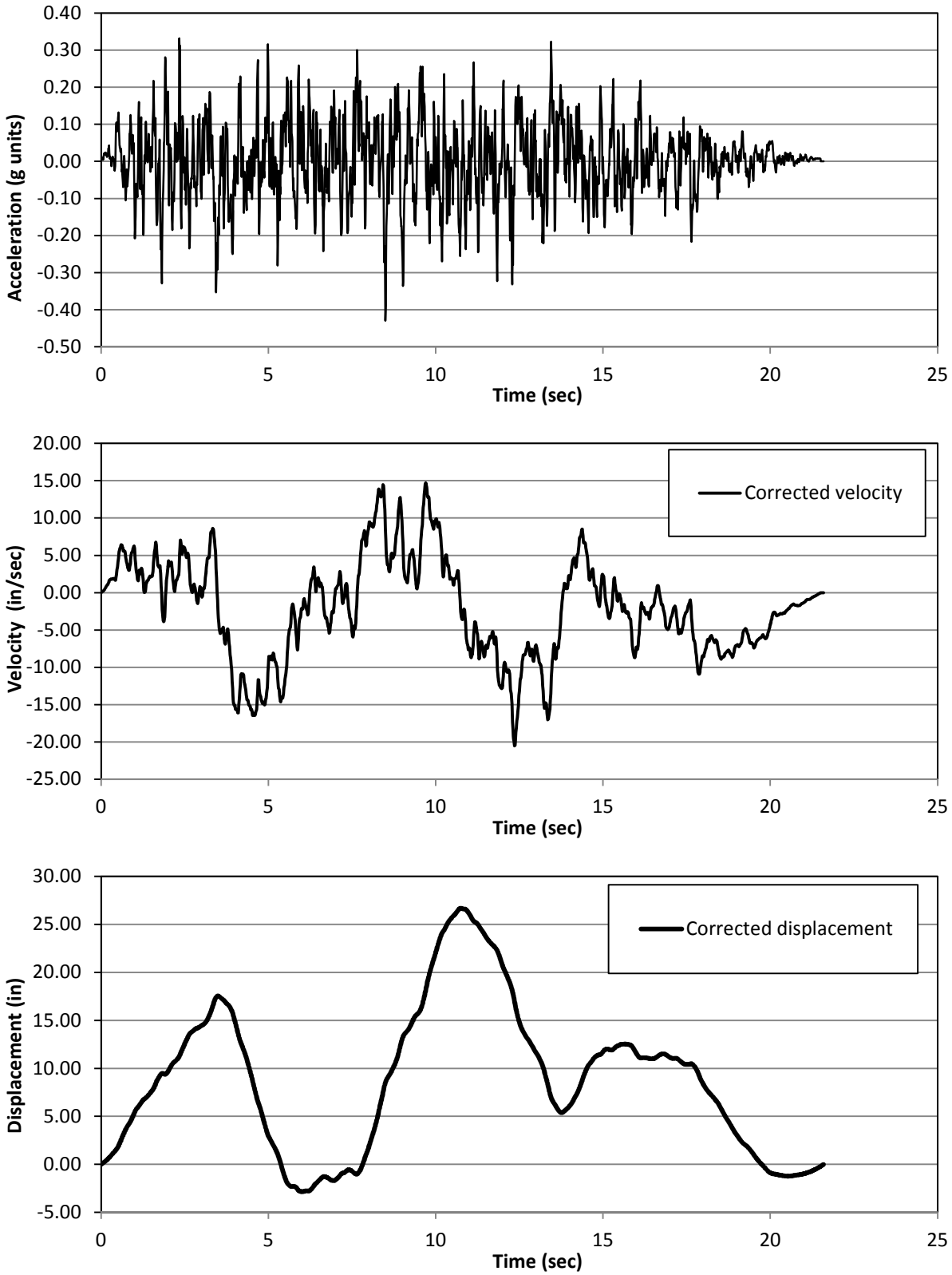

Figure 2-17 Acceleration, velocity and displacement record for seismogram SQK-3

Table 2-9 Correlation coefficient between seismograms generated with SIMQKE-I

Combination	Correlation Coefficient *r*
SQK-1 and SQK-2	-0.0079
SQK-1 and SQK-3	0.0110
SQK-2 and SQK-3	0.0294

After analyzing the features of SIMQKE-I the next conclusions are addressed:

- The input data required for SIMQKE-I is not complex.
- It is necessary to input appropriate duration for the generated seismograms, and that parameter could be estimated using Table 2.3-1 of ASCE 4-98 for an earthquake magnitude and fault distance given by the USGS deaggregation models (U.S. Geological Survey, 2009a).
- The shape of the spectrum from the generated seismograms matches very close with the target spectrum.
- The records of velocity and displacement will need to account for constant of integration to guarantee zero velocity at the end of the record.
- The generated seismograms have statistical independence, which is demonstrated by having a correlation coefficient close to zero.

2.2.2.3 Stochastic seismograms generated by the USGS

The U.S. Geological Survey (USGS) provides artificial acceleration histories appropriate for a site of interest, and those are generated using the software SMSIM_TD, version 2.20, developed by David M. Boore (2000), for the modal Magnitude-Fault distance, M-D, that represent the seismic hazard for the site of interest. This software simulates ground motions based on the stochastic method that Boore (2000) describes as generated ground motions "based on the assumption that the amplitude of ground motion at a site can be specified in a deterministic way, with a random phase spectrum modified such that the motion is distributed over a duration related to the earthquake magnitude and to distance from the source." Documentation about the methodology that SMSIM_TD uses for the generation of acceleration

histories is provided by Boore (2000). The current document focuses on the results of applying this software in the context of evaluating the appropriateness of the generated acceleration histories for linear response history analysis.

Deaggregation models are provided by the USGS for data up to 1996, 2002, and 2008; however, stochastic seismograms are available only for the 2002 deaggregation models (Harmsen, 2010a). Therefore, the stochastic seismograms referred in this document correspond to those generated using the 2002 deaggregation model of the USGS.

According to the documentation provided in the USGS website (2009a), the acceleration histories generated using the stochastic seismograms tool are intended to match their spectral ordinate at a defined period with the spectral ordinate from the maximum considered earthquake (MCE) maps developed by Leyendecker et al. (2000); the latter is referred in this section as the "target spectral acceleration of the stochastic seismograms."

The target spectral acceleration of the stochastic seismograms at a particular period can differ from the spectral acceleration for the same period given by seismic codes such as ASCE 7-98 or ASCE 7-05, because, as stated by Harmsen (2010b), Research Physical Scientist of the USGS, the 2002 deaggregation website "uses a target motion that is in all cases the probabilistic motion;" however, the approach followed by seismic codes such as ASCE 7-98 or ASCE 7-05 might be different, because those codes can include additional factors applicable over the probabilistic code spectral accelerations, and also because such code spectral accelerations can be governed by a deterministic approach instead of a probabilistic one for locations close to a fault region (Harmsen, 2010b). In summary, the target spectral acceleration of the stochastic seismograms can diverge from the spectral acceleration of seismic codes. However, this document will compare the spectra from the stochastic seismograms with the spectrum given by the MCE maps of the American standard ASCE 7-02 (2003), because according to Section C.9.4.1.1 of ASCE 7-02 (2003), USGS (2009a), and Leyendecker et al. (2000), ASCE 7-02 and the stochastic seismograms are both based on the MCE ground motion maps from the 1997 NEHRP Recommended Provisions for Seismic Regulations for New Buildings (FEMA, 1997).

When using the USGS deaggregation models, six stochastic seismograms are generated for the modal magnitude and fault distance that define the seismic hazard of the site of interest. Those six earthquakes are selected from a pool of 60 acceleration histories generated using SMSIM_TD (Boore, 2000); then, a selection procedure described in the USGS website

documentation (U.S. Geological Survey, 2009a) is carried out to select the final six earthquakes. Such procedure is based on the calculation of a factor S_j for each earthquake equal to the weight summation of the logarithm ratios between the spectral ordinate of the generated stochastic seismogram and the spectral ordinates of the MCE maps for the site of interest. Such weight summation is done within a range of periods that varies between 0.2 sec and 1.0 sec. Also, the calculation of this ratio at the period of interest has a weight three times greater than the weight at any other period. The six earthquakes with the smallest values of S_j are reported.

The described selection process has some limitations; for instance, for structures with periods higher than 1.0 sec, the selection of the six stochastic seismograms using the parameter S_j will still be based on the fit between periods of 0.2 sec and 1.0 sec instead of doing the fit in a period region based on the fundamental period of the structure.

Stochastic seismograms were generated for a site with the characteristics described in Table 2-10 in order to evaluate the similarities between the spectra from the stochastic seismograms with the MCE spectrum for the same location according to the American Standard ASCE 7-02 (ASCE/SEI, 2003).

Table 2-10 Location and return period for a site where stochastic seismograms were generated

Parameter	Value
Latitude	39
Longitude	-80
Probability of exceedance	2% in 50 years

The MCE spectrum for the location of interest was developed according to Section 9.4.1.2.6 of ASCE 7-02. The mapped maximum considered earthquake (MCE) 5% damped spectral response acceleration parameter at short periods, $S_{S,}$ and the mapped MCE 5% damped spectral response acceleration parameter at a period of 1sec, $S_{1,}$ were obtained using the software "Seismic Hazard Curves, Response Parameters, and Design Parameters" developed by the U.S. Geological Survey (2009b), and their values are shown in Table 2-11.

Table 2-11 Parameters required to build the MCE spectrum using maps of ASCE 7-02

Parameter	From maps ASCE 7-02 (g units)
S_S	0.166
S_1	0.070

The stochastic maps were analyzed for two different periods of interest, 0.5 sec and 1.0 sec, and the governing modal magnitude, fault distance, epsilon value ε_0 of the scenario that controls the seismic hazard for each period of interest, and the duration of the generated acceleration histories are listed in Table 2-12. The parameter epsilon ε_0 in Table 2-12 is defined by Baker and Cornell (2005) as "the number of standard deviations by which an observed logarithmic spectral acceleration differs from the mean logarithmic spectral acceleration of a ground-motion prediction (attenuation) equation," and it has been included in Table 2-12 for discussion about the closeness of the generated spectra from the stochastic seismograms with the target spectrum. The relation between ε_0 and the spectra of the stochastic seismograms, as reported in the documentation of the USGS website (U.S. Geological Survey, 2009a), establishes that "Best fit is achieved in the cases where the probabilistic motion is not too far from medium motion. This will occur if the modal epsilon or mean epsilon is close to zero."

Table 2-12 Magnitude, distance, epsilon value, and duration of the stochastic seismograms generated for T=0.5 sec and T=1.0 sec.

Parameter	For T = 0.5 sec	For T = 1.0 sec
Magnitude	7.3	7.7
Fault distance (km)	591.7	821.4
ε_0	1.79	1.62
Duration of record (sec)	90	160

Figure 2-18 and Figure 2-19 show the stochastic seismograms generated for T=0.5 sec and T=1.0 sec, respectively. From these plots it can be seen that the duration of the seismograms is different in both cases, and this result is expected, because the magnitude and distance that govern the hazard in both cases is also different. Also it is noticed that the initial time before the ground motion starts is particularly long for both cases.

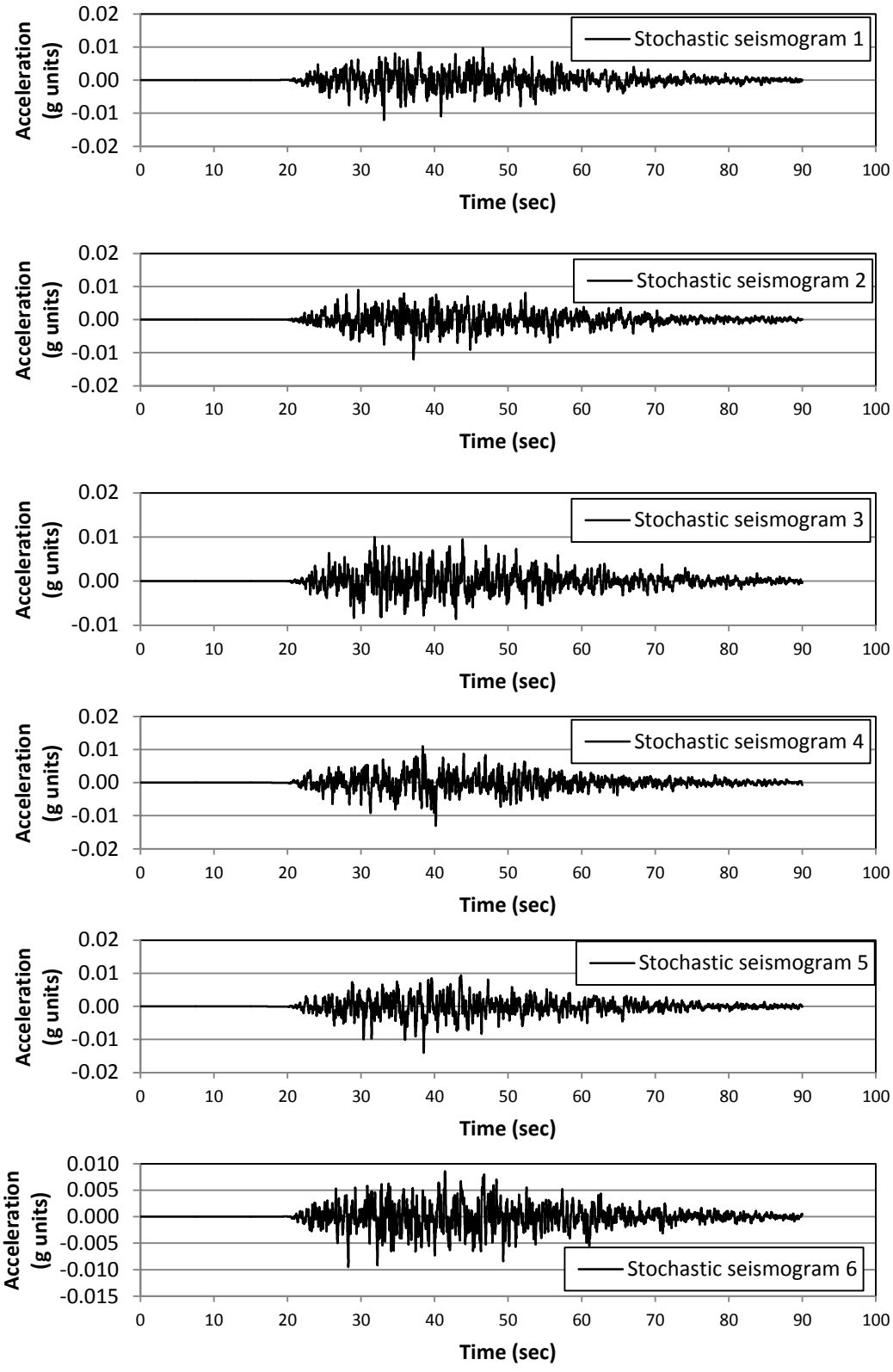

Figure 2-18 Stochastic seismograms generated for the period T = 0.5 sec at a location with latitude 39 and longitude -80

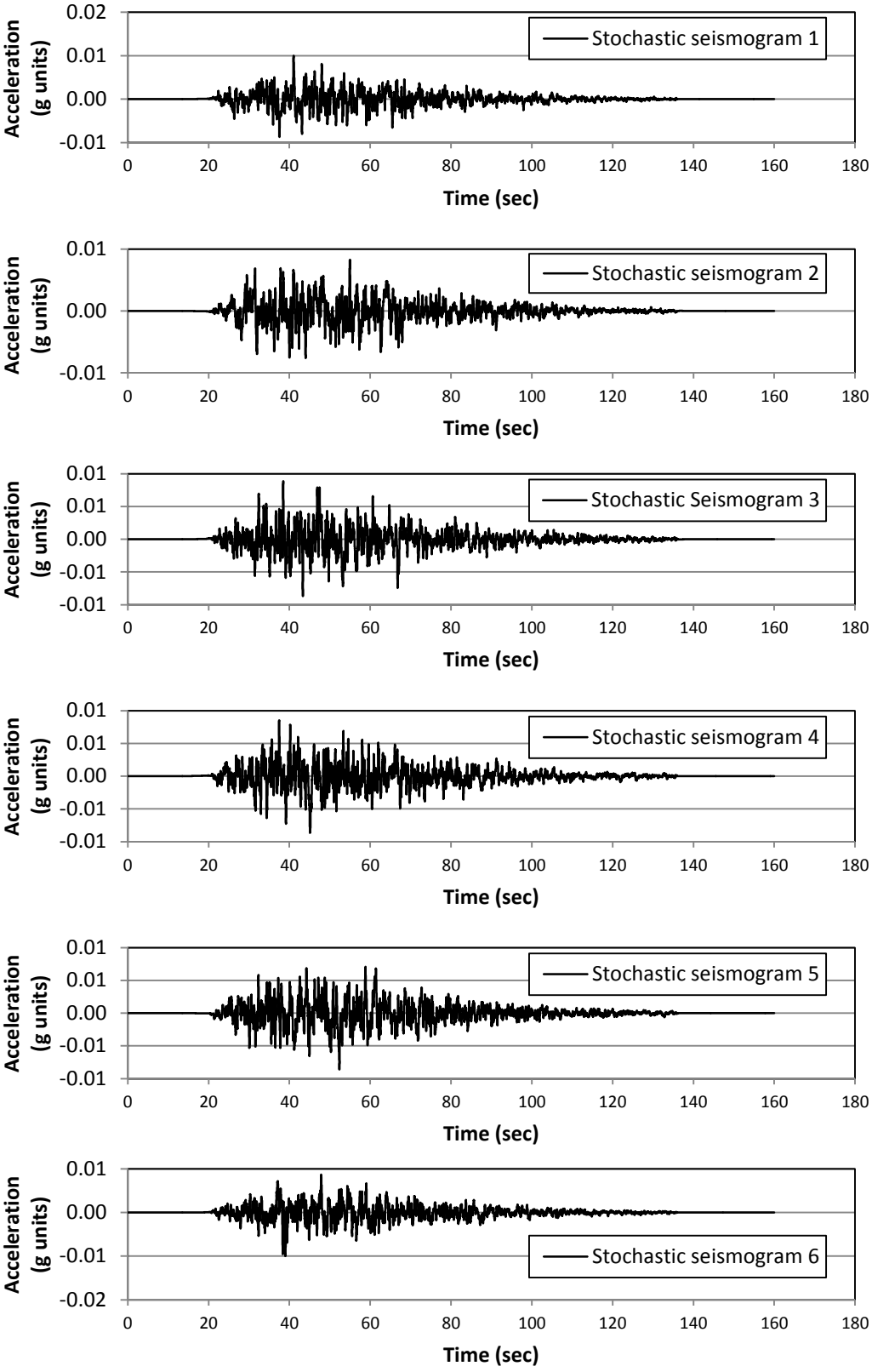

Figure 2-19 Stochastic seismograms generated for the period T = 1.0 sec at a location with latitude 39 and longitude -80

The spectral ordinate at a specified period of the six generated stochastic seismograms is intended to match the spectral ordinate of the target spectrum; however, an exact match is not guarantee because the spectra of the stochastic seismograms are not scaled to match the target acceleration (U.S. Geological Survey, 2009a), and therefore, such scaling has to be done separately by the designer. To illustrate this point, Figure 2-20 shows the spectrum of each stochastic seismogram generated for T=0.5 sec, and it can be seen that the ordinate of those spectra at T=0.5 sec differs considerably from the target acceleration at the same period. Therefore, scaling is necessary, and the resulting scaled spectra are shown in Figure 2-21. The mean of these scaled spectra is shown in Figure 2-22.

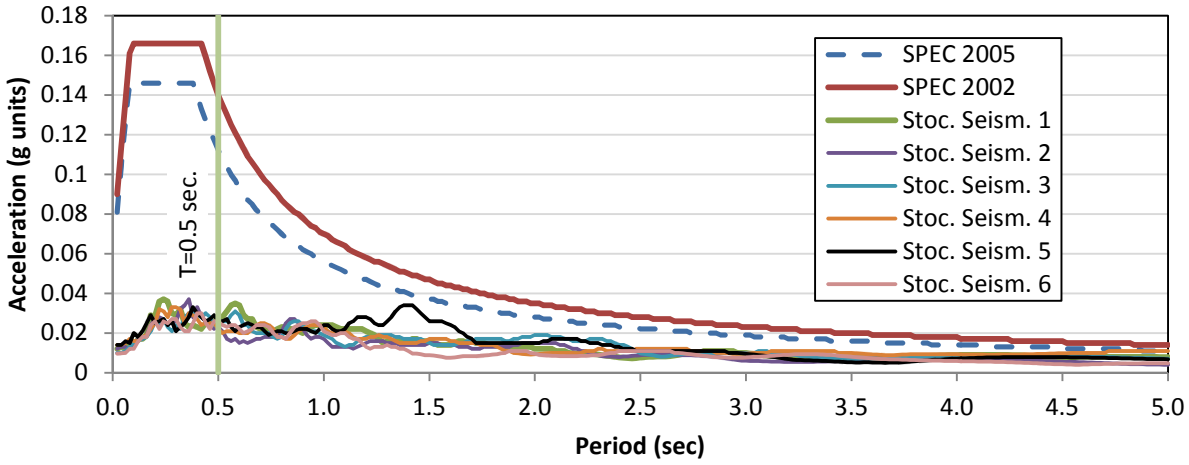

Figure 2-20 Original Spectra of stochastic seismograms for T=0.5 sec

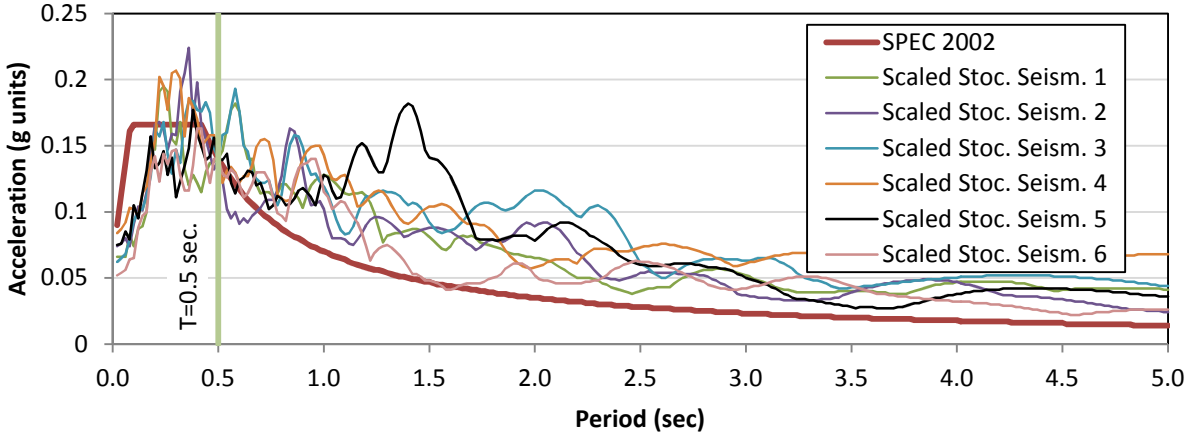

Figure 2-21 Scaled spectra of stochastic seismograms to match target acceleration at T=0.5 sec

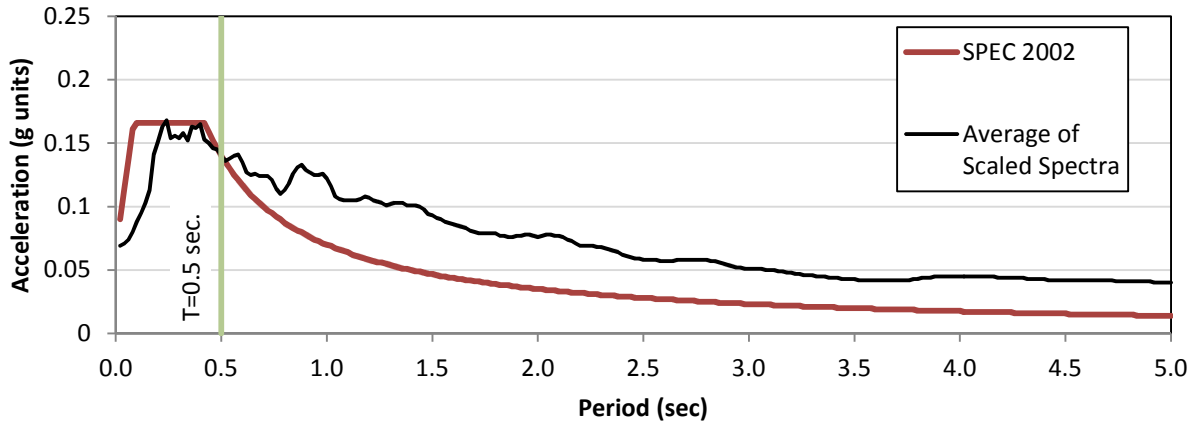

Figure 2-22 Average of scaled spectra from stochastic seismograms for T=0.5 sec

The spectra of the stocastic seismograms generated for a structure with period T=1.0 sec (see Figure 2-19) are plotted in Figure 2-23, and the same spectra scaled to the ordinate of the target spectrum at the period T=1.0 sec is shown in Figure 2-24. Also, the mean of these scaled spectra is shown in Figure 2-25.

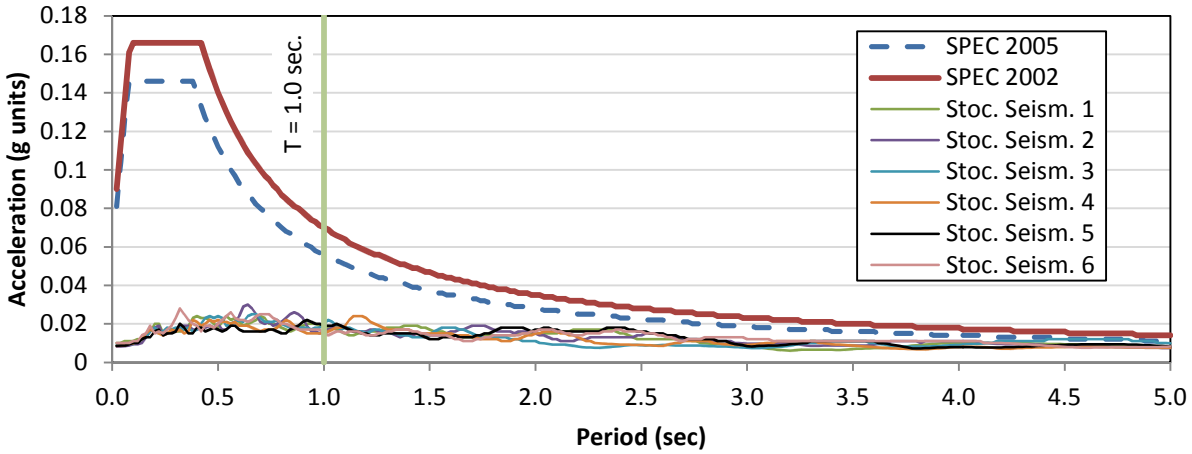

Figure 2-23 Original Spectra of stochastic seismograms for T=1.0 sec

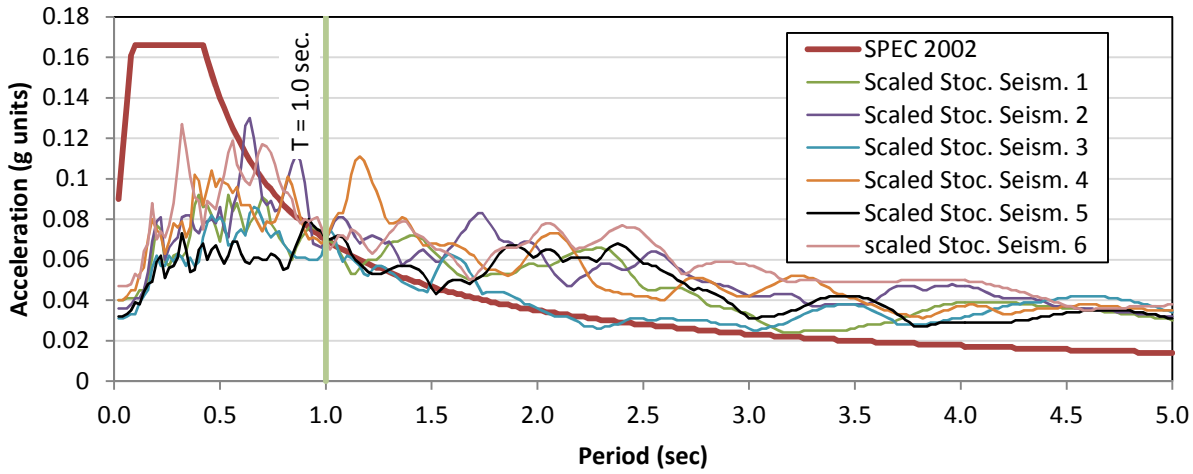

Figure 2-24 Scaled spectra of stochastic seismograms to match target acceleration at T=1.0 sec

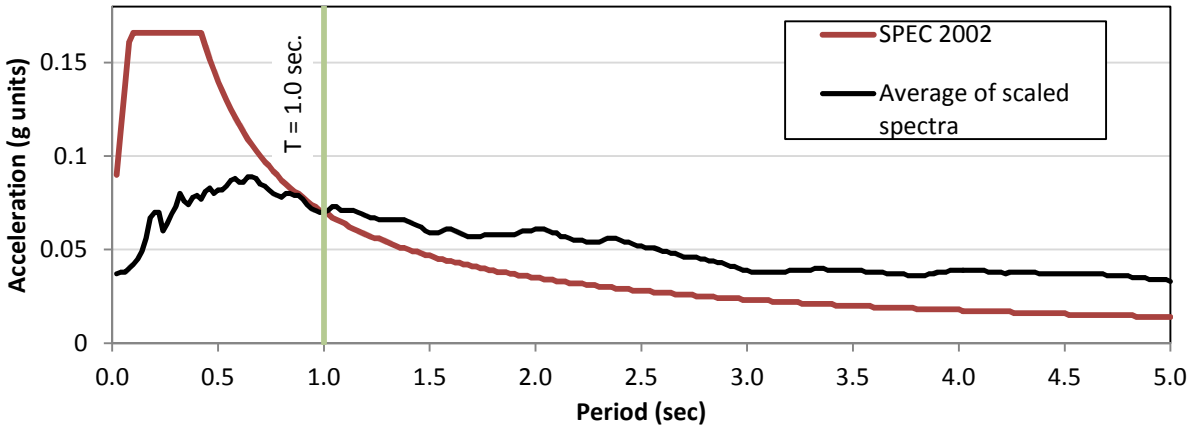

Figure 2-25 Average of scaled spectra from stochastic seismograms for T=1.0 sec

Two aspects can be anlyzed from Figure 2-20 through Figure 2-25: a) the closness of the spectral shape of the original spectra from stochastic seismograms with the target spectrum, and b) the implications of using stochastic seismograms for linear response history analysis. First, it can be seen in Figure 2-20 and Figure 2-23 that the spectral ordinate corresponding to the stochastic seismograms differs a lot from the target spectral acceleration. This result was expected, because as explained it before, a measure of this fit is given by values of ε_0 close to zero; however, the values of ε_0 reported in Table 2-12 are considerably above 0.5, and therefore a good match was not expected.

The use of stochastic seismograms for linear response history analysis has several limitations; for instance, the shape of the average spectrum might not reflect in some cases, as shown in Figure 2-25, the shape of a general spectrum with high accelerations at lower periods and a exponential decrease in spectral accelerations as the period increases. This fact indicates that the generated acceleration histories might not represent the seismic hazard at periods other than the one of interest, which would cause problems in the scaling of those ground motions, because such a scaling procedure requires a good match of the average spectra not only around the fundamental period of vibration but also at a more extense range of periods.

Also, the stochastic seismograms are reported only for the modal scenario Magnitude-Fault distance, M-D; however, more than one scenario M-D might control the seismic hazard for a site, and such additional scenarios will not appear in the stochastic seismograms. Furthermore, the stochastic seismograms can be generated only at the available periods of the 2002 USGS deaggregation models, which are 0.0 sec (PGA), 0.1sec, 0.2 sec, 0.3 sec, 0.5 sec, 1.0 sec, and 2.0 sec; therefore, it will not be possible to generate stochastic seismograms for structures with period different than the ones mentioned. Additionally, the stochastic seismograms using the USGS deaggregation models are based on rock with average shear wave velocity equal to 760 m/s in the upper 30 m for the central eastern United States, CEUS; however, for the western United States, WUS, "the exact NEHRP site class is not specified" (U.S. Geological Survey, 2009a). Therefore, as stated in the USGS website documentation (2009a), "This website does not model variable site conditions such as local soil amplification and attenuation," and its application for types of soil different than the specified one would not be possible. Due to all these limitations it is the opinion of the author that the use of the stochastic seismograms from the USGS deaggregation tools is not appropriate for linear response history analysis.

2.2.3 LRHA using the routine developed by Chapman and the time series generated by the software SIMQKE-I.

The efficiency of the artificial seismograms generated using the routine developed by Chapman as well as of the signals generated by SIMQKE-I was evaluated by analyzing the closeness in structural response results when using any of these two techniques with the results from a response spectrum analysis and from actual records. This analysis does not include the analysis of the USGS stochastic seismograms, because its limitations make it not likely to be applicable for LRHA.

The interstory drifts and interstory shears were calculated in a symmetric eight story building and in a nonsymmetrical twelve story building; both models are described in the Appendix A as Building 1 and Building 2, respectively. The interstory drifts were calculated at the center of mass for Building 1, and they were taken at the intersection of the axis E and 4 of Figure A- 2 for Building 2. The record components used in this analysis correspond to the acceleration histories using Chapman's routine (Ch-1, Ch-2 and Ch-3 as obtained in Section 2.2.2.1), SIMQKE-I (SKQ-1, SQK-2 and SQK-3 as obtained in Section 2.2.2.2), and the original record components used to generate the artificial seismograms from Chapman's routine (A90, B00, and C90 as described in Table 2-6). The loading for both buildings was applied parallel to the Y axis shown in Figure A- 1 for Building 1 and in Figure A- 2 for Building 2. Also, all the acceleration histories were scaled so that their spectrum has the same ordinate as the design spectrum given in Figure 2-4 at the periods 1.72 sec and 2.74 sec for Building 1 and Building 2, respectively. The latter periods correspond to the average of the first period of vibration in the two principal directions, for each building. The average response of the three acceleration records generated with Chapman's routine and the three acceleration records from SIMQKE were compared with the results from a modal response spectrum analysis using the design spectrum given in Figure 2-4 and also with the average response of the scaled record components A90, B00, and C90 of Table 2-5. The modal response spectrum analysis used the Complete Quadratic Combination (CQC) for the modal combination. The interstory drift and interstory shear of Building 1 is presented in Figure 2-26 and Figure 2-27, respectively, and the interstory drift and interstory shear for Building 2 is shown in Figure 2-28 and Figure 2-29, respectively.

It can be seen from Figure 2-26 that the interstory drift using Chapman's routine and SIMQKE yield very similar results than those of a modal response spectrum analysis. This is an expected result because the artificial earthquake signals from Chapman's routine and SIMQKE have a spectrum that matches with the spectrum used in the modal response spectrum analysis. Also, it can be seen in Figure 2-26 that the interstory drifts from both Chapman's routine and SIMQKE are lower than the values obtained using the actual record components. The same behavior described for the interstory drift occurred with the interstory shear as shown in Figure 2-27. This result could be due to the influence in the response of vibration modes other than the fundamental mode. It is possible that the ordinates of the spectrum from the scaled ground motion could be above the ordinates of the spectrum from the signals of Chapman's routine and

SIMQKE, at periods with important contribution to the response. If that is the case, the response parameters (i.e. interstory drift) will be higher when using the scaled actual records than when using the artificially generated spectral matched records.

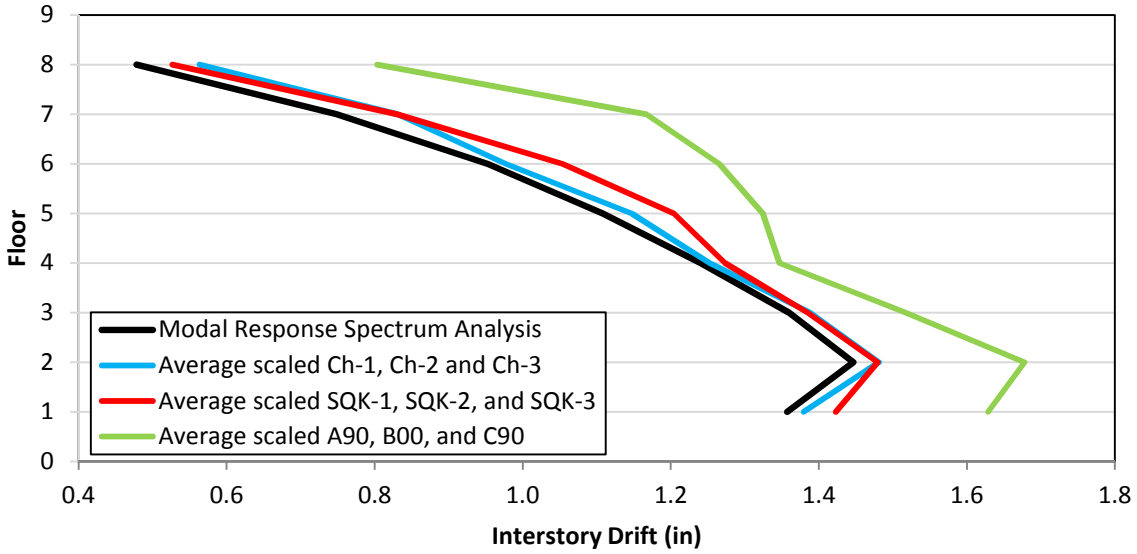

Figure 2-26 Interstory drift in Building 1 using modal response spectrum analysis, artificial accelerograms generated with Chapman's routine (Ch-1, Ch-2, and Ch-3), artificial accelerograms generated with SIMQKE (SQK-1, SQK-2, and SQK-3), and actual acceleration histories (A90, B00, and C90).

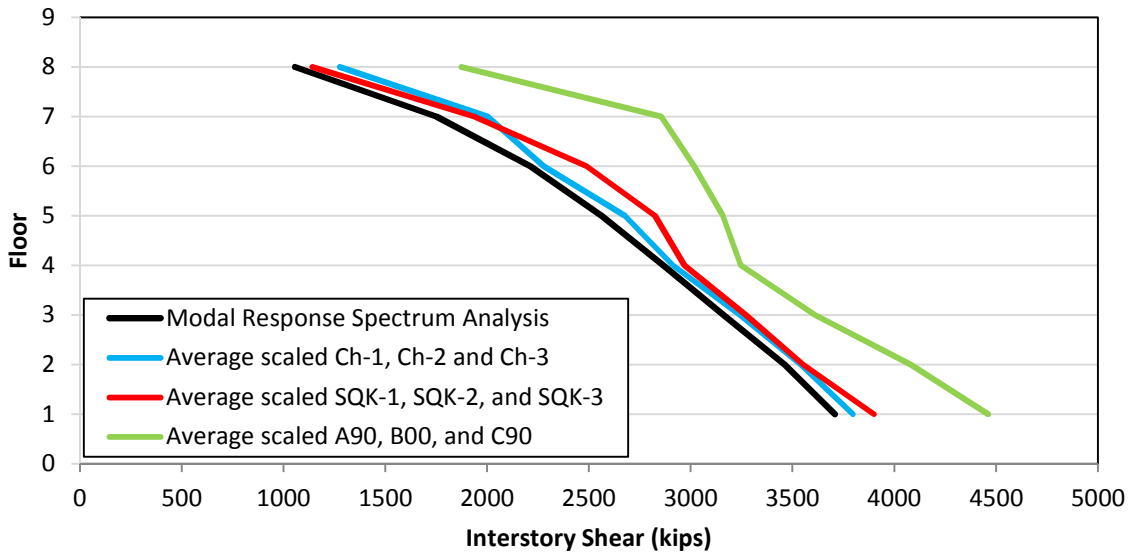

Figure 2-27 Interstory shear in Building 1 using modal response spectrum analysis, artificial accelerograms generated with Chapman's routine (Ch-1, Ch-2, and Ch-3), artificial accelerograms generated with SIMQKE (SQK-1, SQK-2, and SQK-3), and actual acceleration histories (A90, B00, and C90).

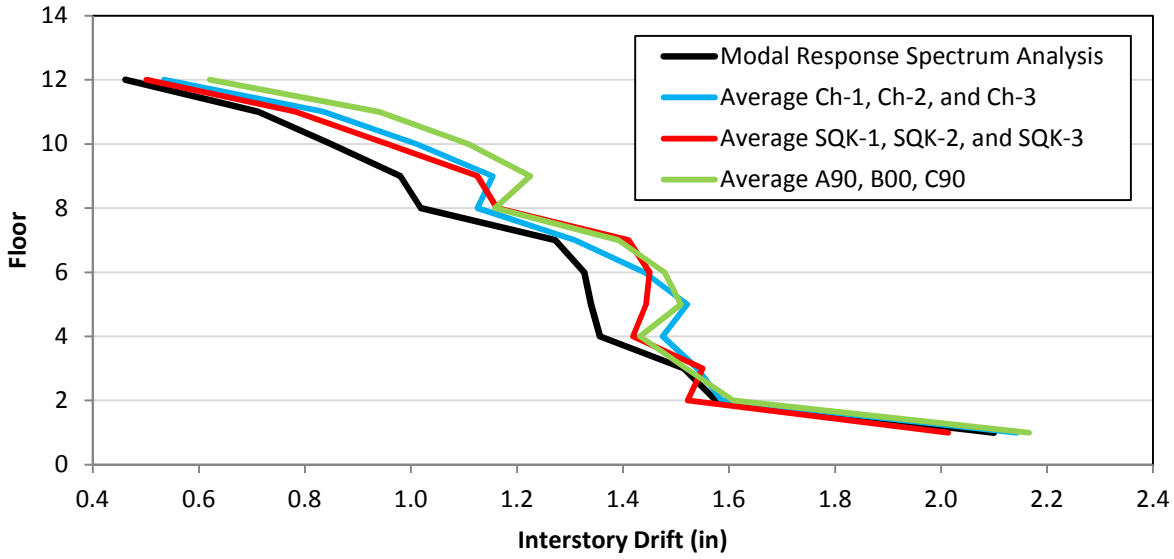

Figure 2-28 Interstory drift in Building 2 using modal response spectrum analysis, artificial accelerograms generated with Chapman's routine (Ch-1, Ch-2, and Ch-3), artificial accelerograms generated with SIMQKE (SQK-1, SQK-2, and SQK-3), and actual acceleration histories (A90, B00, and C90).

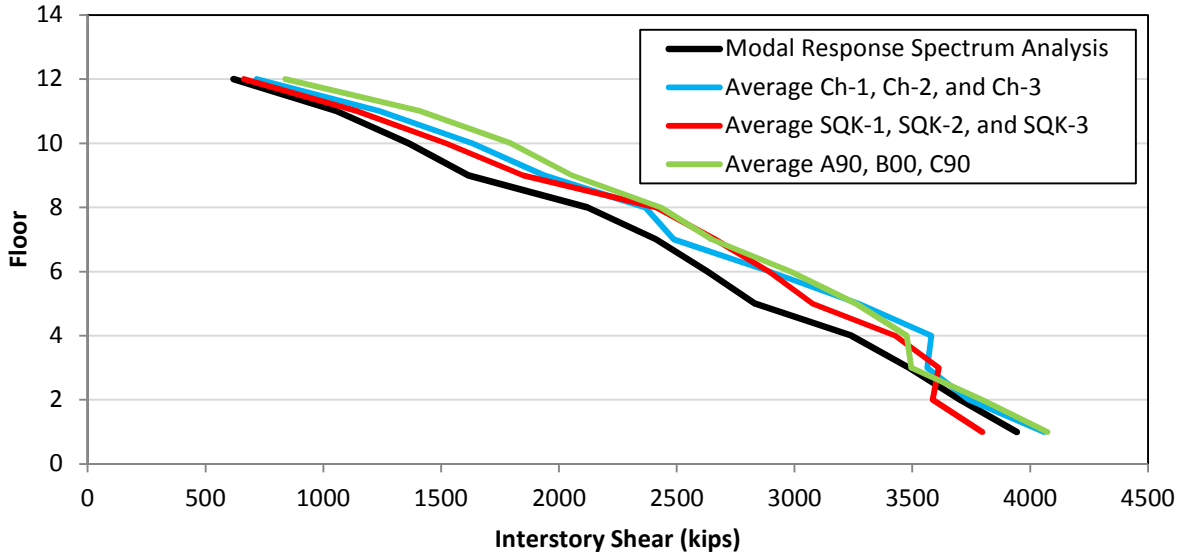

Figure 2-29 Interstory drift in Building 2 using modal response spectrum analysis, artificial accelerograms generated with Chapman's routine (Ch-1, Ch-2, and Ch-3), artificial accelerograms generated with SIMQKE (SQK-1, SQK-2, and SQK-3), and actual acceleration histories (A90, B00, and C90).

From Figure 2-28 it can be noticed that for the case of Building 2, the interstory drifts from Chapman's routine and from SIMQKE are very similar to the values from the actual

acceleration histories; however, they differ slightly from the interstory drifts from a modal response history analysis. Also, for the case of interstory shears in Building 2, as shown in Figure 2-29, the results from Chapman's routine, SIMQKE, actual acceleration histories and modal response spectrum analysis are very similar to each other.

In addition, if looking at Figure 2-26 and at Figure 2-28 or if looking at Figure 2-27 and Figure 2-29, it is remarkable the fact that the results from Chapman's routine and from SIMQKE are closer to the values given by actual records in the case of a nonsymmetrical building (Building 2) than in the case of a symmetrical building (Building 1).

From the analysis of Figure 2-26 through Figure 2-29, it can be concluded that the artificial acceleration histories generated by Chapman's routine and by SIMQKE yield interstory drifts and interstory shears comparable with those given by a modal response spectrum analysis; however, the degree of similarity with the same parameters obtained using recorded acceleration histories could change depending on if the structure analyzed is symmetrical or nonsymmetrical. Finally, the designer should note that the use of several artificial seismograms compatible with a target spectrum will not be efficient, because all of them will predict a similar response, and therefore only one record might be necessary to predict a response compatible with one from a RSA.

The conclusions stated in this section are applicable only for the two buildings analyzed and only to the selected artificial acceleration histories, and more research will be necessary to generalize conclusions.

2.3 Recommendations for selection of earthquakes based on a M-D-SM-ST for code provisions

Based on a literature review of the provisions for the selection of earthquakes from seismic codes other than ASCE 7-10, as well as from the analysis of spectral matched acceleration histories, the following provisions are suggested to be included in future code language of ASCE 7:

- Magnitude and distance appropriate for the site of interest shall be obtained from the deaggregation model provided by the U.S. Geological Survey (2009a). The designer shall consider all the magnitude distance scenarios, M-d, that define the seismic hazard for the site of interest. Modal values M-d from deaggregation are preferred rather than mean values.

- The preferred range of magnitude of the selected earthquakes will be ±0.25 of the target magnitude.
- Near-fault records will be used when the distance from the source given by a hazard analysis is less than 60 km. Use of only near-fault records is preferred for distances less than 20 km.
- Selection of earthquakes should be the same for 2D and 3D analysis.
- Nearly equivalent design response parameters (i.e. base shear or interstory drift) from a modal response spectrum analysis can be obtained if using linear response history analysis with an acceleration record which spectrum matches with the design spectrum.

Chapter 3. SCALING OF GROUND MOTIONS

The scaling and selection of ground motions are typically treated as two separate processes according to the American standard ASCE 7-10 (ASCE/SEI, 2010), because according to this standard, the selection of ground motions is only associated with choosing earthquakes with magnitude, fault distance, source mechanism similar to the ones predicted by a seismic hazard analysis, and the fulfillment of these requirements is independent of the scaling of those ground motions. However, it would be more appropriate to select ground motions so that they would satisfy the current requirements of ASCE 7-10 and that they would also have (after being scaled) a spectrum with shape similar to that given by the design spectrum within a specific range of periods; this way, the selection and scaling of ground motion would be two related procedures.

The scaling of ground motions is discussed in this chapter by including seven different topics as follows:

- Review of scaling procedures in different seismic codes
- Variables that influence the scaling of ground motions
- Scaling procedure if using spectral matched acceleration histories
- New proposal for the selection and scaling procedure
- Example of new suggested method for the selection and scaling of ground motions
- Comparison of scaling procedures using the approach of Charney, the New Zealand Standard (NZS), and the new suggested scaling method
- Differences in the scaling requirements when acceleration histories are intended to be used in linear and nonlinear response history analysis.

The reader is addressed to the Appendix E of this document for explanation of abbreviations not specified within the text.

3.1 Review of scaling procedures

This section will explain in detail the scaling procedure given in the American standard (ASCE/SEI, 2010), which is denoted as ASCE 7-10, a proposed method by Charney (2010a), the method given by the National Building Code of Canada (Canadian Commission on Building and

Fire Codes, 2005), which is denoted as NBCC, the New Zealand Standard (Council of Standards New Zealand, 2004), which is denoted NZS, ATC-63 (ATC, 2008), and other related provisions.

3.1.1 Scaling Procedure given by the American standard ASCE 7-10 (ASCE/SEI, 2010)

ASCE 7-10 states different scaling approaches for structures modeled in two or three dimension. For 2D analysis this standard requires that the average spectra from the scaled arbitrary components of the records to be above the target spectrum within the range of periods between 0.2*T* and 1.5*T,* where *T* is the fundamental period of vibration of the structure. Also, for the case of 3D analysis, it is required to assign scale factors to the ground motions such that the average of the scaled square root of the sum of the square (SRSS) spectrum of each earthquake does not fall below the design spectrum at any ordinate between 0.2*T* and 1.5*T*. The SRSS of each earthquake is obtained as the SRSS of the individual 5 percent damping individual spectrum of each horizontal component. Figure 3-1 and Figure 3-2 show the approach of ASCE 7-10 when the structure analyzed is modeled in 2D or 3D, respectively, when considering three records in the analysis.

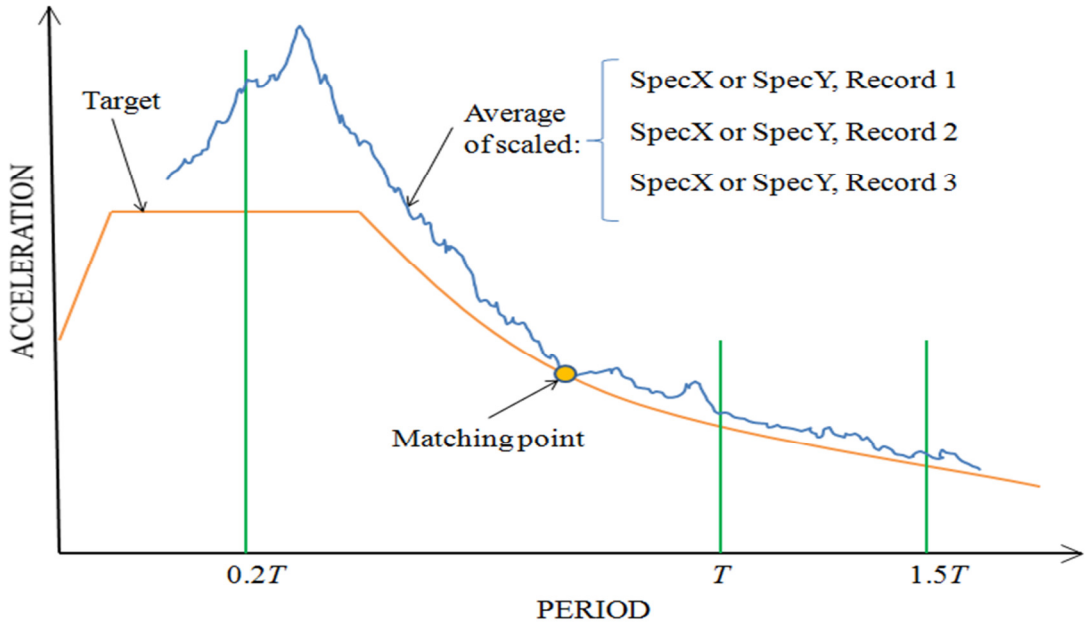

Figure 3-1 Scaling procedure of ASCE 7-10 for structures modeled in 2D

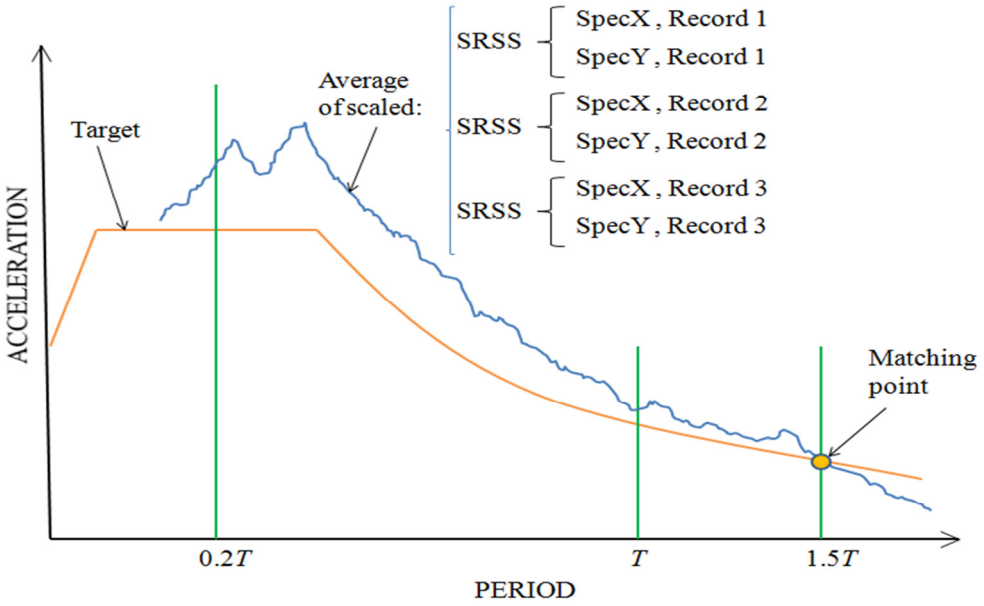

Figure 3-2 Scaling procedure of ASCE 7-10 for structures modeled in 3D

Figure 3-1 and Figure 3-2 show different average scaled spectrum (blue line) and different matching point where such average scaled spectrum is above the target spectrum within the period range of interest. These differences are intended to show that the average scaled spectrum as well as the matching point, are different when following the ASCE 7-10 approach to scale ground motions in structures modeled in 2D or 3D.

3.1.2 Scaling procedure given by Charney (2010a)

Charney (2010a) suggested a more rational scaling procedure so that different designers will come up with the same scale factors when using the same suite of ground motions. The suggested approach has different methodologies when the structure is modeled in 2D or 3D; however, such characteristic of this method was done to reflect the current provisions of ASCE 7-10, although Charney believes that there should be a unique scaling procedure for both 2D or 3D (2009).

For 2D analysis the proposal consists of selecting only one of the components of each record and using its spectrum as the spectral measure of that particular record (see Section 3.2.2 of this document for definition of the spectral measure of a record). Charney mentions that such component can be chosen as the one with peak ground velocity, peak ground acceleration, pseudoacceleration at the fundamental period of vibration, or according to the judgment and experience of the designer. The next step consists of scaling the spectral measure of each

earthquake by a "Fundamental Period Scale factor," denoted hereafter *FPS*, so that the ordinate of the spectral measure of each record (see Section 3.2.2 for definition of spectral measure) and the target spectrum at the fundamental period of vibration of the building would be the same. A different scale factor *FPS* for each record is applied at this stage. Then a second scale factor denoted *SS* (for suite scale factor) is applied so that the average of the scaled spectra does not fall below the design spectrum in the range of periods between 0.2*T* and 1.5*T*. The factor *SS* is the same for all the earthquake records, and the final scale factors for the i^{th} earthquake are calculated by the product of FPS_i*SS.

The procedure is very similar in the case of 3D analysis except that the spectral measure of each earthquake is given by the SRSS of the spectral components of each earthquake. Examples of this technique can be found in Charney (2010a) and Charney et. al. (2010b). Also, two detailed examples of the application of this technique are described in Example 1 and Example 2 of Appendix B considering three and seven ground motions, respectively.

3.1.3 Scaling procedure given by the National Building Code of Canada (Canadian Commission on Building and Fire Codes, 2005)

The commentary of the provisions of the NBCC (Canadian Commission on Building and Fire Codes, 2006) states two main requirements for the scaling of ground motions; the first of them requires the spectral acceleration from the scaled spectrum at the fundamental period *T* to be equal to the one corresponding to the design spectral acceleration at the same period *T*, and the second requirement specifies that for periods below *T*, the ordinates of the scaled spectrum should be equal or higher than those from the design spectrum.

Also it can be noticed that the upper limit of the period range of interest is the fundamental period *T*; however, there is no specification about the lower limit of this range of periods. Another disadvantage of this approach is that it does not explain how to combine the spectra from the two horizontal components of the records and how to combine the spectral measures of all the selected records. Apparently, each record has to be scaled independently.

3.1.4 Scaling procedure given by the New Zealand Standard 1170.5 (Council of Standards New Zealand, 2004)

The approach for scaling ground motions given in Section 5.5 of the New Zealand Standard 1170.5 (Council of Standards New Zealand, 2004), denoted NZS, requires the

calculation of two scale factors denoted k_1 and k_2, and the resulting scale factor for each selected ground motion is the product of these two factors. The purpose of k_1 is "to match the target spectrum over the period range of interest," while the purpose of k_2 is "to ensure that the energy content of at least one record in the family exceeds that of the design spectrum over the target period range." Specific calculation of k_1 and k_2 is explained in the NZS. An additional factor D_1 is considered to check the fitness of the scaled spectrum with the target spectrum. The range of periods considered by the NZS is $0.4T_1$ to $1.3T_1$, where T_1 is defined as the longest period in the direction of interest. Also, the NZS states the limits within the scale factors k_1 and k_2 can change so that the limits reflect if the selected earthquakes are appropriate. Furthermore, the two components of an earthquake are defined as principal and secondary component, and the first of them is defined as the component with the smallest value of k_1 if the value of k_2 is between 1.0 to 1.3; when the value of k_2 is bigger than 1.3 the NZS (Section 5.5.2 (e)) states the procedures to define the principal and secondary components. Also, the NZS states that the scaling procedure should be done for all the directions of interest. An example of the application of this method is shown in the Example 3 of Appendix B.

3.1.5 Scaling procedure given by ATC-63 (ATC, 2008)

Another approach is followed by ATC-63 (ATC, 2008) when describing procedures for the "selection of ground motion record sets for collapse assessment of building structures using nonlinear dynamic analysis (NDA) methods." This technique uses a record scale factor and a set scale factor; the first one is different for each ground motion, and the second one is equal for each record. The record scale factor is obtained so that the peak ground velocity of the record, denoted PGV, is normalized to the median PGV of the unscaled records. Therefore, the record scale factor is equal to the ratio between the median PGV of the unscaled records and the PGV of the record to be scaled. Then, the already scaled records are scaled again "to the point that causes 50 percent of the ground motions to collapse the archetype analysis model being evaluated." This procedure was applied to the 22 far-field records and the 28 near-field records used in ATC-63 (ATC, 2008).

The ATC-63 scaling methodology is applicable to collapse assessment of structures using nonlinear analysis; however, ATC-63 (ATC, 2008) states that the procedure can also be applied to scale records using the maximum considered earthquake, denoted MCE, with the difference that "the median value of the scaled record set need only match the MCE demand at the

fundamental period, *T*, rather than over the range of periods required by ASCE 7/SEI 7-05." This means that the first scale factor would still be the same, but the second factor would change. Also, it is noticed that with this change there is no guarantee in the matching of the MCE at ordinates different than the one given by the fundamental period of vibration. In addition, it is not stated specifically that the target of the scaling procedure could be the spectral ordinate of the design spectrum instead of the one given by the MCE spectrum, although it is not explicitly restricted either. Finally, it should be considered that the purpose of the scaling procedure of ATC-63 (studies regarding collapse prevention) might be different than the purpose of the scaling procedure of ASCE 7-10 for linear response history analysis (design perspective). Therefore, caution is recommended when applying scaling of ground motion procedures with different goals than the ones of ASCE 7-10.

3.1.6 Other scaling procedures

Somerville et al. (1998) described the procedure to generate acceleration histories for performance based design, and they show its application to the Phase 2 of SAC Steel Project. The principle of this scaling technique consisted in modifying the two horizontal components of each record by the same factor, which is calculated so that it minimizes the squared error between the target spectrum and the average spectrum of the two horizontal components of the record over the periods of 0.3 sec and 4.0 sec. Different weights of the squared error are given at different periods, and they are 0.1, 0.3, 0.3, and 0.3 for periods corresponding to 0.3, 1, 2, and 4 sec, respectively. Such scale factor is applied to the three components of the ground motion.

Another technique for the selection and scaling of ground motions was developed by Naeim et al. (2004) using genetic algorithms. One of the interesting features of this technique is that it connects the selection and the scaling of ground motions instead of treating these procedures independently. This technique is capable of evaluating random combination of seven records with random combinations of scaling factors in each record; this way, each selection of records and scale factors has 14 variables. The best selection of records and scale factors is based on the mean squared error between the SRSS of the average scaled spectrum and the target spectrum, and the specific formula for such calculation is provided in Naeim and Alimoradi et al. (2004). Also, this technique is able to control that the average scaled spectrum would be above the target spectrum within the period range of interest (as required by ASCE 7-10), as well as it is capable of choosing the best scale factors if the set of ground motions is a constant instead of a

variable. This approach seems very powerful, because it follows the requirements of ASCE 7-10, and it also allows the user to set up the limits for the scaling factors. Finally, it is mentioned by Naeim and Alimoradi et al. that for design purposes the selection of records should be from a database with records that are associated with magnitude and fault distance appropriate for the site of interest.

The Council on Tall buildings and Urban Habitat provides three procedures to scale ground motions in its document *Recommendations for the Seismic Design of High-rise Buildings* (Willford et al., 2008); all of these procedures apply to time series that have been modified to match a specific target spectrum. The first of these procedures states that each component of the ground motions has to be scaled to a denoted "maximum spectrum." The second procedure states that one of the components should be scaled to the maximum spectrum, and the other component should be scaled to a denoted "minimum spectrum." Finally, the third of these procedures states that one of the components needs to be scaled to the maximum conditional mean spectra while the other component has to be scaled to the minimum conditional mean spectra (Baker and Cornell, 2006). The definition of the maximum and minimum spectra can be found in Huang et al. (2009), which states that the maximum and minimum spectra can be obtained by multiplying the ordinates of a Design Basis Earthquake by the factors F_H and $1/F_H$, respectively. The calculation of the factor F_H is specified in the same reference.

3.2 Variables that influence the scaling of ground motions

The identification of the variables that influence the scaling of the ground motion is the first step to analyze the convenience of the current scaling procedure of ASCE 7-10, and the discussion of such variables will guide the reasoning of suggestions for future editions of this standard. The variables to be studied are:

- Number of earthquakes
- Spectral measure of an earthquake to be compared with the target spectrum
- Treatment of the two components of an earthquake for 2D and 3D analysis
- Spectral ordinate of scaled earthquakes at the fundamental period of vibration of the building
- Limits in the values of the scale factors
- Identification of period at which the 90% of the mass is reached
- Range of periods of interest

- Differences in the scale factors obtained for the same set of ground motions
- Set of periods where any required spectrum is calculated
- Point of matching of the average spectral measure of all the selected earthquakes and the target spectrum

3.2.1 Number of earthquakes

The required number of earthquakes for analysis needs to overcome the uncertainties associated with the physical variability of earthquakes as well as the sensitivity of linear response history analysis (LRHA) with even small differences in the characteristics of the ground motions (Canadian Commission on Building and Fire Codes, 2006). The minimum number of records used in different codes is shown in Table 3-1, and it can be noticed that a minimum of three earthquakes is required in most of the codes analyzed.

Table 3-1 Minimum number of records required by different seismic codes

Standard	Minimum number of records
American standard (ASCE 7-10)	3, for using envelope response of the scaled selected records 7, for using average response of the scaled selected records
National Building Code of Canada (NBCC)	not specified
Seismic Analysis of Safety-Related Nuclear Structures (ASCE 4-98)	1
New Zealand Standard (NZS)	3
Eurocode 8 (EC8)	3
Mexican standard (MXS)	4

The criterion to select the number of earthquakes for analysis should have additional clarifications depending if the selected ground motions are: a) recorded or simulated earthquakes or b) artificial earthquakes. As mentioned in Chapter 2 simulated records correspond to acceleration histories generated by simulation of the source and travel path mechanisms, and artificial records are those acceleration histories generated or modified so that their spectrum matches closely with a defined target spectrum (Gomes et al., 2006). In the case of using recorded or simulated records the latter could be treated as actual recorded motions for the purpose of selecting the number of records for analysis.

Moreover, it will be convenient to relate the selection of records using parameters such as magnitude, fault distance, source mechanism and soil type (M-D-SM-ST) predicted by a hazard analysis with the closeness between the spectral shape of the record and the target spectrum. This connection can be done by selecting first the number of actual earthquake records *m* desired for the analysis, then going to an earthquake database and choose a number *n* of earthquakes records with similar characteristics than those M-D-SM-ST predicted for the site of interest so that $n>m$. Finally, from the set of *n* earthquakes, it will be chosen the *m* earthquakes with best spectrum matching to the target spectrum. A suggested procedure to define the number of earthquakes *n* is to multiply the desired number of earthquakes *m* by 1.5 and approximate any decimal part to the next integer. Table 3-2 shows how this suggestion applies to a different number of records desired for analysis; for instance, if 7 records are desired for analysis, then 11 records with similar properties M-D-SM-ST have to be chosen from an earthquake database.

Table 3-2 Suggested number of earthquakes with similar parameters M-D-SM-ST (*n*) according to the number of records desired for the analysis (*m*)

Number of actual earthquake records desired for analysis (*m*)	Number of earthquake records with similar M-D-SM-ST required for analysis (*n*)
3	5
5	8
7	11

3.2.2 Spectral measure of an earthquake to be compared with the target spectrum

The "spectral measure of a record" is defined as the measure used to combine the spectrum from each of its horizontal components; for instance, the spectral measure of a record could be given by the geometric mean, by the average, by the square root of the sum of the squares (SRSS), or by the envelope of the spectrum from each horizontal component. Also, the spectral measure of a set of records, denoted here as "combined spectral measure," is defined as the combination of the spectral measure from each record; for instance, the combined spectral measure of a set of records could be given by the average, by the SRSS, or by other estimations of the individual spectral measures of each record. The definitions of the spectral measure of a record and the spectral measure of a set of records (or combined spectral measure) has been

given in this section, because those definitions are frequently used in guidelines for the scaling of ground motions; for instance, the combined spectral measure is usually the parameter compared with the target spectrum.

In the case of ASCE 7-10 the combined spectral measure is defined as the average of the already scaled spectral measures from each record, and this definition applies for structures modeled either in 2D or 3D. Also, for ASCE 7-10 the spectral measure of each earthquake is defined as the SRSS of the individual spectra of the horizontal components if the structure is modeled in 3D, but it is equal to any of the two spectral components if the analysis is done in 2D. The following will explore the convenience of using the SRSS as the spectral measure for each record.

The appropriateness of using the SRSS as the spectral measure of a record using ASCE 7-10 is questionable, because other spectral measures, such as the geometric mean, the average, or the envelope of the spectra from the horizontal components, might be more adequate. In fact, the most appropriate spectral measure should be given by the same rule that was used to treat the two components of an earthquake when developing attenuation laws and code seismic maps. ASCE 7 uses maps developed using attenuation models based in some cases in an arbitrary component or in the geometric mean of the component in other cases (Baker and Cornell, 2006); therefore, inconsistencies will arise when using a different combination rule such as the SRSS. Moreover, the same inconsistency would occur for the case where an arbitrary component is used as the spectral measure of an earthquake; however, for this case Baker and Cornell (2006) suggested three methods to transform the results using the arbitrary component in appropriate results as if the geometric mean had been used in the analysis.

Since the use of the geometric mean, denoted hereafter geomean, as the spectral measure of a record seems to be more appropriate than the SRSS in terms of consistency with code maps, an analysis is presented next to evaluate the differences in the scale factors obtained using these two techniques as the spectral measures of each record. Two sets of ground motions, denoted Set 1 and Set 2, were analyzed; the first set consists of the three records shown in Table 2-6, while the second set has the seven records presented in Table B- 3 of Appendix B. In both cases the code spectrum was given by the information presented in Table 2-5 and Figure 2-4, and the scale factors were obtained for different periods using the method suggested by Charney (2010a) (see Section 3.1.2 of this document for explanation of Charney's methodology). The scale

factors for the first set of records were obtained using routines developed in the software Mathcad (Parametric Technology Corporation, 2007), but all those factors were checked with the ones given by the software EQTools (Charney and Syed, 2004, 2010). In the case of the set with the seven records, the scale factors were generated with EQTools directly, but they were checked with routines developed in Mathcad at specific periods. The same set of records was used to calculate the scale factors at all the periods analyzed, although this assumption implies that the same set of records can represent the seismic hazard at all the analyzed periods, which in reality might not be realistic, because structures with different fundamental periods might be governed by different seismic hazard scenarios, which would turn into different sets of ground motions for different periods.

The scale factors obtained for Set 1 when using the SRSS and the geomean as the spectral measures of each record are shown in the last three columns of Table 3-3 and Table 3-4, respectively, and the ratios of the scale factors using these two spectral measures are presented in Table 3-5. The fundamental period scale factor (*FPS*) and the set scale factor (*SS*) suggested by Charney (see Section 3.1.2 of this document for definition of *FPS* and *SS*) have also been included in Table 3-3 and Table 3-4, and those factors are shown to explain the differences in the scale factors when using the SRSS or the geomean as the spectral measure of each record. The maximum difference between the scale factors from Table 3-3 and Table 3-4 and their respective values using EQTools was 2.83%. Such difference is expected to be due to different sets of periods used to compute the response spectrum in EQTools and in the routine developed in Mathcad.

Figure 3-3 shows simultaneously the scale factors from using both spectral measures of an earthquake: the SRSS and the geomean (in this figure SF accounts for scale factor). Also Figure 3-4 shows the ratio between the scale factors calculated using the SRSS and the geomean as spectral measure of each record. By observation of Table 3-3, Table 3-4, and Figure 3-3, it can be seen that the scale factors obtained when using the SRSS as the record spectral measure are smaller than when using the geomean. Additionally, Table 3-5 and Figure 3-4 show that the ratio between the scale factors obtained using the SRSS and the geomean as the spectral measures of each record vary between 0.50 and 0.75.

Table 3-3 Scale Factors for the three records of Set 1 using the SRSS as the spectral measure of each record

Period (sec)	*FPS* factor Record A	*FPS* factor Record B	*FPS* factor Record C	*SS* factor	Scale Factor Record A	Scale Factor Record B	Scale Factor Record C
0.50	0.974	0.612	0.86	1.103	1.074	0.675	0.949
1.00	0.664	0.788	0.912	1.161	0.771	0.914	1.058
1.50	0.488	0.951	1.195	1.067	0.519	1.013	1.273
2.00	0.539	0.826	0.967	1.187	0.64	0.981	1.148
2.50	0.453	0.681	1.415	1.122	0.507	0.762	1.583
2.74	0.407	0.712	1.31	1.187	0.481	0.843	1.55
3.00	0.36	0.777	1.146	1.271	0.458	0.987	1.457
3.50	0.31	0.967	1.328	1.362	0.422	1.316	1.808

Table 3-4 Scale Factors for the three records of Set 1 using the Geomean as the spectral measure of each record

Period (sec)	*FPS* factor Record A	*FPS* factor Record B	*FPS* factor Record C	*SS* factor	Scale Factor Record A	Scale Factor Record B	Scale Factor Record C
0.50	1.398	0.929	1.263	1.074	1.501	0.998	1.356
1.00	0.989	1.115	1.348	1.141	1.128	1.272	1.538
1.50	0.93	1.346	1.695	1.078	1.003	1.451	1.828
2.00	0.946	1.181	1.641	1.129	1.068	1.333	1.852
2.50	0.789	0.963	2.331	1.086	0.857	1.046	2.531
2.74	0.735	1.007	2.062	1.162	0.854	1.17	2.396
3.00	0.635	1.099	1.646	1.429	0.908	1.57	2.353
3.50	0.55	1.382	1.889	1.53	0.841	2.113	2.889

Table 3-5 Ratio of scale factors for Set 1 using the SRSS to the scale factors using the Geomean as the spectral measure of each earthquake

Period (sec)	Record A	Record B	Record C
0.50	0.72	0.68	0.70
1.00	0.68	0.72	0.69
1.50	0.52	0.70	0.70
2.00	0.60	0.74	0.62
2.50	0.59	0.73	0.63
2.74	0.56	0.72	0.65
3.00	0.50	0.63	0.62
3.50	0.50	0.62	0.63

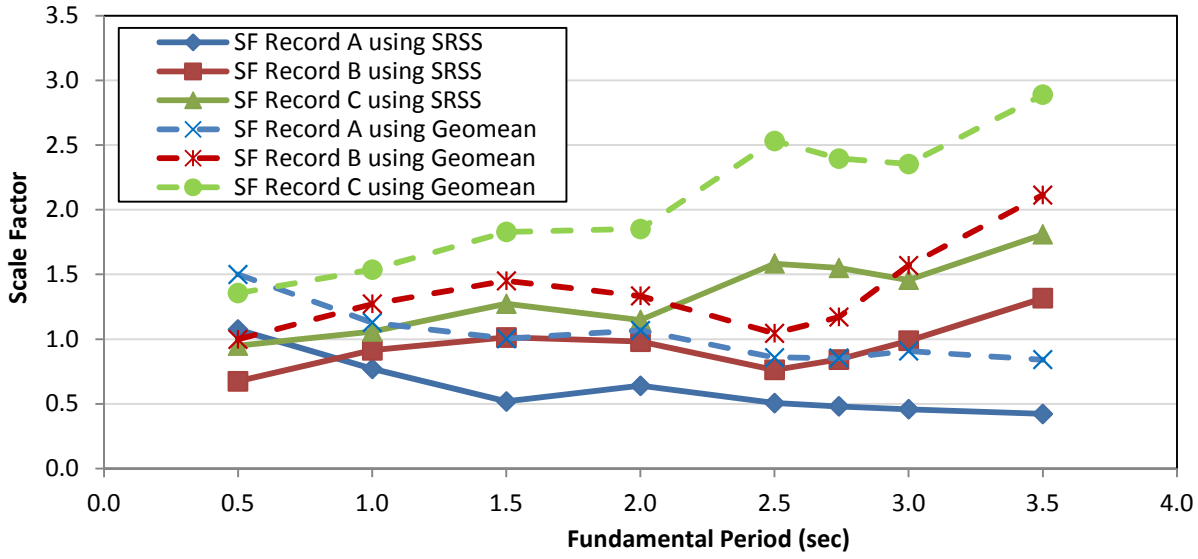

Figure 3-3 Scale Factors for the three records of Set 1 using the SRSS and the geomean as the spectral measure of each record, and using an arithmetic scale for the scale factors

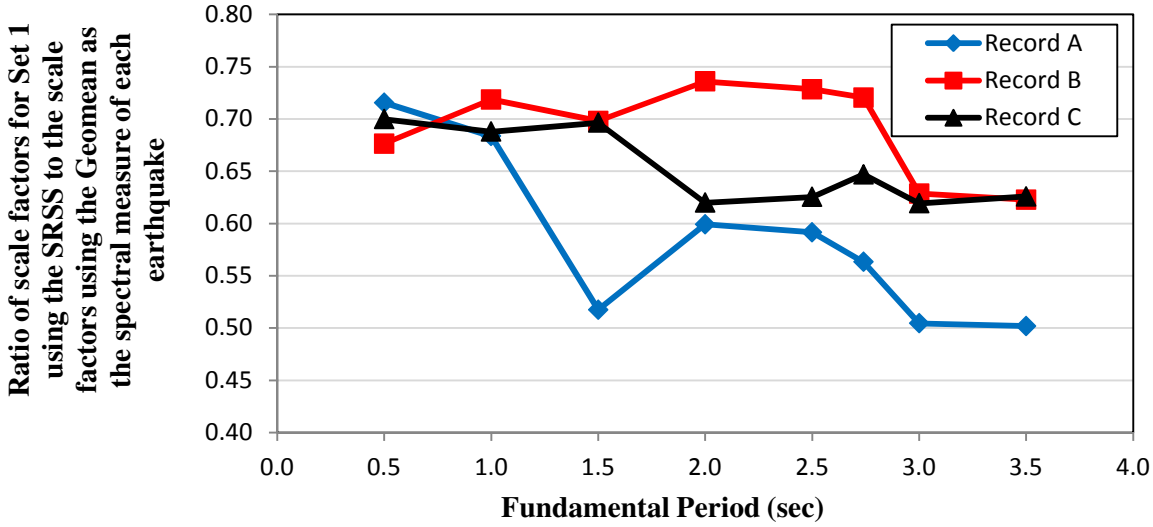

Figure 3-4 Ratio of scale factors for Set 1 using the SRSS to the scale factors using the Geomean as the spectral measure of each earthquake

The reason why the scale factors obtained using the geomean as the spectral measure of a record are higher than those when using the SRSS can be explained by analyzing the two scale factors *FPS* and *SS* used in Charney's methodology (2010a) (see Section 3.1.2 of this document

for definition of these factors). The scaling methodology proposed by Charney obtains the scale factors for each record by doing the product of their respective factors *FPS* and *SS*, and therefore the differences in the scale factors using the geomean or the SRSS as the spectral measures of each record need to be analyzed in each of these factors.

It is expected that the *FPS* factor using the SRSS will be smaller than the *FPS* factor when using the geomean, because it is always true that the SRSS of two numbers is higher than their geomean; therefore, the curve defining the SRSS of the spectrum from each horizontal component of a record will always be above the curve defined by the geomean of the spectrum from the same horizontal components. Both curves are defined hereafter as "SRSS spectrum curve" and "geomean spectrum curve." Then, if it is assumed that the SRSS spectrum curve and the geomean spectrum curve are both above the design spectrum, it is expected that the *FPS* factor in both cases would be a positive number less than 1.0. However, because the SRSS spectrum curve is at a further distance from the design spectrum than the geomean spectrum curve, it is expected that the SRSS spectrum will need a stronger reduction than the geomean spectrum when scaling to the ordinate of the design spectrum at a particular period. Therefore, in this case the *FPS* factor applied to the SRSS spectrum curve of a record will be smaller than that *FPS* factor applied to the geomean spectrum curve.

Also, if it is assumed that the SRSS and the geomean spectrum curves are both below the design spectrum, it is expected for this case that the *FPS* factors will be bigger than 1.0. Then, because the SRSS spectrum curve would be closer to the design spectrum than the geomean spectrum curve, the *FPS* factor for the SRSS spectrum curve will be smaller than that for the geomean spectrum curve. This way, it is concluded that regardless of the matching period, the *FPS* factor will be higher when using the geomean as the spectral measure of a record than when using the SRSS. This conclusion is confirmed if comparing the *FPS* factor of records A, B, and C in Table 3-3 and in Table 3-4 where any of the *FPS* factors of Table 3-3 is smaller than its respective *FPS* factor in Table 3-4.

In the case of the set scale factor *SS* of the method proposed by Charney, it is unpredictable if this factor using the average of the SRSS spectra would be higher or lower than the same factor when using the average of geomean spectra. This unpredictability is because the curve defining the average of the spectrum using each spectral measure (SRSS or geomean) is different and then the matching point (point of the average scaled spectrum closer to the target

spectrum within the period range of interest) to satisfy the requirement of ASCE 7-10 of having such average curve above the design spectrum within a period of interest will also be different. For instance, it can be seen in Table 3-3 that for T=0.5 sec the SS factor (1.103) is higher than its respective value in Table 3-4 (1.074); however, the opposite case occurs for T=3.5 sec because the SS factor from Table 3-3 (1.362) is lower than its respective value in Table 3-4 (1.530).

Moreover, Table 3-3 and Figure 3-3 show how the magnitude of a scale factor changes for structures with different periods of vibration; for instance, the scale factor of the Record A using SRSS is equal to 1.074 at T=0.5 sec and 0.422 at T=3.5 sec. The case where a scale factor is close to 1.0 is preferable, because it would imply almost no modification of the intensity of the record (the designer should be aware that a scale factor that modifies equally the ordinates of the complete accelerogram does not change its characteristics of frequency content or duration); this way, the record A would be more appropriate for scaling purposes for a structure with period T=0.5 sec, instead of a structure with period T=3.5 sec. Therefore, it can be concluded for this particular case that the same ground motions might not be equally useful for scaling purposes for structures with different fundamental periods of vibration, and this statement is based on the magnitude of the amplification or deamplification of the characteristics of the original record.

Also, the designer should consider that a better measure of the amplification or deamplification of a record can be done when using a logarithmic scale in the vertical axis of Figure 3-3 instead of an arithmetic one, because the first case can represent equal magnitude of record modification for scaling factors equal to SF and 1/SF (where SF accounts for scaling factor), while the arithmetic scale cannot do that. This fact shows that scale factors equal to 3.0 and 0.33 are equivalent in the sense that the first implies an amplification of 3 times while the second implies a reduction of 3 times. Figure 3-5 shows the same data of Figure 3-3 but using a logarithmic scale in the vertical axis, and the magnitude of the modification of a record is given by the distance between the scale factors to the horizontal line where the scale factor is equal to 1.0. Also, Figure 3-5 shows the limits in the scale factors SF given by the NZS (the limits refer to the factor k_1 as explained in Section 3.2.5 of this document) which are SF=0.33 and SF=3.0.

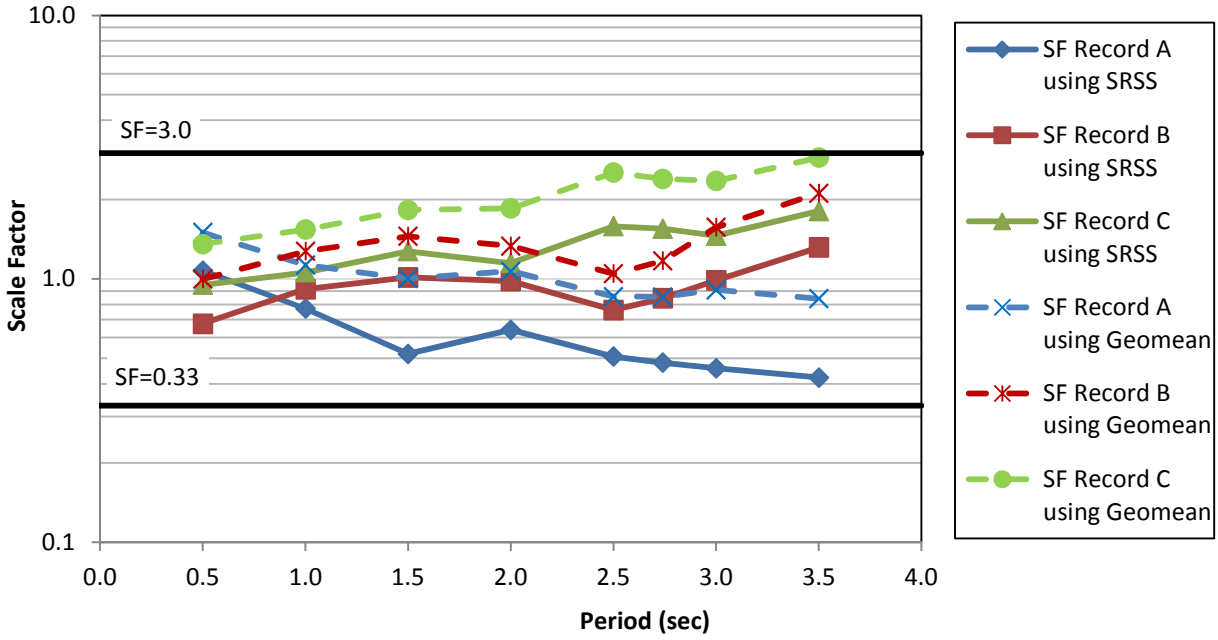

Figure 3-5 Scale Factors for the three records of Set 1 using the SRSS and the geomean as the spectral measure of each record, and using a logaritmic scale for the scale factors

Similar information was obtained for the second set of ground motions (7 records), which has scale factors that are presented in Table 3-6 for the case of using the SRSS as the spectral measure of these records and in Table 3-7 for the case of using the geomean as the spectral measure. Also, Table 3-8 shows the ratio of the scale factors using the SRSS to the scale factors using the geomean, and it can be seen that all the ratios are less than one, which indicates that the scale factors using the SRSS are smaller than the scale factors when using the geomean. The fact that the scale factors using the SRSS are smaller than those when using the geomean is confirmed in Figure 3-6 where the scale factors from both spectral measures (SRSS and geomean) using a logarithmic scale have been plotted together.. Also, Figure 3-7 shows the ratios of the scale factors described in Table 3-8, and it can be seen that those ratios vary between 0.61 and 0.74.

Table 3-6 Scale Factors for the seven records of Set 2 using the SRSS as the spectral measure of each record

Record	Period (sec)						
	0.5	**1.0**	**1.5**	**2.0**	**2.5**	**3.0**	**3.5**
A	2.871	1.537	1.445	1.407	2.632	3.561	4.980
B	0.919	1.474	2.008	2.583	3.095	3.766	3.773
C	1.333	1.386	1.597	1.143	1.721	1.430	1.664
D	1.351	1.006	0.668	0.680	0.812	0.838	0.820
E	3.019	2.199	1.813	1.174	0.998	0.920	1.088
F	0.827	0.534	0.426	0.382	0.407	0.601	0.605
G	1.558	0.689	0.442	0.326	0.250	0.325	0.399

Table 3-7 Scale Factors for the seven records of Set 2 using the Geomean as the spectral measure of each record

Record	Period (sec)						
	0.5	**1.0**	**1.5**	**2.0**	**2.5**	**3.0**	**3.5**
A	4.082	2.281	2.041	2.162	3.712	5.414	7.687
B	1.336	2.080	2.889	3.482	4.378	5.610	5.482
C	1.956	2.029	2.252	1.832	2.810	2.164	2.377
D	1.912	1.432	0.960	1.042	1.145	1.282	1.279
E	4.271	3.078	2.577	1.583	1.420	1.409	1.625
F	1.192	0.774	0.604	0.562	0.633	0.909	0.865
G	2.336	0.964	0.678	0.437	0.358	0.485	0.585

Table 3-8 Ratio of scale factors for Set 2 using the SRSS to the scale factors using the Geomean as the spectral measure of each earthquake

Record	Period (sec)						
	0.50	**1.00**	**1.50**	**2.00**	**2.50**	**3.00**	**3.50**
A	0.70	0.67	0.71	0.65	0.71	0.66	0.65
B	0.69	0.71	0.70	0.74	0.71	0.67	0.69
C	0.68	0.68	0.71	0.62	0.61	0.66	0.70
D	0.71	0.70	0.70	0.65	0.71	0.65	0.64
E	0.71	0.71	0.70	0.74	0.70	0.65	0.67
F	0.69	0.69	0.71	0.68	0.64	0.66	0.70
G	0.67	0.71	0.65	0.75	0.70	0.67	0.68

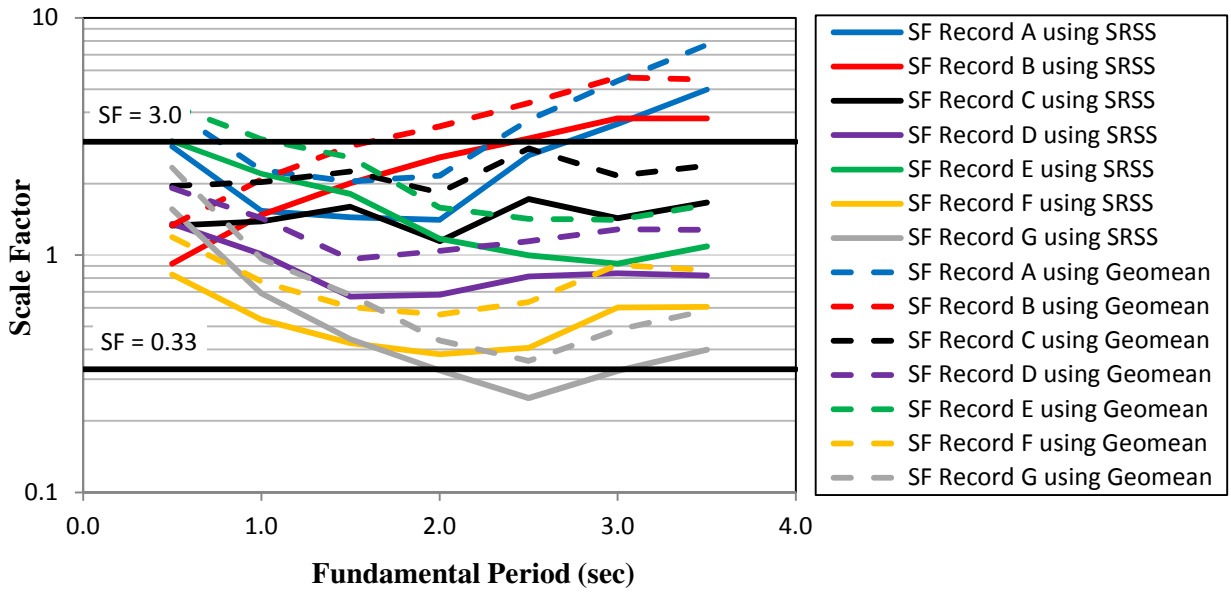

Figure 3-6 Scale Factors for the seven records of Set 2 using the SRSS and the geomean as the spectral measure of each record

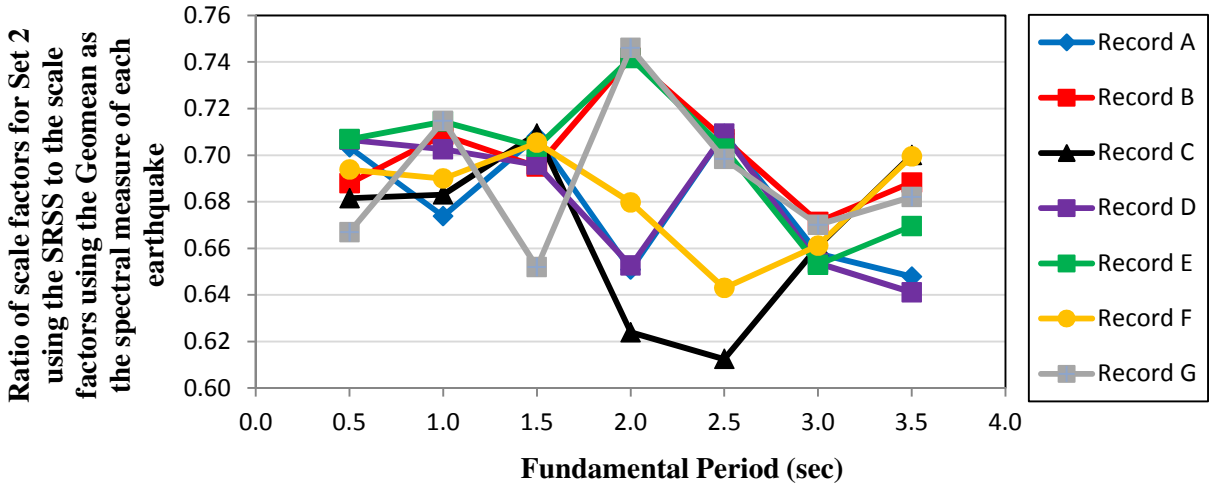

Figure 3-7 Ratio of scale factors for Set 1 using the SRSS to the scale factors using the Geomean as the spectral measure of each earthquake

It can be noticed in Figure 3-6 that the scale factors in some records are very close to 1.0 for small periods but very high at long periods; for instance, the record B using SRSS has a scale factor of 0.919 for T=0.5 sec and 3.773 for T=3.5 sec. However, other scale factors, like the one corresponding to the Record C using SRSS, do not change significantly with the fundamental

period of the structure analyzed. For instance, the scale factor of that record is 1.333 for T=0.5 sec and 1.664 for T=3.5 sec. Furthermore, it can be seen that some scale factors can be as high as 7.687 (Record A using the geomean for T=3.5sec) or as low as 0.250 (Record G using SRSS for T=2.5 sec), and these values represent extreme modification to the original record, and therefore, they might not be appropriate for scaling purposes. This way, the Set 2 of records will be more effective when it is used in the design of structures with small fundamental periods of vibration.

After the analysis of these two sets of records, it is concluded that the use of the geomean produces higher scale factors than when using the SRSS as the spectral measure when the scaling method is the one suggested by Charney (2010a), if the ratio (FPS_{SRSS}*SS_{SRSS}) / (FPS_{GEOM}/SS_{GEOM}), is bigger than 1.0, where:

FPS_{SRSS} is the fundamental period scale factor calculated using the SRSS as the record spectral measure.

FPS_{GEOM} is the fundamental period scale factor calculated using the geomean as the record spectral measure.

SS_{SRSS} is the set scale factor calculated using the SRSS as the record spectral measure.

SS_{GEOM} is the set scale factor calculated using the geomean as the record spectral measure.

It is concluded after this discussion that the use of the SRSS as the combined spectral measure for 3D analysis is arguable, and the use of the geomean might be more appropriate because seismic maps of ASCE 7 were developed using either the geomean or an arbitrary component of the two components of each record (Baker and Cornell, 2006). This document still recommends the use of the SRSS only for consistency with previous editions of ASCE 7, however, the author believes that more research is needed about this topic; particularly, it is necessary to re-evaluate the reasons for which the SRSS was used in earlier editions of ASCE 7.

3.2.3 Treatment of the two components of an earthquake record for 2D and 3D analysis

ASCE 7-10 specifies a different treatment of the record components depending if the analysis is performed in two dimensions (2D) or in three dimensions (3D) as explained in Section 3.1.1 of this document. For the case of 2D analysis the number of scale factor combinations for the same suite of ground motions is equal to 2^n where n is the number of

selected records having two horizontal components. The number of combinations equal to 2^n is because according to ASCE 7-10, the spectrum of either of the two components of each record can be used as its spectral measure (see Section 3.2.2 of this document for specific definition of the spectral measure of a record). In the case of a 3D analysis, ASCE 7-10 specifies the spectral measure of a record as the square root of the sum of the squares (SRSS) of the spectrum in each horizontal component, and the scale factors will be different than those in a 2D analysis. Table 3-9 specifies nine different combinations of scale factors for the same suite of ground motions, which corresponds to the three earthquake records given in Table 2-6; the first eight combinations corresponds to scale factors obtained as if a 2D analysis were to be performed, and the different record components defining the spectral measure of each record are also specified in Table 3-9. The scale factors from the last combination were obtained as if a 3D analysis were to be performed. The data of Table 3-9 was obtained using the scaling method suggested by Charney (2010a) for a structure with fundamental period of vibration equal to 2.74 sec.

Table 3-9 Sets of scale factors obtained for the same suite of ground motions

Combination	Record A		Record B		Record C		Scale Factors		
	A00	A90	B00	B90	C00	C90	Record A	Record B	Record C
1	x		x		x		0.403	0.957	2.719
2	x		x			x	0.565	1.341	1.931
3	x			x	x		0.448	1.036	3.018
4	x			x		x	0.647	1.496	2.209
5		x	x		x		1.458	1.182	3.359
6		x	x			x	1.970	1.597	2.300
7		x		x	x		1.388	1.098	3.198
8		x		x		x	1.845	1.458	2.154
9	Combination for 3D						0.481	0.843	1.550

It can be seen in Table 3-9 that the scale factors vary for each combination, and such a situation is not realistic, because the same earthquake will hit the structure regardless if it was modeled in 2D or 3D. Therefore, it is recommended to have a scaling procedure for 3D and apply it with no difference to 2D analysis (in case that a 2D analysis would be allowed).

3.2.4 Spectral ordinate of scaled earthquakes at the fundamental period of vibration of the building

The current scaling procedure of ASCE 7-10 does not connect the scaling procedure with the spectral ordinate of the target spectrum at the fundamental period of the structure, and it should be recognized that satisfying the requirement to have the average of the scaled spectral measures of each record above the target spectrum in the period range of interest, the minimum scale factors are obtained when the ordinate of such average spectra is as close as possible to the ordinate of the target spectrum at the fundamental period of vibration. For example, the commentary section of the NBCC (Canadian Commission on Building and Fire Codes, 2006) states that recorded earthquakes " should be scaled so that the spectral acceleration at the fundamental period of the structure corresponds to the design spectral response acceleration for the particular site." An appropriate procedure to account for the importance of matching the combined spectral measured with the ordinate of the target spectrum at the fundamental period of vibration is the approach developed by Charney (2010a), which is explained in Section 3.1.2.

3.2.5 Limits in the values of the scale factors

Caution is recommended when applying high or low scale factors to earthquake records, because excessive modification of the magnitudes of the original signal without changes in the frequency content or duration might not represent the ground motions for the site of interest. For instance, as mentioned by Brendon Bradley (2010), Professor of Department of Civil and Natural Resources Engineering at the University of Canterbury, "The aim of the limits on scale factor is to ensure that, for example, a small magnitude event recorded at a long distance is not excessively scaled up to represent a large magnitude event at close distances (the latter should have a much longer duration than the former, something which is not considered when only looking at response spectra)."

In the case of ASCE 7-10 there is no regulation about lower and upper limits for the scale factors; however, the New Zealand Standard NZS 1170.5, denoted NZS, does have those limits. The scaling procedure of the NZS applies two different scale factors, k_1 and k_2, to the ground motions as explained in Section 3.1.4; the first one is a record factor different for each record, and the second one is a set factor that applies equally to all the records selected. The acceptable values of such factors are $0.33<k_1<3.0$ and $1.0<k_2<1.3$, and according to Brendon Bradley (2010), those limits "are based more on engineering judgment than any formal analysis that has

been conducted." In general sense, the NZS disqualifies records with a signal that is amplified or reduced by more than a factor of 3, and a similar criterion is needed in future editions of ASCE 7-10.

3.2.6 Identification of period at which the 90% of the modal mass is reached

Section 12.9.1 of ASCE 7-10 requires the analysis to include the number of modes such that 90 percent of the mass of the building is reached in each of the orthogonal directions considered in the analysis. Therefore, it could be assumed that the period at which 90 percent of the mass of the building is reached, denoted T_{90}, is the smallest period with significant contribution to the response, and it could be considered in linear response history analysis to define a lower limit in the period range for the scaling of ground motions as it is explained in Section 3.4.

Also, the frequency corresponding to T_{90}, denoted F_{T90}, needs to be compared with the Nyquist frequency of the selected records. The Nyquist frequency is defined as half of the sampling frequency of a discrete signal, and the sampling frequency is the number of samples per second taken from such discrete signal (Santamarina and Fratta, 2005). For the case where F_{T90} is greater than the Nyquist frequency of each record used in the analysis, it will be an indicator that the mode at which T_{90} occurs does not have any energy component, and therefore, that particular earthquake might need to be replaced if the period T_{90} plays an important role in the scaling procedure. For instance, if T_{90} and F_{T90} for a particular structure are 0.025 sec and 40 Hz, respectively, then the Nyquist frequency of all the records used in the analysis has to be greater than 40 Hz. If the scaling procedure had been done with the earthquakes shown in Table 3-10, it is noticed that the record 3 might need to be replaced.

Table 3-10 Example showing the relation between the frequency of the period T_{90} and the Nyquist frequency

Earthquake Record	Δt	Sampling Frequency	Nyquist Frequency
	(sec)	(Hz)	(Hz)
1	0.005	200	100
2	0.01	100	50
3	0.02	50	25

Finally, a question arises about the definition of T_{90} considering that there is a different T_{90} for each translational direction; therefore, the value of T_{90} used for scaling procedures can be defined as the smaller value between T_{90X} and T_{90Y}, where T_{90X} and T_{90Y} are the periods at which 90% of the mass is reached in each of the principal directions of the structure.

3.2.7 Range of periods of interest

The scaling of ground motions is done within a specific range so that the lower limit will capture the effects of higher vibration modes, while the upper limit will account for the lengthening of the period of the structure due to cracking and yielding in seismic events (FEMA, 2009). ASCE 7-10 specifies $0.2T$ and $1.5T$ as the period range of interest for the scaling of ground motions where T is the fundamental period of vibration of the structure. Also, the NZS uses $0.4T$ and $1.3T$ for these limits (where T has been replaced by its original nomenclature T_1) with the additional requirement that T has to be bigger than 0.4 sec. Moreover, the NBCC only specifies the fundamental period T as the upper limit of the period range of interest; however, it does not provide any recommendation for the lower limit. Other provisions such as the EC8 states that the period range of interest needs to be between $0.2T$ and $2.0T$ (where T has been replaced by its original nomenclature T_1), while the *Recommendations for the Seismic Design of High-rise Buildings* of the Council on Tall Buildings and Urban Habitat (Willford et al., 2008), denoted hereafter CTBUH, states that a usual measure of the lower limit can be given by the period corresponding to the 4^{th} translational mode while the upper limit can be given by $1.5T$. Figure 3-8 shows the period range of interest for all the described provisions.

There are issues regarding the applicability of these limits; for example, the use of a period larger than the fundamental period as the upper limit is not justified for design purposes using LRHA, because the period of the structure will never increase in a linear elastic analysis (although a period higher than T as the upper limit of the period range of interest could be considered appropriate if it is intended to provide a margin of safety to the uncertainty in the computation of T). As it can be seen from Figure 3-8, the only scaling method for which the upper limit is the fundamental period T is the one given by the NBCC. Also, the procedures for the scaling of ground motions as stated in ASCE 7-10, NZS, NBCC, EC8 and CTBUH, define the period range of interest as a function of the fundamental period of vibration in the direction analyzed; however, this fact would yield a different set of scale factors for each orthogonal direction in almost any case, which is a fictitious case because both orthogonal directions of a

building should be loaded with the original record components multiplied by the same scale factor to maintain the relative strength of the two components. The use of different scale factors in each component could still be used for satisfying code requirements regarding minimum strength in each principal direction of the structure; however, it is a fictitious condition.

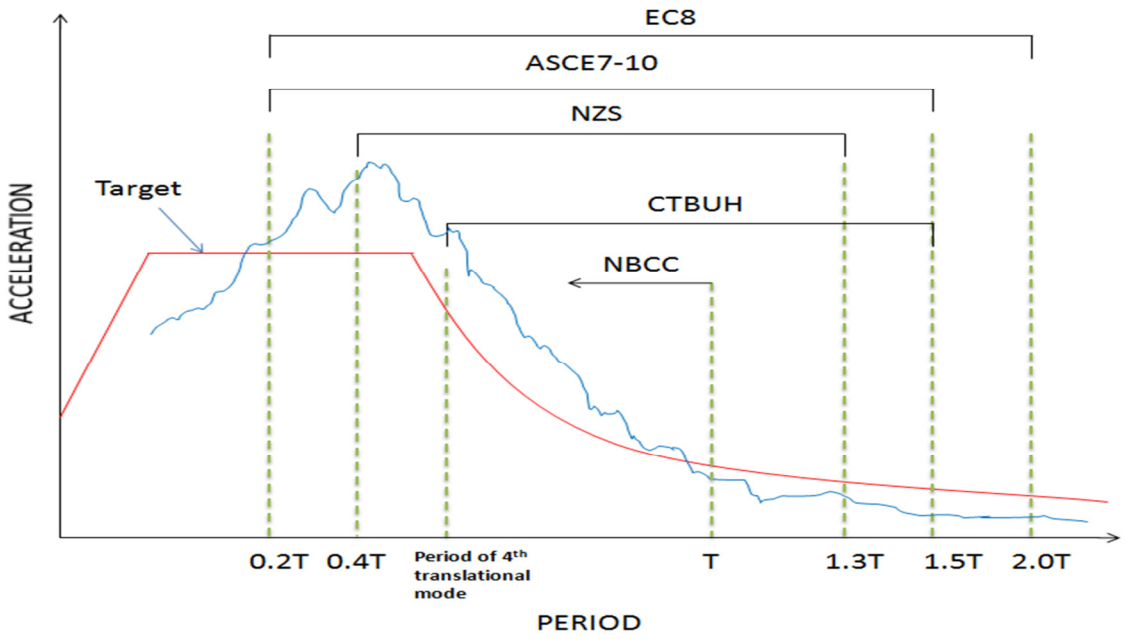

Figure 3-8 Period range of interest given by different seismic provisions

In addition, there is a complexity when scaling each orthogonal component based on its own fundamental period *T*, and such complexity arises because different fundamental periods can yield different pairs of Magnitude-Fault distance in a deaggregation model of the seismic hazard for the site of interest, which in turn might imply different selected records for scaling purposes in each orthogonal direction. From the discussion above it can be concluded that having different scale factors in both orthogonal direction would create additional complexity in the application of linear response history analysis, and therefore it might be more convenient to have a unique set of scaling factors for both directions.

An alternative to achieve the same scale factors in both orthogonal directions is to use the average of the two translational periods in each direction as the value of *T* when it is required in the calculation of the period range of interest. An additional recommendation is given in the Section C6.4.3 of the commentary of the NZS (Council of Standards New Zealand, 2004b), and

it consists of using the smaller translational period in the calculations of the lower limit and using the largest translational period instead of T if required for calculations of the upper limit of the period range of interest.

3.2.8 Differences in the scale factors obtained for the same set of ground motions.

It is important to have a rational procedure for scaling ground motions where different designers could arrive at the same scale factors when using the same set of ground motions. However, that is not the case in the current provisions of ASCE 7-10 and more than one result can be obtained by different designers. For instance, Table 3-11 shows different sets of scale factors for the same set of ground motions so that any set of scale factors satisfies the requirements of Chapter 16 of ASCE 7-10 for linear response history analysis. The scale factors of Table 3-11 were obtained for a structure with fundamental period T equal to 2.74 sec, the set of ground motions corresponds to the records described in Table 2-6, and the target spectrum is defined in Table 2-5 and Figure 2-4. The scale factors from Set 1 through set 5 were generated in three steps: first, random scale factors were assigned to the SRSS spectrum of each record, then the average of the scaled SRSS spectra was calculated from the previous step, and finally the scaled average SRSS spectrum was scaled again so that it would be above the target spectrum within the period range of interest. The Set 6 of scale factors was obtained using the method suggested by Charney (see Section 3.1.2 of this document).

The results from Table 3-11 can be interpreted as the scale factors obtained by six different structural engineers using the same set of ground motions, and it reflects the inconsistency of the current scaling procedure of ASCE 7-10.

Table 3-11 Different sets of scale factors that satisfy ASCE 7-10 requirements of scaling ground motions, for the same set of ground motions, and for a structure with fundamental period T=2.74

Record	NGA Record	Set 1	Set 2	Set 3	Set 4	Set 5	Set 6
A	879	0.904	1.061	0.170	1.705	1.532	0.481
B	725	0.904	1.061	2.556	0.024	0.306	0.843
C	139	0.904	0.530	0.681	1.218	1.021	1.550

Also, Figure 3-9 shows the scaled average of the SRSS spectra of each record for the different sets of scale factors of Table 3-11, and as required by ASCE 7-10, all these scaled

average spectra are above the target spectrum within the periods between 0.2*T* and 1.5*T*. Furthermore, Figure 3-9 shows different shapes in the spectra particularly at low periods, and it can have influence if higher modes of the structure contribute significantly to the response.

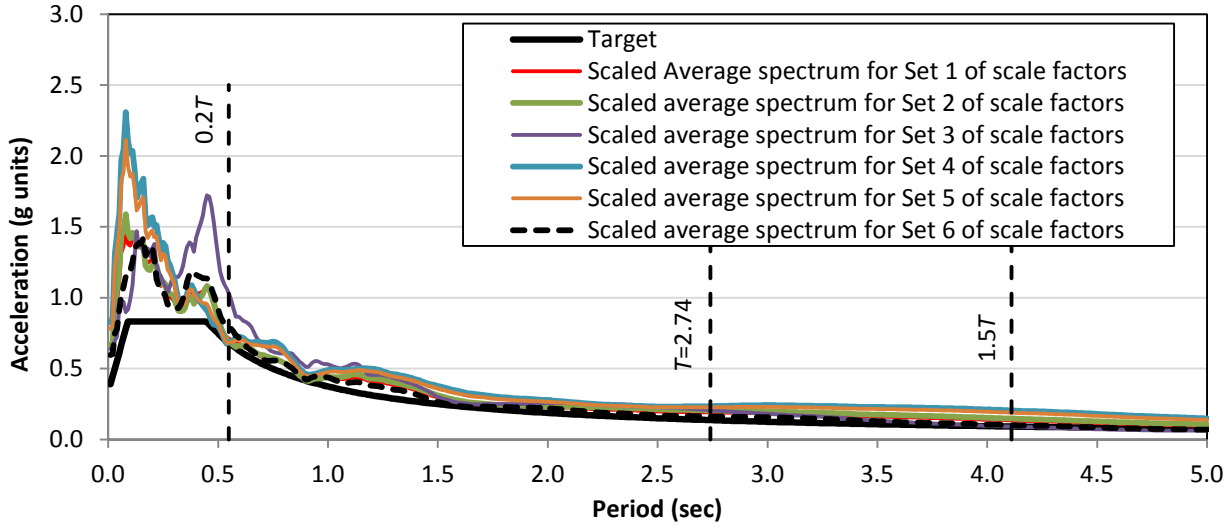

Figure 3-9 Scaled average spectra for different sets of scale factors that satisfy ASCE 7-10 requirements of scaling ground motions, and for a structure with fundamental period *T*=2.74 sec.

Special attention should be given to the difference between the spectral ordinate of the target spectrum and the one from the different scaled average spectra at the fundamental period of vibration *T*=2.74 sec. Table 3-12 shows the ratios of the ordinate of the scaled average spectrum from each set of scale factors from Table 3-11 to the ordinate of the target spectrum at the period of interest *T*=2.74 sec, and it can be seen that for the Set 4 of scale factors such ratio is equal to 1.72 which indicates that the response parameters (i.e. interstory displacement or interstory shear) in a linear response history analysis using those scale factors will be considerably higher than in a modal response spectrum analysis.

Table 3-12 Ratio of the ordinate of the scaled average spectrum to the ordinate of the target spectrum at *T*=2.74 sec

Parameter	Target	Set 1	Set 2	Set 3	Set 4	Set 5	Set 6
Ordinate of average spectrum at T=2.74 sec (g units)	0.136	0.19	0.205	0.206	0.234	0.226	0.162
Ratio of the ordinate of the scaled average spectrum to the ordinate of the target spectrum at T=2.74 sec	1.00	1.40	1.51	1.51	1.72	1.66	1.19

Also, it is shown in Table 3-12 that the Set 6 of scale factors, which were obtained using the methodology suggested by Charney (see Section 3.1.2 of this document) produces the smallest ratio (1.19) between ordinate of the scaled average spectrum and the ordinate of the target spectrum at T=2.74 sec.

The same records used in Table 3-11 were also used to generate six random sets of scale factors for a structure with fundamental period equal to T=0.6 sec. The intention of calculating sets of scale factors based on a different fundamental period is to see if the region of the scaled spectra corresponding to high frequencies (very small periods) has influence on the scaling factors, since it was noticed in Figure 3-9 that in this region of the spectrum the shape of the scaled average spectrum varies significantly for each set of scale factors. Table 3-13 shows the sets of random scale factors that satisfy the scaling of ground motion requirements of Chapter 16 of ASCE 7-10. As in Table 3-11, Set 1 through Set 5 of Table 3-13 are random sets of scale factors obtained with the same methodology used for calculating the scale factors of Table 3-11. Also, the Set 6 of scale factors in Table 3-13 was calculated using the methodology suggested by Charney.

Table 3-13 Different sets of scale factors that satisfy ASCE 7-10 requirements of scaling ground motions, for the same set of ground motions, and for a structure with fundamental period T=0.6

Record	NGA Record	Set 1	Set 2	Set 3	Set 4	Set 5	Set 6
A	879	0.866	1.049	0.137	1.750	1.558	1.074
B	725	0.866	1.049	2.062	0.025	0.312	0.675
C	139	0.866	0.525	0.550	1.250	1.039	0.949

Figure 3-10 shows the scaled average spectrum from each set of scale factors of Table 3-13, and it can be seen that for the Set 3 of scale factors, the lower point of the scaled average spectrum is in the region of constant acceleration of the target spectrum, which is also a region of high frequency periods.

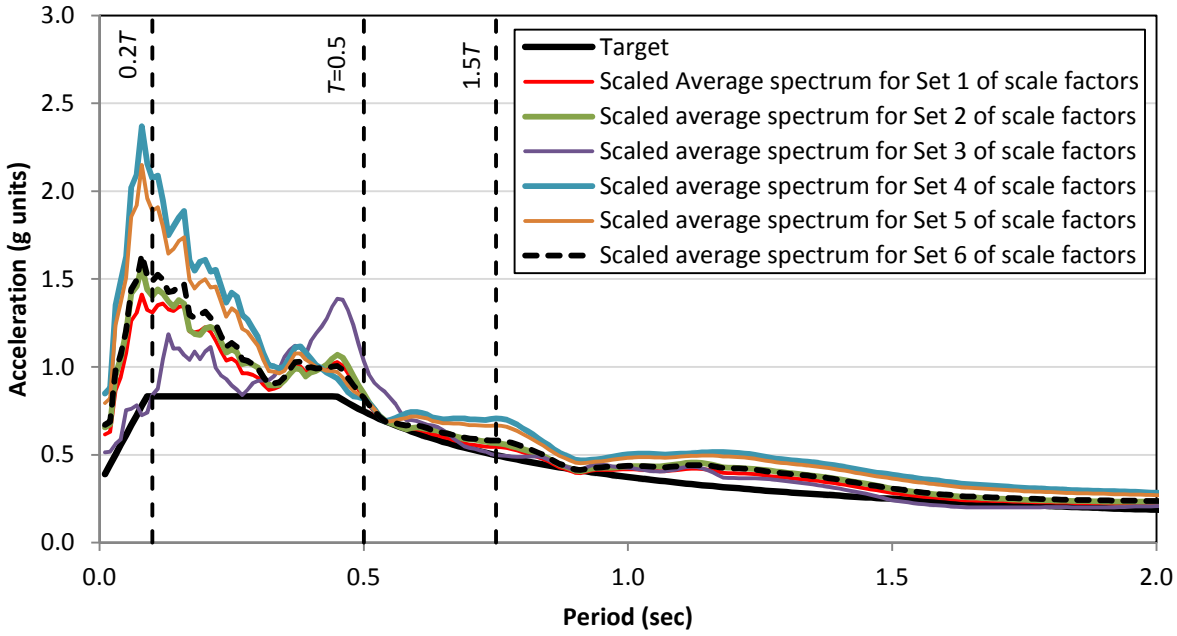

Figure 3-10 Scaled average spectra for different sets of scale factors that satisfy ASCE 7-10 requirements of scaling ground motions, and for a structure with fundamental period T=0.5 sec.

From the analysis of this section, it is concluded that the current scaling of ground motion procedure of ASCE 7-10 provides several sets of scale factors for the same suite of ground motions, and it requires modification to this procedure so that it will yield a unique set of scale factors for a specific set of records. Finally, it is mentioned that the scaling procedures of the NZS and the one proposed by Charney yield unique scale factors for the same set of ground motions, and that is an advantage of these methods in comparison with the current provisions of ASCE 7-10.

3.2.9 Set of periods where any required spectrum is calculated

Given the period range where the spectrum of a record is desired, the number of points in which this range is divided might have a strong influence in the shape of the spectrum, and therefore, it could affect directly the scale factors used in the procedures for the scaling of ground motions. For instance, Figure 3-11 shows the 5% damped spectrum for the component LCN260 of the Landers earthquake (see Table 2-6) using different number of points per logarithmic increment (i.e. from 0.01 to 0.1 or from 0.1 to 1). These spectra were calculated using the software NONLIN (Charney, 1995, 2003).

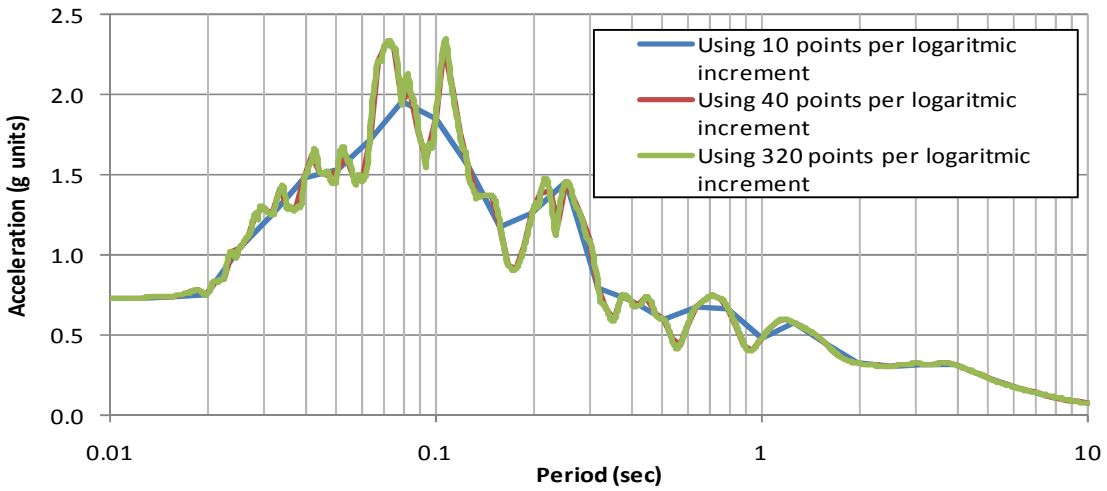

Figure 3-11 Spectra for the component LCN260 of the Landers earthquake, when using 10, 40, and 320 points per logarithmic increment.

From the figure above it can be seen that the spectral shape when using 10 points per logarithmic increment differs from the one using 40 points per logarithmic increment; however, there is no significant difference between the two spectra using 40 and 320 points per logarithmic increment.

A provision regarding recommended periods for the calculation of the spectrum is stated in ASCE 4-98, which provides in its Table 2.3-2 recommended increments in the frequency for different frequency ranges of the spectrum. For example, for the region of the spectrum where the frequency varies between 0.5 Hz and 3.0 Hz (periods between 0.333 sec and 2 sec) the recommended increment of the frequency is 0.10Hz. Also, ASCE 4-98 states an alternative procedure where each frequency used to calculate its spectral ordinate must be within 10% of the previous frequency.

The establishment of a specific procedure to define all the periods where a spectrum is calculated could also serve to define the periods used to calculate any measure that involves comparison between the spectrum under consideration and the target spectrum. For example, if it is desired to obtain a factor that minimizes the summation of the squared error between the spectrum under consideration and the target spectrum within the period range of interest, then guidelines are necessary to specify the periods used in that calculation. For instance, the NZS states that "…. the periods used to determine k_1 are to be selected so that each period is within

10% of the preceding one, except that an increment not greater than 1 sec may be used for periods greater than 5 seconds." The definition of the factor k_1 is explained in Section 3.1.4 and in the Example 3 of Appendix B.

Figure 3-11 indicates that forty periods per logarithmic scaled would be enough for getting no significant variation of the spectrum with the number of periods; however, the recommendation of this document is to use at least one hundred periods per logarithmic scale because Figure 3-11 corresponds to a particular case only, and higher levels of discretization might be required if considering other ground motions. Nevertheless, more research is required in this topic.

3.2.10 Point of matching of the average spectral measure of all the selected earthquakes and the target spectrum

If the scaling of ground motions procedure from any seismic provisions states that the spectral measure to be compared with the target spectrum needs to be above such target within a period range of interest, then at least two steps are required to obtain appropriate scale factors. Each of these steps, as described below, will yield separate scale factors denoted $k1_i$ and $k2$, respectively, and the final scale factors for each record will be the product of the scale factors $k1_i$ and $k2$.

Scale factor $k1_i$:

An initial set of scale factors denoted $k1_i$ which could be different for each record, can be obtained as follows:

- Randomly
- By adjusting the ordinate of the spectral measure of each record (see Section 3.2.2 for definition of spectral measure of a record), i.e. the SRSS or the geomean of the spectra from each horizontal component of a record, to the spectral ordinate of the target spectrum at the fundamental period (approach suggested by Charney as explained in Section 3.1.2)
- By minimizing the difference between the spectral measure of each record and the target spectrum within the period range of interest
- By minimizing the error between the combination (i.e. the average) of the spectral measures of each record within the period range of interest (which is part of the procedure developed by Naeim and Alimoradi et al. as explained in Section 3.1.6)

Scale factor *k2*:

A second scale factor denoted *k2* is required so that the final spectral combination be above the target spectrum within the period range of interest, and that factor will be equal for all the records analyzed.

When this methodology is used for scaling purposes, there is a matching point where the combined spectral measure (see Section 3.2.2 for definition of combined spectral measure of a set of records) coincides with the target spectrum, and at any other period within the range of interest, the combined spectral measure is above the target spectrum. The closeness of the period corresponding the matching point to the fundamental period of vibration *T* plays a very important role in the magnitude of the response, because it indicates how the spectral ordinate at the fundamental period *T* is increased by the scale factor *k2*. For example, Figure 3-12, Figure 3-13, and Figure 3-14 show three different locations of the matching point assuming that the factor $k1_i$, as described before, is calculated using Charney's methodology (2010a) . Figure 3-12 describes a situation where the matching point occurs at a point very close to the fundamental period *T*, and a small difference can be noticed between the ordinate of the combined spectral measure and the ordinate of the target spectrum at the fundamental period *T*. However, Figure 3-13 and Figure 3-14 show scenarios where the matching point is towards the upper limit (T_{UL}) and towards the lower limit (T_{LL}) of the period range of interest, and for these cases the increase in the ordinate of the combined spectral measure with respect to the ordinate of the target spectrum at the period *T*, is significant. Therefore, these last two cases are undesired scenarios.

Some reflections come from analyzing Figure 3-12 through Figure 3-14; first, the current scaling procedure of ASCE 7-10 does not provide any commentary about the location of the matching point. Also, it might be desirable for scaling purposes to set up a limit value of the combined spectral measure at the fundamental period; for instance, such ordinate could not be greater than a specific percentage of the ordinate of the target spectrum at the same period. Moreover, the scenario where the matching point is towards the lower period limit is not "fair" in the sense that it should be allowed for the combined spectral combination to be below the target spectrum at periods where the contribution to the response of the structure is no longer significant; for example, a reasonable matching point of Figure 3-14 could be given by Figure 3-15 where the combined spectral combination is allowed to be below the target spectrum for

periods smaller than $T_{maximum\ contribution}$, which is defined as the period at which the contribution to the response of the structure from smaller periods is no longer significant.

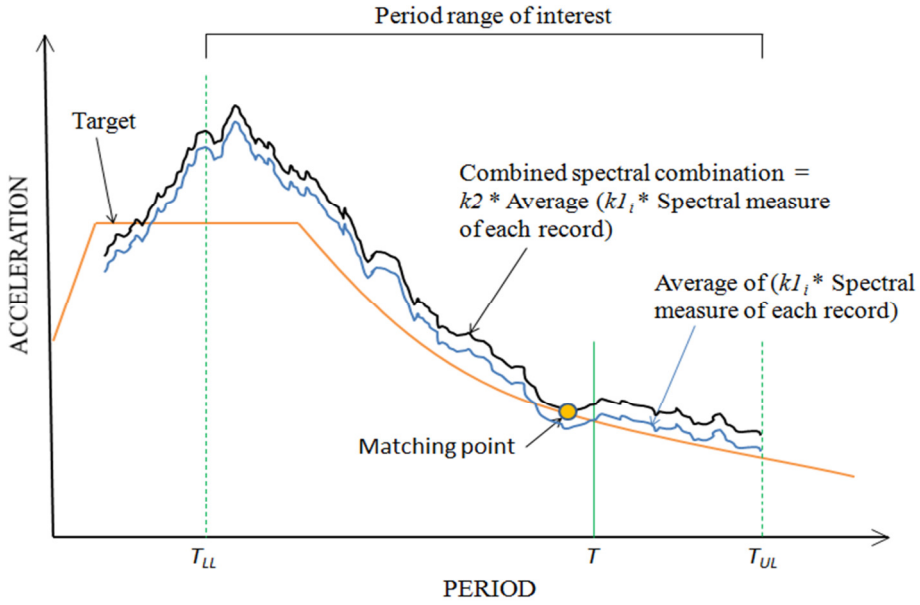

Figure 3-12 Scaling procedure when the matching point is close to the fundamental period of vibration T

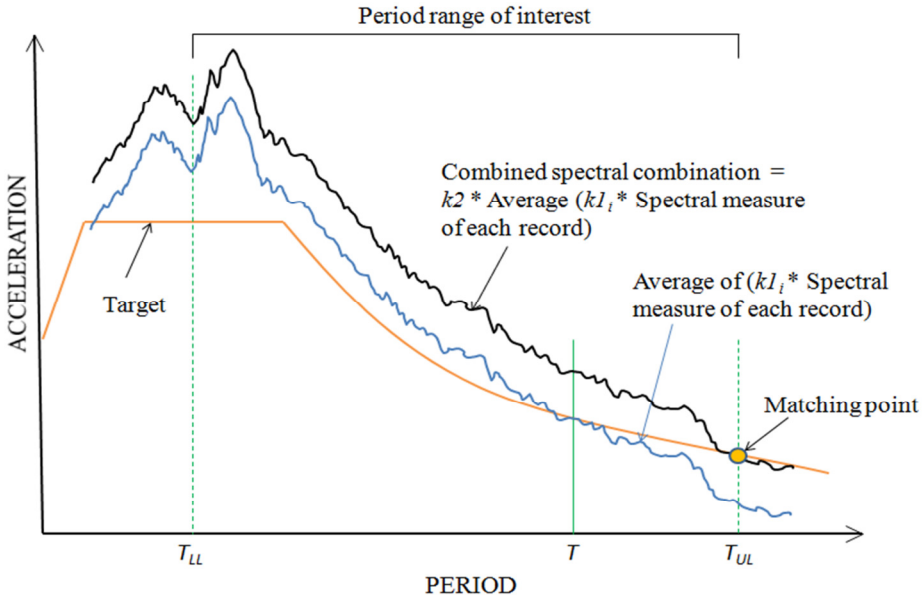

Figure 3-13 Scaling procedure when the matching point is close to the upper limit of the period range of interest

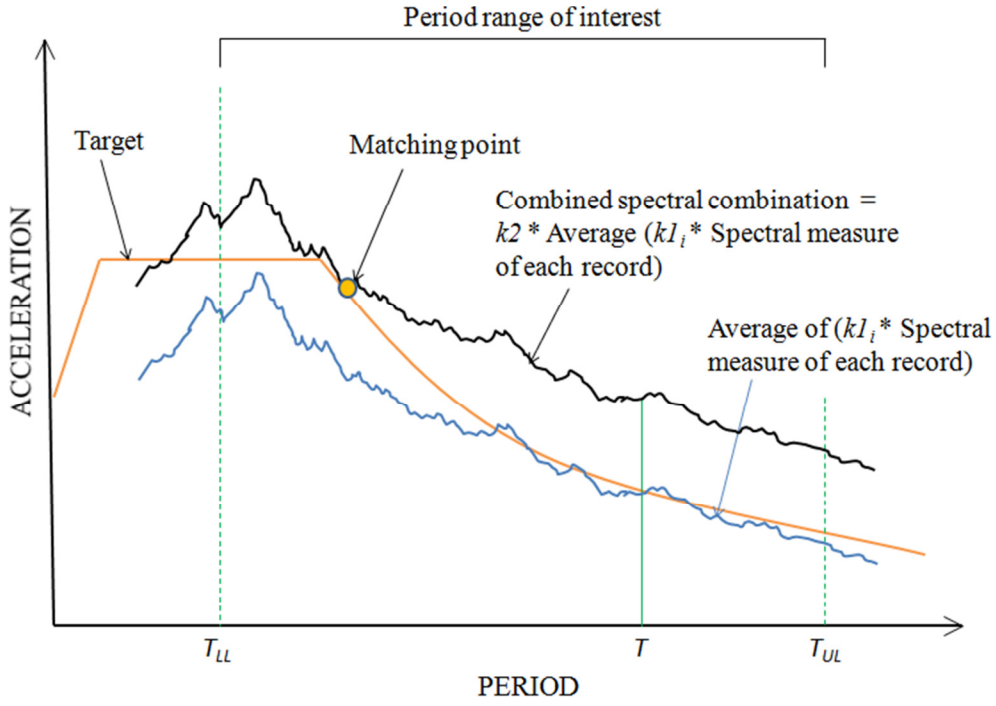

Figure 3-14 Scaling procedure when the matching point is close to the lower limit of the period range of interest

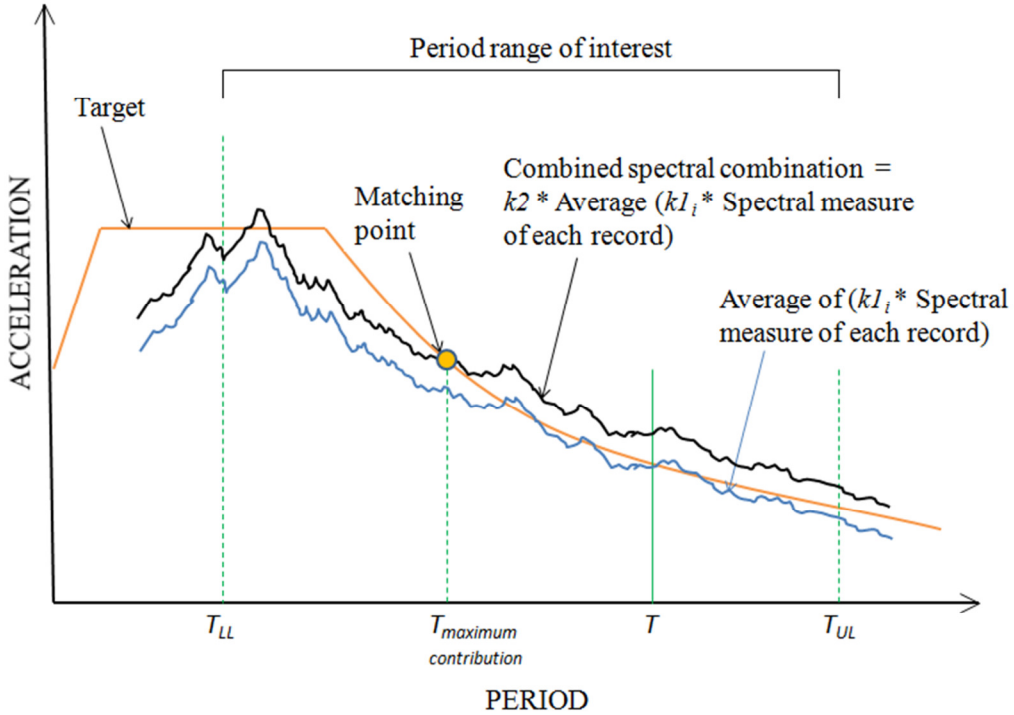

Figure 3-15 Acceptable Scaling procedure when the matching point is close to the lower limit of the period range of interest

The procedure given by ASCE 7-10 could be improved by giving different weights or levels of importance to the matching at different periods. For instance, it will be very important to have the ordinate of the combined spectral measure at the fundamental period of vibration of the structure at least equal or above the target ordinate at the same period; however, a less restrictive criterion can be used for other periods.

3.3 Scaling procedure if using artificial seismograms with a spectrum that matches with the target spectrum

Artificial acceleration series generated so that their spectrum is compatible with a target spectrum might also need to be scaled, because their spectra usually moves up and down relative to the target spectrum as shown in Figure 2-8 and Figure 2-14, and that characteristic might violate the scaling requirements of ASCE 7-10. Different spectral measures could be compared with the target spectrum. For instance, the artificial records could be scaled individually so that their spectrum should be above the target spectrum in the period range of interest. Also, the artificial records could be combined using their average and then this average could be compared with the target spectrum. It is the opinion of the author that an individual scaling is preferable, although in either case the scaling factors are expected to be very close to 1.0.

3.4 New proposal for the selection and scaling procedure

Having discussed in Chapter 2 and Chapter 3 several of the variables that influence the selection and scaling of ground motions, new guidelines are suggested in order to provide a more detailed procedure applicable to LRHA. The guidelines referring to the selection of ground motions are stated in this chapter instead of in the previous one, because the new suggested method treats the selection and the scaling of ground motions as one variable instead of considering two independent procedures. This section covers the philosophy and the principles of the new scaling procedure; it also describes specific code language for this proposal, and it provides a commentary based on explanations given in Chapter 2 and in Section 3.2.

3.4.1 Philosophy of proposed scaling procedure

These are the principles in which the new proposal is rooted.

- The set of records selected take into account not only the appropriate parameters M-D-SM-ST, but it also accounts for an initial measure of the fitness between the spectrum of the horizontal components of the record and the target spectrum.
- The spectral measure of each record is the SRSS of the individual response spectra of each horizontal component. Also, the combined spectral measure, which is compared with the target spectrum, is the average of the SRSS of each record.
- The scaling procedure is specified for structures modeled in 3D, because this document recommends that 2D analysis is not allowable for linear response history analysis.
- The scale factor of a record should have an upper and lower limit such that:
    - The upper limits of the period range of interest do not need to account for periods larger than the fundamental period of vibration of the structure.
    - The lower limit of the period range of interest should account for information such as the period at which the structure reaches the 90% of the modal mass, the Nyquist frequency of the records, and the current lower limit given in ASCE 7-10.
- Equal scaling factors should be applied in both principal directions of the structure for the case of using real records.
- The matching of the combined spectral measure with the target spectrum is more important in the first translational modes than at higher modes.
- Minimum resolution of the number of periods when calculating the response spectrum from an acceleration record.

3.4.2 Description of proposed scaling procedures

Section 3.4.2.1 describes the new suggested approach when using real records while Section 3.4.2.2 describes the new suggested method when using artificial records (see pg. 8 for definition of real and artificial).

3.4.2.1 Selection and Scaling of ground motions for the case of using real records

These next steps will be addressed for the selection and scaling of ground motions for LRHA when using real records.

Step 1: Calculation of the fundamental period of vibration of the structure

The average of the first fundamental periods of vibration in each principal direction can be used as the representative fundamental period of the structure.

Step2: Definition of the seismic hazard

Considering the fundamental period given by step 1 and having the specific location of the structure under analysis, then the definition of the seismic hazard for the site of interest can be defined using the deaggregation models provided by the USGS in their website: http://eqint.cr.usgs.gov/deaggint/2008/. Such seismic hazard will be in the form of a pair of magnitude and distance, denoted M-D, of the modal event that controls the seismic hazard. Also, the probability of exceedence used as input in the deaggregation model can be chosen as 2% for 50 years for design purposes using LRHA.

Step 3: Selection of ground motions from a database

Ground motions with properties close to the target M-D need to be selected from a database, and the number of ground motions selected will be bigger than the number of ground motions intended to use for LRHA. The minimum number of records selected from a database will be equal to 1.5 times the number of earthquakes intended for LRHA, and any decimal number will be rounded to the next integer. This set of ground motions is denoted as the pre-selected earthquake set. Also, the preferred range of magnitude of the selected earthquakes will be ±0.25 of the target magnitude. If the number of records from a database is less than the number required, then simulated records with two horizontal components (and a vertical component if possible) need to be generated.

Step 4: Control of the statistical independence of the horizontal components of the preselected earthquakes

The statistical independence between the horizontal components of a record will be guaranteed if the absolute value of the correlation coefficient between their acceleration histories is less than 0.3.

Step 5: Calculation of the acceleration design spectrum for the location of interest

The design spectrum is given by the Section 11.4.5 of ASCE 7-10.

Step 6: Calculation of the SRSS spectrum of the spectral components of each record

The number of periods used to calculate any spectra should be enough to guarantee that the resulting scale factors are not affected by this selected number of periods. A minimum resolution of 100 periods per logarithmic scale (i.e. 100 points between 0.1 sec and 1.0 sec, equally spaced in logarithmic scale) is suggested.

Step 7: Scaling of the pre-selected records to the fundamental period of vibration using the factor *FPS*

A fundamental period scale factor, denoted *FPS*, will be calculated for each pre-selected earthquake so that their SRSS spectrum will have the same ordinate of the design spectrum at the fundamental period of vibration.

Step 8: Definition of the period range of interest

The upper limit of the period range of interest will be given by the fundamental period defined in Step 1, and it has to be smaller than the maximum usable period of each pre-selected earthquake. The maximum usable period should be available from the database where the ground motions are selected. On the other hand, the lower limit of the period range of interest, denoted T_{LL}, is given by the greatest of:

- The period when 90% of the modal mass is reached
- The period corresponding to the smallest Nyquist frequency of the set of records
- $0.2T$ where T is the fundamental period defined in Step 1
- 4^{th} translational period
- The maximum of the minimum usable period for each record, which should be available from the database where the ground motions were selected

Step 9: Selection of the records that best fit the design spectrum.

At least one error measure will be used to define the best fit between the scaled (by *FPS*) SRSS spectra of each earthquake (see Step 7) within the period range of interest defined in the

previous step. Also, such error measures can include weighting functions that give more weight to the periods closer to the fundamental period than at periods away from the fundamental period. Then, the pre-selected earthquakes that yield smaller errors will be assigned as the selected records for analysis.

Step 10: Recalculation of the lower limit of the period range of interest, if needed

The period range of interest will be recalculated, if needed, considering only the characteristics of the selected records.

Step 11: Calculation of the average of the scaled (by *FPS*) SRSS spectra of the selected earthquakes

Step 12: Definition of the new target spectrum

The target spectrum is defined for three different scenarios as described next:

Scenario 1: $T_{LL} < T_S$ and $T_S < T_{2Tr}$, as shown in Figure 3-16

Scenario 2: $T_{LL} < T_{2Tr}$ and $T_{2Tr} < T_S$, as shown in Figure 3-17

Scenario 3: $T_{LL} > T_S$ and $T_{2Tr} > T_{LL}$, as shown in Figure 3-18

The equations corresponding to each scenario are:

For scenario 1:

$$\text{Target Spectrum} = \begin{cases} k S_{DS} & \text{if } T_{LL} < T < T_S \\ c\left(T - T_{2Tr}\right)^2 + S_{2Tr} & \text{if } T_S \le T < T_{2Tr} \\ \qquad \text{where} \quad c = \dfrac{k S_{DS} - S_{2Tr}}{\left(T_S - T_{2Tr}\right)^2} & \\ \text{Design Response Spectrum (Section 11.4.5 of ASCE 7-10)} & \text{if } T_{2Tr} \le T \le Tn \end{cases}$$

For scenario 2:

$$\text{Target Spectrum} = \begin{cases} k S_{DS} & \text{if } T_{LL} < T < T_{2Tr} \\ \text{Design Response Spectrum} & \text{if } T_{2Tr} \le T \le Tn \\ \text{(Section 11.4.5 of ASCE 7-10)} & \end{cases}$$

For scenario 3:

$$\text{Target Spectrum} = \begin{cases} c\left(T - T_{2Tr}\right)^2 + S_{2Tr} & \text{if } T_{LL} \le T < T_{2Tr} \\ \text{where } c = \dfrac{k S_{DS} - S_{2Tr}}{\left(T_{LL} - T_{2Tr}\right)^2} & \\ \text{Design Response Spectrum} & \text{if } T_{2Tr} \le T \le Tn \\ \text{(Section 11.4.5 of ASCE 7-10)} & \end{cases}$$

where k is a constant equal to 0.7

S_{DS} is the design spectral response acceleration parameter at short periods

S_{D1} is the design spectral response acceleration parameter at 1 sec

S_{2Tr} is the ordinate of the design spectrum at the period T_{2Tr}

T_{2Tr} is the least of the second translational period in each principal direction

T_{LL} is the period corresponding to the lower limit of the period range of interest

T_S is the ratio between S_{D1} and S_{DS}

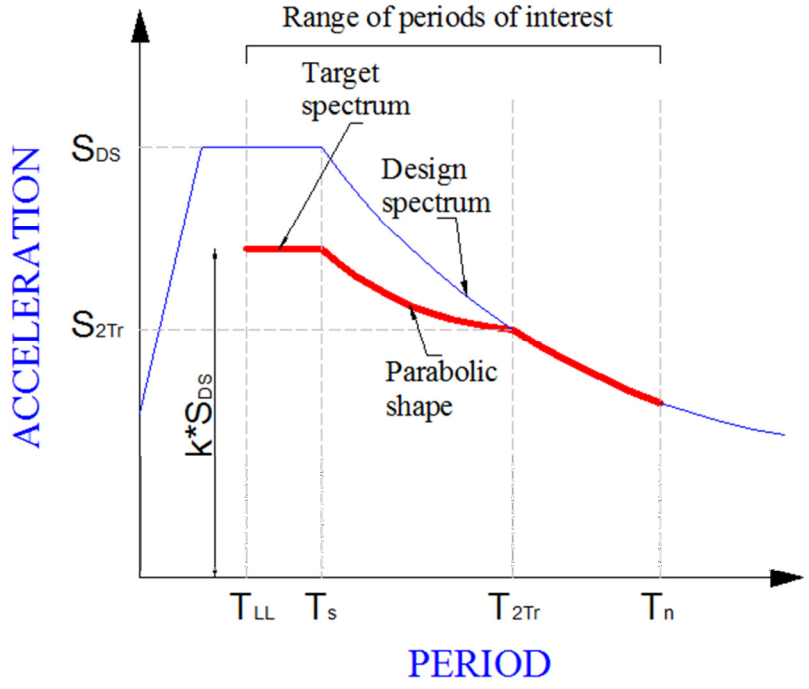

Figure 3-16 Target Period of proposed scaling of ground motion procedure, Scenario 1

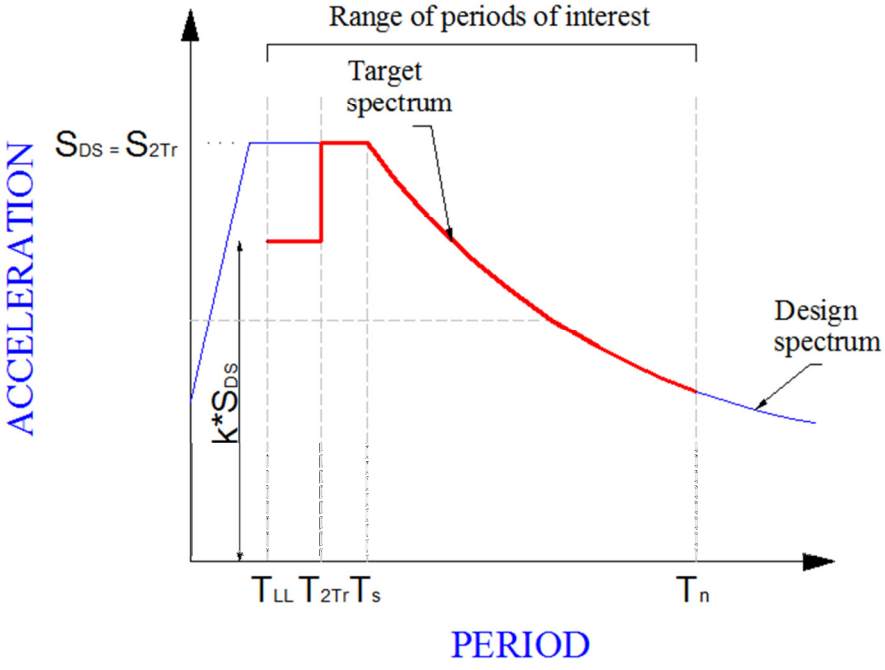

Figure 3-17 Target Period of proposed scaling of ground motion procedure, Scenario 2

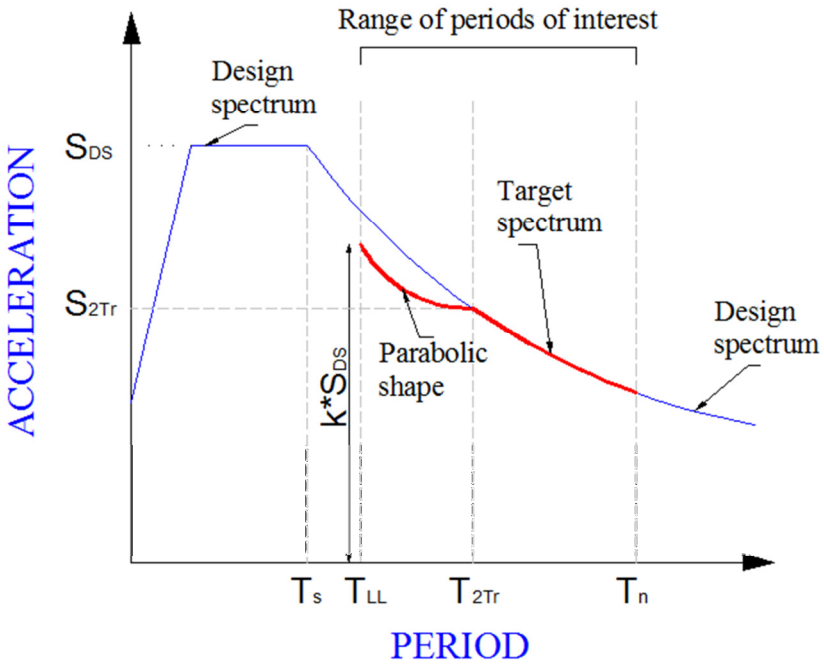

Figure 3-18 Target Period of proposed scaling of ground motion procedure, Scenario 3

Step 13: Calculation of the set scale factor *SS*

The set scale factor *SS* will be calculated so that the average of the scale (by *FPS*) SRSS spectrum is above the new target spectrum within the period range of interest.

Step 14: Calculation of final scale factors

The final scale factors are given by the product of the factor *FPS* for each record by the set scale factor *SS*.

Step 15: Control of the maximum and minimum allowable limits of the final scale factors

The final scale factors need to be within the range $0.33 < FPS_i * SS < 3.0$, where FPS_i is the fundamental period scale factor of the i^{th} earthquake and *SS* is the set scale factor.

Step 16: Calculation of the average PGA from the selected records and comparison with PGA from design spectrum

The PGA from each record (not scaled) will be obtained as the geometric mean of the PGA of each horizontal component. Then, the average of the PGA values from each record needs to be above the PGA value given by the design spectrum.

The proposed scaling procedure described above contains several steps, and its application might require a significant amount of time. However, the intention of this section was to provide an algorithm that could be implemented with computer software.

3.4.2.2 Selection and Scaling of ground motions for the case of using artificial records

This section states the suggested method for the scaling of ground motions using artificial records. The steps are as follows:

Step 1: Selection of the desired number of records for analysis

One spectral matched acceleration history will be required to perform linear response history analysis with artificial records

Step 2: Control of the acceptability criterion for artificial records

An artificial record will consist of two statistically independent components as described in the Step 4 of Section 3.4.2.1.

Step3: Scaling of acceleration histories

The artificial records will be scaled as described next: The spectrum from each component of the artificial records will be scaled by a factor *F*, so that its spectrum is above the new target spectrum described in Step 12 of Section 3.4.2.1, within the period range of interest defined in Step 8 of Section 3.4.2.1.

3.4.3 Commentary of proposed scaling procedure

Some commentaries about the principles and steps of the new suggested method are explained below:

- The spectral measure for each record is kept as the SRSS of the spectrum from the horizontal component, even though it was discussed in Section 3.2.2 that the geomean might be more appropriate. The decision of keeping the SRSS as the spectral measure is for consistency with the current procedure of ASCE 7-10.

- Special attention is given at the ordinate of the combined spectral measure at the fundamental period of vibration as it was mentioned in Section 3.2.4. The new suggested method follows very closely the methodology used by Charney (2010a); the differences of these two procedures are the target spectrum and the period range of interest.
- Regarding the upper and lower limits for the scale factors, the proposed scaling technique follows the recommendations given in the NZS that were explained in Section 3.2.5. Such regulation states that a record should be amplified or de-amplified by no more than a factor of 3.
- The upper limit of the period range of interest does not need to be bigger than the fundamental period of vibration of the structure as explained in the second paragraph of Section 3.2.7. Therefore, the upper limit of the proposed scaling procedure is $1.0T$ where T is the fundamental period of vibration of the structure.
- A critical stage in the scaling is the comparison of the combined spectral measure of all the earthquakes with the target spectrum. As mentioned in Section 3.2.10, higher importance should be given to the first translational modes and lower importance to higher modes. This can be achieved by defining a new target spectrum as shown in Figure 3-16, Figure 3-17, and Figure 3-18. The factor k used in these figures was established arbitrarily as 0.7, and more research is required to calibrate this number.

3.5 Example of new suggested method for the selection and scaling of ground motions

A very detailed example of the new suggested method for the selection and scaling of ground motions is presented in Example 4 of Appendix B.

3.6 Comparison of scaling procedures using the approach of Charney, the NZS, and the new suggested scaling method

The scale factors from two sets of three earthquakes were obtained using the new suggested method, the method suggested by Charney (2010a) and the provisions from the New Zealand Standard NZS 1170.5 (Council of Standards New Zealand, 2004). These scale factors were obtained for structures with different fundamental periods of vibration in order to have a better understanding in the trends of the scale factors when changing the fundamental period T. The two sets of earthquakes are denoted Set 1 and Set 2, and the first of them correspond to the records A, B, and D described in Table B- 13 (which are the records used in the Example 4 of

Appendix B), while the second set contains the earthquakes described in Table 2-6 (which are the same records use by Charney et al. (2010b)). The three records of each set are denoted as Record 1, Record 2, and Record 3.

The period range of interest used in the method suggested by Charney was from 0.2*T* to 1.5*T* as required by ASCE 7-10, and the range given by the NZS was from 0.4*T* to 1.3*T* where *T* is the fundamental period of vibration. Also, and only for comparison purposes, it was assumed that the lower limit of the new suggested method was governed by 0.2*T*, and the period of the second translational mode, T_{2Tr}, was assumed to be equal to 0.4*T*.

Also, it is mentioned that Set 1 originally represented the seismic hazard for a structure with fundamental period equal to 2.74 sec at a specific location (see Example 4 in Appendix B), and its use for other periods will depend on the deaggregation model at other periods. However, it was assumed that the same records govern at other periods only for comparison reasons. The same assumption is applied to the Set 2 except that these records were originally chosen not based on the seismic hazard at a specific location but in the closeness of their spectral shape to a specific design spectrum.

The scale factors obtained using the Set 1 of earthquakes are shown in Table 3-14, and it can be noticed there that the NZS almost always yields scale factors higher than those when using the other two techniques (the only exceptions are the scale factor for Record 3 at *T*=2.0 sec and the scale factor of Record 2 at *T*=2.5 sec). Also, it can be noticed that the new suggested method yields scale factors that are in some cases equal to the ones obtained by the method developed by Charney (i.e for *T*=0.5 sec), or even lower (i.e. for *T*=1.0 sec, 1.5 sec, 2.0 sec, 2.5 sec, and 3.0 sec); this is an expected result because the new suggested method is set up so that its scale factors are equal or lower than the ones obtained from the method developed by Charney.

The nature of having scale factors smaller or equal to those using the method suggested by Charney (2010a) depends on the location of the matching point. For instance, Figure 3-19 shows simultaneously the location of the scaled average SRSS spectrum when using the method suggested by Charney and the new suggested method considering a fundamental period *T*=0.5 sec. It can be seen from Figure 3-19 that the matching point is the same in both cases, and therefore there will be no difference in the scale factors. This will be the case when the matching point of the new suggested method is between *T* and T_{2Tr} (see Figure 3-17 and Figure 3-18).

Table 3-14 Scale factors for the Set 1 of earthquakes using different methodologies

Scale Factors using the method suggested in this document						
Record	**Fundamental Period (sec)**					
	0.50	**1.00**	**1.50**	**2.00**	**2.50**	**3.00**
1	1.801	1.648	1.447	1.752	2.11	2.034
2	1.069	0.96	1.204	0.975	1.417	1.212
3	0.537	0.339	0.479	0.473	0.433	0.513

Scale Factors using the method developed by Charney						
Record	**Fundamental Period (sec)**					
	0.50	**1.00**	**1.50**	**2.00**	**2.50**	**3.00**
1	1.802	1.98	1.577	2.019	2.526	2.657
2	1.07	1.154	1.311	1.124	1.696	1.584
3	0.537	0.408	0.522	0.545	0.519	0.671

Scale Factors using the New Zealand Standard						
Record	**Fundamental Period (sec)**					
	0.50	**1.00**	**1.50**	**2.00**	**2.50**	**3.00**
1	2.413	2.646	2.481	2.423	2.689	3.246
2	1.389	1.571	1.65	1.552	1.65	2.017
3	0.804	0.551	0.524	0.529	0.598	0.76

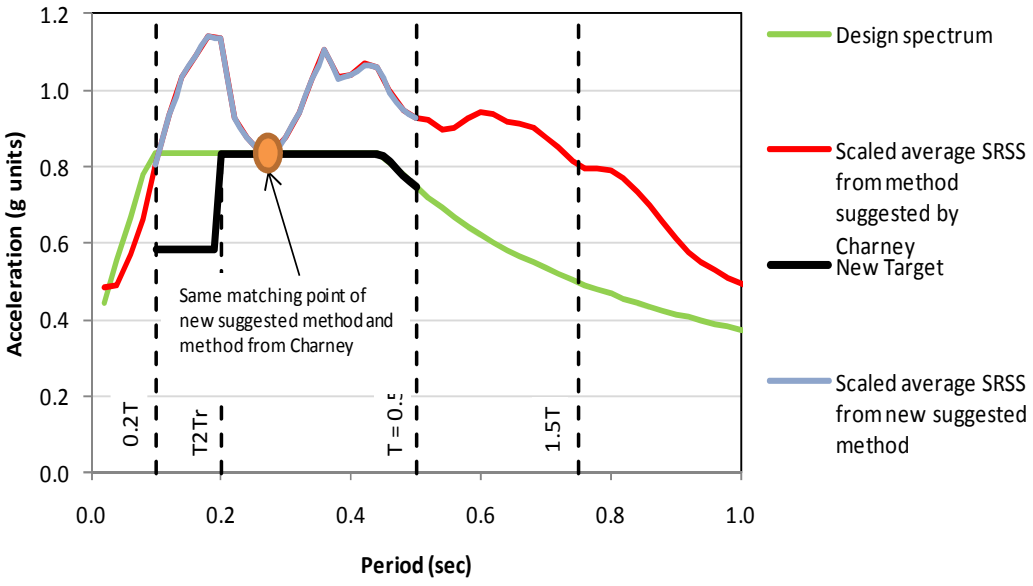

Figure 3-19 Matching point in the scaling of ground motions using the method suggested by Charney and the new suggested method for the Set 1 of earthquakes and for a structure with fundamental period T=0.5 sec

A different case occurs if analyzing the new suggested method and the method from Charney for a structure with fundamental period T=1.0 sec. Figure 3-20 shows the scaled average SRSS spectra and respective matching point when using these two methodologies, and it can be seen that the matching point when using Charney's methodology is towards the left of the matching point obtained with the new suggested method, which result in smaller scale factors for the latter case.

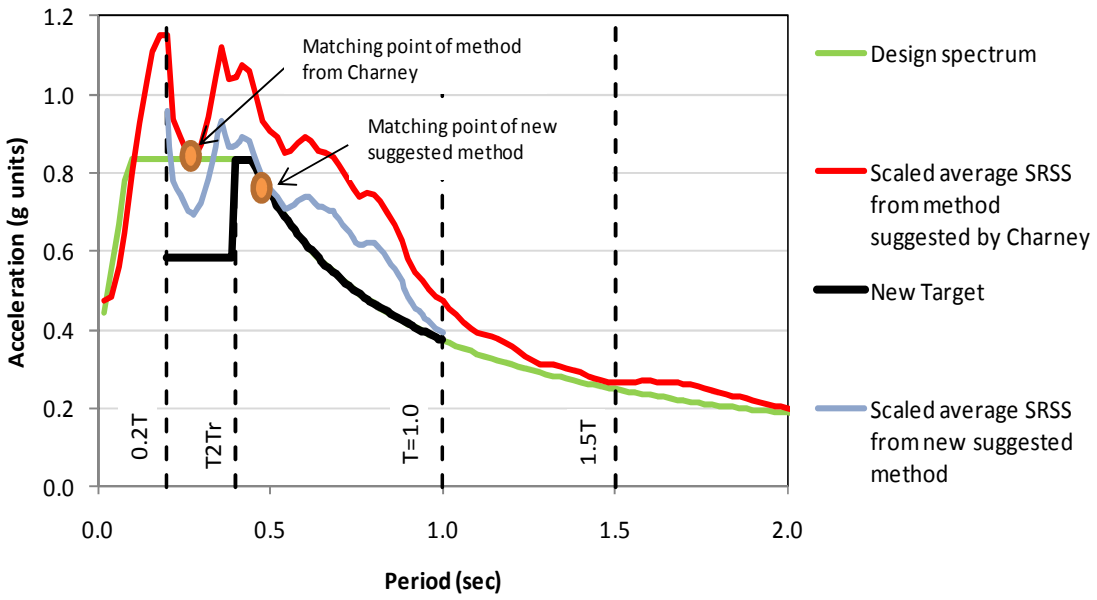

Figure 3-20 Matching point in the scaling of ground motions using the method suggested by Charney and the new suggested method for the Set 1 of earthquakes and for a structure with fundamental period T=1.0 sec

A different location of the matching point occurs when analyzing the new suggested method and the method from Charney for structures with fundamental period T=1.5 sec, 2.0 sec, 2.5 sec and 3.0 sec. In these cases, as it is shown in Table 3-14, the scale factors from the new suggested method are smaller than the ones when using the method suggested by Charney, and it is because the matching point when using the new suggested method occurs at a period close to the fundamental period T, while in the second case the matching point is close to 1.5T. This situation is presented in Figure 3-21, which corresponds to the particular case of a structure with period T=3.0 sec.

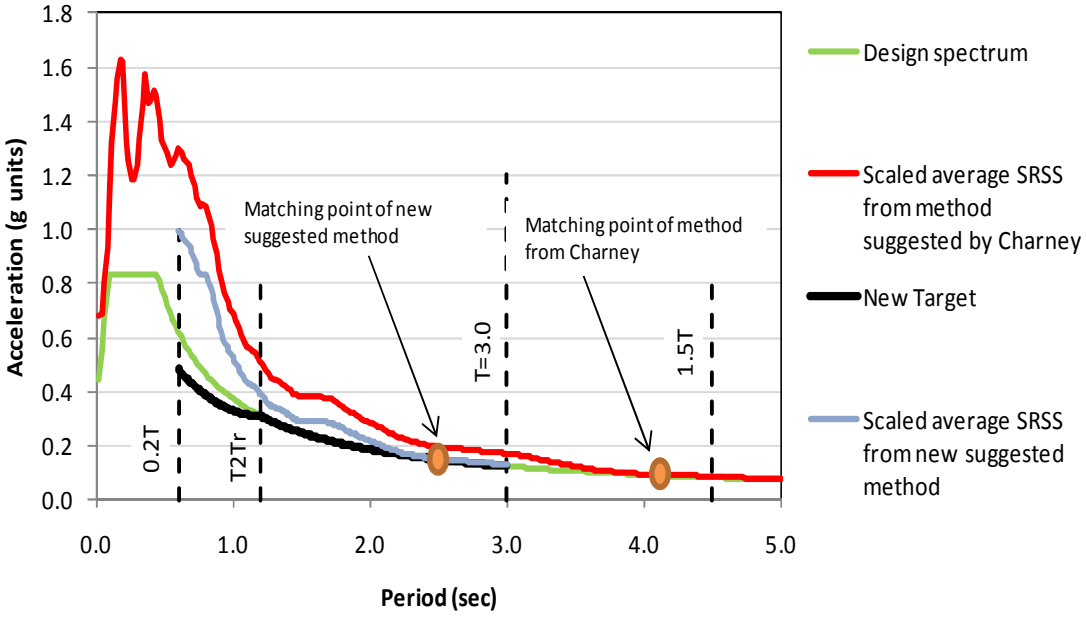

Figure 3-21 Matching point in the scaling of ground motions using the method suggested by Charney and the new suggested method for the Set 1 of earthquakes and for a structure with fundamental period T=3.0 sec

A second set of ground motions, denoted Set 2, was tested with the three methodologies used before, and the resulting scale factors are shown in Table 3-15. It can be seen from Table 3-15 that the suggested method yields scale factors equal to the ones calculated using the method suggested by Charney (2010a), and this occurred because the matching point in all these figures was between the T_{2Tr} and T. Therefore the target spectrum of the new suggested method coincides with the design spectrum, which is the target spectrum of the method suggested by Charney.

3.7 Differences in the scaling procedure for linear and nonlinear structural analysis

Given the variables that influence the scaling of ground motions for LRHA, it is important to discuss the differences in the criteria for linear response history analysis and for nonlinear response history analysis. Some of these differences are explained next.

The range of periods of interest for non-linear response history analysis (NLRHA) should consider a lower and upper limit based on the fundamental period of vibration of the structure T. The upper limit will be required to be bigger than T to account for elongation of the period while

Table 3-15 Scale factors for the Set 2 of earthquakes using different methodologies

Scale Factors using the method suggested in this document						
Record	**Fundamental Period (sec)**					
	0.50	**1.00**	**1.50**	**2.00**	**2.50**	**3.00**
1	0.974	0.770	0.517	0.640	0.506	0.456
2	0.612	0.914	1.009	0.980	0.761	0.982
3	0.860	1.057	1.268	1.147	1.582	1.449

Scale Factors using the method developed by Charney						
Record	**Fundamental Period (sec)**					
	0.50	**1.00**	**1.50**	**2.00**	**2.50**	**3.00**
1	1.074	0.771	0.519	0.64	0.507	0.458
2	0.675	0.914	1.013	0.981	0.762	0.987
3	0.949	1.058	1.273	1.148	1.583	1.457

Scale Factors using the New Zealand Standard						
Record	**Fundamental Period (sec)**					
	0.50	**1.00**	**1.50**	**2.00**	**2.50**	**3.00**
1	1.287	1.155	0.844	0.737	0.610	0.591
2	1.383	1.289	1.522	1.437	1.339	1.489
3	1.561	1.571	1.650	1.650	1.650	1.874

the structure loses stiffness during the earthquake. This is a difference with the LRHA where the upper limit does not need to be bigger than *T*.

Also, ground motions for nonlinear structural analysis might have a different treatment than in LRHA. For instance, Shome and Cornell (1998) stated two different stages described as normalization and scaling of ground motions. The goal of this normalization process is to reduce the dispersion in the damage measures without creating a bias in the parameters that define the structural response. The normalization process is done over a set of records with similar properties magnitude-distance M-R appropriate for the site of interest, and it is intended that the records would have equal intensity based on a specific ground motion parameter. The selected records can be normalized to a single frequency (like PGA or the lowest frequency of the structure), normalized to the median spectral acceleration at the frequency of the structure using high damping levels, or normalized to the average spectral acceleration between a range of frequencies (Shome and Cornell, 1998). On the other hand, the scaling of the already normalized

records might or might not be necessary, since it is intended to modify the already normalized records such that they would represent a different pair M-R (Shome and Cornell, 1998).

In addition, the criteria to evaluate appropriate artificial seismograms for nonlinear analysis should have different or additional requirements than those for linear analysis because as stated by Somerville et al. (1998) "The nonlinear response of structures is strongly dependent on the phasing of the input ground motion and on the detailed structures of its spectrum." To illustrate this point it should be noticed that when using LRHA with two different record components with compatible spectrum, the results of both signals will be very similar. However, if the same record components are used for nonlinear analysis, then the similarities of the response might be unpredictable. Lastly, the number of ground motions required could be different for linear analysis than for nonlinear analysis, because the level of uncertainty in the response is higher when using nonlinear analysis.

Chapter 4. DIAPHRAGM FLEXIBILITY AND ACCIDENTAL TORSION

This chapter is divided in two sections: the first section refers to the assumptions used for the flexibility of diaphragms when modeling the floors of a building, and the second section refers to accidental torsion for linear response history analysis (LRHA). The first part of this chapter studies the behavior of buildings when their floors are modeled using rigid and semirigid diaphragms. Floors modeled with rigid diaphragms are defined here as those floors modeled as having the same lateral (or planar) displacements at all the nodes modeled within the same floor so that internal forces (or strains) are not developed inside the diaphragms. On the other hand, semirigid diaphragms are defined here as those floors modeled with shell elements so that there are no constraints between the degrees of freedom of nodes located within the same floor; this way, each shell element within a diaphragm, and therefore the whole diaphragm, are able to develop internal forces (or strains). The definitions of rigid and semirigid diaphragms given in this document differ from the definition of rigid diaphragm and semirigid diaphragm (diaphragm not satisfying the conditions of rigid or flexible diaphragms) given in Section 12.3.1 of ASCE 7-10, which defines the flexibility of a diaphragm as a measure relative to the stiffness of the vertical elements being part of the seismic force-resisting system. However, different definitions of diaphragm flexibility have been considered in this document because it is intended to explore how linear response history analysis (LRHA) can be applied in buildings modeled using the given definitions of rigid and semirigid diaphragms.

The modeling aspects of rigid and semirigid diaphragms are discussed in the first part of this chapter, and the differences between these two diaphragm conditions are shown by calculating the interstory drift in four buildings subjected to acceleration histories such that their spectrum matches a defined target spectrum. The second section of this chapter refers to accidental torsion for linear response history analysis, and it gives background in the basis of accidental torsion, it describes the provisions given by other seismic codes, and it analyzes static and dynamic procedures for modeling accidental torsion assuming static methods as an alternative to measure accidental torsion in a dynamic analysis. Static methods given by different seismic codes are described as well as new suggested methods that include variables not considered yet in ASCE 7-10. Moreover, the discussion of torsional records and torsional

spectrum is discussed in this chapter. Finally, recommendations are given for modeling the effects of diaphragm flexibility and accidental torsion.

The reader is addressed to the Appendix E of this document for explanation of abbreviations not specified within the text.

4.1 Diaphragm Flexibility

The modeling of a building floor using rigid diaphragms can be used if it is desired to reduce the number of degrees of freedom (DOF) of a system when using response spectrum analysis (RSA) or linear response history analysis (LRHA); however, the capabilities of current available software do not require a reduction in the DOF, because the response of a building including those DOF can be obtained in a short amount of time. For instance, Table 4-1 shows the time required for the analysis of three acceleration histories using Modal response spectrum analysis (Modal RSA), Modal linear response history analysis (Modal LRHA), and Direct Integration, in four buildings modeled with semirigid and rigid diaphragms. The three acceleration histories used in this analysis correspond to the record components with highest PGA of the records A, B, and D in Table B- 13. The number of points and the time step of these acceleration records is specified in Table B- 13. Additionally, the values corresponding to the Direct Integration procedure in Table 4-1 did not include the time required to find the mode shapes. Six mode shapes were used for modal analysis of these buildings to guarantee the inclusion of at least 90% of the effective mass in all the models. The analyses were run with SAP2000 (Computer and Structures Inc, 2009) in a computer with processor Intel I5 2.53GHz.

Table 4-1 Time required for running the analysis of three acceleration histories using modal response spectrum analysis, modal linear response history analysis, and direct integration, in four buildings with the same plan view and different number of stories

Number of stories	Using semirigid diaphragms			Using rigid diaphragms		
	Time for Modal LRHA (hours)	Time for Modal RSA (hours)	Time for Direct Integration (hours)	Time for Modal LRHA (hours)	Time for Modal RSA (hours)	Time for Direct Integration (hours)
5	0:00:14	0:00:05	0:24:54	0:00:06	0:00:02	0:20:07
15	0:00:20	0:00:10	1:05:43	0:00:10	0:00:06	1:00:24
25	0:00:27	0:00:16	1:50:09	0:00:15	0:00:10	1:42:05
35	0:00:33	0:00:21	*	0:00:19	0:00:14	*

*The time required for these analyses exceed 5 hours, which is considered a period of time excessive and impractical in consulting practice. Therefore, these analyses were interrupted at 5 hours.

From Table 4-1 it can be noticed that the analysis of the three selected acceleration histories using Modal LRHA and Modal RSA is very small and takes only a few seconds regardless if the floors are modeled using rigid or semirigid diaphragms. This fact demonstrates that the time required to perform a modal linear response history analysis is small and equivalent to the time required for a modal response spectrum analysis. However, when the buildings were analyzed using direct integration, the time required for the analysis increased significantly for both diaphragm conditions (rigid and semirigid) if comparing to the same values required for a Modal LRHA.

4.1.1 Linear Response History Analysis using rigid diaphragms

The modeling of buildings with rigid diaphragms for linear response history analysis can be done using two procedures. First, the mass of each floor can be distributed along each shell element used for the modeling of that floor, and the rigid condition is applied by creating a constraint such that all the nodes within the floor will displace the same amount. The second procedure consists in using shell elements with zero mass for the modeling of each floor, and concentrating the translational and rotational mass of that floor at its center of mass Then, a constraint for equal displacement of the nodes within the floor (including the node located at the center of mass of each floor) is applied. The translational mass in each floor is equal to its own mass while the rotational mass is given by the following expression:

$$I_o = \int_{Vol} r^2 dm = \rho t(I_x + I_y) \qquad \textbf{Eq. 4- 1}$$

where all the terms apply to a specific floor, and:

I_o is the rotational mass

r is the distance from the center of mass to any point in that floor

dm is the differential of mass

ρ is the mass density in units of mass per volume

t is the thickness of the slab of that floor

I_x is the moment of inertia of that floor about the axis X

I_y is the moment of inertia of that floor about the axis Y

X and Y are two orthogonal axis that pass through the center of mass of that floor

For the particular case of a rectangular floor with dimensions a and b, total mass m, and center of mass coinciding with the geometric center of the floor, Eq. 4- 1 produces:

$$I_o = \frac{m(a^2 + b^2)}{12} \qquad \textbf{Eq. 4- 2}$$

Furthermore, the rotational mass at each floor has contributions from any linear mass associated usually with the mass of the perimeter walls. For design purposes it is tedious to include the contributions from the linear masses; however, the results obtained are more accurate when including them. For instance, Table 4-2 shows the contributions to the rotational mass in each floor by the diaphragm and by the linear masses for the building analyzed by Charney et al. (2010b). The average of the contribution of linear masses is 9.3% of the total rotational mass excluding the floor 1, which has a bigger contribution due to the fact that the mass of the basement walls was also associated to this floor. The assumption of ignoring the calculation of the linear masses depends on the designer; however, a good approach in this case would be to amplify the rotational mass from the diaphragm itself by a factor to include the contribution of the linear masses. For instance, such factor would be equal to 1.0/(1.0-0.093) = 1.10 for the example shown; however, it will depend in each case of the weight of the perimeter walls.

Table 4-2 Contribution to the rotational mass at each floor by the mass of the diaphragm and by the linear masses, for the building analyzed by Charney et al. (2010)

Level	Contribution Diaphragm (%)	Contribution Linear Masses (%)	Total
13	90.97	9.03	100
12	88.70	11.30	100
11	88.70	11.30	100
10	88.70	11.30	100
9	93.54	6.46	100
8	90.45	9.55	100
7	90.45	9.55	100
6	90.45	9.55	100
5	94.13	5.87	100
4	91.39	8.61	100
3	91.39	8.61	100
2	89.70	10.30	100
1	71.27	28.73	100

The contribution from the linear masses to the rotational moment of inertia can be analyzed in a rectangular floor with sides *a* and *b* and total mass *m* by looking at the ratio I_2/I_1, where I_1 is the rotational moment of inertia of a story with mass *m* distributed within the diaphragms only and where I_2 is the rotational moment of inertia of a story with mass *m* distributed so that αm is a linear mass distributed along the perimeter of the story and $(1-\alpha)m$ is the mass distributed within the diaphragm as it is shown in Figure 4-1.

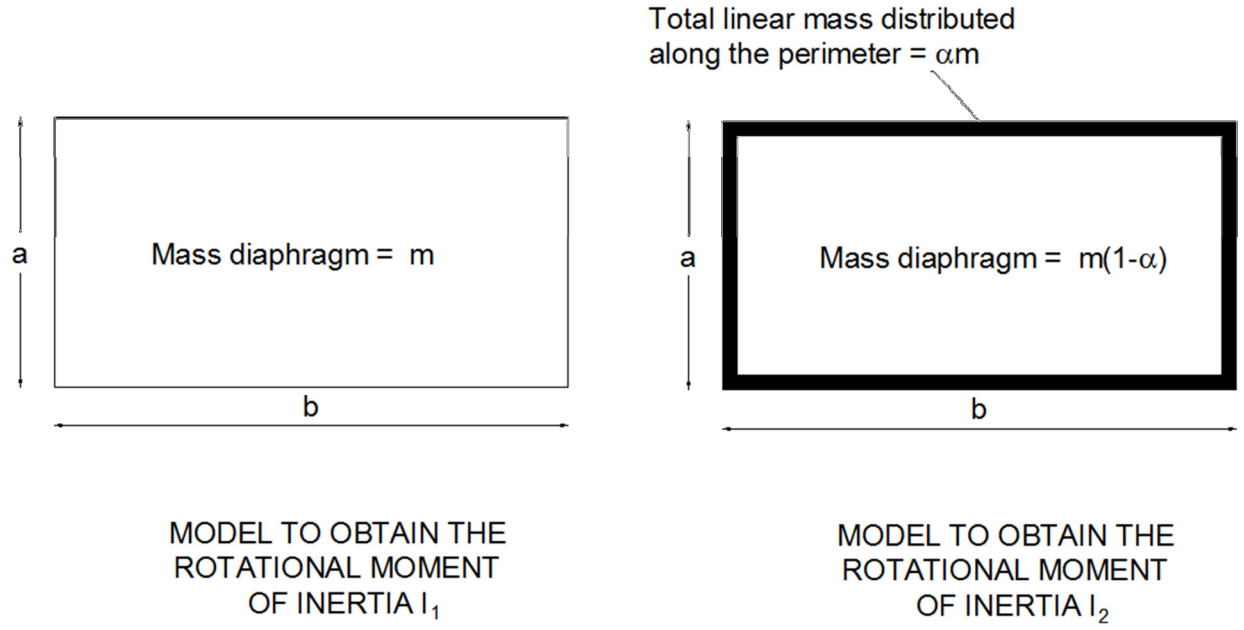

Figure 4-1 Models to obtain the rotational moment of inertia I_1 and I_2 when the a portion of the mass of the diaphragms is distributed along the perimeter of a rectangular floor

The ratio I_2/I_1 depends on the ratio a/b, and it varies according to the equation shown below:

$$\frac{I_2}{I_1} = \frac{\left(\frac{a}{b}\right)^2 + 2\alpha\left(\frac{a}{b}\right) + 1}{\left(\frac{a}{b}\right)^2 + 1} \qquad \textbf{Eq. 4- 3}$$

Figure 4-2 shows the ratios I_2/I_1 plotted for different ratios a/b, and it can be noticed that I_2 is always greater than 1.00 for any value of α, which means that the rotational moment of inertia in each floor of a rectangular shape building when modeling specifically perimeter linear

masses is greater than the rotational moment of inertia when distributing such linear masses as a uniform mass within the diaphragm.

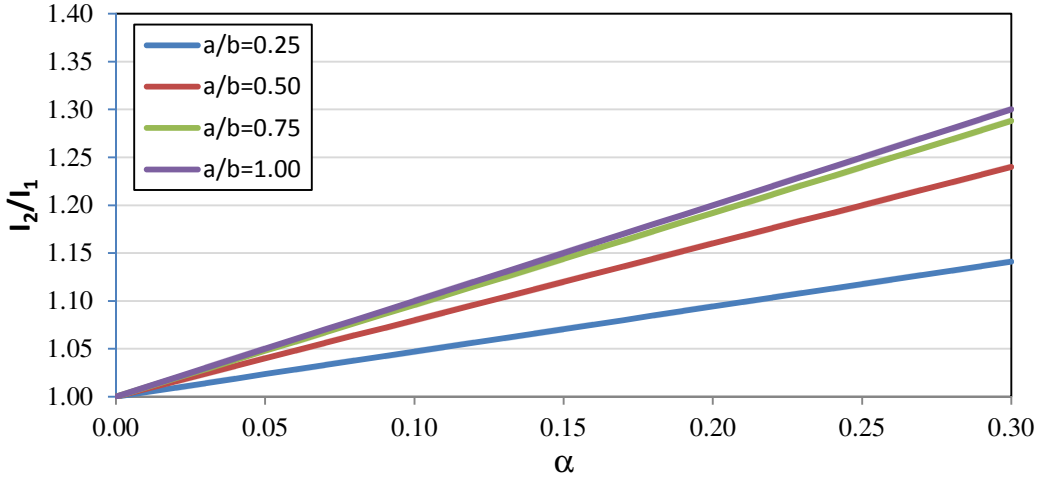

Figure 4-2 Ratio of rotational moments of inertia I_2/I_1 for different values of α and for different ratios a/b

4.1.2 Linear response history analysis using semirigid diaphragms

When using linear response history analysis in buildings with floors that are modeled with semirigid diaphragms, the mass of each floor is distributed along the shell elements used in the modeling of that floor. There is not any type of constraint applied to the nodes within a floor when using semirigid diaphragms. Also, the effect of linear masses can be easily captured when using semirigid diaphragms, because the contributions from these linear masses to the global mass matrix can be directly accounted by the structural analysis program used, i.e. SAP 2000 (Computer and Structures Inc, 2009).

4.1.3 Differences in results for linear response history analysis (LRHA) when using rigid and semirigid diaphragms

The differences in the results when doing linear response history analysis in buildings modeled with rigid and semirigid diaphragms can be significant when using different structural systems in parallel resisting planes of a building (i.e. dual systems), because in such cases, the differences in the stiffness of the resisting planes causes larger forces and strains in the diaphragms.

Four different buildings were subjected to three different ground motions in order to study the differences in the interstory drifts when they are modeled using rigid and semirigid diaphragms. The buildings correspond to the Building 1, Building 2, Building 3, and Building 4 as specified in the Appendix A, and they were analyzed by orienting the ground motions in their Y direction (the direction Y of each building is specified in the same Appendix A). These four buildings had different lateral load resisting systems; for instance, Building 1 had concrete moment frames resisting the lateral loads, while Building 2 had steel perimeter frames. Also, Building 3 had concrete shear walls to resist lateral load and Building 4 had steel perimeter frames. The four buildings are denoted in this section as B1, B2, B3, and B4 corresponding to the Buildings 1, 2, 3, and 4, respectively. The buildings B1, B3, and B4 were symmetrical and only B2 was nonsymmetrical. Only one building with a dual system was chosen (B3), and future research about the differences in buildings modeled with rigid and semirigid diaphragms should include the analysis of more buildings of this type.

Regarding the record components used in the analysis, they correspond to the components with highest PGA of the records A, B, and D of Table B- 13. Such record components are denoted as EQ1, EQ2, and EQ3 in correspondence with the records A, B, and D, respectively.

The modeling of these buildings using semirigid diaphragms was done by adding superficial gravity loads to the shell elements in each floor, while for the case of rigid diaphragms the calculations of the translational and rotational mass in each floor are shown in Table C- 1, Table C- 2, Table C- 3, and Table C- 4 (Appendix C) for Building 1, 2, 3, and 4, respectively.

The diaphragms were modeled with shell elements using the same thickness for membrane and bending elements. In the case of the buildings B1, B3, and B4 the thickness of the shell elements correspond to the slab thickness specified in the Appendix A, and those values correspond to 5 in, 5 in, and 5.5 in for buildings B1, B3, and B4, respectively. The same thickness was used at all the stories in buildings B1, B3, and B4. For the case of the building B2 the thickness of each story was modified to include the weight of all the additional superficial load (i.e. ceiling, mechanical) within the thickness of the slab, and specific calculations of these thickness can be found in Charney et al. (2010b).

The results for the interstory drift of the four described buildings under the records EQ1, EQ2, and EQ3 are shown in Figure 4-3, Figure 4-4, and Figure 4-5, respectively, where the abbreviations R and SR account for the models build using rigid (R) and semirigid (SR) diaphragm conditions. From these figures it can be seen that almost identical results were obtained for the four buildings using both diaphragm assumptions.

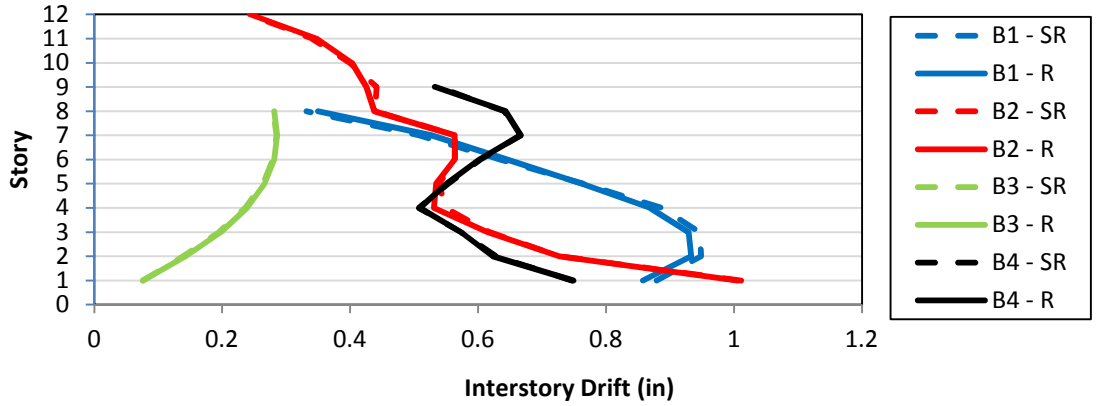

Figure 4-3 Envelope of interstory drift in Buildings 1 (B1), Building 2 (B2), Building 3 (B3) and Building 4 (B4) for the earthquake EQ1

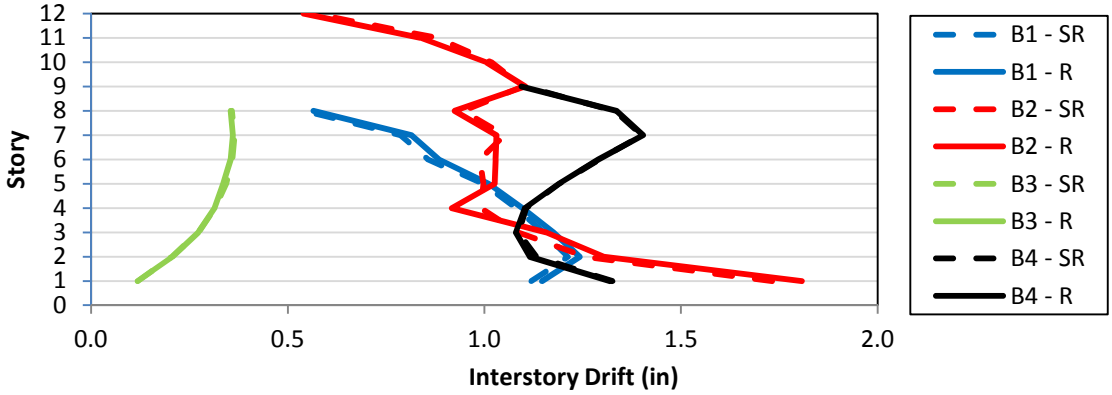

Figure 4-4 Envelope of interstory drift in Buildings 1 (B1), Building 2 (B2), Building 3 (B3) and Building 4 (B4) for the earthquake EQ2

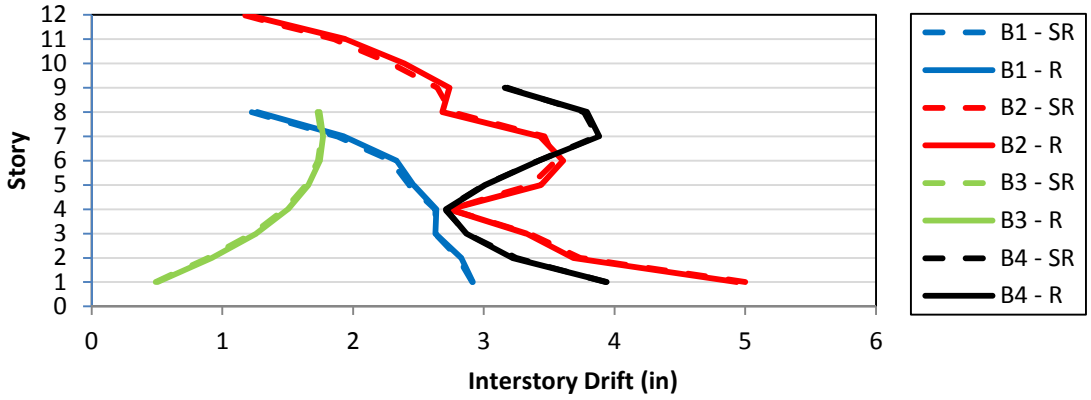

Figure 4-5 Envelope of interstory drift in Buildings 1 (B1), Building 2 (B2), Building 3 (B3) and Building 4 (B4) for the earthquake EQ3

Although the interstory drift for each of the four buildings analyzed was very similar when using rigid and semirigid diaphragms, it is recognized that large differences of the shears in the structural components are possible with even minor differences in the drifts. The shears in the structural components could be the issue with more sensitivity to the assumptions in the flexibility of the diaphragms, and therefore further research is encouraged in this topic.

Another issue of significant importance is the level of the discretization of the mesh used for the modeling of the floor diaphragms. If the designer prefers the use of rigid diaphragms, a mesh with one shell element per floor panel (rectangular region between with adjacent columns in each corner) could be enough to perform a lateral load analysis. However, the same model might require a higher level of discretization for gravity load analysis (or any combination of gravity and lateral load) because in this case the connectivity between the diaphragm and the beams is of significant importance to obtain appropriate design forces in the beams. Also, if the designer prefers the use of semirigid diaphragms, the modeling with one shell element per panel might not be appropriate because one of the purposes of modeling with semirigid diaphragms could be to identify differential displacements at different locations within the same floor panel.

4.1.4 Recommendation for diaphragm flexibility

The preference of using rigid or semirigid diaphragms depends on the magnitude of the stiffness of the diaphragm relative to the stiffness of the seismic components, and without a pre-analysis using both diaphragm conditions, it will be very difficult to predict which assumption would be more appropriate. Therefore, it is recommended to do a pre-analysis calculating

response measures like interstory shear or interstory displacement using rigid and semirigid diaphragms, and if the results are similar, it could be more convenient to use rigid diaphragms. However, if the differences in the results are important then the use of semirigid diaphragms would be a better option.

Also, caution should be considered with respect to the required number of modes to capture 90% of the mass, since this number might be considerably bigger when using semirigid diaphragms than when using rigid diaphragms. Additionally, the appropriateness of using rigid or semirigid diaphragms will depend on how the accidental torsion is modeled in each case, and such modeling of the accidental torsion for both diaphragm assumptions is covered in the next section.

4.2 Accidental Torsion

The modeling of accidental torsion in linear response history analysis (LRHA) might have different approaches depending on if the diaphragms are modeled using rigid or semirigid diaphragms. This section explores the basics of accidental torsion, the variables that have to be considered for accidental torsion in any code procedure, the code language for accidental torsion in different codes, and the appropriateness and alternatives of using static and dynamic procedures that could be used to include accidental torsion in LRHA.

4.2.1 Basics of accidental torsion

The sources of torsion in a building can be divided in two groups: inherent torsion and accidental torsion. The inherent torsion accounts for the coupling between translational and torsional response due to lack of symmetry of the building, while the accidental torsion accounts for uncertainties in the location of the center of mass, differences between the theoretical and real stiffness, excitation at the base of the building due to rotational component of ground motions, and other sources of accidental torsion not included specifically in the analysis (De la Llera and Chopra, 1994a). Building codes usually account for torsional effects by applying the lateral forces at a distance e_d from the center of stiffness given by:

$$e_d = \alpha e_s + \beta b \qquad \textbf{Eq. 4- 4}$$

$$e_d = \gamma e_s - \beta b \qquad \textbf{Eq. 4- 5}$$

where $e_d =$ eccentricity measured from the center of stiffness (denoted hereafter CS)

e_s = static stiffness eccentricity (difference between the center of mass and the center of stiffness of an specific floor)

α, β, and γ = parameters that vary with different seismic codes (see Table 4-3)

b = maximum dimension in the direction perpendicular to the applied load

Figure 4-6 explains graphically the terms used in Eq. 4- 4 and Eq. 4- 5 for a floor symmetric about the vertical axis Y and nonsymmetrical with respect to the X axis and the intended location to apply an acceleration record $a_{gy}(t)$ parallel to the Y axis. It is identified in Figure 4-6 the center of mass of the floor CM, the center of stiffness CS, the static eccentricity e_s, and the two design eccentricities e_d corresponding to Eq. 4- 4 and Eq. 4- 5. Also, it has been identified in the same figure the stiff and flexible sides of the floor, which are defined as follows: the stiff side is defined as the distance between the center of stiffness CS to the edge located towards the opposite direction of center of mass CM relative to the CS; for instance, in the case of Figure 4-6 the stiff side is located towards the right side of the CS because the CM is located towards the left of the CS. On the other hand, the flexible side of a floor is the distance between the CS and the edge of the floor located in the same direction of the CM relative to the CS.

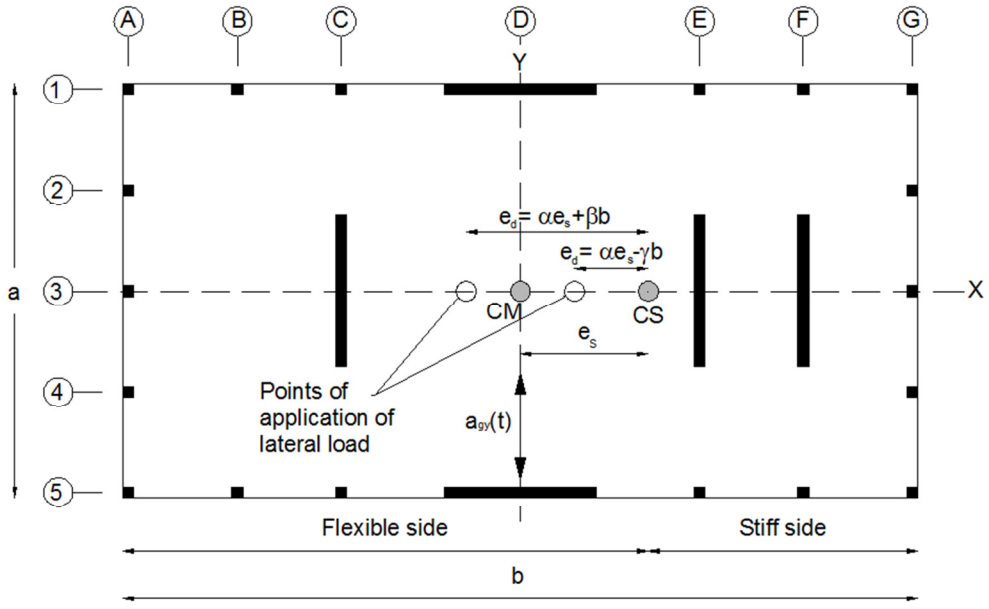

Figure 4-6 Terminology for the definition of inherent and accidental torsion in seismic codes

The resisting planes of a structure can be defined as the structural systems (i.e. moment frames, shear walls) along axis parallel to the applied lateral load; for instance, in the case of Figure 4-6 the resisting planes for earthquake loads applied parallel to the Y direction are the lateral load resisting systems that pass through the axes A, B, C, D, E, F, and G. Eq. 4- 4 and Eq. 4- 5 control the design of the resisting planes located at the flexible and stiff sides of the building, respectively. The first term in Eq. 4- 4 and Eq. 4- 5 accounts for inherent torsion (distance between the center of mass CM and the center of stiffness CS), while the second term accounts for accidental torsion.

When α or γ in Eq. 4- 4 and Eq. 4- 5 are different than 1.0, the design eccentricities require the explicit calculation of the location of the center of stiffness of each floor, although procedures have been implemented to skip this step (Goel and Chopra, 1993). Since ASCE 7-10 does not require amplification of the inherent torsion ($\alpha = \gamma = 1.0$), the location of the actual center of rigidity is not required. The values of α, β, and γ used by different codes are shown in Table 4-3, and such information will be complemented in Section 4.2.2. Also, the note "implicit" in the values of α and γ of Table 4-3 indicates that these seismic codes assume implicitly values of α and γ equal to 1.00 since they require measurement of the design eccentricity relative to the center of mass of the building CM instead of relative to the center of stiffness CS.

Table 4-3 Values of α, β, and γ for definition of inherent and accidental eccentricity given by different seismic code

Code	Parameter		
	α	γ	β
ASCE7-10	1.00 (implicit)	1.00 (implicit)	0.05
NBCC	1.00*	1.00*	0.10**
NZS	1.00 (implicit)	1.00 (implicit)	0.10
MXS	1.50	1.00	0.10
EC8	1.00 (implicit)	1.00 (implicit)	0.05

* Defined explicitly for accidental torsion using static procedures and defined implicitly for accidental torsion in dynamic procedures

** It allows β=0.05 for some cases as explained in Section 4.2.2.2 of this document.

From Table 4-3 it can be seen that the design eccentricities for ASCE 7-10 are equal to ±0.05b as shown in Figure 4-7.

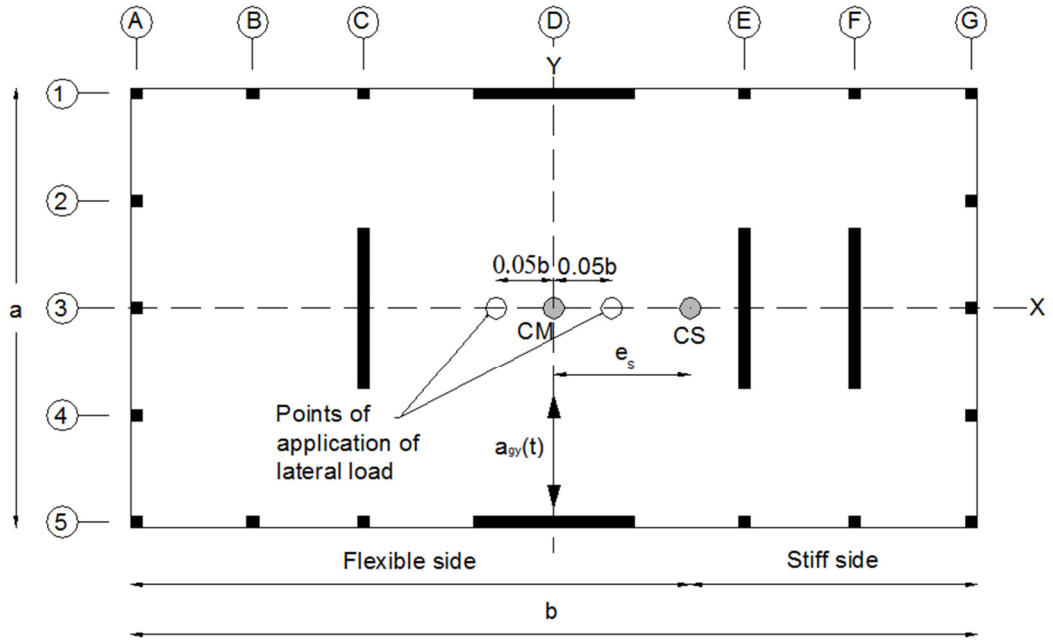

Figure 4-7 Design eccentricities used in the American standard ASCE 7-10

Also, it is important to identify the most important variables that influence the results of accidental torsion, because those are the factors that are required to be present in any seismic code language regarding application of accidental torsion. Some of these variables, which have been mentioned by De la Llera and Chopra (1994a), are:

T_x, T_y, T_θ: Uncoupled lateral vibration periods of the structure (T_x and T_y), and fundamental torsional period (T_θ). The corresponding circular frequencies of these periods are ω_x, ω_y, and ω_θ, and they can be estimated using Rayleigh's method (De la Llera and Chopra, 1994a). Another procedure for obtaining the lateral uncoupled periods T_x and T_y in a non-symmetrical building consists in adding restraints to the perimeter nodes of the mathematical model of the building such that it allows displacement only along its principal direction (no twisting).

Ω: "Ratio between ω_θ and ω_y (or ω_x), the fundamental torsional and lateral frequencies of hypothetical symmetric-plan building defined by lateral and torsional stiffness matrices K_y (or K_x) and K_θ, equal to those of the actual

building." (De la Llera and Chopra, 1994a). It should be noticed that K_y, K_x and K_θ, correspond to the stiffness matrixes of a hypothetical (and not real) symmetrical building where the translational and rotational periods are uncoupled, and it does not mean that the total stiffness matrix of the real system could be obtained as $K = K_x + K_\theta$.

e/r: Ratio of the static eccentricity to the rotational radius of gyration

b: Largest dimension of the building perpendicular to the applied lateral load

b/a: Aspect ratio, where b is the plan dimension of the building perpendicular to the lateral load and a is the other dimension of the building

4.2.2 Provisions for accidental torsion given in seismic codes

The provisions to include accidental torsion in ASCE 7-10 and other seismic codes were explored to study the differences in each method and to investigate if there is any specific provisions for linear response history analysis (LRHA). The application of accidental torsion with static and dynamic methods is revised considering that the possible complexities associated with the application of accidental torsion with dynamic methods might force the use of static torques for measuring accidental torsion in LRHA.

4.2.2.1 Accidental torsion provisions of ASCE 7-10

Section 16.1.5 of ASCE 7-10 addresses the application of accidental torsion in LRHA with the same procedure specified for the equivalent lateral force (ELF) method in its section 12.8.4. This provision was recently added to ASCE 7-10 because ASCE 7-05 did not have such requirement. The provisions for the application of accidental torsion using the ELF method specifies that the design has to include the moments produced by the inherent torsion and by the accidental torsion, and the latter can be obtained by assuming the center of mass is displaced 5% of the dimension perpendicular to the lateral loads applied. The displacement of the center of mass is justified, because studies done by De la Llera and Chopra (1994a) showed that the uncertainty in the center of mass together with the uncertainty in the stiffness of the elements contributes to 70% of the total increase in response due to accidental torsion. The response measure corresponds to the mean-plus-one standard deviation of the "normalized edge displacement," which is defined as the ratio of μ_x* and μ_x, where μ_x* is the displacement at the edge of a floor considering the effect of all the sources of accidental torsion and μ_x is the

displacement at the same location but neglecting accidental torsion. Also, the inherent torsion can be taken into account directly by applying the resultant of the lateral loads of each floor at the center of mass of that level instead of applying those loads at the center of stiffness.

Dynamic analysis including torsional effects can be included in structures modeled with rigid diaphragms by displacing the center of mass the eccentricity ±0.05b; however, the application of torsional effects using dynamic procedures for structures modeled using semirigid diaphragms is not specified in ASCE 7-10 (nor it is specified in the NBCC, NZS, EC8, MXS or the CHS). Also, the conditions for the amplification of accidental torsion in ASCE 7-10 for LRHA are the sane than those given when applying the ELF method, and they are specified in Section 12.8.4.3 of ASCE 7-10.

4.2.2.2 Accidental torsion provisions of the National building Code of Canada (NBCC)

The NBCC (Canadian Commission on Building and Fire Codes, 2005) establishes a limit where static and dynamic methods can be applied to estimate accurately the increase in response due to accidental torsion. This limit is established by calculation of the torsional sensitivity factor B, which is defined as the biggest value of B_x in each orthogonal direction where B_x is equal to:

$$B_x = \frac{Max\ Disp}{Ave\ \ Disp} \qquad \textbf{Eq. 4- 6}$$

where Max Disp is, according to the NBCC, the "maximum *storey* displacement at the extreme points of the structure, at level x in the direction of the earthquake induced by the equivalent static forces acting at distances ±0.10 D_{nx} from the centers of mass at each floor."

Ave Disp is, according to the NBCC, the "average of the displacements at the extreme points of the structure at level x produced by the above mentioned forces." The expression "above mentioned forces" refers to the equivalent static forces that are used to calculate Max Disp.

B_x is given by the maximum of the individual values of B_x at each floor

D_{nx} is the widest building dimension perpendicular to the lateral load applied

The NBCC specifies that accidental torsion can be taken into account by static moments with eccentricity $0.10D_{nx}$ from the center of mass if B is less than 1.7; otherwise, and for the case where $I_E F_a Sa(0.2) \geq 0.35$, it is required to follow a dynamic procedure using the design eccentricities given by the NBCC (see Eq. 4- 4, Eq. 4- 5, and Table 4-3). The coefficients I_E and F_a, are defined in the NBCC as the earthquake importance factor and the acceleration-based site coefficient, while $Sa(0.2)$ is the 5% spectral response acceleration in g units for a period T=0.2 sec. The limit of $B \leq 1.7$ was derived so that the ratio Ω between the uncoupled torsional and translational frequencies would be greater than 1 (Humar et al., 2003), because values of Ω less than that produces a significant increase in structural response that cannot be predicted by static analysis.

For the case of dynamic analyses (either RSA, LRHA, or NLRHA) two procedures are stated in the NBCC to account for accidental torsion; the first of them is applicable to any value of the torsional sensitivity factor B, and it requires the application of static moments resulting from displacing the center of mass $0.10D_{nx,}$ and using lateral forces derived from a static or dynamic analysis. Then these results need to be combined with those from the dynamic analysis without accidental torsion. The second of these procedures is applicable only for the case where $B<1.7$ (structures defined in the NBCC as not torsionally sensitive), and it requires the calculation of torsional effects displacing the center of mass by only $0.05D_{nx}$ (instead of $0.10D_{nx}$) as long as a dynamic analysis is performed. As it can be noticed, the eccentricity of the center of mass in both procedures is different, and it is larger for the case when using static moments, because as stated in the Commentary section of the NBCC (Canadian Commission on Building and Fire Codes, 2006) the first procedure (eccentricity from the center of mass $0.10D_{nx,}$) "includes a dynamic amplification of the static effect of accidental eccentricity."

4.2.2.3 Accidental torsion provisions of the New Zealand Standard (NZS)

The provisions for accidental torsion given by the New Zealand Standard NZS 1170.5 (Council of Standards New Zealand, 2004) state that the accidental eccentricity has to be measured from the center of mass, and it is equal to ±0.10 of the dimension perpendicular to the load applied. Also, the NZS provides important information about the direction of the eccentricity at various levels, and the procedure to follow when the lateral loads are applied in directions not coinciding with the principal axis of the structure (the principal axis of a structure could be defined as the axis parallel to the directions given by the mode shapes corresponding to

the fundamental translational periods). The latter case might be useful for buildings located near fault regions where the analysis might require the application of lateral load not coinciding with the principal axis of the structure, because in this case, the realistic orientation of expected ground motions relative to the orientation of the analyzed building has to be considered.

The NZS in its Section 5.3.2 states that "The eccentricity shall be applied in the same direction at all levels," and this requirement is not stated anywhere in the ASCE 7-10 provisions. Also, the NZS states that "For actions applied in other directions, the accidental eccentricity may be assumed to lie on the outline of an ellipse with semi-axis equal to the eccentricities specified for the orthogonal directions." The application of this principle is presented in Figure 4-8 where it is assumed that the principal directions of the building are given by the X and Y axis. Figure 4-8 shows the original location of the center of mass, denoted CM, and it shows the points P and Q that corresponds to the center of mass displaced towards the left and towards the right, respectively; such points P and Q are obtained from the intersection of a line perpendicular to the direction of ground motion that crosses the center of mass and the ellipse with semi-axis equal to 0.10a and 0.10b where a and b are the biggest dimensions of the building in the two principal directions for that particular story.

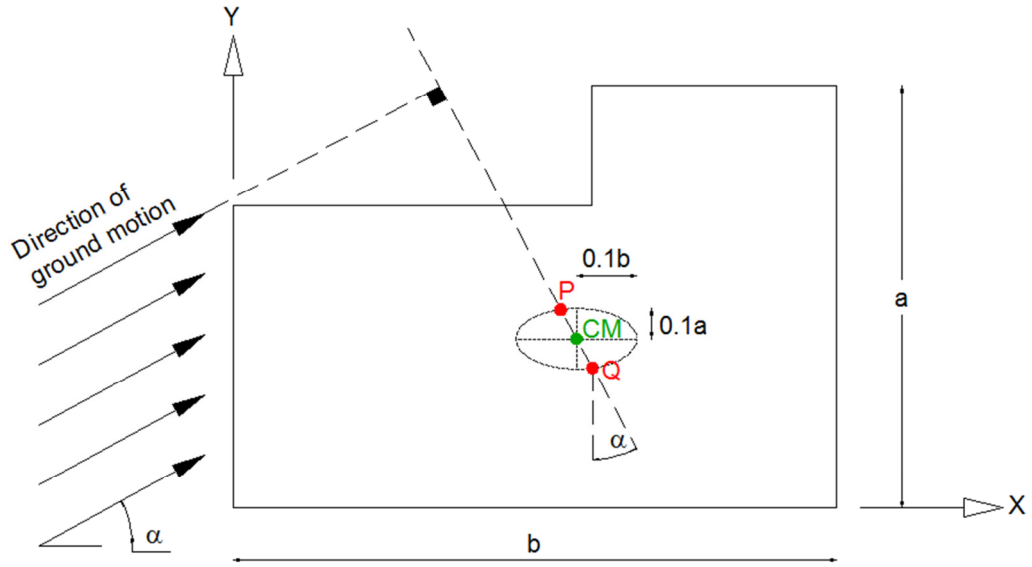

Figure 4-8 Application of accidental torsion according to the New Zealand Standard for a ground motion which direction differs from both principal axis of a structure

Additional provisions for torsion are described in Section 6.3.5 of the NZS, which corresponds to the modal response spectrum method, and it limits the use of static analysis for torsional effects only for regular structures "not classified as plan irregular" (plan irregularity conditions according to the NZS are defined in its Section 4.5.2) that are analyzed with a bi-dimensional model. For other type of structures, it is specified two options to include the torsional effects in a three-dimensional model; the first of them consist in adjusting the location of the center of mass with the design eccentricity (0.10b) but keeping the original value of the rotational inertia of the floor, while the second method states to keep the location of the center of mass constant but adjust the line of action of the earthquake load so it is applied eccentrically. Specifications for the application of the second method are given in the commentary to the NZS (Council of Standards New Zealand, 2004b). These two approaches are explicit for the case of using rigid diaphragms.

The NZS does not describe specific procedures for the application of accidental torsion for the case of LRHA, but it could be assumed that those guidelines should follow the procedures specified for the modal spectrum analyses as described in the paragraph above.

4.2.2.4 Accidental torsion provisions of the Eurocode 8 (EC8)

When using a static analysis for lateral loads, Section 4.3.3.2.4 of the Eurocode 8 (British Standards, 2004) states two procedures; the first of them requires the calculation of static moments using the design eccentricity $0.05L_i$ (measured from the center of mass), where L_i is the dimension of the building perpendicular to the load applied for that particular floor. Also, the second method uses an amplification factor that magnifies the results in each frame, without considering accidental torsion, by a factor that is proportional to the distance of such frame to the center of mass of the floor under consideration. The specific formula to calculate the amplification factor is given in the EC8 (Eq. 4.12), and it includes the terms x and L_e, where x is defined as the distance between the analyzed frame and the center of mass, and L_e is the distance between the outermost lateral resisting frames. Figure 4-9 shows the definitions of x and L_e, and Table 4-4 indicates the resulting amplification factors for frames located at different distances from the center of mass.

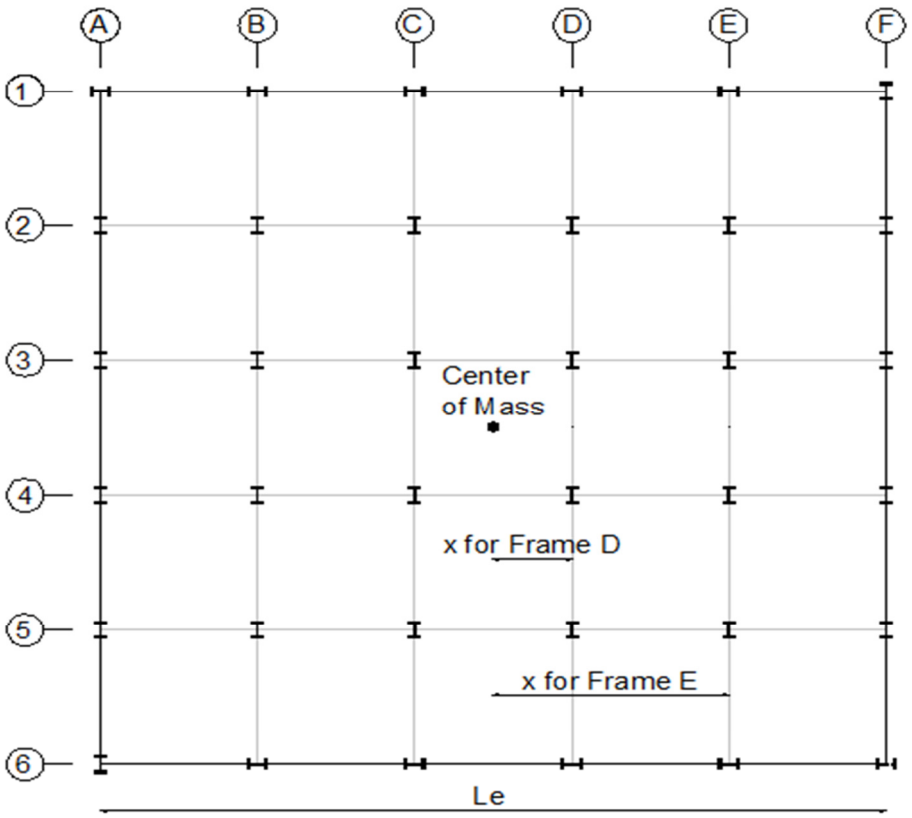

Figure 4-9 Definition of parameters x and Le required for the calculation of the amplification factor for accidental torsion given by the EC8

Table 4-4 Amplification factor for accidental torsion given by the EC8 for frame located at different distances from the center of mass

Distance from center of mass: x	Amplification Factor
$0.0L_e$	1.00
$0.1L_e$	1.06
$0.2L_e$	1.12
$0.3L_e$	1.18
$0.4L_e$	1.24
$0.5L_e$	1.30

As it can be seen in Table 4-4, the amplification factor varies from 1.0 for a frame located along the line that passes through the center of mass to 1.3 for the most exterior frame. This methodology is specified only for structures where the mass and the lateral stiffness are symmetrically distributed along the floor, and there are additional requirements for structures modeled only in two dimensions, where the EC8 specifies that the design eccentricity should be increased from $0.05L_i$ to $0.1L_i$ (for more accurate procedures than the one explained using amplification factors), and the upper limit of the amplification factor should be increased from 1.3 to 1.6.

For the case of doing a modal response spectrum analysis, the EC8 specifies the use of static moments to account for accidental torsion, and those moments will be obtained by multiplying the static lateral forces by the design eccentricity $0.05L_i$ for structures modeled in 3D and by the design eccentricity $0.10L_i$ for structures modeled in 2D.

4.2.2.5 Accidental torsion provisions of the Chilean Standard (CHS)

The Chilean standard (Instittuto Nacional de Normalizacion, 1996) requires the application of static torques to consider the effects of accidental torsion in static analysis, and those static moments are calculated using the eccentricity given by:

$$e = \pm 0.10\, b\, Z / H \qquad \textbf{Eq. 4- 7}$$

where b is the dimension of the floor in the direction perpendicular to the load applied
Z is the high of the analyzed floor measured from the base
H is the high of the building measured from the base

For the case of modal spectrum analysis, the Chilean standard specifies two procedures; the first of them is the same method used for static analysis, and the second procedure states to displace the center of mass an eccentricity 0.05b with the same direction at all the floors.

There is a fact of particular importance in the Chilean standard, and it is that the eccentricity given for the application of the static moments is not a constant for each floor, but it varies linearly from the base of the building until it gets a maximum value of 0.1b at the top of the building. Figure 4-10 shows different values of the required eccentricity at different ratios of Z/H which can also be interpreted as different heights of a building.

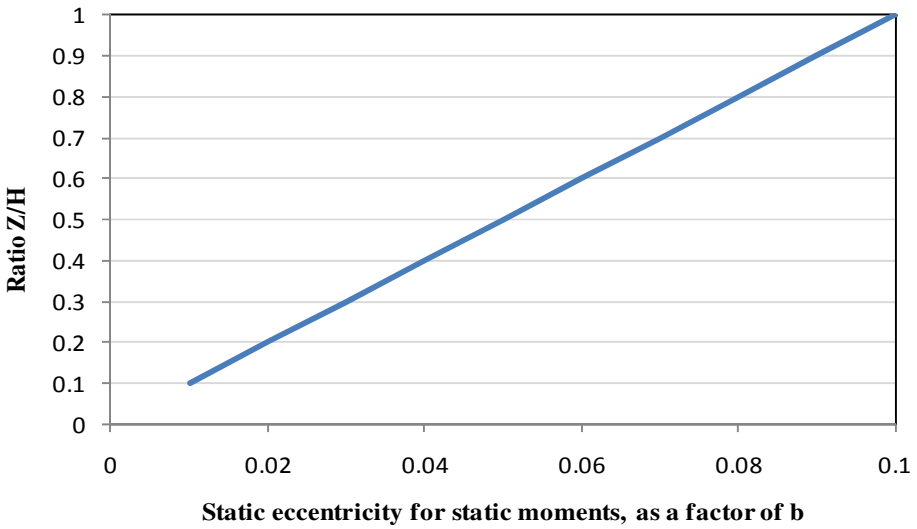

Figure 4-10 Static eccentricity for application of static moments in the Chilean Standard for different ratios Z/H

The linear distribution of eccentricities implies having a static moment distribution different than the distribution of the static forces since eccentricities and static forces are multiplied together to get the final distribution of moments. For instance, Table 4-5 shows the calculation of the static moments for the same set of lateral loads using the constant eccentricity of ASCE 7-10 and the variable eccentricity of the Chilean standard. The set of lateral loads denoted as F_x in the fourth column of Table 4-5 corresponds to the lateral loads used by Charney et al. (2010b) in the analysis of a twelve story building. It can also be noticed in Table 4-5 that the total static moments, which are 11807 kips-ft for ASCE 7-10 and 16979 kips-ft for the CHS, are significantly different. Figure 4-11 shows the resulting static moments from Table 4-5, and as expected, the static moments from the CHS are smaller than those of ASCE 7-10 for the lower half of the building and bigger for the upper half of the building. It should be noticed that at the highest level of the building the static moment from the CHS is twice the one from ASCE 7-10.

After reviewing the regulations from different seismic codes regarding accidental torsion, it was noticed that the application of static moments is considered an option to account for accidental torsion in a dynamic analysis; therefore, it is necessary to analyze alternative procedures that use the results from a static analysis to estimate the effects due to accidental

torsion in a dynamic analysis. These alternative procedures include variables not specified in the current provisions of ASCE 7-10

Table 4-5 Comparison of static moments between ASCE 7-10 and the CHS, for the same set of static lateral loads corresponding fo the Building 2 of Appendix 1

Level	Z	Z/H	F_x	Ecc. ASCE 7-10*	Ecc. CHS **	Static Moment ASCE7-10	Static Moment CHS	Accum. Torque ASCE7-10	Accum. Torque CHS
	(ft)		(k)	(ft)	(ft)	(k-ft)	(k-ft)	(k-ft)	(k-ft)
13	155.50	1.00	186.92	10.50	21.00	1963	3925	1963	3925
12	143.00	0.92	154.01	10.50	19.31	1617	2974	3580	6900
11	130.50	0.84	129.86	10.50	17.62	1364	2289	4943	9188
10	118.00	0.76	107.63	10.50	15.94	1130	1715	6073	10903
9	105.50	0.68	186.25	10.50	14.25	1956	2654	8029	13557
8	93.00	0.60	100.83	10.50	12.56	1059	1266	9088	14823
7	80.50	0.52	77.04	10.50	10.87	809	837	9897	15661
6	68.00	0.44	56.24	10.50	9.18	590	516	10487	16177
5	55.50	0.36	71.42	10.50	7.50	750	535	11237	16713
4	43.00	0.28	31.47	10.50	5.81	330	183	11567	16895
3	30.50	0.20	16.58	10.50	4.12	174	68	11742	16964
2	18.00	0.12	6.26	10.50	2.43	66	15	11807	16979
*Calculated as 0.05b					Total	**11807**	**16979**		
**Calculated as 0.1b(Z/H) Ecc = Eccentricity									

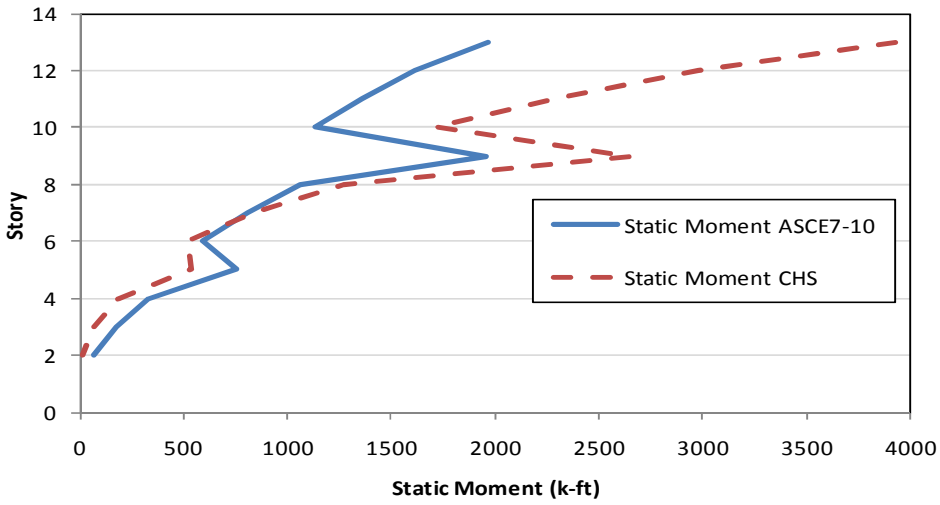

Figure 4-11 Comparison of static moments between ASCE 7-10 and the CHS, for the same set of static lateral loads corresponding fo the Building 2 of Appendix 1

4.2.3 Improvements in static procedures to measure accidental torsion

It is important to analyze improved static procedures that include the effects of accidental torsion. Such methods could be used to model accidental torsion in LRHA when using semirigid diaphragms, because the direct inclusion of the dynamic effects of accidental torsion using LRHA might have some difficulties for this particular diaphragm condition, and then a static procedure to measure accidental torsion could be an option.

Also, any provision for accidental eccentricity should include the effect of the parameter Ω, which as explained in Section 4.2.1 represents the ratio of the uncoupled fundamental translational and rotational periods. Three improved methods that consider the parameter Ω are presented next, and such methods were developed by De la Llera and Chopra (1994a), Escobar et. al. (2004), and Dimova and Alashki (2003). These methods were derived by analyzing the dynamic response of single degree of freedom systems subjected in each method to a different spectrum.

4.2.3.1 Procedure developed by De la Llera and Chopra (1994a) to account for accidental torsion

De la Llera and Chopra suggested a new method to implement accidental torsion in seismic codes. The proposed method include several sources of accidental torsion, such as uncertainty in the location of the center of mass, uncertainties in the stiffness of the structural elements, effects due to rotational ground motion, uncertainties in the stiffness of other floors different to the one considered, and the influence of Ω; therefore it is considered a more appropriate method than the current provision of accidental torsion for static analysis provided in ASCE 7-10. The advantage of this method is that it will reflect a better consistency in the effects due to accidental torsion using static analysis with those compared using dynamic analysis. The steps to follow are summarized next:

Step 1: Calculate the parameter Ω as the ratio between the uncoupled torsional and translational fundamental frequencies (or the ratio between the uncoupled translational and rotational fundamental periods) of the building, and use this value of Ω to reflect if the structure is torsional stiff if $\Omega>1$ or torsional flexible if $\Omega<1$. The definition of the uncoupled translational and rotational fundamental periods was given in section 4.2.1 of this document.

Step 2: Obtain the increase in displacements $\hat{u}_{b/2}$ at the edge of the building resulting from all sources of accidental torsion. The parameter $\hat{u}_{b/2}$ represents a factor that multiplies the displacement at the edge of the building calculated without including accidental torsion in order to obtain the approximate displacement at the same location but including torsional effects. The parameter $\hat{u}_{b/2}$ is calculated using the following expression which has been taken from De la Llera and Chopra (1994a):

$$\hat{u}_{b/2} = \begin{cases} A & 0 \le \Omega \le 1 \\ A - \dfrac{A-1}{\Omega_c - 1}(\Omega - 1) & 1 < \Omega \le \Omega_c \\ 0 & \Omega > \Omega_c \end{cases} \qquad \textbf{Eq. 4- 8}$$

where the value of A is given by:

$$A = 1 + 0.0475(b/r)^2 \qquad \textbf{Eq. 4- 9}$$

and $\Omega_c = 1.8$

The value of A computed in this way corresponds to an implicit probability of exceedance of 30% that the accidental eccentricity is equal to 0.05b.

Step 3: Compute the increase in displacements due to accidental torsion at the locations of all interior resisting planes (the increase in displacements due to accidental torsion in the exterior resisting planes is given by $\hat{u}_{b/2}$). Such increase in response can be approximated using a linear variation in the amplification factor $\hat{u}_{b/2}$ varying from 1.0 at the CM until $\hat{u}_{b/2}$ at the edge of the plan.

Step 4: Compute the forces of the structural members of each resisting plane by amplifying the forces corresponding to the system with no accidental torsion by the factors determined in the previous step.

This method was developed for symmetric structures, and its applicability to nonsymmetrical systems is not addressed, although the original report of De la Llera and Chopra (1994a) includes an example of applying this procedure to an nonsymmetrical building with

results relatively close to those from a dynamic analysis. This technique was further tested using real measurements in twelve asymmetric buildings in California (Lin et al., 2001), and it showed appropriate results. Another advantage of this procedure is that it requires only one analysis to calculate the amplifications due to torsional effects in one direction of the building, instead of the classical two analyses (+ - 5% eccentricity) required to apply accidental torsion in each direction of the load.

4.2.3.2 Procedure developed by Escobar, Mendoza and Gomez (2004) to account for accidental torsion

This procedure simplifies the calculations of accidental torsion from dynamic procedures to a set of calculations based on the loading of a structure with static loads only. This technique requires the calculation of a normalized radius of gyration denoted ρ that is associated with the ratio of uncoupled torsional to lateral frequencies, Ω. Then, this method specifies the calculation of a "Torsional Amplification Factor" (FAT), which has different formulations for the resisting elements on the stiff and rigid size (definitions of stiff and rigid size are explained in Section 4.2.1 of this document). The application of this procedure requires the calculation of the shear center and the center of rigidity of each floor, and the definition of these parameters as well as specific formulas for their calculation are given in Escobar et al. (2004). Additionally, an advantage of this technique is that it applies to symmetric and nonsymmetrical structures.

4.2.3.3 Procedure developed by Dimova and Alashki (2003) to account for accidental torsion

Dimova and Alashki studied the accuracy of the provisions for accidental torsion in the Eurocode 8 motivated by their awareness that the current method of that standard to account for dynamic effects of accidental torsion by static moments (as explained in Section 4.2.2.4 of this document) cannot properly represent the dynamic effects from accidental torsion. This method suggests the application of a corrected coefficient C that affects the forces in the resisting planes at the edge of the building. This parameter C is intended to reflect the increase in displacement at one edge of the building when moving the CM a distance 0.05b compared to the displacement of the same point when ignoring accidental torsion. The increase of the displacements and element forces at other locations are calculated using a linear variation of the corrected

coefficient C, varying from 1 at the center of rigidity to C at the edge of the building. Detail calculation of the factor C is presented in Dimova and Alashki (2003).

4.2.4 Application of static moments to account for accidental torsion when using rigid and semirigid diaphragms

So far static procedures to account for accidental torsion have been discussed, and they have been explained considering that these techniques could be used to predict accidental torsion when using LRHA. The static procedures described in Section 4.2.2 and 4.2.3 follow two approaches; the first of them consists of applying static moments calculated with the set of lateral loads and an appropriate eccentricity, and the second approach consists in amplifying the forces in each frame from an analysis without torsion. Any of these two approaches could be easily implemented when using rigid diaphragms; for instance, the modeling of the eight load cases of accidental torsion shown in Figure 4-12 can be performed in the same mathematical model and with only one analysis.

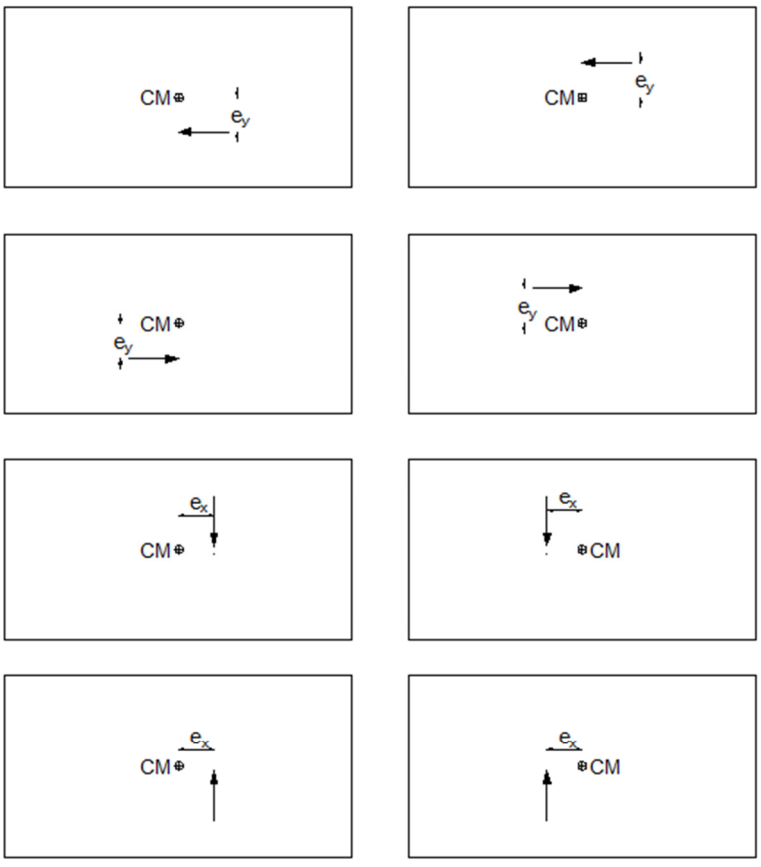

Figure 4-12 Combinations required to apply accidental torsion

Additional definitions are required to implement static loading procedures for buildings modeled with semirigid diaphragms, and these additional definitions refer to the application of lateral loads and static torques in semirigid diaphragms. The lateral loads when using semirigid diaphragms still need to be applied at the center of mass of each floor; however, as it is shown in Figure 4-13, it will not be often the case where the center of mass coincides with one of the nodes of the grid used within that floor. Therefore, the static lateral load *Fi* at each floor has to be replaced by two equivalent forces *Pi* and *Qi* acting on two nodes *P* and *Q* located close to the center of mass as it is shown in Figure 4-14. The procedure to calculate the equivalent forces *Pi* and *Qi* is shown in Figure 4-15, and it only requires finding the reactions of a simple supported beam with length equal to the distance between the nodes *P* and *Q* and under the load *Fi* corresponding to that specific floor.

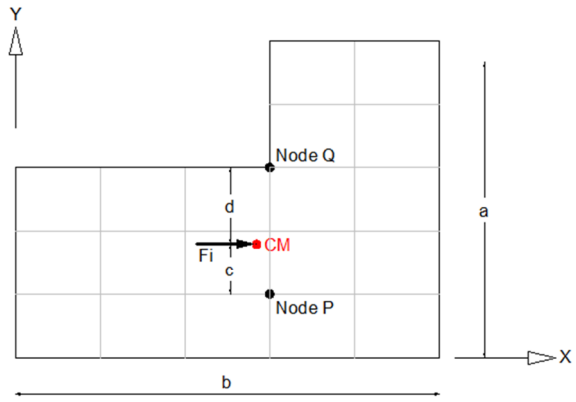

Figure 4-13 Center of mass not coinciding with the nodes of a grid for a building modeled with semirigid diaphragms

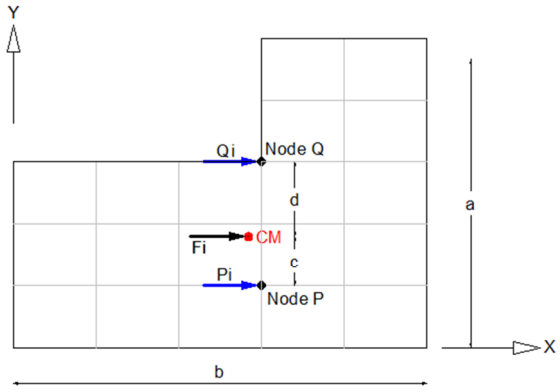

Figure 4-14 Application of lateral loads for the case of semirigid diaphragms

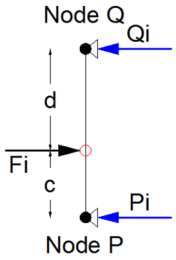

Figure 4-15 Calculation of forces *Pi* and *Qi*

Also, for the case when static moments need to be applied in a structure with semirigid diaphragms, a similar procedure can be implemented. For instance, if the static moment Mi needs to be applied as shown in Figure 4-16, then such static moment can be replaced by two equivalent forces *Gi* acting in nodes *P* and *Q* in different directions. This methodology is shown in Figure 4-17.

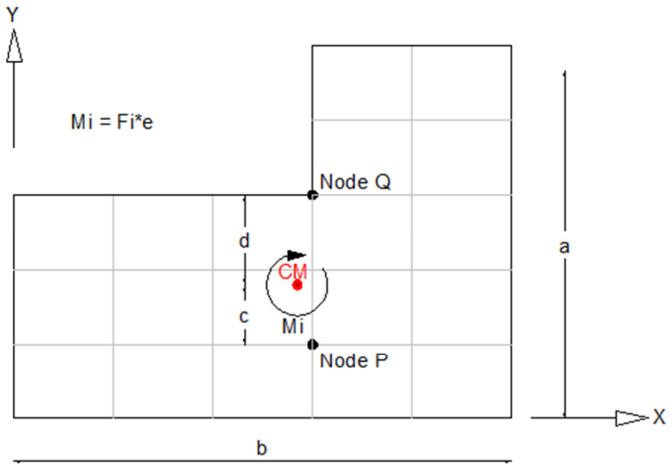

Figure 4-16 Application of static moments for buildings modeled with semirigid diaphragms

The calculation of the forces *Gi* is given by:

$$Gi = \frac{Mi}{c+d} = \frac{Fi*e}{c+d} \qquad \textbf{Eq. 4- 10}$$

where *Mi* is the static moment to account for accidental torsion

c is the distance from the center of mass to the node P according to Figure 4-17

d is the distance from the center of mass to the node Q according to Figure 4-17

Fi is the lateral force corresponding to that floor

e is the design eccentricity (i.e. 0.05a for the case of ASCE 7-10)

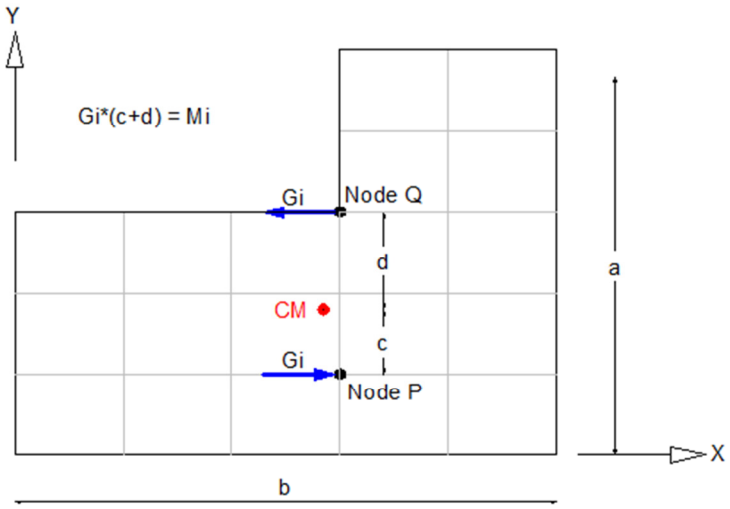

Figure 4-17 Equivalent Forces *Gi* to produce an equivalent static moment for buildings modeled with semirigid diaphragms

This approach to model lateral loads and accidental torsion in semirigid diaphragms was implemented in the twelve story building analyzed by Charney et al. (2010b). The application of forces *Pi* and *Qi* or forces *Gi* for modeling of lateral load and torsional effects, respectively, will not be an appropriate procedure when the diaphragm is too flexible, because the region around the nodes where the concentrated lateral loads are applied will experience undesired local deformations. This case has been represented in Figure 4-18, which indicates that an area of local distortion will probably be formed around the node O due to application of the lateral force P. An alternative to avoid local distortion around the node O could be to distribute the load P in smaller nodal forces applied over the area of the diaphragm.

So far it has been discussed in detail only static procedures to account for accidental torsion; however, there are also alternatives to include the effects of accidental torsion from LRHA by dynamic procedures, and that is the topic of the next section.

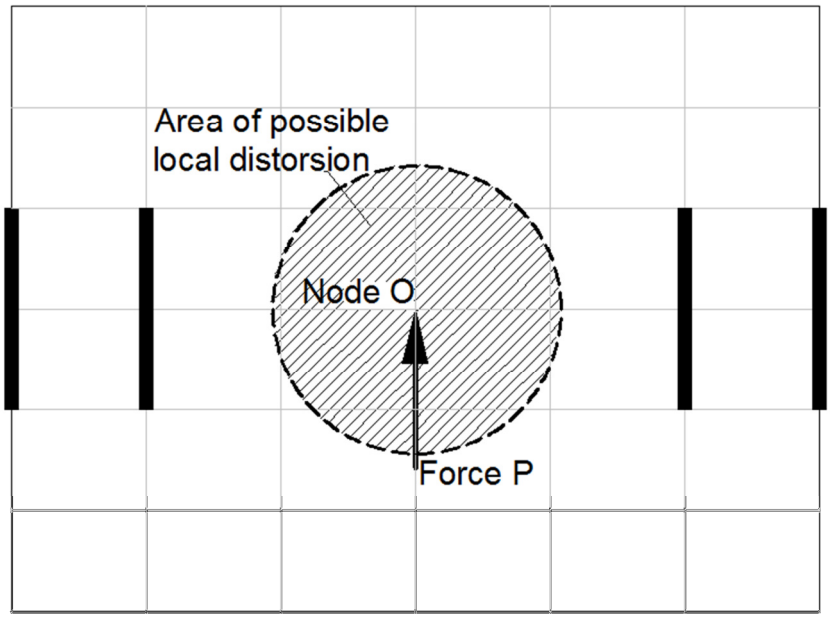

Figure 4-18 Possible local distorsion in a floor modeled with semirigid diaphragms due to application of a lateral load P on the Node O.

4.2.5 Application of dynamic procedures to account for accidental torsion when using rigid and semirigid diaphragms

This section is divided in two parts; the first one refers to modeling issues of accidental torsion when using rigid diaphragms, and the second part provides a procedure to incorporate accidental torsion in semirigid diaphragms. Both parts consider linear response history analysis as the type of loading that causes accidental torsion when it is applied at a specified eccentricity from the center of mass.

4.2.5.1 Accidental torsion in rigid diaphragms using dynamic procedures

As it was already mentioned, the application of accidental torsion using LRHA can be easily applied for the case of having rigid diaphragms by displacing the center of mass by the design eccentricity; however, it requires the construction of the four different mathematical models shown in Figure 4-19, and the handling of all the output information from these mathematical models could demand a very extensive amount of time.

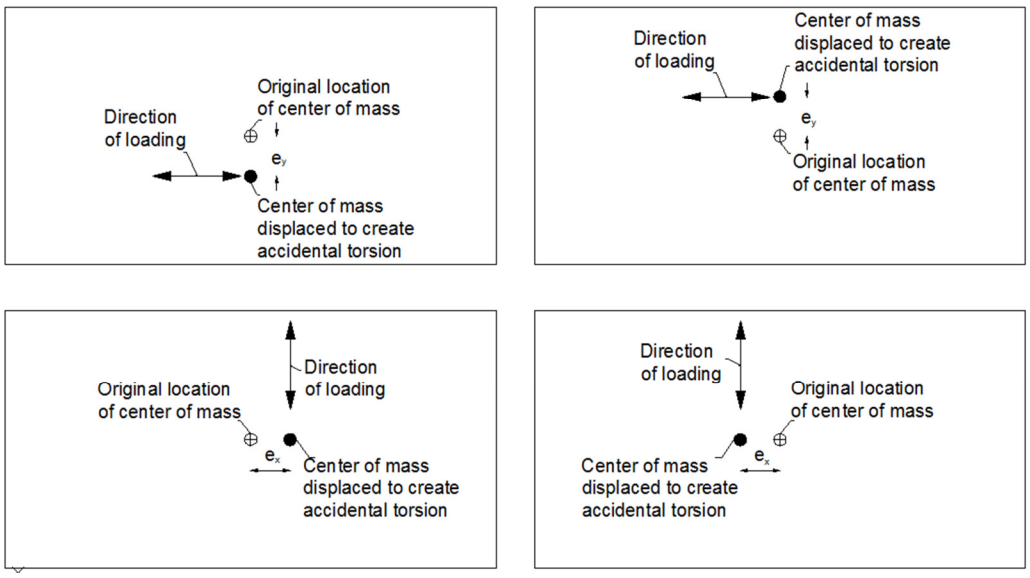

Figure 4-19 Mathematical models that need to be constructed to run LRHA using rigid diaphragms

Furthermore, the displacement of the center of mass in each floor to account for accidental torsion in buildings modeled with rigid diaphragms implies a change in the mass matrix of the system if the DOFs associated with the center of mass is kept at the original location of the center of mass (without accidental eccentricity). However, the displacement of the center of mass implies a change in the stiffness matrix if the DOFs associated with the center of mass move accordingly with the center of mass after applying the desired eccentricity. The change in either, the mass matrix or the stiffness matrix, will produce changes in the fundamental period, modal shapes, and dynamic base shear. For instance, Figure 4-20 shows the change in the fundamental translational periods T_x, T_y, and in the fundamental rotational period T_{rot} when a modal analysis was done in the Building 1, Building 2, Building 3 and Building 4 described in the Appendix A, and which are denoted as B1, B2, B3, and B4, respectively. The fundamental periods T_x, T_y and T_{rot} in these four buildings were calculated with and without displacement of the center of mass (eccentricity 0.05b was used for all the buildings). All the buildings were modeled with rigid diaphragms, and for the models including accidental torsion, the center of mass was displaced parallel to the X direction of each building (see Appendix A for orientation of X axis for each building). From Figure 4-20 it can be seen that the fundamental translational and rotational periods do not change significantly for any of the buildings.

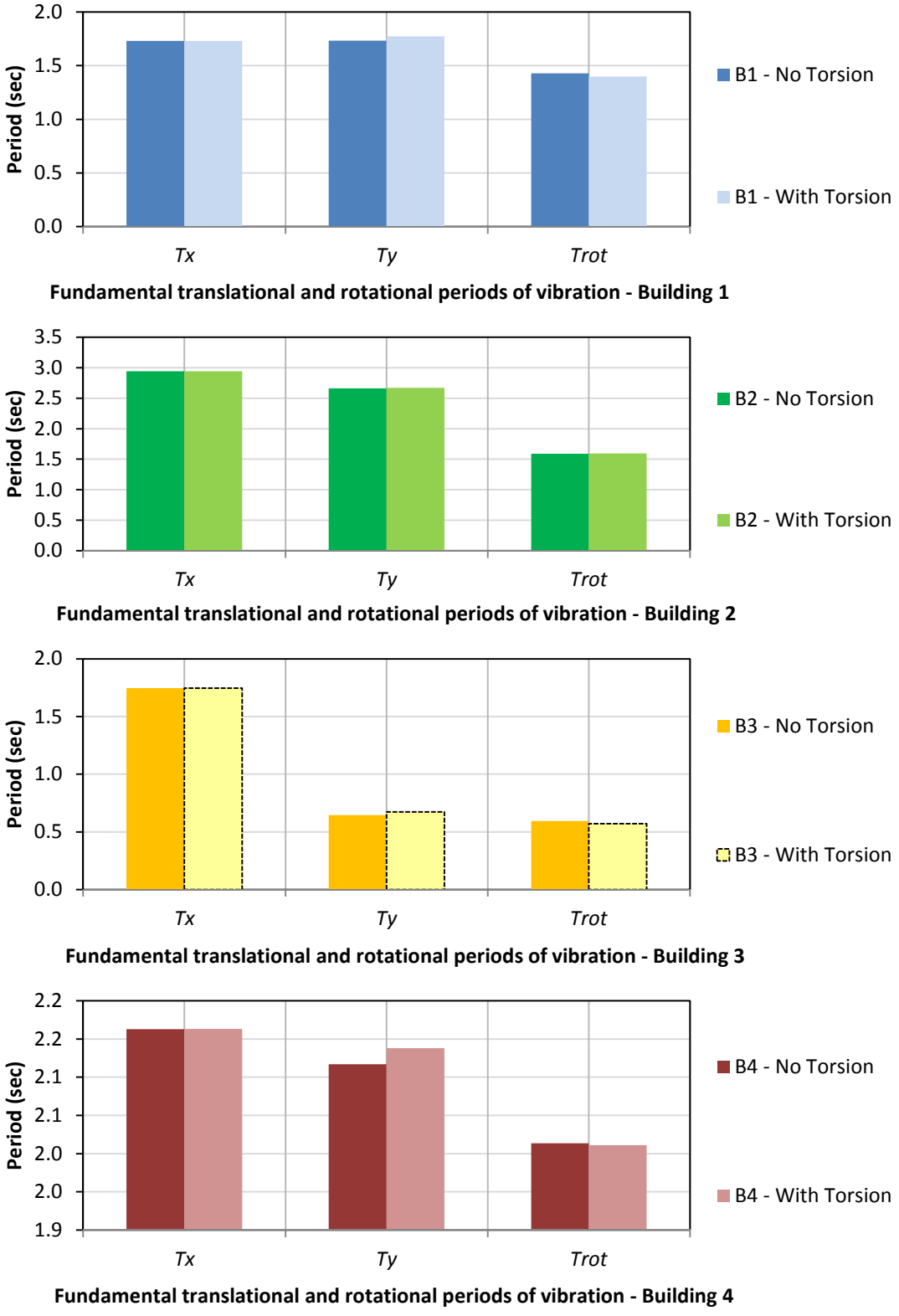

Figure 4-20 Fundamental Periods of vibration of Building 1, Building 2, Building 3, and Building 4 modeled with rigid diaphragms and with and without accidental torsion

Also, Figure 4-21 shows the mass participation factor (as a percentage of the effective mass of each building) corresponding to T_x, T_y, and T_{rot}, and it can be noticed that it can change considerably in some cases when displacing the center of mass. For instance, the mass participation factor of the building B3 corresponding to the fundamental period in the Y direction changes from 69.36% to 53.64% (of the effective mass) when displacing the center of mass. A similar change can be noticed in the mass participation factor corresponding to the rotational period T_{rot} for the same building B3, which changes from 69.74% to 44.35% when displacing the center of mass in the X direction.

The fact that the mass participation factor of the fundamental periods can change when including and not including accidental torsion in buildings modeled with rigid diaphragms indicates that the number of modes required for reaching 90% of the mass might also change when displacing the center of mass to account for accidental torsion. Therefore, it will be convenient to check the number of modes used in the analysis before and after displacing the center of mass. Also, it is noticed in Figure 4-21 that the mass participation factor does not change for the fundamental period in the X direction, and this is an expected result, because the applied eccentricity (moving the center of mass in the X direction) does not affect the mass participation factor in the X direction for symmetrical systems (Buildings B1, B3, and B4), and it affects only slightly for the case of nonsymmetrical systems (Building B2).

In addition, the designer might consider increasing the mass moment of inertia of a diaphragm in order to create accidental torsion in buildings using rigid diaphragms with lumped masses. However, this procedure does not create accidental torsion because if the analyzed building is symmetric the response under lateral load applied at the center of mass will not change regardless of the mass moment of inertia used in the calculations.

4.2.5.2 Accidental torsion in semirigid diaphragms using dynamic procedures

A suggested method is provided in this section to account for accidental torsion in buildings modeled with semirigid diaphragms and loaded with acceleration histories. This suggested approach is based on the fact that accidental eccentricity can be artificially created by reducing the mass of the diaphragm and putting that removed mass at the edge of the considered floor so that the total mass is still the same. The amount of mass moved to the edge of the building will be such that two goals are accomplished:

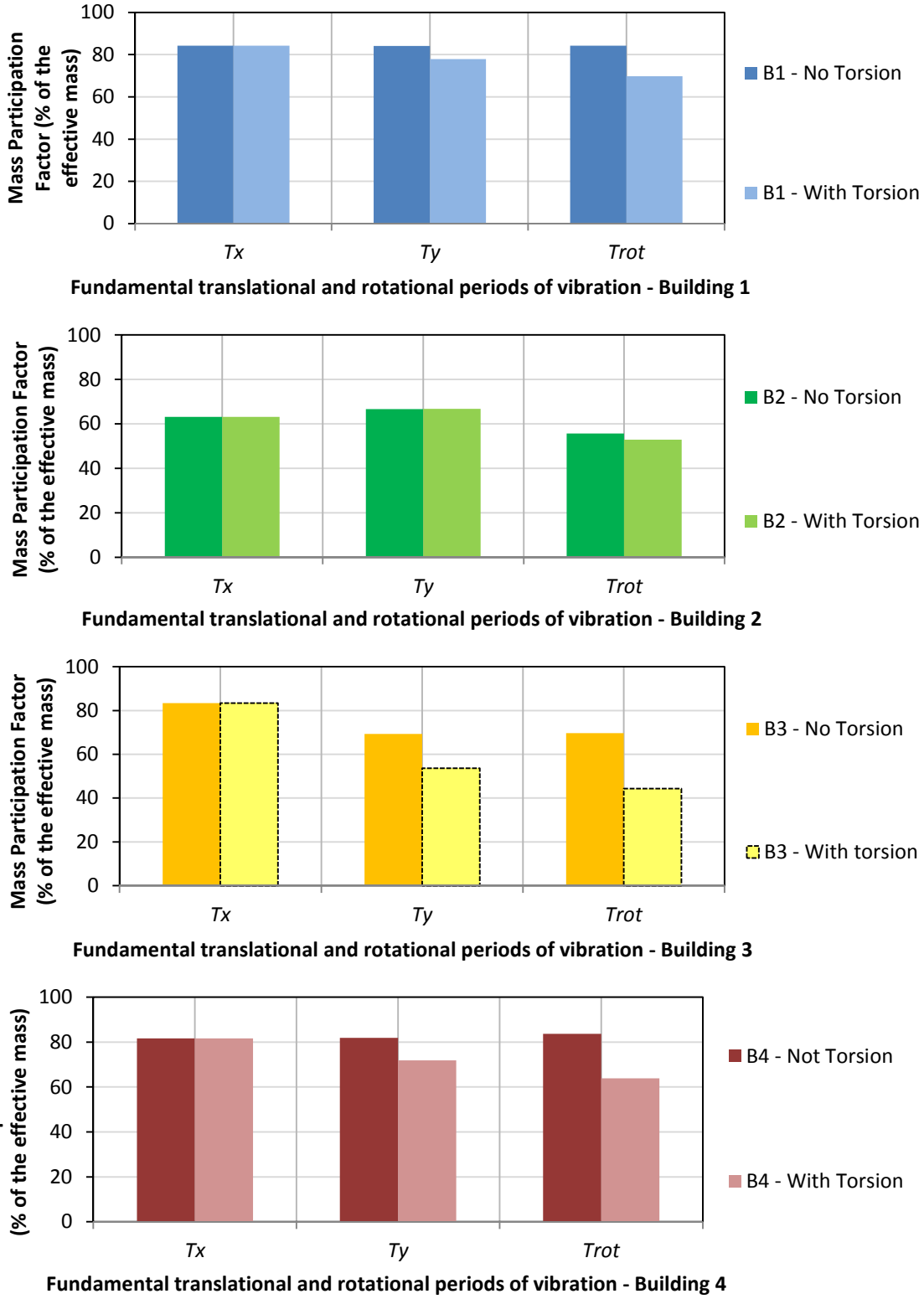

Figure 4-21 Mass participation factor of the fundamental periods of Building 1, Building 2, Building 3, and Building 4 modeled with rigid diaphragms when including and not including accidental torsion

1. The center of mass will be displaced an eccentricity equal to the one specified by the appropriate code, in the direction of interest.
2. The center of mass will be displaced only in one of the two orthogonal directions of analysis but it will keep the same ordinate (as in the original model without accidental eccentricity) in the other direction.

For the case of a rectangular shape floor, width dimension a, and length dimension b, it can be demonstrated that removing 10% of the mass of the slab and locating it as a uniform mass along the width of the floor displaces the center of mass a distance 0.05b (as required by ASCE 7-10) along the length of that floor as shown in Figure 4-22. This particular procedure guarantees that the center of mass will be displaced in the direction parallel to the side with dimension b in Figure 4-22, but it will not be displaced in the direction parallel to the side with dimension a.

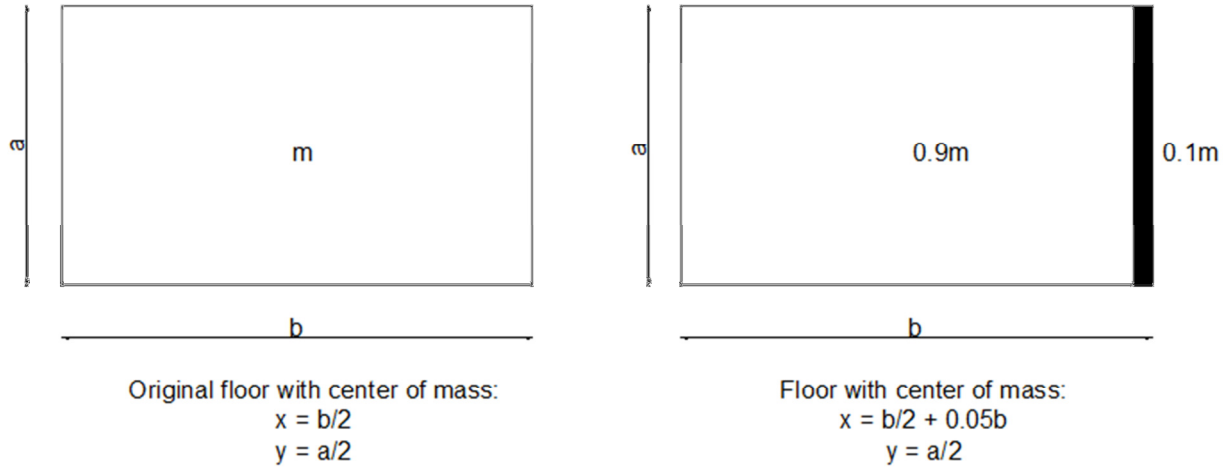

Figure 4-22 Artificial motion of the center of mass of a rectangular shape floor modeled with semirigid diaphragms.

This approach is more appropriate when it is reasonable to ignore the contributions from the linear masses to the total rotational mass, and it implicitly changes the rotational mass of the analyzed floor, although the translational mass is the same. In order to study the change in the rotational mass, the ratio I_2/I_1 was calculated, where I_1 is the rotational moment of inertia of a story with mass m distributed within the diaphragms only, and where I_2 is the rotational moment of inertia of a story with mass m distributed so that λm is a linear mass distributed along one of

the sides of a floor and (1-λ)m is the mass distributed within the diaphragm as it is shown in Figure 4-23.

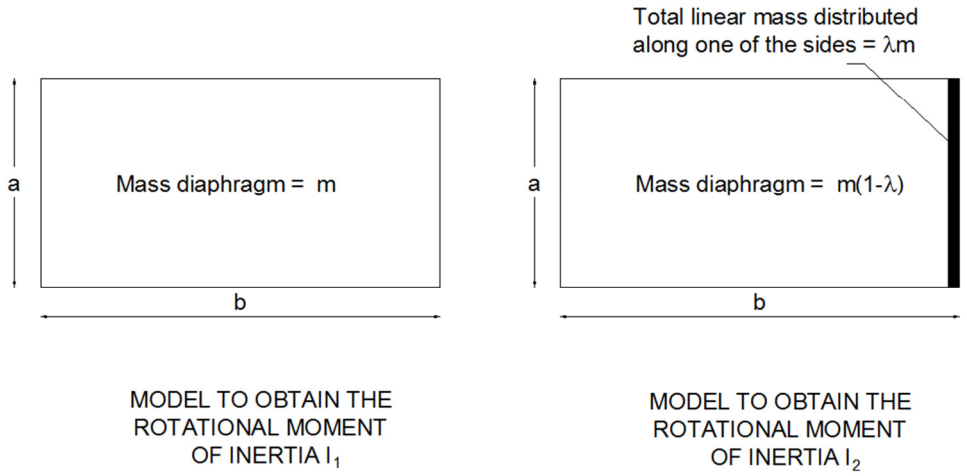

Figure 4-23 Models to obtain the rotational moment of inertia I_1 and I_2 when the a portion of the mass of the diaphragms is distributed along one of the sides of a rectangular floor

The ratio I_2/I_1 depends on the ratio a/b, and it varies according to the equation shown below:

$$\frac{I_2}{I_1} = \frac{\left(\frac{a}{b}\right)^2 + 1 + 2\lambda}{\left(\frac{a}{b}\right)^2 + 1} \qquad \textbf{Eq. 4- 11}$$

Figure 4-24 shows the ratios I_2/I_1 plotted for different ratios a/b, and it can be noticed that I_2 is always greater than 1.00 for any value of λ, and this fact indicates that the suggested procedure of displacing in each diaphragm a percentage of the mass towards one of its sides in order to create accidental torsion increases the rotational moment of inertia with respect to the model without accidental torsion.

For the particular case of λ=0.10, which creates an accidental torsion of 0.05b (see Figure 4-22), Figure 4-25 shows the variation of I_2/I_1 for different ratios a/b, and it can be noticed that the minimum and maximum increase in the rotational moment of inertia I_2 with respect to I_1 is 10% for a/b=1.0 and 20% for a/b=0.0 (a/b=0.0 indicates that the dimension b is very large respect to the dimension a).

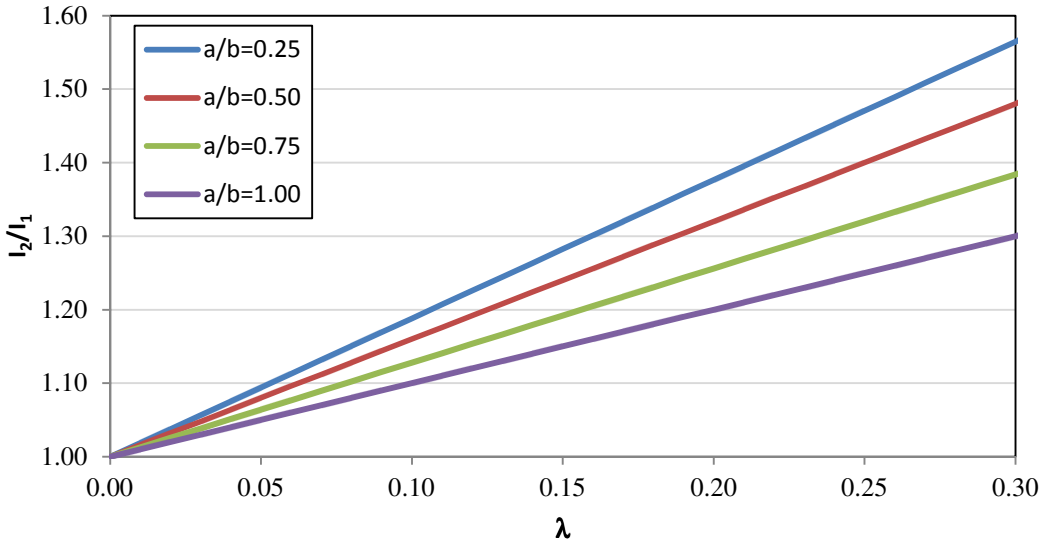

Figure 4-24 Ratio of rotational moments of inertia I_2/I_1 for different values of λ and for different ratios a/b

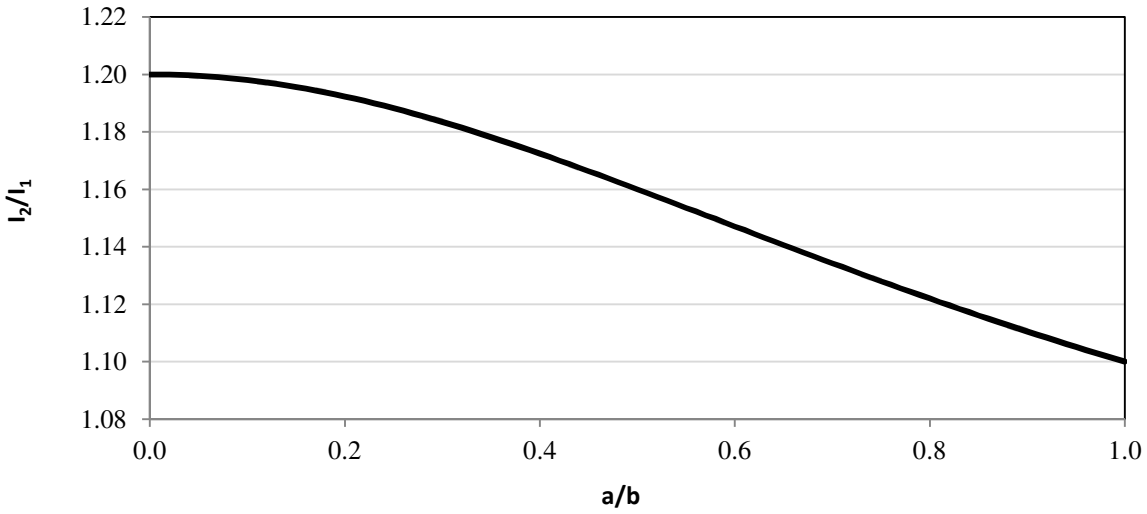

Figure 4-25 Ratio of rotational moments of inertia I_2/I_1 for different ratios a/b and for λ=0.1

For the case of an L shape floor, as shown in Figure 4-26, the shifting of the center of mass is more complex because two different linear masses w1 and w2 are required so that the center of mass is displaced along the X direction only and not along the Y direction. The use of a unique value for the linear mass along the sides with dimensions c and d (see Figure 4-26) is not possible.

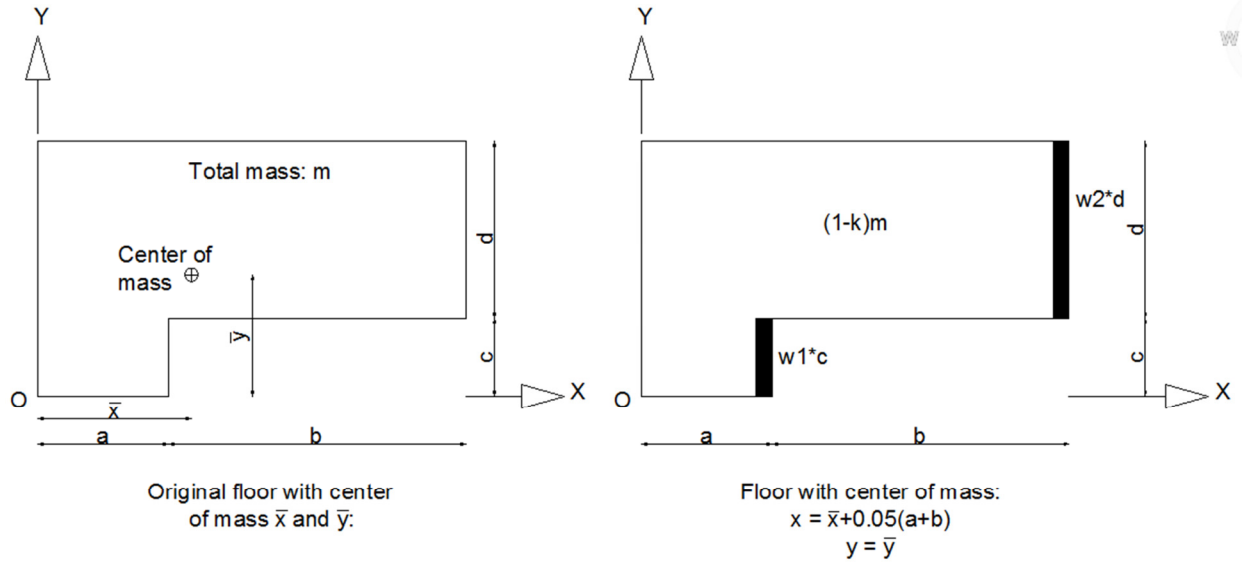

Figure 4-26 Artificial displacement of the center of mass of L shape floor modeled with semirigid diaphragms

The corresponding values of the linear masses w1 and w2 acting on the sides with dimensions c and d, respectively, so that the center of mass is displaced an eccentricity equal to 0.05(a+b) along the X direction with no displacing of the mass in the Y direction, are given by solving the following system of equations:

$$A_{11}(w1)+A_{12}(w2)=0.05m(a+b)$$

$$A_{21}(w1)+A_{22}(w2)=0 \qquad \textbf{Eq. 4- 12}$$

where:

$$A_{11}=ac-c\bar{x} \qquad \textbf{Eq. 4- 13}$$

$$A_{12}=ad+bd-d\bar{x} \qquad \textbf{Eq. 4- 14}$$

$$A_{21}=\frac{c^2}{2}-c\bar{y} \qquad \textbf{Eq. 4- 15}$$

$$A_{22}=\frac{d^2}{2}+cd-d\bar{y} \qquad \textbf{Eq. 4- 16}$$

$\bar{x}$ and $\bar{y}$ are the coordinates of the center of the mass along the X and Y directions as shown in Figure 4-26

A parameter k is defined as the fraction of the mass of the slab that is distributed to the sides c and d, and it is given by:

$$k = \frac{w1 * c + w2 * d}{m} \qquad \textbf{Eq. 4- 17}$$

where k is not unique, but it depends on the dimension of the L shape floor.

The procedure described in this section could also be applied to account for accidental torsion in buildings modeled using rigid diaphragms with the mass distributed along the diaphragms (the procedure for the case of rigid diaphragms with floor mass concentrated at the center of mass was discussed in Section 4.2.5.1 of this document).

The specific application of the procedure described above to account for accidental torsion in buildings modeled with semirigid diaphragms by artificially displacing the location of the center of mass will be applied to an eight story concrete building denoted as Building 1 in the Appendix A, and the results of the suggested technique will be compared with the same values from running an analysis using rigid diaphragms. The center of mass will be displaced artificially along the X axis according to Figure 4-22 since the building has a rectangular shape; therefore, 10% of the mass of each floor was distributed as a linear mass over the Frame F of the building (see Figure A- 1), and the remaining 90% of the weight was applied as a uniform load over the slab. The resulting uniform load applied in each floor and the linear mass applied on Frame F is shown in the columns 4 (Col4) and 5 (Col5) of Table 4-6, respectively.

Table 4-6 Calculations for application of accidental torsion using LRHA in Building 1 modeled with semirigid diaphragm

Level	Col 1	Col2 = 0.9*Col1	Col3 = 0.1*Col1	Col4 = Col2/Area*	Col5 = (Col3/g)/960**
	Total Load	**Distributed weight = 0.9M**	**Weight for linear mass = 0.1M**	**Uniform Load for SAP2000**	**Linear Mass for SAP2000**
	(kips)	**(kips)**	**(kips)**	**(psf)**	**(kips-sec^2/in)/in**
R	2507	2256	251	188.03	0.000676
8	2351	2116	235	176.35	0.000634
7	2351	2116	235	176.35	0.000634
6	2351	2116	235	176.35	0.000634
5	2351	2116	235	176.35	0.000634
4	2351	2116	235	176.35	0.000634
3	2351	2116	235	176.35	0.000634
2	2368	2131	237	177.61	0.000638

* Area = 150*80 = 12000 ft2
** 960 is the dimension of the building (in inches) of the side of the building along the axis F.

Figure 4-27 and Figure 4-28 show the interstory shears in frames A and F, and C and D, respectively, that corresponds to Building 1 modeled with semirigid diaphragms when including accidental torsion with the suggested technique, and using the spectral matched acceleration histories Ch-1, Ch-2, and Ch-3 obtained in Section 2.2.2.1 of this document. These interstory shears obtained in Building 1 were compared to the same values obtained in Building 1 modeled with rigid diaphragms and under response spectrum analysis loading. In addition, Figure 4-27 and Figure 4-28 show the interstory shears in frames A and F, and C and D without including accidental torsion. The center of mass was displaced along the X direction of Building 1 (see Figure A- 1 for X direction of Building 1) and towards the right edge. The nomenclature of RD, SR, RSA, and LRHA in Figure 4-27 and Figure 4-28 accounts for the cases when Building 1 was modeled using rigid diaphragms, semirigid diaphragms, response spectrum analysis and linear response history analysis, respectively. Also, the "Average of Ch-1, Ch-2, Ch-3" represents the average interstory shears obtained from doing the analysis with the three spectral matched acceleration histories Ch-1, Ch-2, and Ch-3.

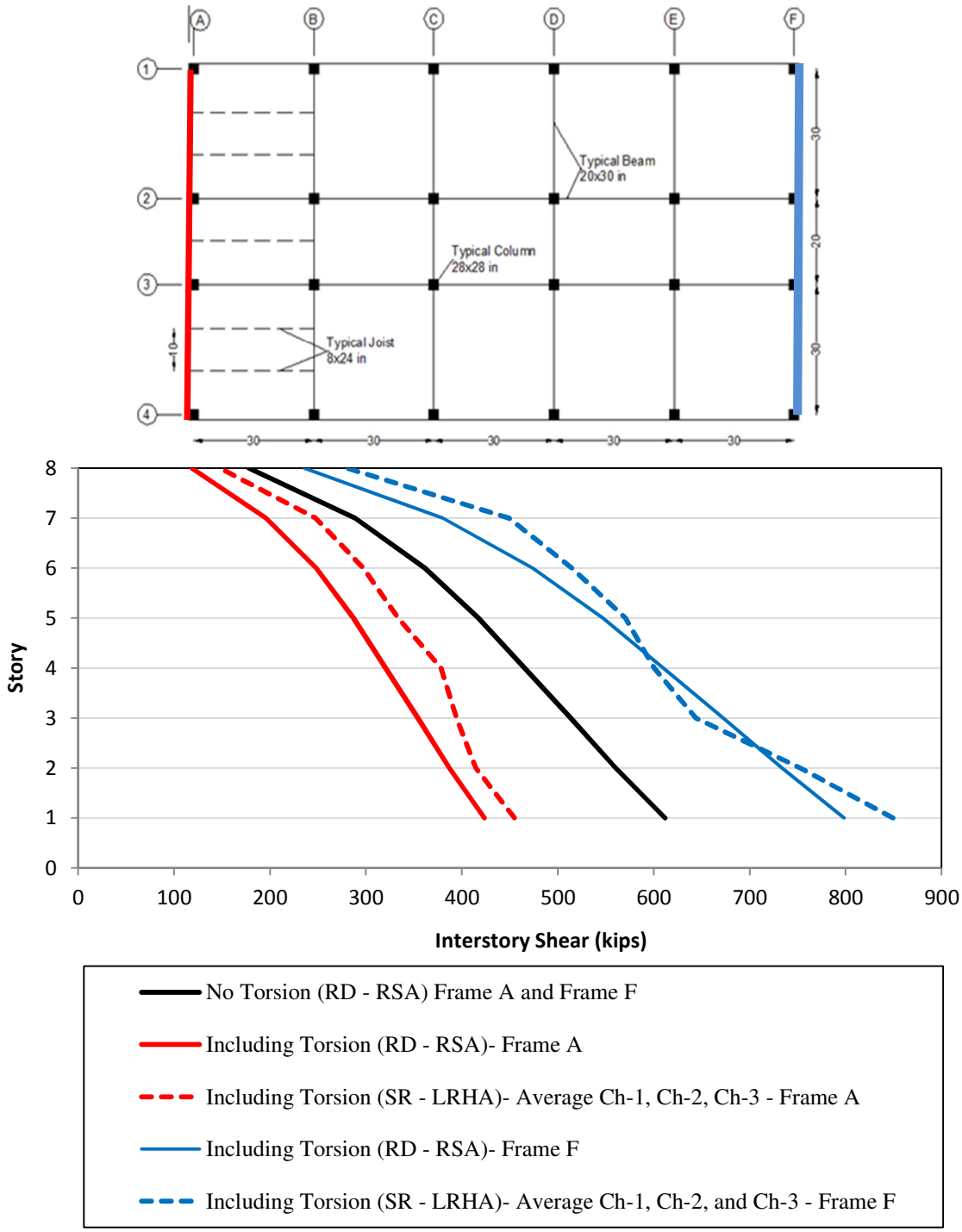

Figure 4-27 Interstory shear along frames A and F of Building 1 modeled with semirigid diaphragms shen including accidental torsion from modal response spectrum analysis and from the average of three different spectral matched acceleration histories

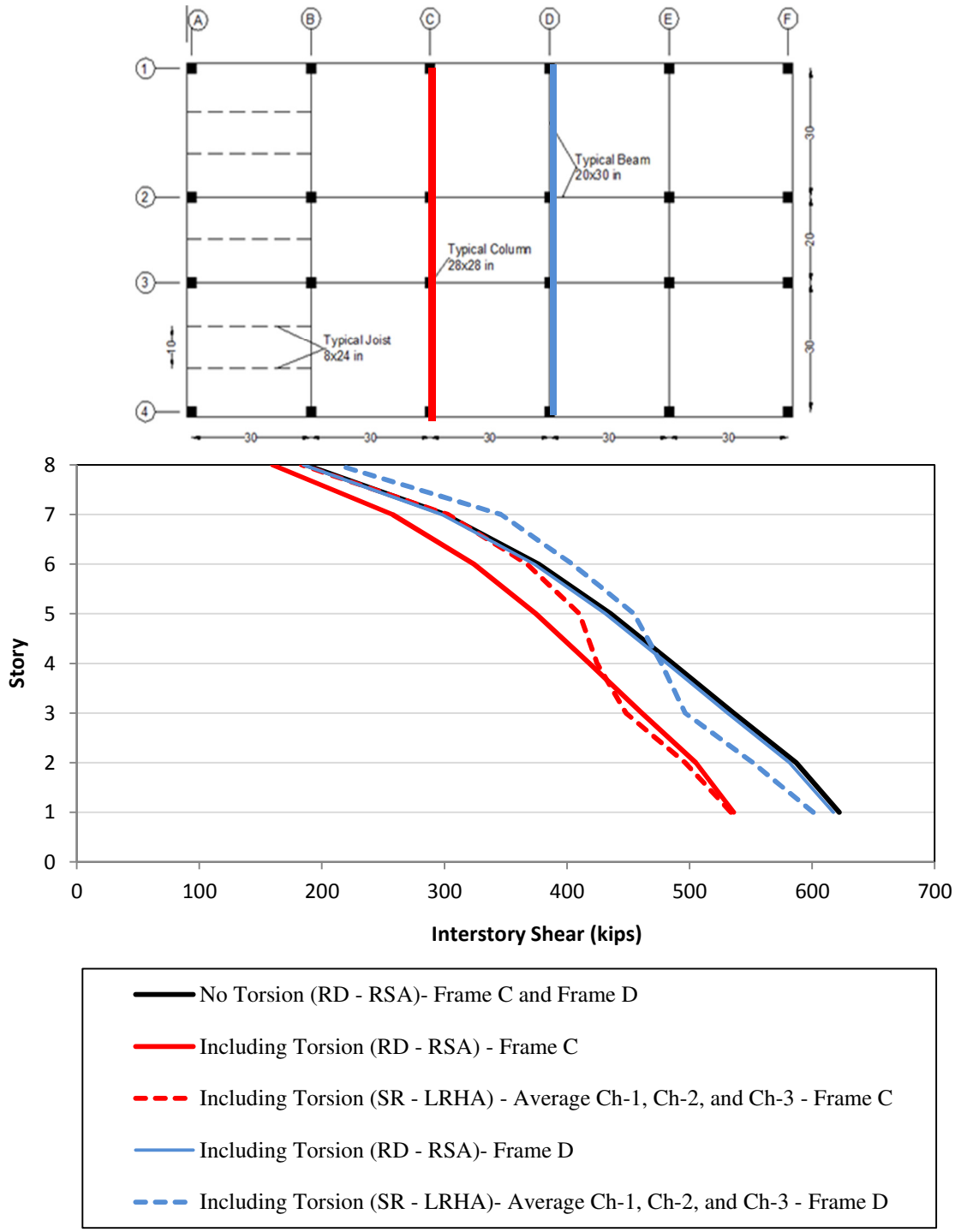

Figure 4-28 Interstory shear along frames C,and D of Building 1 modeled with semirigid diaphragms shen including accidental torsion from modal response spectrum analysis and from the average of three different spectral matched acceleration histories

Several observations can be made from Figure 4-27 and Figure 4-28. First, the interstory shears without torsion are very similar for frames A and F and for frames C and D because of symmetry. Also, the interstory shears from frames C and D are bigger than those in frames A and F because the location of the frames C and D (interior frames) makes them stiffer than frames A and F (exterior frames). Also, it is seen that for frames C, D, and F, the suggested technique to include accidental torsion in buildings modeled with semirigid diaphragms and subjected to spectral matched acceleration histories yields comparable interstory shears to those of a response spectrum analysis using rigid diaphragms; however, for the case of Frame A the interstory shears using both techniques differs more significantly.

Also, when comparing the values including and not including accidental torsion it can be noticed that the interstory shears in frame F when including accidental torsion are considerably higher than the interstory shears in the same frame when not including accidental torsion. This is because the resultant of the seismic loads is closer to frame F when including accidental torsion than when excluding it. On the other hand, the interstory shears in Frame A when including accidental torsion are smaller than the interstory shears in the same frame when excluding accidental torsion. This occurs because the resultant of the seismic loads is located at a further distance than frame A when displacing the center of mass to include accidental torsion.

In summary, the suggested technique to include accidental torsion in buildings modeled with semirigid diaphragms subjected under spectral matched acceleration histories yields comparable results to those resulting from a response spectrum analysis with rigid diaphragms in the building analyzed; however, more research is required to evaluate the differences resulting in all the interstory shears or other response parameters (i.e. interstory drift including accidental torsion) in buildings with more resisting frames and with different structural systems (i.e. shear walls, braced systems).

4.2.6 Comparison of static and dynamic procedures to account for accidental torsion

Some of the methodologies described previously to account for accidental torsion by static and dynamic procedures were analyzed by calculating the interstory shear in the frames D and F of Building 1 modeled with rigid diaphragms (See Figure A- 1). The analyzed techniques are divided into two groups; the first of them is associated with accidental torsion implemented with dynamic procedures, and it includes accidental torsion using modal response spectrum analysis and also with linear response history analysis. For the latter case the results represent

the average of the response from the three spectral matched acceleration histories described in Section 2.2.2.1. The second group of techniques applies accidental torsion using the static procedures given in the American standard ASCE 7-10 (ASCE/SEI, 2010), the Chilean standard (Instituto Nacional de Normalizacion, 1996), the two methods of the Eurocode 8 (British Standards, 2004) presented in section 4.2.2.4, and the method developed by De la Llera and Chopra (already explained in Section 4.2.3.1). The interstory shears for frame D and F are shown in Figure 4-29 and Figure 4-30, respectively.

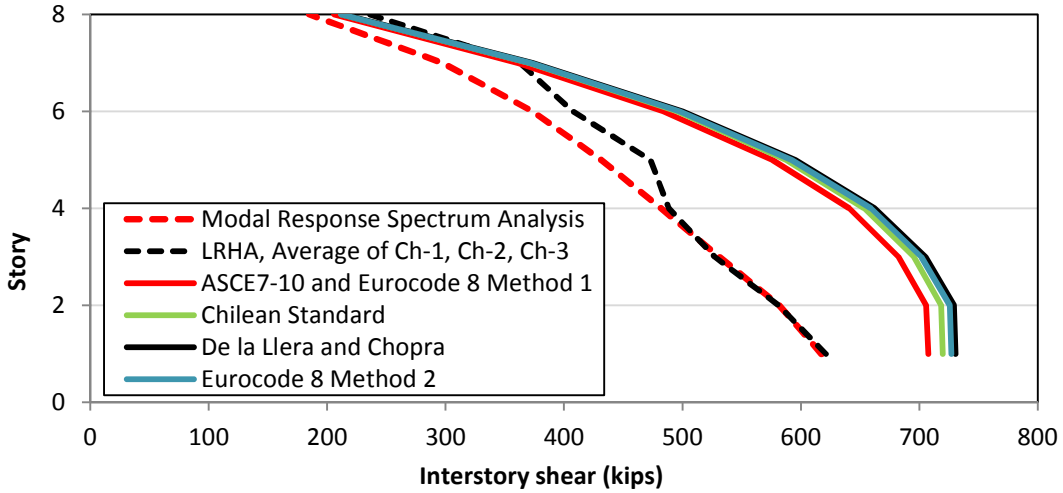

Figure 4-29 Interstory shear in Frame D of Building 1 when applying different techniques to account for accidental torsion

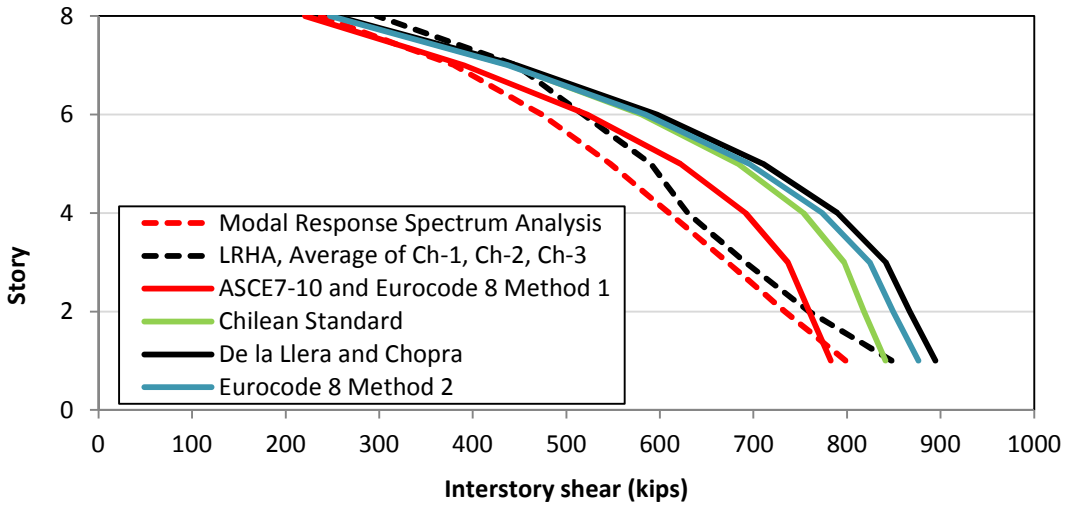

Figure 4-30 Interstory shear in Frame F of Building 1 when applying different techniques to account for accidental torsion

For this building in particular it is shown that the effects of accidental torsion differ when using static and dynamic procedures, and such difference is larger for frame D than for frame F. Also, it can be seen that all the techniques that use static forces produce similar shears for frame D, but their results differ when analyzing frame F. Additionally, it is shown that the interstory shears from using static forces are closer to those using dynamic procedures at the upper floors than at the bottom floors. Furthermore, the base shears in frame D (shears corresponding to Story 1) when using static forces differ considerably from those base shears when using a dynamic analysis; however, this difference is reduced for the case of frame F. An interesting fact noticed in Figure 4-30 is that the base shear in frame F reported using static forces from ASCE 7-10 can be even smaller than those reported for the response spectrum analysis. Finally, it can be noticed that the average of the interstory shears using spectral matched acceleration histories gives similar results than those from response spectrum analysis.

It could not be possible to generalize any conclusion because these results correspond only to the particular case of Building 1; however, this section has shown an initial relationship between accidental torsion implemented with static forces, modal response spectrum analysis, and linear response history analysis. This current section has compared static and dynamic methods of accidental torsion using standard procedures; however, it is intended in this document to present alternative concepts such as rotational records and rotational spectrum as possible procedures to measure the effects of accidental torsion, and these topics are studied in the next section.

4.2.7 Rotational records and rotational response spectrum

An approach used to generate a rotational acceleration record is to use the translational records of two parallel channels at the base of a building and calculate the rotational acceleration by dividing the difference of the translational signals over the distance between them. This approach was used to study the accidental torsion in 30 buildings in California (De la Llera and Chopra, 1994b), and here, the characteristic of one of those torsional records will be described.

Figure 4-31 shows the orientation of the signals recorded for one of the buildings analyzed by De la Llera and Chopra (1994b). Those signals correspond to the Channel 9 (Ch9), Channel 10 (Ch10), and Channel 13 (Ch13) of the Watsonville four story building, which is denoted as CSMIP Station No. 47459 by the Center of Engineering Strong Motion Data

(California Department of Conservation's Strong Motion Instrumentation Program (CSMIP) and USGS National Strong Motion Program (NSMP), 2007).

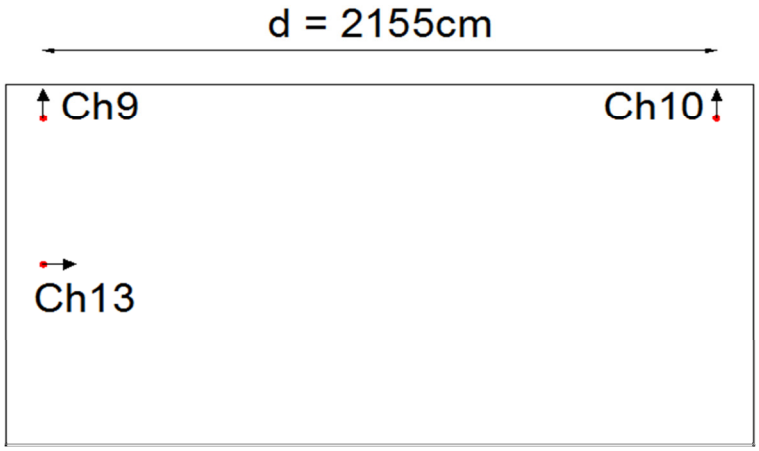

Figure 4-31 Location of instrumentation and orientation of the acceleration histories recorded at the ground floor of the CSMIP Station no. 47459 during the Loma Prieta earthquake in 1989

As it can be seen in Figure 4-31, Ch9 and Ch10 are the translational signals that are used to obtain the corresponding torsional record, and the acceleration record of these translational signals is presented in Figure 4-32, where it can be noticed a close similarity between the two signals as it was expected. An appropriate measure of the ground acceleration corresponding to the axis parallel to Ch9 and Ch10 could be given by the average of these two signals.

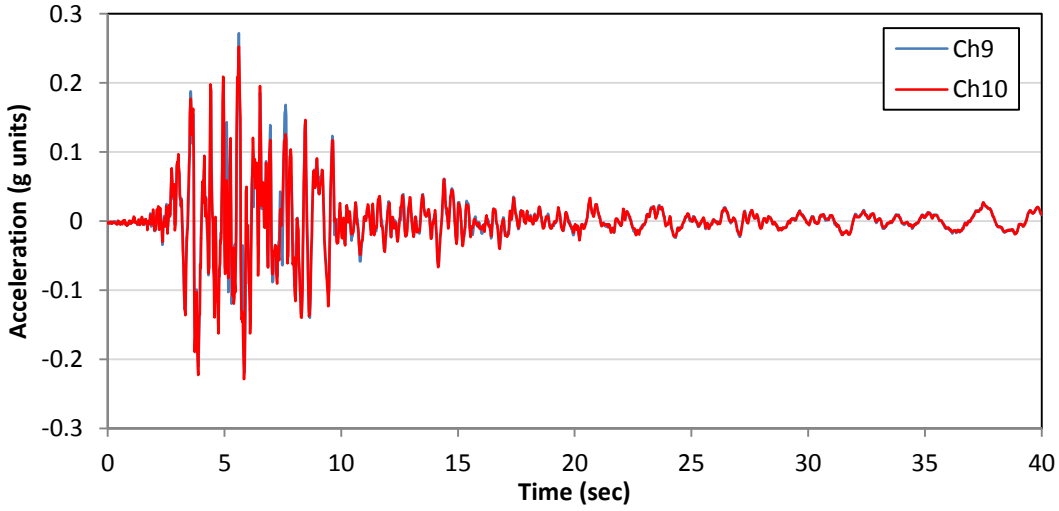

Figure 4-32 Acceleration records from Ch9 and Ch10

Furthermore, Figure 4-33 shows the correlation between those translational signals, and it tends to be a linear plot as expected due to their similarity. As a matter of fact, the correlation coefficient between the two translational signals was calculated to be 0.956, which indicates that the two signals are virtually identical.

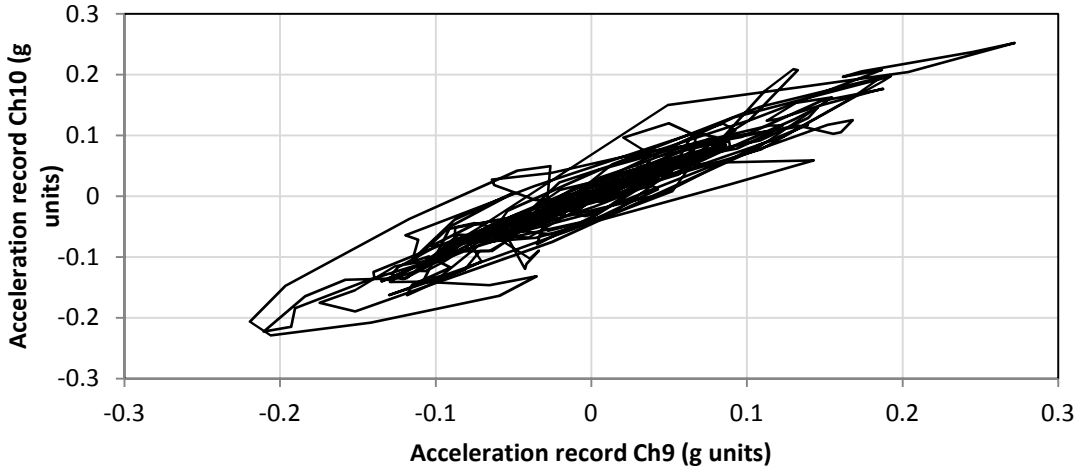

Figure 4-33 Correlation between the acceleration records Ch9 and Ch10

Also, the spectrum from the signals Ch9 and Ch10 is shown in Figure 4-34, and it can be noticed that both signals have almost equal ordinates for periods higher than 0.5 sec; however, the ordinates at very short periods differed from one signal to another as it is shown in Figure 4-34. The difference in the two spectra is more significant for periods less than 0.6 sec, and such differences could be associated with the rotational component of the ground motion.

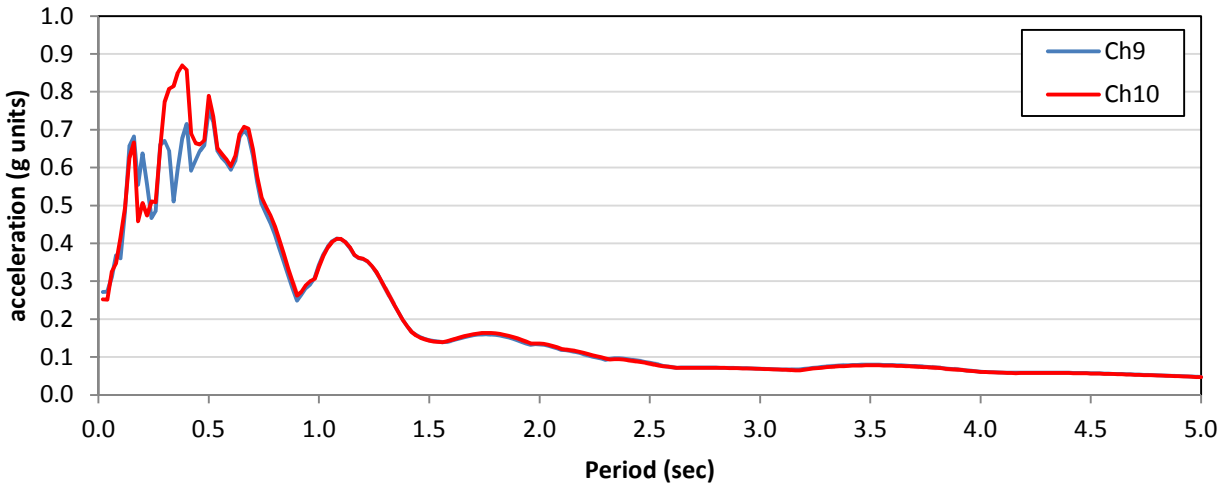

Figure 4-34 Spectrum from Channel 9 (Ch9) and Channel 10 (Ch10)

The rotational record was calculated then using the expression:

$$\text{Rotational Record} = \frac{Ch9 - Ch10}{d} \qquad \textbf{Eq. 4- 18}$$

The resulting record is shown in Figure 4-35, where the units of the vertical axis are g units per cm, which are equivalent to rad/sec^2 if the vertical axis is multiplied by g=386.4 in/sec^2.

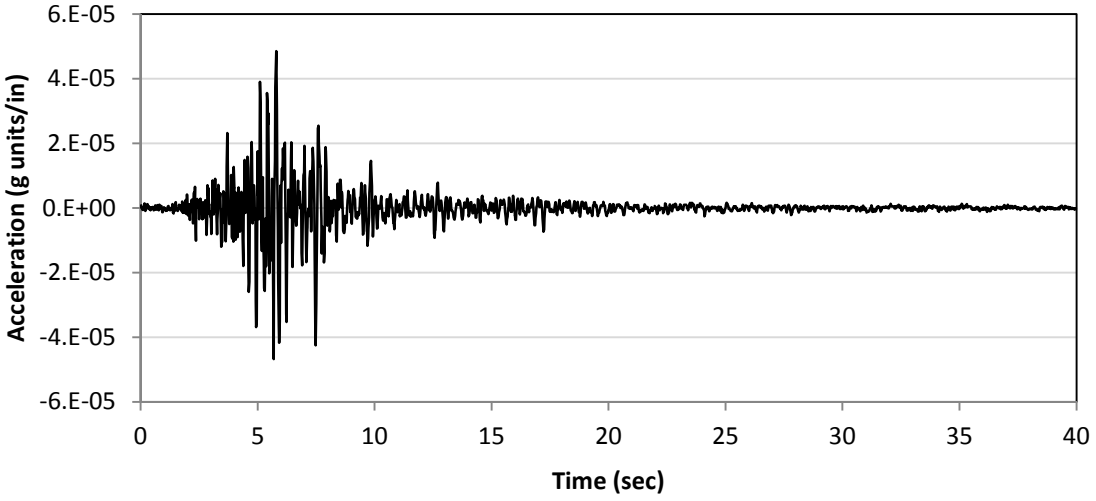

Figure 4-35 Rotational record generated from the translational acceleration histories Ch9 and Ch10

When the rotational record is obtained in this way, it is possible to have some level of dependence between the translational and the rotational records. For this particular case this dependence was investigated in Figure 4-36 where the translational and rotational records are plotted in the same figure, and it can be noticed that there is no trend between both records. This relation was further investigated with the correlation coefficient between the translational and the rotational records, which happened to be 0.001; therefore, it was confirmed that the translational and rotational record for this particular case were independent from each other.

Another procedure to derive rotational records can be based not only in using two translational records but using multiple stations; this methodology, denoted "geodetic method", was developed by Spudich et al. (1994). Ghayamghamian et al.(2009) used the geodetic method to derive rotational records using the data of multiple stations of the Chiba array in Japan. Nine of those rotational records were used to test the response of an idealized single story building and establish the relation with code procedures. It is shown in such study that accidental eccentricity

tends to be larger at small periods T and with small values of Ω, where T is the fundamental period in the direction analyzed, and Ω is the ratio of the fundamental translational and rotational periods. Values of accidental eccentricity for these cases were found to vary between 0.6b to 0.08b; however for long periods T and long ratios Ω, the equivalent accidental eccentricity was equal to 0.01b. It should be noticed that accidental eccentricities of 0.6b are twelve times bigger than those given by the ASCE 7-05.

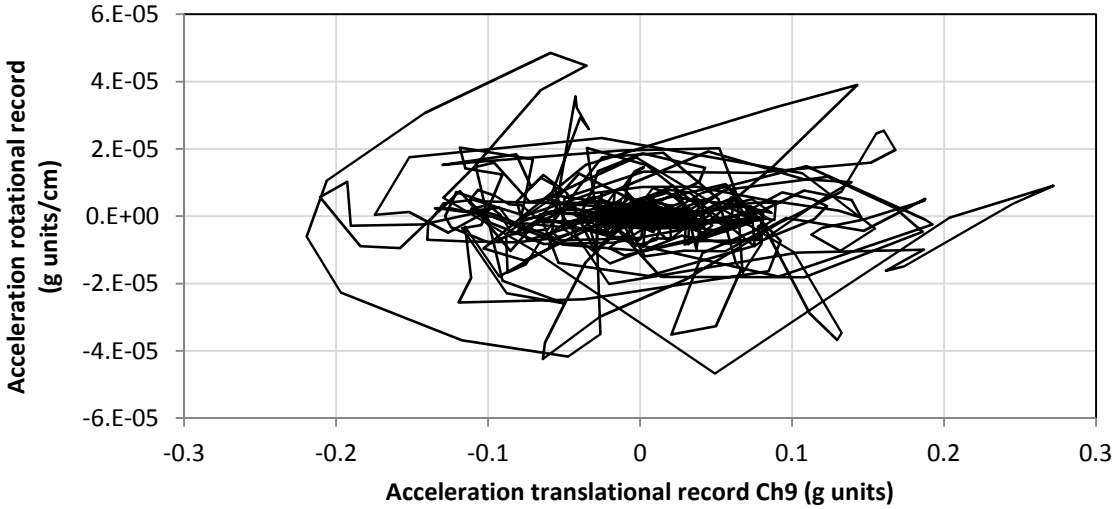

Figure 4-36 Correlation between the trnaslational record Ch9 and the generated rotational record

From the previous paragraphs it is concluded that rotational seismograms could be derived from translational records, and the availability of these rotational seismograms makes it possible to define the equation of motion of a single degree of freedom torsional oscillator under torsional excitation in terms of the angular acceleration, velocity, and rotation of the system. The maximum responses of angular acceleration, angular velocity and angular rotation under a specific torsional period can be used to generate a rotational spectrum, and the equation governing such spectrum, which has been taken from Tso and Hsu (1978), can be written as:

$$\ddot{\Psi}(t) + 2\xi\omega_{nRot}\dot{\Psi}(t) + \omega_{nRot}^2\Psi(t) = -\overset{**}{\phi}(t) \qquad \textbf{Eq. 4- 19}$$

where $\ddot{\Psi}(t)$ is the relative angular acceleration of the torsional oscillator

$\dot{\Psi}(t)$ is the relative angular velocity of the torsional oscillator

$\Psi(t)$ is the relative angular displacement of the torsional oscillator

ξ is the fractional critical damping

ω_{nRot} is the angular velocity corresponding to the torsional natural frequency

$\overset{**}{\phi}(t)$ is the computed rotational acceleration

The equation above is very similar to the equation governing the spectrum of a translational record. Also, the solution of the equation above implies the definition of ω_{nRot} as the square root of the ratio between a defined rotational stiffness K_{Rot} and a rotational mass M_{Rot}. If following this criterion, Figure 4-37 shows the rotational spectrum corresponding to the rotational record shown in Figure 4-35 for different levels of damping.

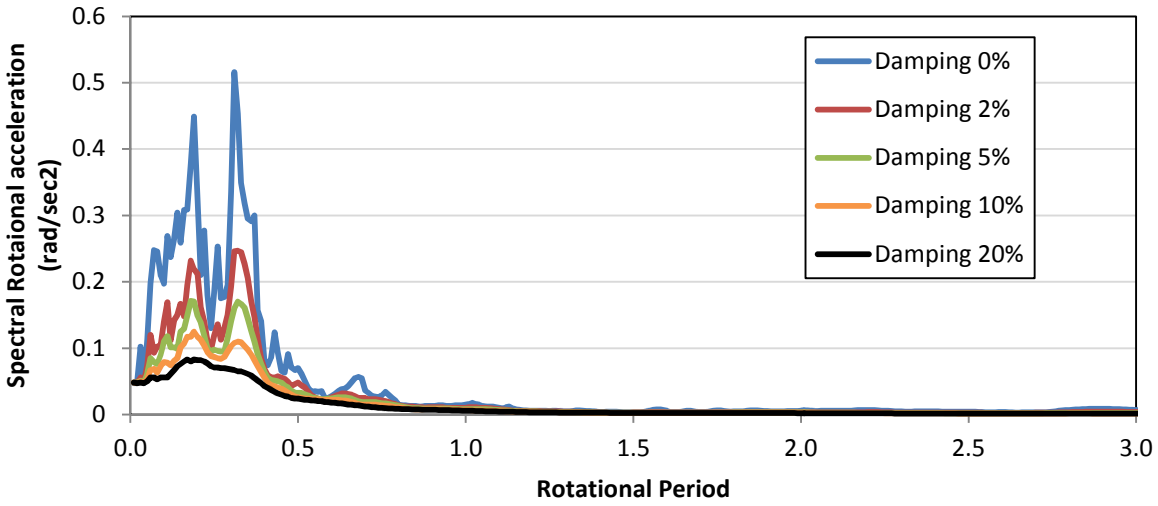

Figure 4-37 Rotational acceleration spectrum for different damping ratios considering the rotational record generated from the translational records Ch9 and Ch10

From Figure 4-37 it can be noticed that the rotational component of the ground motion has more influence at small periods, and this trend was also seen in Figure 4-34. More research is needed to explore this behavior.

It is of interest to compare the magnitude of the ordinates of the rotational spectrum relative to the ordinates of the translational spectrum, and with this purpose, Figure 4-38 shows the rotational spectra from Figure 4-37 together with the translational spectrum corresponding to the signal Ch9 for different levels of damping. Also, Figure 4-39 shows the same plot as Figure 4-38 but with the focus on periods less than 0.5 sec. The coordinates of the rotational spectrum have been multiplied by 1077.5 cm, which is half of the distance between Ch9 and Ch10 in Figure 4-31. This way, the translational and rotation spectrum of Figure 4-38 and Figure 4-39 have the same units. It can be seen in Figure 4-38 that the ordinates of the translational spectrum are higher than those of the rotational spectrum in the order of one magnitude; however, this difference in magnitude is reduced at short periods, as it is shown in Figure 4-39.

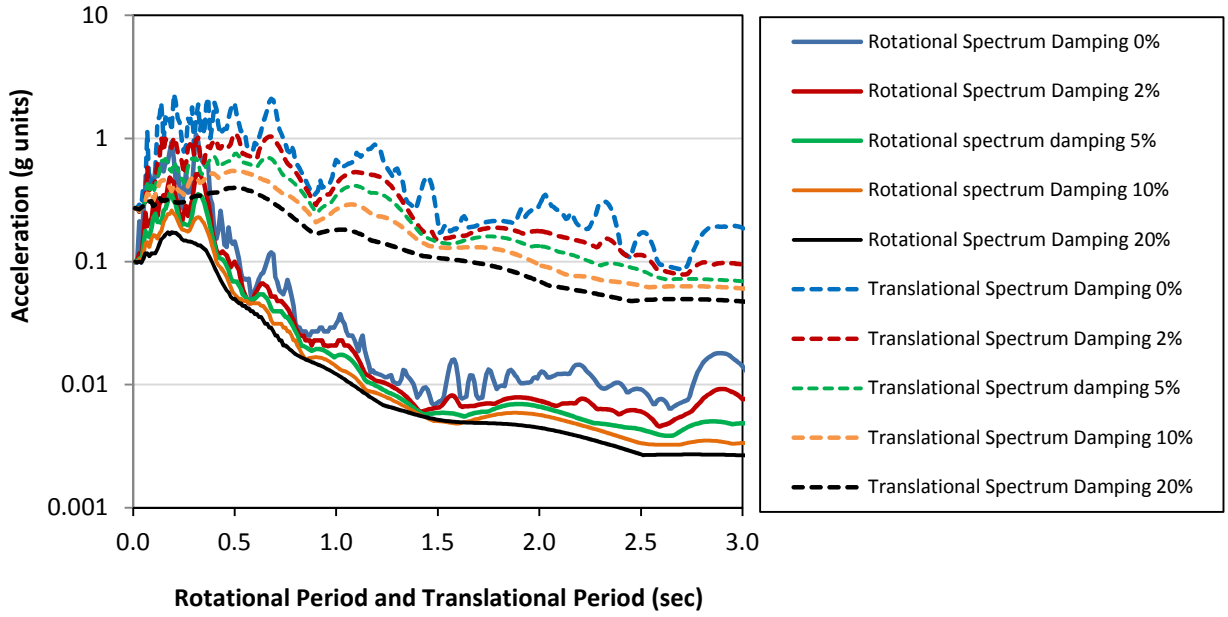

Figure 4-38 Rotational and translational spectrum of signal Ch9 for different levels of Damping

Another technique to develop the rotational spectrum using translational records was developed by Tso and Hsu (1978), and it is based on the treatment of an earthquake record as the "superposition of two non-dispersive propagating waves." The application of this method requires data of the angle θ between the orientation x and y corresponding to the local axis of the seismograms and the X and Y axis that define the orientation of the earthquake waves respect to

the epicenter. Figure 4-40 explains the definition of the x and y axis, the X and Y axis, and the angle θ. Furthermore this procedure requires the shear wave velocity of the soil.

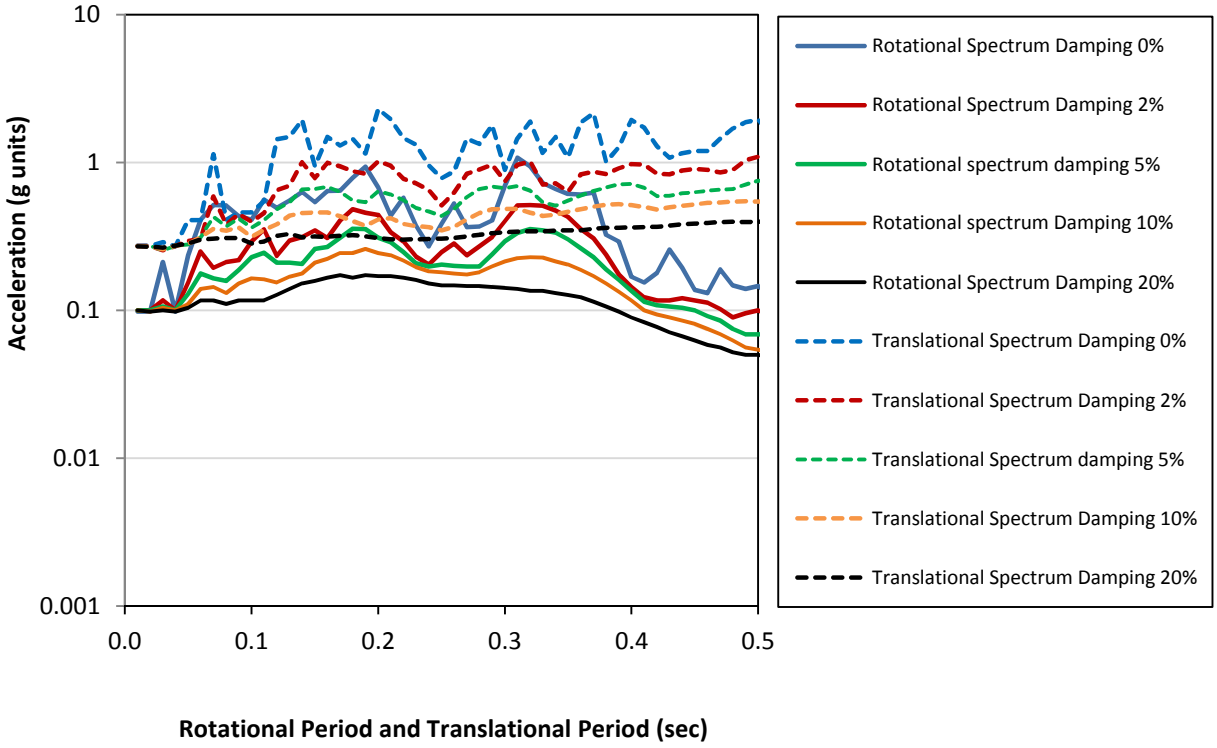

Figure 4-39 Rotational and translational spectrum of signal Ch9 for different levels of Damping – Detail at short periods

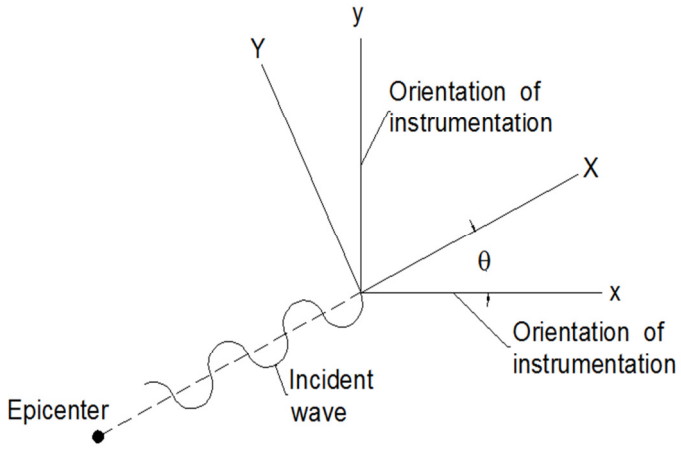

Figure 4-40 Definition of angle θ required for the calculation of the rotational spectrum using the method of Tso and Hsu (1978)

The procedure of Tso and Hsu calculates the contribution to the rotational spectrum from each of the translational components of a record, and the rotational spectrum is the summation of both components.

Tso and Hsu (1978) applied their technique to build the rotational spectrum of the El Centro earthquake in 1940; however, the specific source of this record is not stated. For this document computational routines were developed in the software Mathcad (Parametric Technology Corporation, 2007) to calculate the torsional spectrum using the approach of Tso and Hsu. The record corresponding to El Centro earthquake in 1940 was also used in these computational routines for comparison reasons. The record of El Centro was taken from the Center of Strong Motion Data database (California Department of Conservation's Strong Motion Instrumentation Program (CSMIP) and USGS National Strong Motion Program (NSMP), 2007). The resulting angular velocity spectrum was calculated by obtaining the maximum response of $\dot{\Psi}(t)$ in Eq. 4- 19 for different torsional periods, and the contribution to the angular velocity spectrum from the wave propagation along the X direction (see Figure 4-40) is shown in Figure 4-41, while the contribution to the rotational spectrum from the wave propagated in the Y direction is shown in Figure 4-42. All these spectra have been calculated for different damping ratios. Then, the total rotational spectrum, which is the summation of the contributions of Figure 4-41 and Figure 4-42, is presented in Figure 4-43.

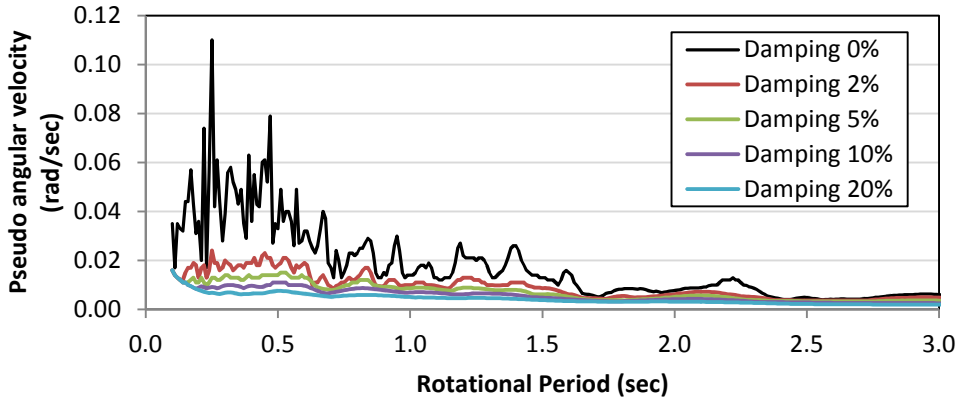

Figure 4-41 Angular velocity spectrum for wave propagation along the X direction (earthquake El Centro 1940)

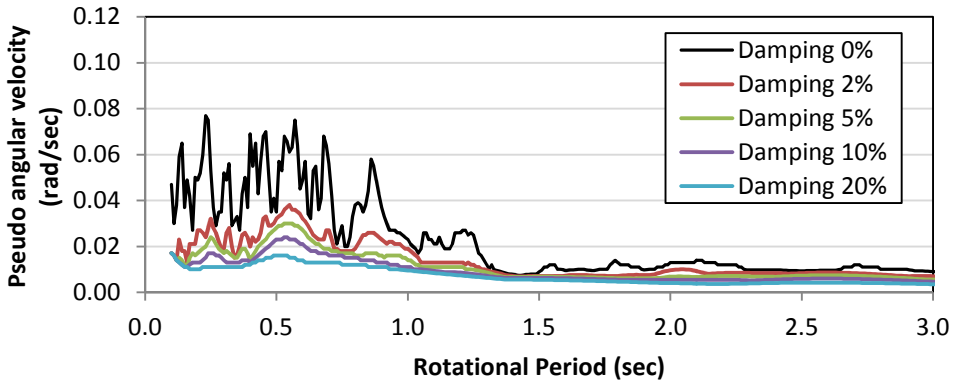

Figure 4-42 Angular velocity spectrum for wave propagation along the Y direction (earthquake El Centro 1940)

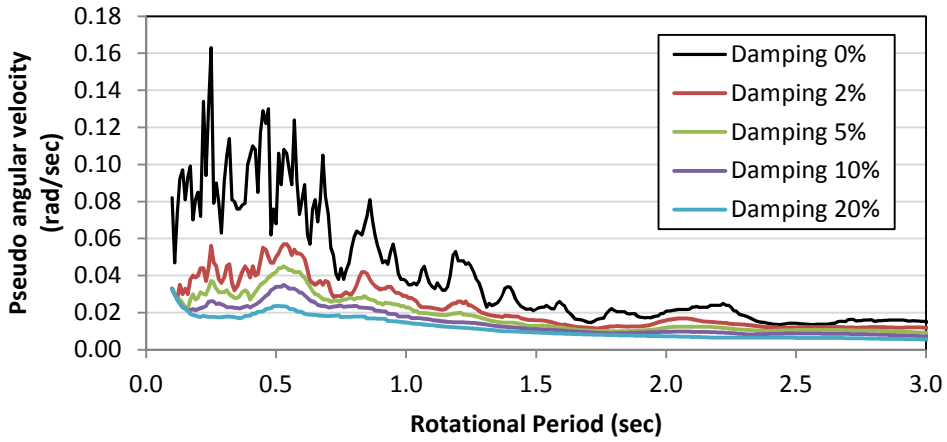

Figure 4-43 Angular velocity for wave propagation along the X and Y directions (earthquake el Centro 1940)

Figure 4-41 and Figure 4-42 of this document were compared with Figure 2 and Figure 3 of Tso and Hsu (1978), and the comparison showed very similar results of the original plots with the results from the computational routines developed for this document. Moreover, it can be seen in Figure 4-43 that the higher the damping the smother the angular velocity spectrum as was expected.

Also, it should be noticed that Figure 4-37 and Figure 4-43 represent two different rotational spectra; Figure 4-37 is an angular acceleration spectrum, while Figure 4-43 is an angular velocity spectrum; however, the angular velocity spectrum is related with the angular

rotation spectrum and the angular acceleration spectrum by the following relations which have been taken from Tso and Hsu (1978):

$$R_d = |\Psi(t)|_{max}$$
$$R_v = w_{nRot} R_d \qquad \textbf{Eq. 4- 20}$$
$$R_a = w_{nRot}^2 R_d$$

where: R_d is the angular rotation spectrum

R_v is the angular velocity spectrum

R_a is the angular acceleration spectrum

The method of Tso and Hsu is based on the method to draw the torsional response spectrum proposed by Newmark and Rosenblueth (1971). This section has discussed different procedures to obtain rotational records as well as torsional spectra; this information could be used to predict the effects of accidental torsion with dynamic procedures, and particularly with linear response history analysis; however, this topic of research was not investigated in this document. Also, it is believed that the rotational component of the ground motion might not represent a major contribution to accidental torsion since the ordinates of the rotational spectrum (normalized to the same units of the translational spectrum) are generally smaller by one order of magnitude with respect to the ordinates of the translational spectrum.

The application of rotational records or rotational spectra in building codes to capture accidental eccentricity is a topic that requires further research.

4.2.8 Recommendations for accidental torsion in LRHA

Based on the literature review of different seismic codes, as well as particular analysis developed in this chapter regarding accidental torsion in semirigid diaphragms, it is possible to establish some recommendations about the application of accidental torsion in LRHA; these recommendations are as follows.

The design eccentricity measured from the center of mass will be equal to 0.05b, where b is the longest dimension in direction perpendicular to the lateral load applied. For the case of lateral loading acting not parallel to the principal axis of a structure, the lateral forces will act on an ellipse with a center that coincides with the center of mass and with semi-axes that are equal to the design eccentricities in the principal directions of the building.

The eccentricity in each floor of a structure with more than one story will be applied in the same directions for all the floors of a building, and for the case of using rigid diaphragms, the rotational mass from the model without accidental torsion will not need to be changed when displacing the center of mass. Linear masses, if they exist, should be considered in the calculation of the rotational moment of inertia of each floor.

The calculation of torsional effects using static moments will be allowed only for the cases where the parameter Ω, which is the ratio of the fundamental translational and rotational period, is greater than 1. For other cases torsional effects will be calculated using dynamic procedures by artificially displacing the center of mass of each floor. Particularly for the case of rectangular diaphragms, the displacement of the center of mass with the eccentricity 0.05b can be done by removing 10% of the mass of the diaphragm and distributing this mass as a linear mass located at the edge of the building parallel to the force applied. For shapes of diaphragms different than rectangular, the designer should study other possibilities to displace the center of mass the desired eccentricity.

Chapter 5. MODELING

The assumptions made when modeling a structure for linear response history analysis (LRHA) are critical because the response values, i.e. nodal displacements or element forces, will be influenced by to those assumptions. This chapter will describe some of the key issues in the modeling of buildings when LRHA is the analysis technique to be used. The topics described in this chapter are:

- Orientation of ground motions.
- Use of the vertical component of ground motion
- Scaling of design parameters
- Orthogonal loading
- Explicit definition of load combinations
- Combinations of results
- Solution techniques of LRHA and damping assumptions
- Number of modes required when doing LRHA with modal analysis
- Combination of modal responses when doing LRHA with modal analysis
- P-Delta effects
- Modeling of the basement
- Calculation of drifts for structures modeled with semirigid diaphragms.

The reader is addressed to the Appendix E of this document for explanation of abbreviations not specified within the text.

5.1 Orientation of ground motion axis

After selecting the set of records to be used for linear response history analysis a careful analysis is necessary to find the appropriate orientation for which the two record components of each selected record will hit the structure so that it will cause the highest demands in the response parameters (i.e. interstory displacement, base shear). Two cases are mentioned next where designers are responsible for selecting the appropriate orientation of the two components of an earthquake record with respect to the principal axis of a structure.

First, it could be the case that the designer had identified the location of the source, the appropriate earthquakes for design purposes with components GMx and GMy and the orientation of these components relative to the source. However, the orientation of the structure itself might

not be well defined yet. This case, shown in Figure 5-1, might occur at initial stages of a project, and it will imply several analyses considering all the possible orientations of the structure.

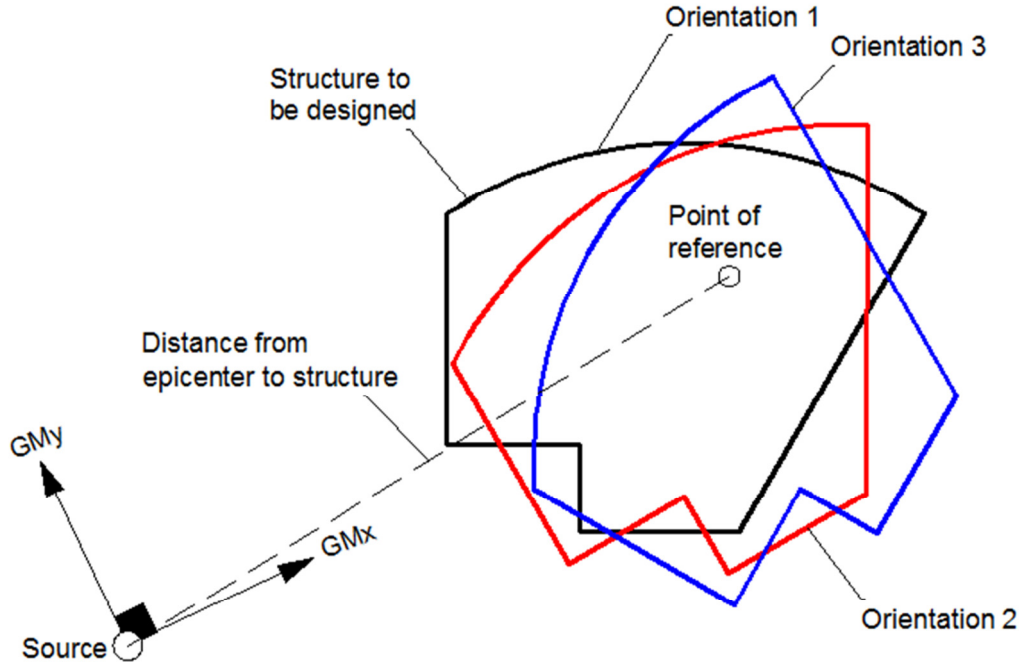

Figure 5-1 Case where the location of the source and the orientation of the record components GMx and GMy are known, but the final orientation of the structure is unknown

A second case needing a thoughtful analysis of the orientation of the record components relative to the structure might occur when the principal axis X and Y of the structure, the distance from the analyzed structure to the seismic source and the magnitude of the expected seismic event is known, but the specific ground motions for design purposes, the orientation of the components of such earthquakes, and the specific location of the seismic source is unknown. This case might occur when the deaggregation maps of the USGS (2009a) are used to define the probabilistic seismic hazard for the site of interest because those maps provide modal and mean values of the magnitude of an earthquake as well as the expected fault distance to the structure (for a structure with a specific period and probability of exceedance) but they do not provide the specific location of the source. For this case, which is shown in Figure 5-2, appropriate ground motions need to be taken from an earthquake database, and different orientations of the components of these selected earthquakes need to be analyzed.

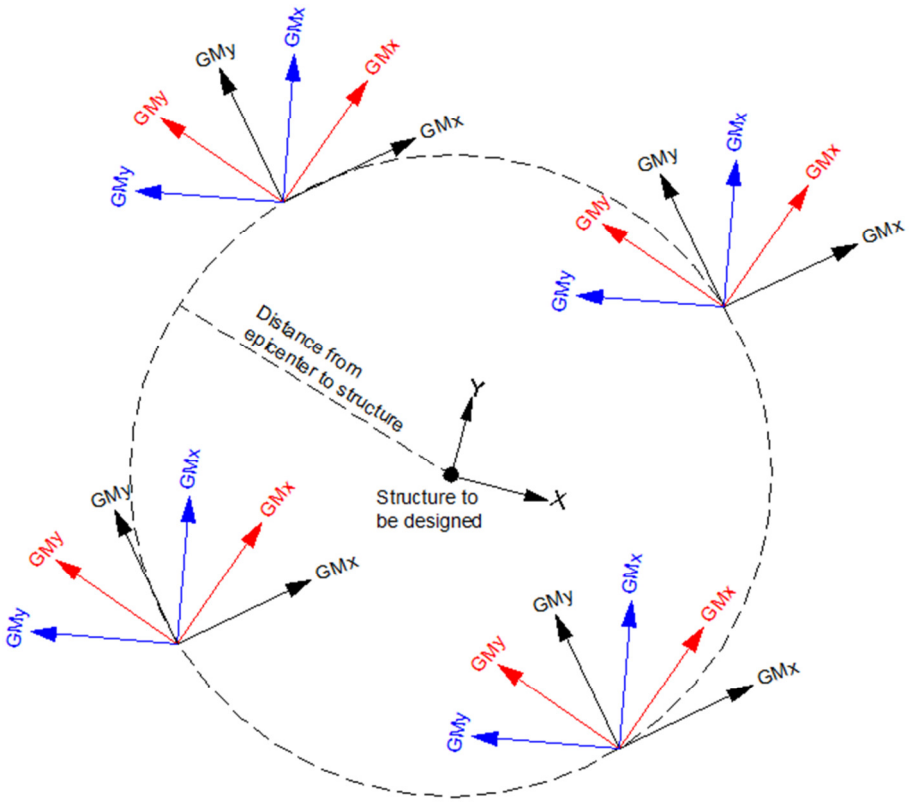

Figure 5-2 Case where the principal axis of the structure, the magnitude of the expected earthquake event, and the distance from the expected epicenter to the structure is known, but the specific earthquakes for design, the orientation of the record components GMx and GMy, and the exact location of the seismic source is unknown

A complexity associated with the last case refers to near field earthquakes, because it requires appropriate orientation of the ground motion components GMx and GMy relative to the structure due to rupture and directivity effects associated with the fault-normal and fault-parallel components of the ground motion. It has to be clear that for the last case mentioned above that the record components GMx and GMy can rotate at different angles with respect to the orientation of the principal axis X and Y of the structure, and this rotation does not change the components GMx and GMy but only implies a change in the angle of attack (angle between the axis of the record components and the principal axis of the structure analyzed). A different case happens when analyzing the acceleration histories generated if the equipment used to record the earthquake signals had been oriented in a different angle. In such a case, different orientations of the equipment would yield different acceleration histories

Based on Figure 5-3, the acceleration histories for different angles θ of the instrumentation could be obtained by using the following linear transformations:

$$\begin{aligned} GMx'_i &= GMx_i \cos\theta + GMy_i \sin\theta \\ GMy'_i &= -GMx_i \sin\theta + GMy_i \cos\theta \end{aligned} \quad \text{or} \quad GM' = \begin{bmatrix} \cos\theta & \sin\theta \\ -\sin\theta & \cos\theta \end{bmatrix} GM \qquad \textbf{Eq. 5- 1}$$

where GMx_i is the i^{th} acceleration of the original record in the component x

GMy_i is the i^{th} acceleration of the original record in the component y

θ is the rotation angle of the axis of the original record

GMx'_i is the i^{th} acceleration of the generated record in the component x'

GMy'_i is the i^{th} acceleration of the generated record in the component y'

GM' is equal to $\begin{bmatrix} GMx'_1 & GMx'_2 & GMx'_3 & \ldots\ldots & GMx'_i & \ldots\ldots & GMx'_n \\ GMy'_1 & GMy'_2 & GMy'_3 & \ldots\ldots & GMy'_i & \ldots\ldots & GMy'_n \end{bmatrix}$

GM is equal to $\begin{bmatrix} GMx_1 & GMx_2 & GMx_3 & \ldots\ldots & GMx_i & \ldots\ldots & GMx_n \\ GMy_1 & GMy_2 & GMy_3 & \ldots\ldots & GMy_i & \ldots\ldots & GMy_n \end{bmatrix}$

The axis x and y follow the direction of the original components GMxi and GMyi

The axis x' and y' follow the direction of the generated components GMx'_i and GMy'_i

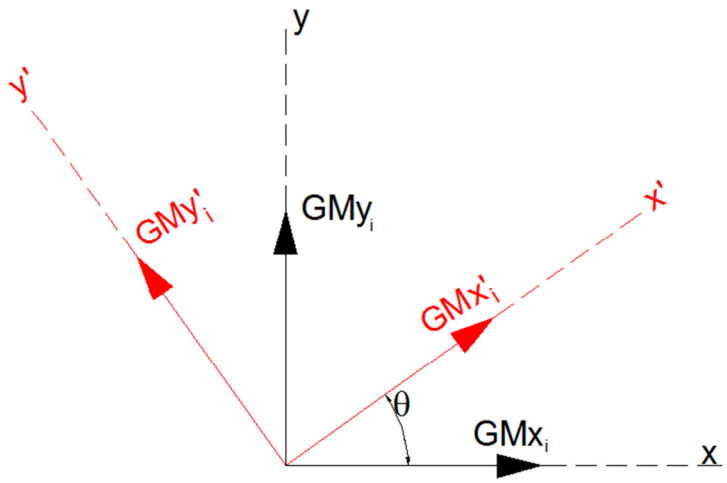

Figure 5-3 Transformation of the acceleration coordinates from the original record (components GMx_i and GMy_i) to a new record obtained (components GMx_i' and GMy_i') rotating the original acceleration coordinates an angle θ

In the strictest sense it is not technically correct to use Eq. 5- 1 because those transformations assume linear behavior of the soil; however, during an earthquake the soil might behave nonlinearly and then Eq. 5- 1 will be only an approximation.

Each of the acceleration histories generated with Eq. 5- 1 implies a different response of the structure, and these differences can be investigated using a "Orbit Spectrum" which is a graph in polar coordinates (ρ,θ) that shows the spectral response measure ρ (either spectral acceleration, spectral velocity or spectral displacement) at a specific period *T* from acceleration histories obtained when decomposing the axis of the record components into a new set of axis rotated an angle θ. The orbit spectrum is drawn without rotating the components of the ground motion itself, but just decomposing them in principal directions.

Figure 5-4 and Figure 5-5 show the procedure to obtain the acceleration orbit spectrum, and the same methodology applies for obtaining the velocity and displacement orbit spectra. Figure 5-4 shows the acceleration response spectrum corresponding to three record components generated by decomposing the original record components along a pair of new axis rotated an angle of $\theta 1$, $\theta 2$, and $\theta 3$, with respect to the orientations of the original record (see Figure 5-3). The spectrum corresponding to the component of the original record ($\theta = 0$) has also been included in Figure 5-4. The acceleration orbit spectrum for a particular period *T* can be obtained by plotting in polar coordinates the spectral acceleration at the period *T* for each angle θ, as it is shown in Figure 5-5.

The advantage of using the orbit spectrum is that it defines the angle for which the maximum spectral acceleration, velocity or displacement is obtained based on the response to the first mode. This particular angle is defined as the "critical angle", and it can be used to define the "principal axis of a ground motion". For instance, the critical angle for the case of Figure 5-5 is $\theta 2$ because it produces the highest spectral ordinate. Also, the acceleration history corresponding to the critical angle is denoted as the "critical acceleration history" or the "critical component", and it is independent of the angle of attack of the earthquake. Moreover, because the orbit spectrum is drawn for a specific period, it is expected that each principal direction of a building might have a different critical acceleration history when the fundamental periods in those principal directions are different. Additional explanations of the orbit spectrum can be found in Beyer et. al. (2007).

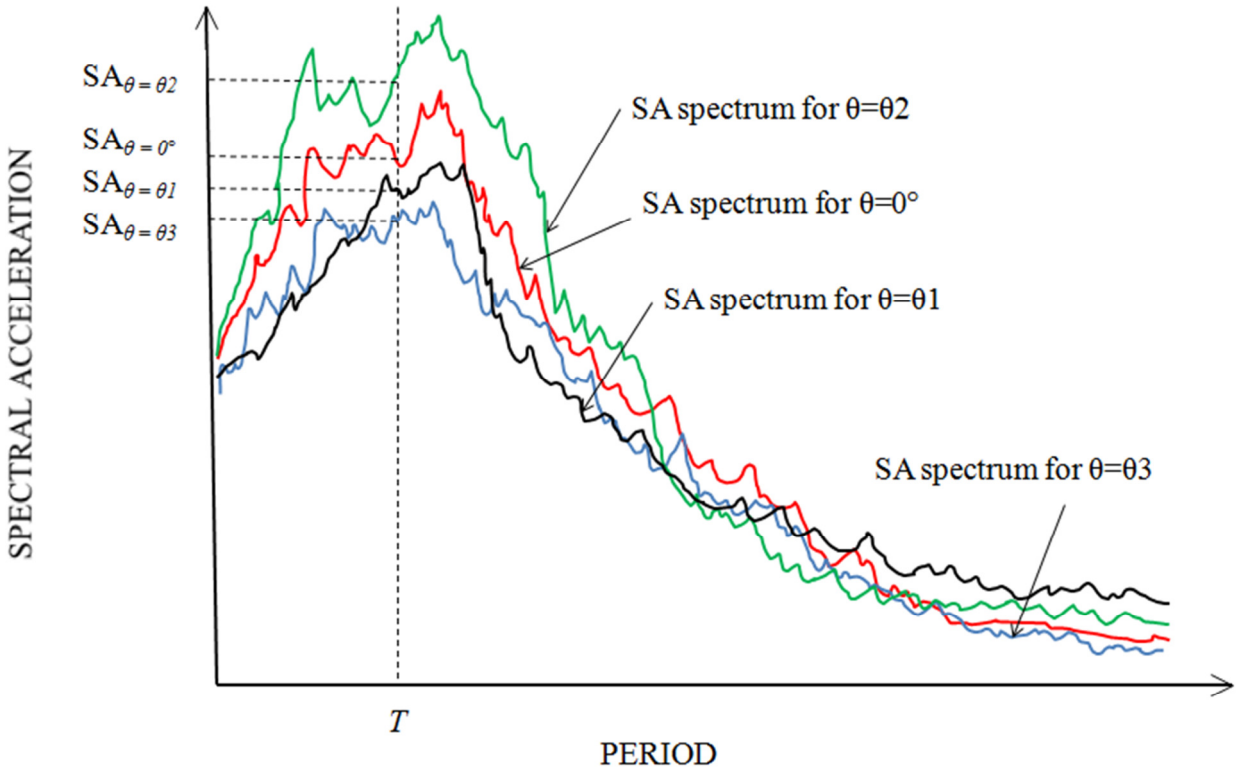

Figure 5-4 Procedure to obtain the data for the Acceleration Orbit Spectrum

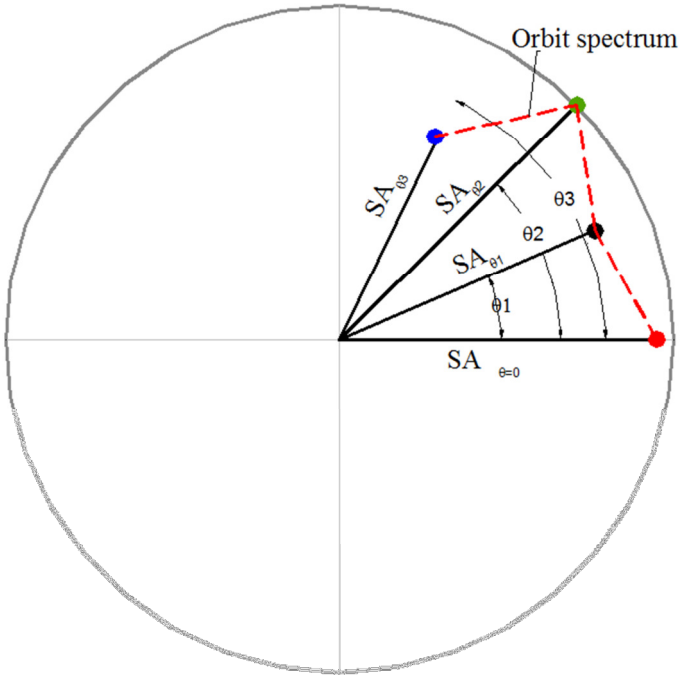

Figure 5-5 Construction of the Orbit Spectrum

As an example of the applications of the orbit spectra, the program EQTools (Charney and Syed, 2004, 2010) was used to obtain different orbit spectra for the Building 2 of Appendix A. This building has an average period in both orthogonal directions of 2.74 sec, and the selected acceleration histories are the records A, B, and C of Table 2-6. As noted in Table 2-6, the horizontal components of the records A, B, and C are A00 and A90 for record A, B00 and B90 for record B, and C00 and C90 for record C.

Table 5-1 shows the maximum spectral accelerations at the period T=2.74 sec of the record components A00 and A90 when different angles were used to decompose the original components of Record A. The spectral accelerations corresponding to an angle of zero degrees represent the spectral accelerations at *T*=2.74 sec of the original signals without any rotation of the record components. Also, Table 5-1 shows the geometric mean (geomean) of the spectral accelerations A00 and A90.

Table 5-1 Data corresponding to the acceleration orbit spectrum of Record A for a period T=2.74 sec.

Angle	**Spectral Acceleration**		
	A00	**A90**	**Geomean of A00 and A90**
(degrees)	**(g units)**	**(g units)**	**(g units)**
0	0.319	0.110	0.187
30	0.241	0.229	0.235
60	0.103	0.313	0.180
75	0.093	0.327	0.174
90	0.110	0.319	0.187
120	0.229	0.241	0.235
150	0.313	0.103	0.180
180	0.319	0.110	0.187
210	0.241	0.229	0.235
240	0.103	0.313	0.180
270	0.110	0.319	0.187
300	0.229	0.241	0.235
330	0.313	0.103	0.180
345	0.327	0.093	0.174
360	0.319	0.110	0.187

It can be noticed in Table 5-1 that the maximum spectral acceleration of a rotated record component differs from the spectral acceleration when the original record component is not rotated (Angle = 0). For instance, the maximum spectral acceleration for the rotated record component A00 is 0.327g at an angle equal to 345 degrees, while the spectral acceleration using the original components (at angle = 0°) is 0.319g. The information provided in Table 5-1 was used to generate the acceleration orbit spectrum of Record A which is shown in Figure 5-6.

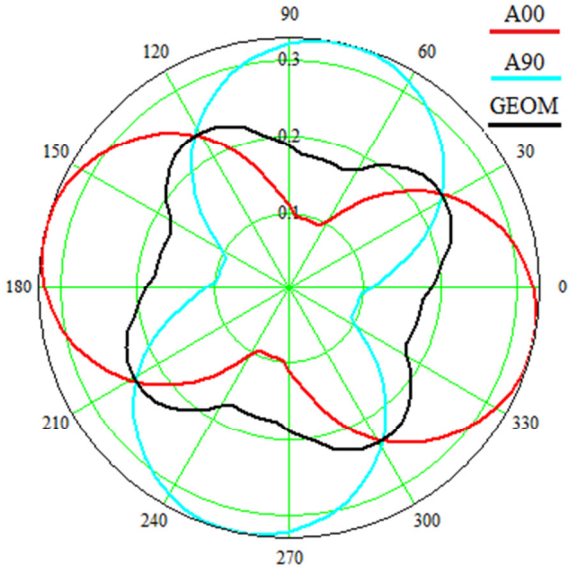

Figure 5-6 Acceleration orbit spectrum of Record A for a period *T*=2.74 sec

Figure 5-6 shows in polar coordinates the same information of Table 5-1 except that the spectral accelerations at *T*=2.74 sec have been calculated at 1 degree angle interval. The red line in Figure 5-6 represents the variation of the spectral acceleration of the rotated record component A00 for different angles, and as it was mentioned before, it can be seen that the maximum spectral acceleration occurs for an angle of 345 degrees. Also, it can be noticed that the spectral acceleration of the record component A90 is in phase 90 degrees with the spectral acceleration of the record component A00, which means that when the acceleration of the record component A00 reach its maximum (at 345°) then the spectral acceleration in the record component A90 reach its minimum, as it is shown in Figure 5-6. In the same way, when the spectral acceleration of the record component A90 reaches its maximum (at 345+90=75°) the spectral acceleration of the record component A00 reaches its minimum. In addition, from Figure 5-6 it can be noticed that the spectral acceleration in each record component varies considerably when changing the

angle; however, not major change is noticed in the spectral accelerations given by the geomean of the spectral accelerations of A00 and A90.

The acceleration orbit spectrum of record A (Figure 5-6) has been repeated for convenience in Figure 5-7, and the acceleration orbit spectrum of Records B and C is shown in Figure 5-11 and Figure 5-15, respectively. As it was already noticed for record A, Figure 5-11 and Figure 5-15 show that in the case of records B and C the maximum spectral acceleration for the period T=2.74 sec does not occur when using the original record components (rotation equal to zero degrees), and the rotation angle θ defining the critical acceleration history of each record component is shown in Table 5-2.

Table 5-2 Angle θ needed to obtain maximum spectral acceleration

Record	θ
A00	345°
A90	75°
B00	45°
B90	135°
C00	75°
C90	165°

A different procedure to study the maximum responses of spectral acceleration, velocity, and displacement is to calculate the ratios between the spectral acceleration, velocity and displacement given by the orbit spectra and the same parameters obtained in the original records with no rotation angle. The resulting ratios can be denoted as "Normalized Response", and a particular value of normalized response bigger than 1.0 will indicate an angle at which the spectral measure of interest (spectral acceleration, velocity or displacement) after rotation of the record components is greater than the same spectral measure from the original record components with no rotation. The normalized response for the spectral acceleration of the records A, B, and C is shown in Figure 5-8, Figure 5-12, and Figure 5-16, respectively; the normalized response for the spectral velocity of the records A, B, and C is shown in Figure 5-9, Figure 5-13, and Figure 5-17, respectively, and the normalized response for the spectral displacement of the records A, B, and C is shown in Figure 5-10, Figure 5-14, and Figure 5-18, respectively. The critical angles in these plots can be obtained by identifying the angle at which the normalized spectral response is the highest.

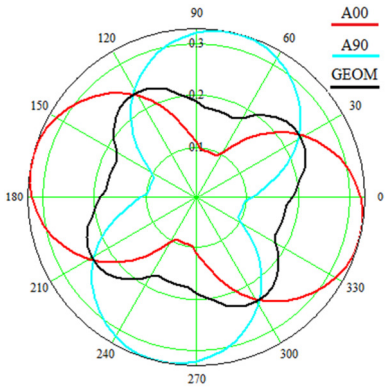

Figure 5-7 Acceleration orbit spectrum of earthquake A for a period T=2.74 sec.

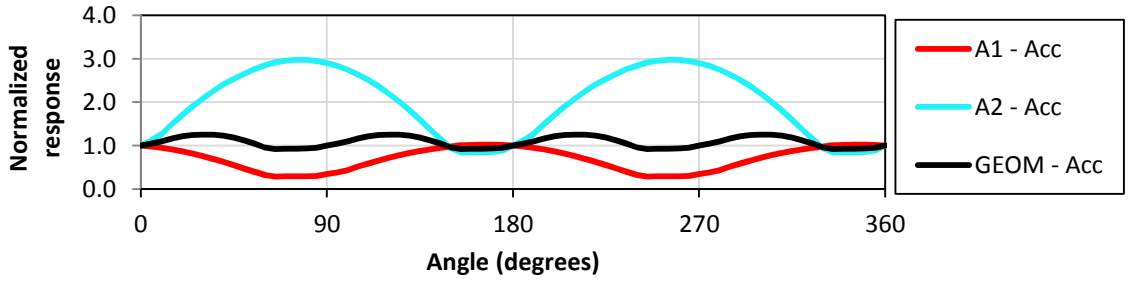

Figure 5-8 Normalized response of spectral acceleration corresponding to the earthquake A, for different angles of the orbit spectrum, and for structure with fundamental period T=2.74 sec.

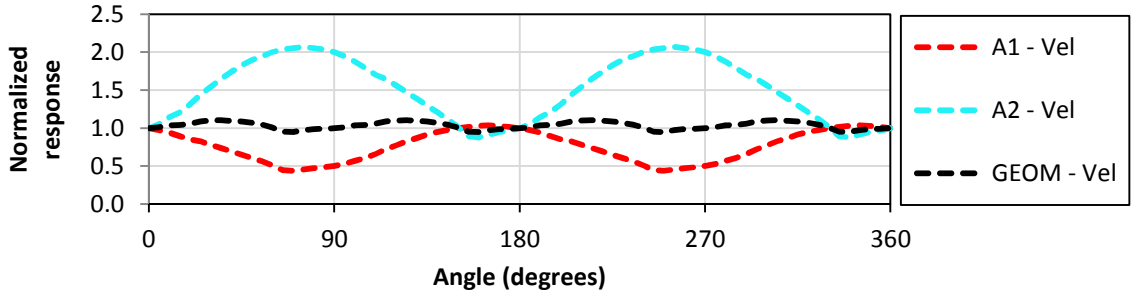

Figure 5-9 Normalized response of spectral velocity corresponding to the earthquake A, for different angles of the orbit spectrum, and for structure with fundamental period T=2.74 sec.

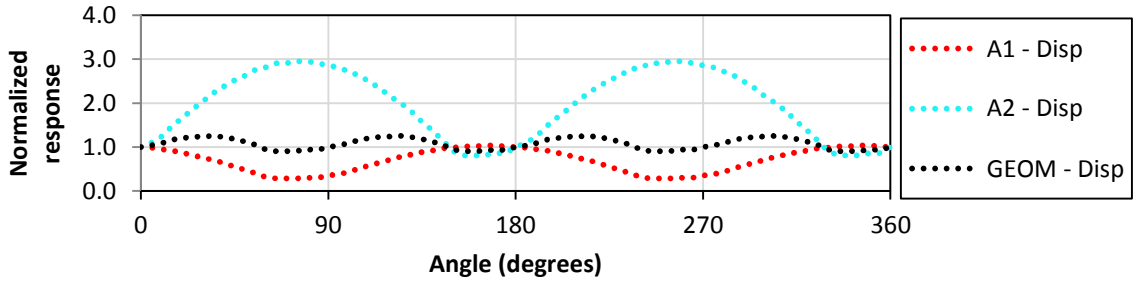

Figure 5-10 Normalized response of spectral displacement corresponding to the earthquake A, for different angles of the orbit spectrum, and for structure with fundamental period T=2.74 sec.

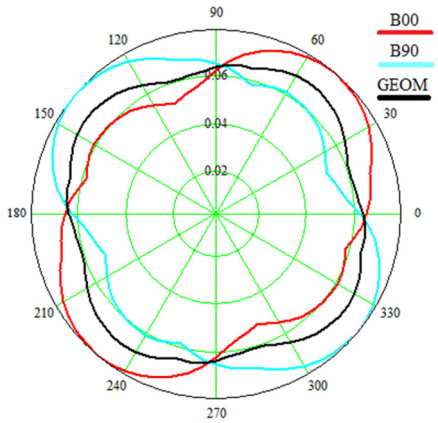

Figure 5-11 Acceleration orbit spectrum of earthquake B for a period T=2.74 sec.

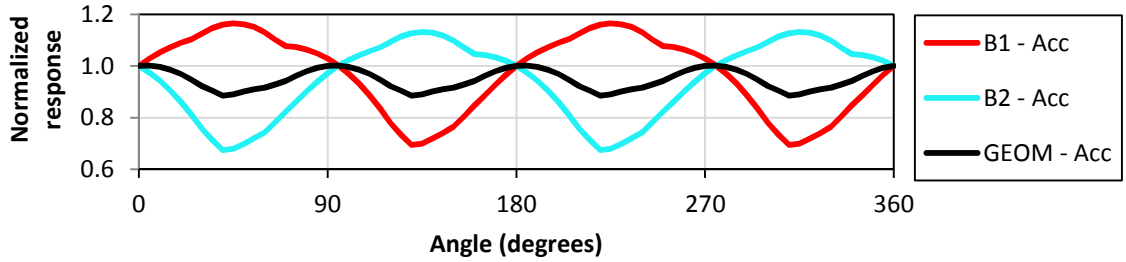

Figure 5-12 Normalized response of spectral acceleration corresponding to the earthquake B, for different angles of the orbit spectrum, and for structure with fundamental period T=2.74 sec.

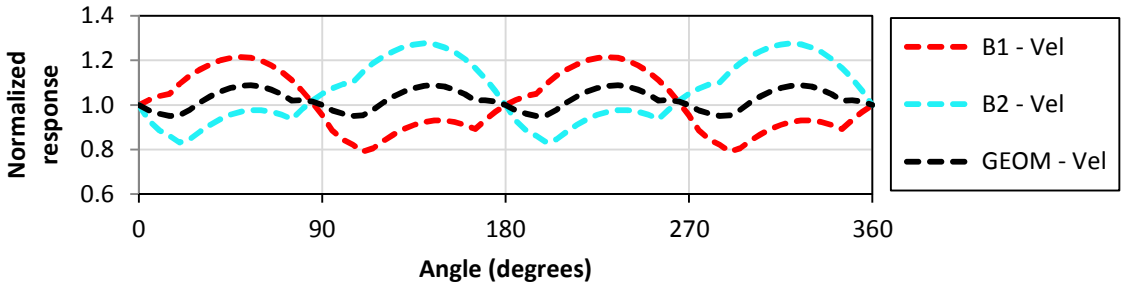

Figure 5-13 Normalized response of spectral velocity corresponding to the earthquake B, for different angles of the orbit spectrum, and for structure with fundamental period T=2.74 sec.

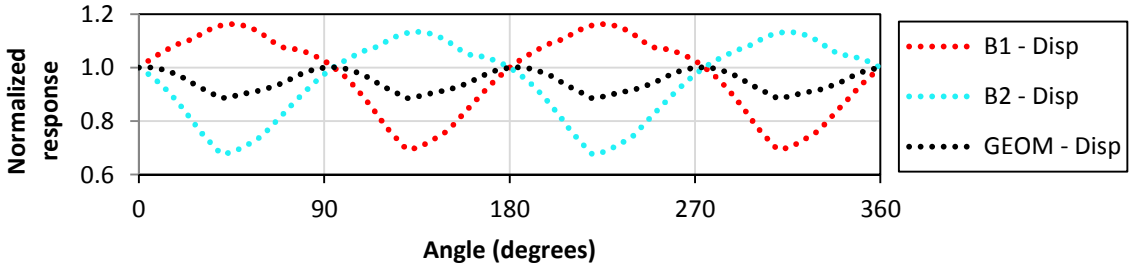

Figure 5-14 Normalized response of spectral displacement corresponding to the earthquake B, for different angles of the orbit spectrum, and for structure with fundamental period T=2.74 sec.

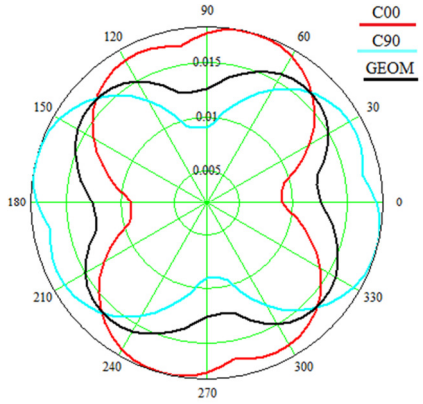

Figure 5-15 Acceleration of Orbit spectrum of earthquake C for a period T=2.74 sec.

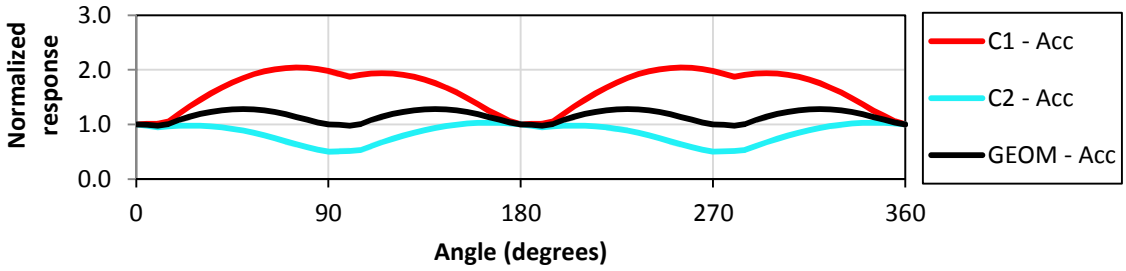

Figure 5-16 Normalized response of spectral acceleration corresponding to the earthquake C, for different angles of the orbit spectrum, and for structure with fundamental period T=2.74 sec.

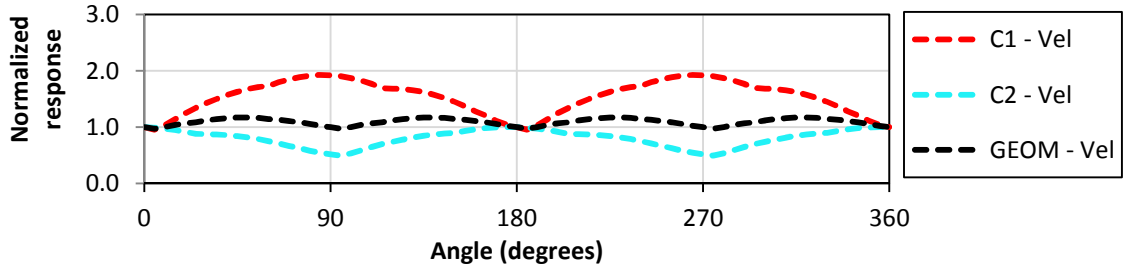

Figure 5-17 Normalized response of spectral velocity corresponding to the earthquake C, for different angles of the orbit spectrum, and for structure with fundamental period T=2.74 sec.

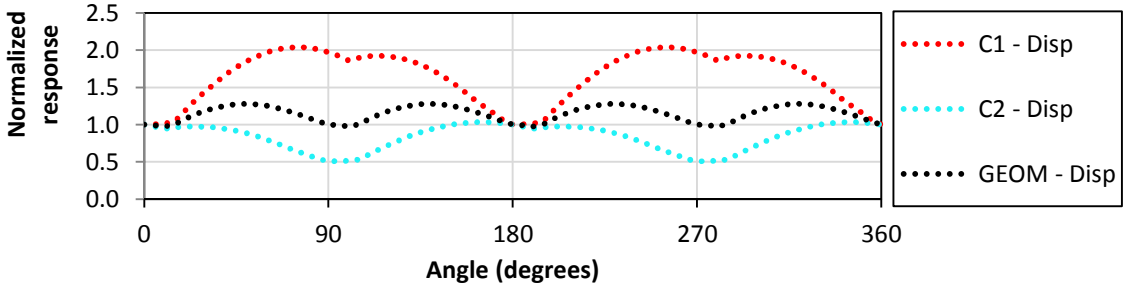

Figure 5-18 Normalized response of spectral displacement corresponding to the earthquake C, for different angles of the orbit spectrum, and for structure with fundamental period T=2.74 sec.

It can be noticed in Figure 5-8 and Figure 5-10, Figure 5-12 and Figure 5-14, and Figure 5-16 and Figure 5-18 that the normalized responses of the spectral acceleration and the spectral displacement are the same; however, the shape of the normalized response of the velocity spectrum (Figure 5-9, Figure 5-13, and Figure 5-17) is similar to normalized responses of spectral acceleration and displacement but it has different numerical values. The reason for this behavior is because the acceleration and velocity orbit spectra calculated in this document used the actual values of spectral acceleration and velocity, instead of pseudo values that are dependent of the actual spectral displacement ($PSV=\omega D$ or $PSA=\omega^2 D$, where PSV and PSA are the pseudo velocity spectrum and the pseudo acceleration spectrum, respectively, and D is the spectral displacement). The actual and pseudo velocity spectrum can differ significantly (Chopra, 2007), and therefore, different normalized responses, and therefore different critical angles, are expected when using actual and pseudo velocity spectrum. The normalized responses and the critical angles would be the same for the acceleration, velocity, and displacement, if the pseudo spectra were used to calculate the normalized responses. However, because this is not the case, it is expected different normalized responses and critical angles for velocity and acceleration.

The case is different for the normalized responses and critical angles from acceleration and displacement, because the actual and pseudo acceleration spectra are very similar for low levels of damping (Chopra, 2007), which indicates that actual and pseudo spectral acceleration will have the same normalized response. Also, because the pseudo spectral acceleration is directly related with the spectral displacement ($PSA=\omega^2 D$), the normalized responses from displacement and acceleration will be the same, and therefore, they will also have the same critical angle. Then, it is concluded that the critical angles are the same for the orbit acceleration and for the orbit displacement spectra; however, it could differ for the orbit velocity spectrum.

It could be thought that the defined "critical acceleration history" (see pg. 166) will produce the worst effects in a structure; however, this might not be always the case because the orbit spectrum reflects the spectral response of a structure only under its first fundamental period, and it does not include the effects of higher modes. This way, it is not guaranteed that the critical angle will provide the highest value of a particular response parameter. This issue was further investigated by obtaining the interstory shears in Building 2 of Appendix A using the original components and the critical acceleration histories generated for the three earthquakes A,

B, and C from Table 2-6. The components of each record as well as the critical acceleration histories corresponding to the critical angle were modified by the scale factors provided in Charney et al. (2010b).

The results after applying all the acceleration histories of interest in the X direction are shown in Figure 5-19, Figure 5-20, and Figure 5-21 for the earthquakes A, B, and C, respectively. Also, the results after applying all the acceleration histories of interest in the Y direction are shown in Figure 5-22, Figure 5-23, and Figure 5-24 for the acceleration histories of the earthquakes A, B, and C, respectively.

From Figure 5-19 through Figure 5-24 it can be noticed that the critical acceleration histories tends to produce higher interstory shears than any of the original record components but this is not always the case. For instance, Figure 5-21 and Figure 5-24 show some floors where the interstory shear from one of the original components is higher than the one given by the critical acceleration history, and this could be due to the influence of the higher modes.

After discussing in detail some issues regarding the orientation of the ground motion axis, some recommendations are presented as follows:

Recommendation for orientation of ground motion axis*:* It is recommended to find the critical angle of each earthquake used in the analysis, and then obtain the respective critical acceleration history. The critical acceleration history could be used to calculate the maximum base shear when a structure is loaded only in one of its principal directions, and for this case, the base shear from LRHA could be defined as the higher value resulting from applying the original components of the ground motion and the critical acceleration history in the direction parallel to the principal axis of the structure. A similar definition could be applied to define the loading of the structure when it is desired to obtain interstory drifts. Finally, for calculations involving simultaneous loading in the two principal axis of the structure, using the original components of the ground motions instead of using the critical acceleration history will be allowed. This recommendation assumes that it has been already defined the principal axis of the structure.

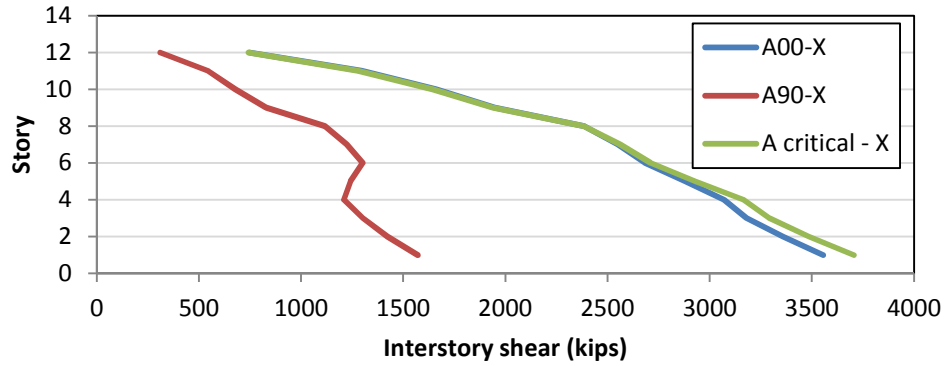

Figure 5-19 Interstory shear in the X direction of Building 2 for the two components and for the critical acceleration history of the earthquake A

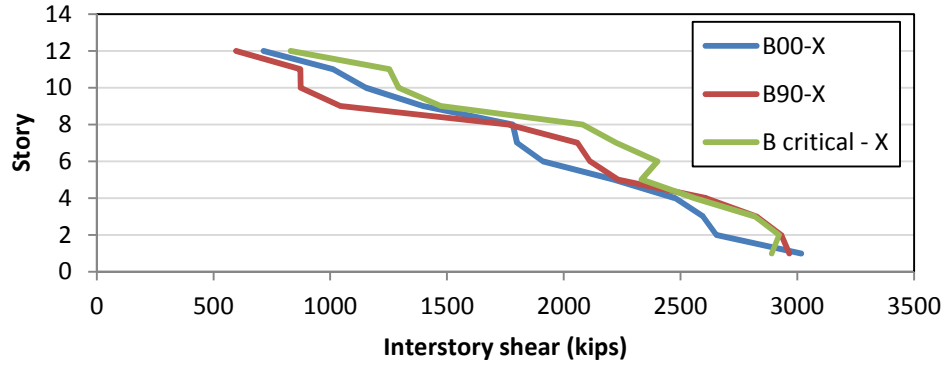

Figure 5-20 Interstory shear in the X direction of Building 2 for the two components and for the critical acceleration history of the earthquake B

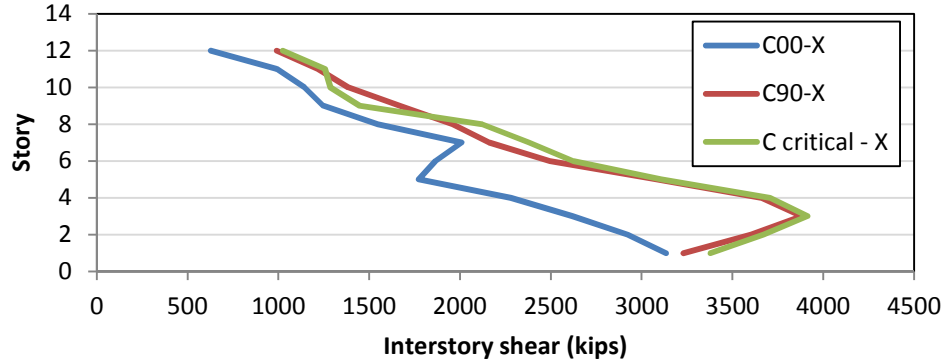

Figure 5-21 Interstory shear in the X direction of Building 2 for the two components and for the critical acceleration history of the earthquake C

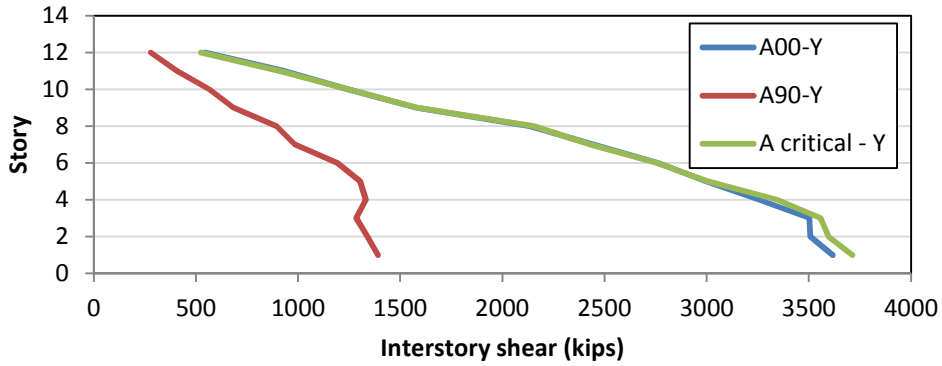

Figure 5-22 Interstory shear in the Y direction of Building 2 for the two components and for the critical acceleration history of the earthquake A

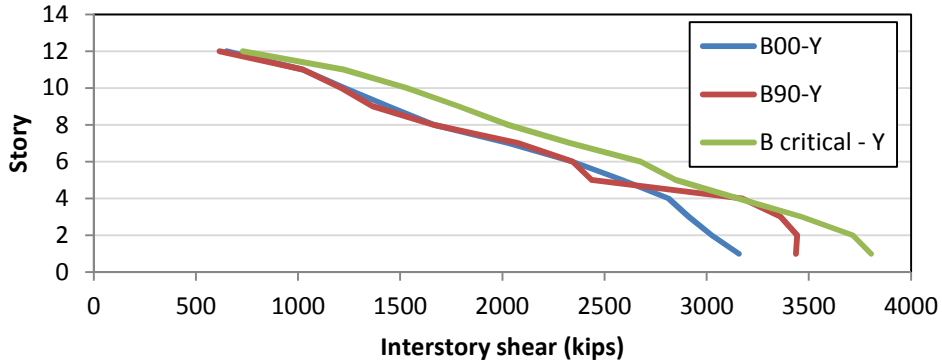

Figure 5-23 Interstory shear in the Y direction of Building 2 for the two components and for the critical acceleration history of the earthquake B

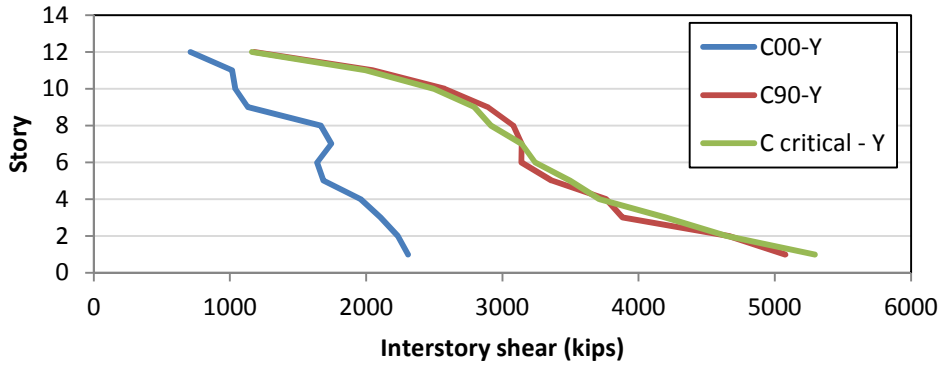

Figure 5-24 Interstory shear in the Y direction of Building 2 for the two components and for the critical acceleration history of the earthquake C

5.2 Use of the vertical component of the ground motion

Most of the earthquake records available in strong motion databases such as the NGA database (PEER, 1999) or the COSMOS database (2007), include the two horizontal and the vertical component of the ground motion; however, the LRHA specified in ASCE 7-10 does not require the analysis to include the vertical component of the earthquake, and instead this effect is indirectly accounted for in the definition of the earthquake load E given in section 12.4.2 of this standard which has being repeated here for convenience:

$$E = E_h + E_v \qquad \text{Eq. 12.4-1 of ASCE 7-10}$$

where E is the seismic load effects for use in the load combinations of ASCE 7-10.

E_h is the effect of horizontal seismic forces.

E_v is the effect of vertical seismic forces.

In Eq. 5- 2 the effect of the vertical component of the earthquake is accounted by the term E_v which is calculated as follows:

$$E_v = 0.2 S_{DS} D \qquad \text{Eq. 12.4-4 of ASCE 7-10}$$

where D is the effect of dead loads

S_{DS} is the design spectral response acceleration parameter at short periods defined in section 11.4.4 of ASCE 7-10

As it can be noticed in the two equations above the effect of the vertical component of ground motions is accounted in ASCE 7-10 by an increment of the dead load instead of being considered explicitly with the vertical acceleration history record. Also, it should be noticed in Eq. 12.4-4 of ASCE 7-10 that the factor that multiplies the effect of dead loads, $0.2S_{DS}$, is equal to 0.5 times the PGA (g units) predicted by the design response spectrum of ASCE 7-10.

The New Zealand Standard NZS 1170.5 (Council of Standards New Zealand, 2004) specifies that the vertical component of acceleration "may be necessary when considering the response of structures or parts that are sensitive to vertical accelerations such as for horizontal cantilevers or some items of equipment". Also, Section 4.3.3.5.2 of Eurocode 8 states that the effects of the vertical component need to be included when the vertical acceleration is greater than 0.25g but only in specific elements such as:

- Horizontal structural members spanning 20m or more.

- Horizontal cantilevers longer than 5m.
- Horizontal pre-stressed elements.
- Beams supporting columns.
- Base isolated structures.
- Supporting elements of all the components mentioned above.

Future editions of ASCE 7-10 might consider following a similar approach to that given by the Eurocode 8, and it would require a threshold value of the vertical acceleration after which the vertical component would need to be included in linear response history analysis procedures and to specify the structural elements that are more sensitive to vertical accelerations. Additionally, the vertical acceleration component of a ground motion would need to be scaled by the same factors used to scale the horizontal components of the earthquake before that peak vertical acceleration is compared with the threshold value.

Finally, an issue that needs further research is the appropriateness of applying the response modification coefficient R and the deflection amplification factor C_d, as defined in ASCE 7-10, to the vertical accelerations and displacements, respectively. Such research would be intended to relate the factors R and C_d with reductions or amplifications of the vertical load and displacements when the vertical component of the ground motion is actually used in the analysis.

5.3 Scaling of design parameters

When using linear response history analysis (LRHA) as the analysis technique for seismic loading, it is possible to obtain element forces or nodal displacements that are below a minimum required, and the further scaling will be necessary. This section refers to the requirements of scaling of element forces and nodal displacements (and therefore drifts), discussing them separately.

5.3.1 Scaling of element forces

When the selected ground motions for LRHA are scaled using the design response spectrum of Section 11.4.5 of ASCE 7-10, the first step to obtain the design element forces is to multiply the element forces from the analysis by I_e/R where I_e is the importance factor and R is the response modification coefficient (as defined in ASCE 7-10).

The second step to obtain the design element forces is specified in Chapter 16 of ASCE 7-10, and these guidelines are based on the minimum base shear forces given by Eq. 12.8-5 and 12.8-6 of this standard which have been repeated here for convenience:

$$C_S = 0.044\, S_{DS} I_e \geq 0.01 \qquad \text{Eq. 12.8-5 of ASCE 7-10}$$

$$C_S = 0.5\, S_1/(R/I_e) \qquad \text{Eq. 12.8-6 of ASCE 7-10}$$

where C_S is the base shear coefficient

S_{DS} is the design spectral response acceleration parameter at short periods

S_1 is the mapped MCE spectral response acceleration at a period of 1 sec.

The base shear for each ith record, denoted Vi, is obtained from a response history analysis and scaled by I_e/R. ASCE 7-10 states that for values of Vi less than $0.85V$, the member forces still need to be further multiplied by V/Vi where V is defined by Eq. 12.8-5 of ASCE 7-10. A similar criterion is given for structures where V is governed by Eq. 12.8-6. The base shear for design, denoted V_{Design}, when following the criterion of ASCE 7-10 for $V_i < 0.85V$ and for $V_i > 0.85V$ is illustrated in Figure 5-25 and Figure 5-26, respectively.

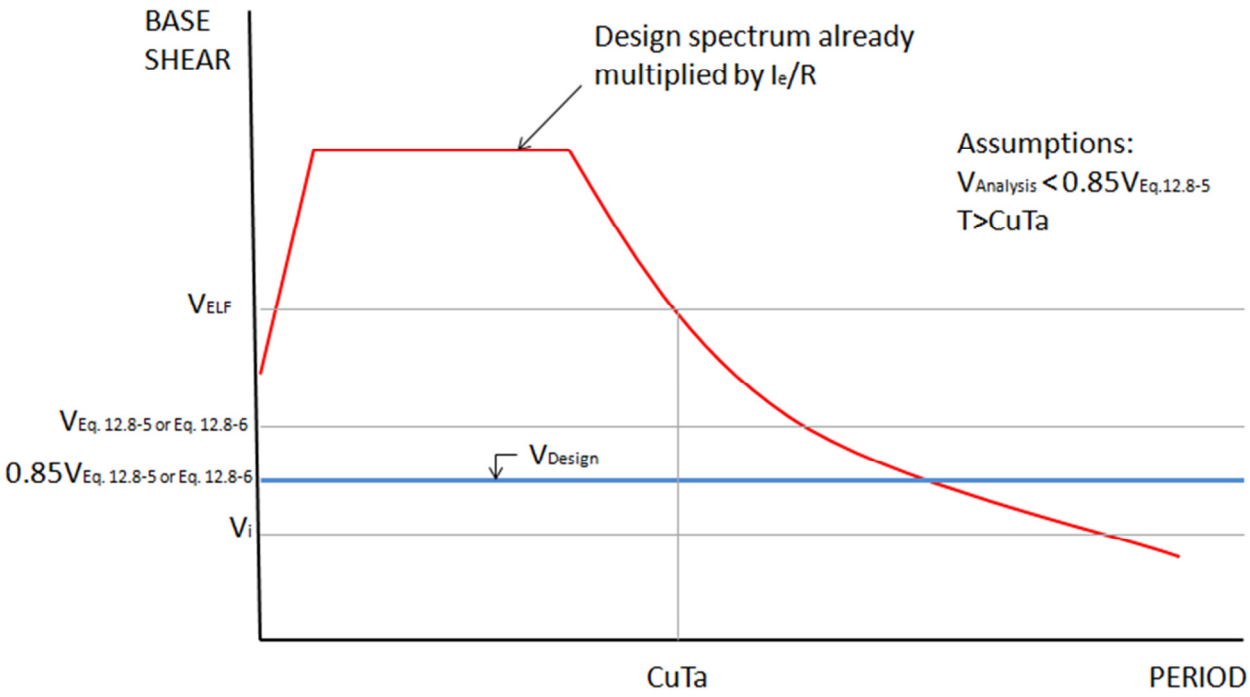

Figure 5-25 Design base shear for design for the case where $Vi < 0.85V$

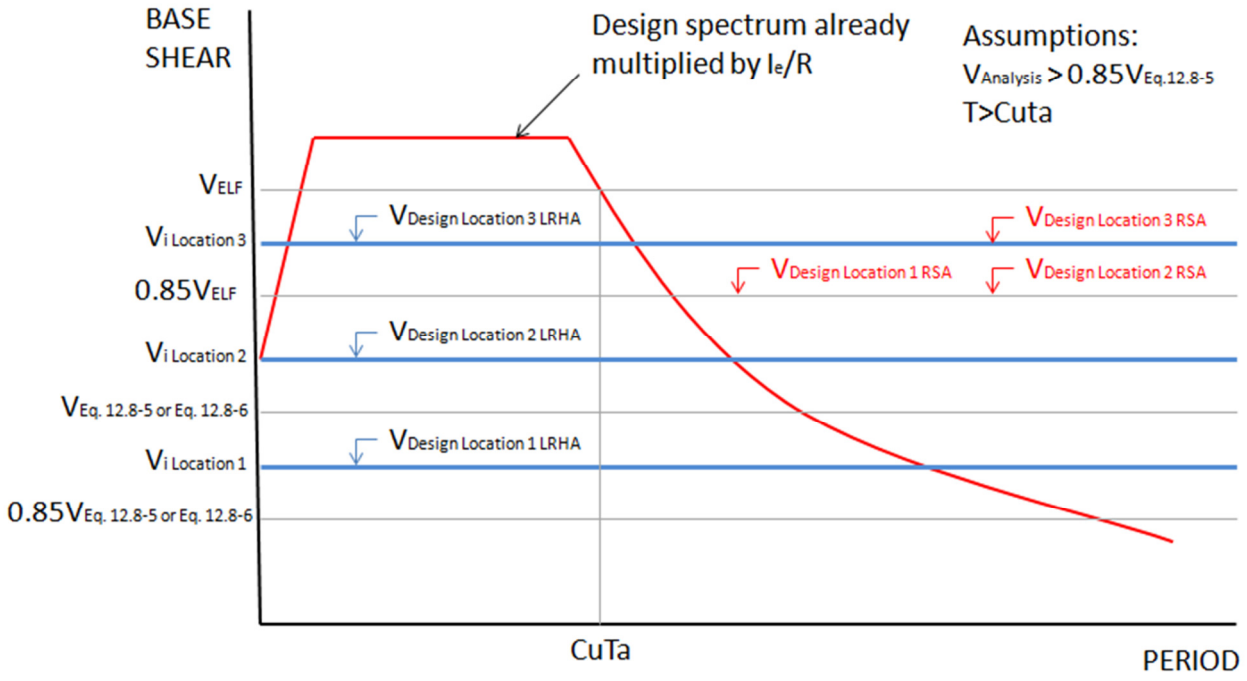

Figure 5-26 Design base shear for design for the case where *Vi* > *0.85V*

The current approach of ASCE 7-10 for scaling base shears and element forces guarantees a minimum design base shear equal to 0.85*V*; however, it can be noticed that *V* is independent of the value of the base shear predicted by the ELF procedure using equations 12.8-2, 12/8-3 and 12.8-4 of ASCE 7-10. This fact shows an inconsistency between the scaling of base shears and element forces predicted by a RSA and by a LRHA because for RSA Section 12.9.4.1 of ASCE 7-10 states that "Where the combined response for the modal base shear (*Vt*) is less than 85 percent of the calculated base shear (*V*) using the equivalent lateral force procedure, the forces shall be multiplied by 0.85*V*/*Vt*". The inconsistency occurs because similar base shears obtained with RSA and LRHA will yield different design base shears. For instance, Figure 5-26 shows the base shear from three different analyses and their respective design base shear according to the RSA and LRHA procedures. Also, the inconsistency is even more evident when using spectral matched acceleration histories in LRHA because the base shear using these signals will be very close to the base shear given by RSA; however, the design base shears could be considerably different which is not reasonable. Therefore; it would be necessary to adjust the scaling requirements of LRHA at least to the level of the scaling requirements of RSA.

Additionally, it is important to mention that the requirement of RSA of adjusting, when necessary, the design base shear from the analysis to 85% of the base shear given by the ELF procedure, might not be appropriate for RSA (and therefore for LRHA) because ATC 63 analyses have shown the collapse of models scaled to 85% of the ELF base shear (Charney, 2010c). This topic is under current research.

Furthermore, three definitions are still needed for a more complete definition of the scaling of the response parameters. First, the scaling requirements when the earthquake load is not applied along the principal axis of the structure needs to be defined, because it is not clear for this case how to calculate the base shear *Vi*. Also, ASCE 7-10 needs to clarify how to proceed with the scaling of element forces when simultaneous loading is acting in both directions, and finally, another aspect that needs to be clarified in ASCE 7-10 is how this scaling affects the forces and displacements calculated when including accidental torsion in the analysis.

In the case of the National Building Code of Canada (Canadian Commission on Building and Fire Codes, 2005), denoted NBCC, the base shear from each scaled ground motion needs also to be multiplied by the parameter I_e and then divided by R_dR_o where I_e is the importance factor and R_d and R_o are respectively the ductility-related force modification factor and the overstrength-related force modification factor as defined in the NBCC. This step is considered to be identical to the one in ASCE 7-10 because the response modification coefficient R in this standard is calculated including the ductility required R_d and the overstrength factor Ω_0 (FEMA, 2009). The second step in the NBCC is to identify if the structure is regular or not because for the case of irregular structures requiring a dynamic analysis, the base shear V_d needs to be taken as the maximum of the base shear from the ground motion V_i (already multiplied by I_e/R_dR_o) and 100% of V where V is the base shear calculated for the equivalent static force method. For other structures (regular structures and irregular structures not needing a dynamic analysis) if the base shear V_i from a linear response history analysis is less than $0.80V$ then the dynamic base shear V_d needs to be taken as $0.80V$, and then the element forces will also need to be multiplied by the factor $0.80V/Vi$.

The approach followed by the NBCC is similar to the one given for the RSA of ASCE 7-10, since the base shear of reference is the one corresponding to the equivalent lateral force procedure (V_{ELF}). The difference is that the NBCC considers a minimum base shear of $0.80V_{ELF}$

instead of $0.85V_{ELF}$ as given by ASCE 7-10. Also, the scaling requirements in the NBCC are equal for RSA and for LRHA.

In the case of the Eurocode 8 the step consisting of dividing the element forces by a factor associated to the ductility and the overstrength is not required, and this is because a similar factor denoted as behavior factor q is already included in the definition of the design spectrum. However, this standard does not provide a further scaling to adjust, if necessary, the dynamic base shear to some fraction of the static base shear.

After analyzing the provisions from ASCE 7-10 and other seismic codes, it is possible to provide a recommendation about the scaling of base shear and element forces.

Recommendation for the scaling of base shears and element forces for LRHA: It is reasonable to have consistency between the scaling procedures of RSA and LRHA, and considering that scaling of the NBCC uses the base shear from static force procedures as a reference, it is recommended for LRHA to provide the same approach of scaling base shears and element forces given by Section 12.9.4.1 of ASCE 7-10, which correspond to the provisions of RSA. When following the described approach, the design base shears of Figure 5-26 will change as given by Figure 5-27.

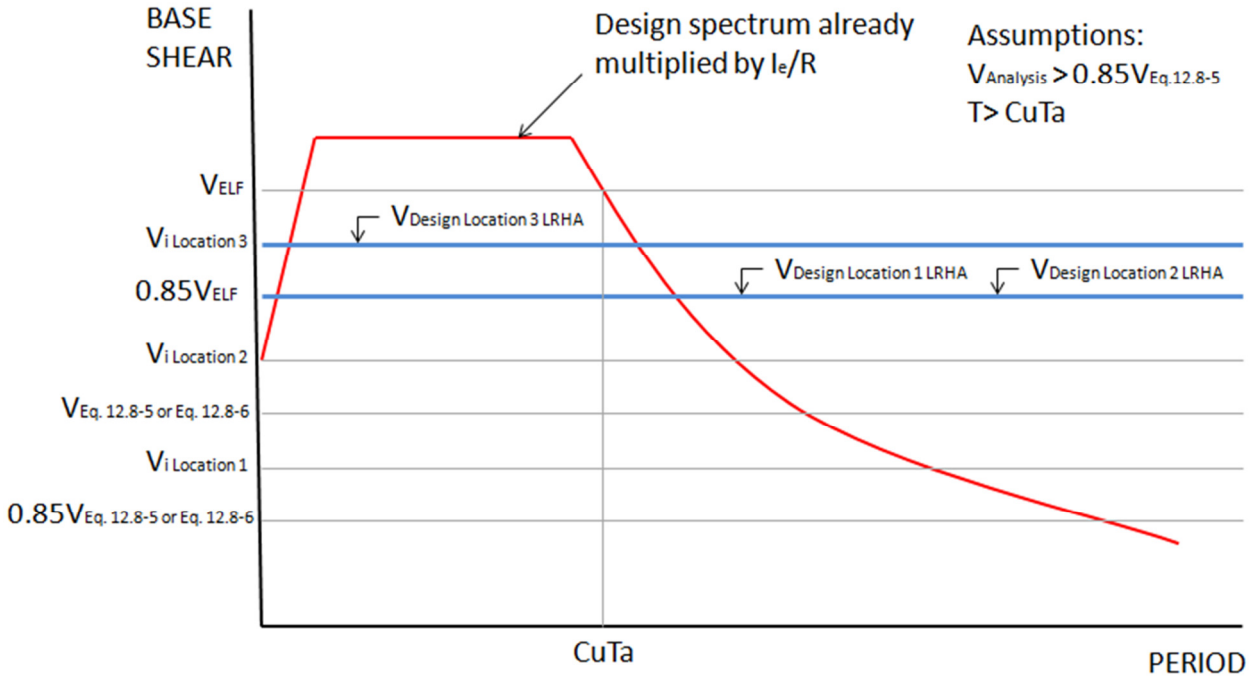

Figure 5-27 Design base shear suggested for different base shears values from analysis

Also, it is important to mention that Chapter 16 of ASCE 7-10 does not require any scaling of the element forces when the base shear from analysis is greater than 85% of the ELF base shear.

5.3.2 Scaling of displacements (and drifts)

For the case of drifts, Chapter 16 of ASCE 7-10 states that "Where the maximum scaled base shear predicted by the analysis, *Vi*, is less than $0.85C_sW$ drifts shall be multiplied by $0.85C_sW/Vi$", where *Cs* is defined in Eq. 12.8-6 of the same standard. This is the only scaling that needs to be done for calculation of drifts according to ASCE 7-10. If *Vi* is greater than $0.85C_sW$ drifts do not need any scaling. Also, when analyzing the provisions for the scaling of drifts from RSA and for LRHA in ASCE 7-10, it can be noticed consistency between these two approaches because the only difference in RSA is that *Vi* is changed by *Vt* where *Vt* is the combined response for modal base shear; however, *Vi* and *Vt* represent both the shear force from the analysis, and therefore they are equivalent.

The NBCC requires the scaling of the displacements using the same criterion used for scaling base shears and element forces as described in the previous section; however, the base shear from the equivalent static force method needs to be re-calculated using a period *Ta* as defined in the NBCC. For the case of the Eurocode 8, the step of multiplying the displacement from an elastic analysis by an amplification factor q_d defined as the displacement behavior factor is specified, and no further scaling is necessary. After analyzing the provisions from ASCE 7-10 and other seismic codes no inconsistence have been noticed in the current approach of ASCE-10 for the scaling of deformations of drifts; therefore, there are no suggestions about changes in this topic.

5.4 Orthogonal loading

This section is divided in three parts; the first part describes the current methods of applying orthogonal load in different seismic codes, the second part contains three alternatives to account for orthogonal effects in LRHA using real records, and the third part describes briefly procedures for orthogonal loading when using artificial seismograms (spectral matched seismograms).

5.4.1 Methods to account for orthogonal loading in different seismic codes

Procedures for the application of orthogonal loading are specified in ASCE 7-10 in Section 12.5, and they depend on the seismic design category (SDC); for instance, for the case of structures corresponding to seismic design category B orthogonal loading effects can be neglected, and the earthquake loads can be applied independently in each orthogonal direction. For the case of structures corresponding to SDC C, the requirements for SDC B and SDC C are considered a minimum. The structures having Nonparallel Systems-Irregularity, which according to ASCE 7-10 (ASCE/SEI, 2010) occurs when "the vertical lateral force-resisting elements are not parallel to the major orthogonal axes of the seismic force-resisting system" are forced to use any of the orthogonal loading procedures specified for SDC C. It is important to mention that structures with vertical lateral force-resisting system that are not symmetric about the major orthogonal axis of the seismic force-resisting system were also defined as having a Nonparallel Systems-Irregularity in ASCE 7-05 (ASCE/SEI, 2006), but that is not the case in ASCE 7-10. Also, two specific procedures for SDC C are mentioned. ; the first of them can be applied to ELF, RSA, and LRHA, and it consists in applying 100% of the load in one direction and 30% of the load in the other direction. This technique is denoted hereafter as the "30% rule". The second method of analysis applies only to LRHA or NLRHA, and it specifies the analyst to apply simultaneously both components of the ground motions in order to account for the orthogonal effects. Moreover, for the case of structures corresponding to SDC D through F, the procedures for SDC C are considered as a minimum, and additional conditions are specified for columns or walls intersecting seismic force-resisting systems.

A method to account for all the possible orientations of the two components of ground motion relative to a structure was developed by Wilson (1995), and it consists in applying separately 100% of the load in each orthogonal direction, and then taking the square root of the sum of the squares (SRSS) to get element forces for design. This method was originally developed for modal response spectrum analysis but it has also been suggested for application in response history analyses as stated in Section 3.2.7.2 of ASCE 4-98 (ASCE, 2000). In addition, ASCE 4-98 suggests the application of a 40% rule (instead of a 30% rule) when the LRHA is done separately in each component, and such 40% rule is described as follows:

$$R = \pm \begin{bmatrix} R_x \pm 0.4R_y \pm 0.4R_z \\ R_y \pm 0.4R_z \pm 0.4R_x \\ R_z \pm 0.4R_x \pm 0.4R_y \end{bmatrix} \qquad \textbf{Eq. 5- 2}$$

where R_x is the maximum response from one of the horizontal record components.

R_y is the maximum response from the other horizontal record component.

R_z is the maximum response from the vertical record component.

R is the maximum response of each selected record.

According to ASCE 4-98 Eq. 5- 2 is applicable as long as the components of the record are statistically independent (see Section 2.1.4.1 of this document for conditions of statistical independence). Also, it can be noticed in Eq. 5- 2 that ASCE 4-98 includes the effect of the two horizontal and the vertical component of the ground motion. This is a difference with the 30% rule described in Section 12.5.3 of ASCE 7-10 which accounts for the combination of the horizontal components of a record but it excludes the influence of the vertical component.

In the case of the NBCC, it is specified that "Earthquake forces shall be assumed to act in any horizontal direction" but the NBCC provides alternative methods to provide adequate strength to the structure. The treatment of the orthogonal effects using these alternative procedures (Section 4.1.8.8 of the NBCC) depends on the orientation of the seismic force resisting system (SFRS), and on the product of the parameters $I_E F_a Sa(0.2)$. These coefficients I_E and F_a, are defined respectively as the earthquake importance factor and the acceleration-based site coefficient, while $Sa(0.2)$ is the 5% spectral response acceleration in g units for a period T=0.2 sec. The NBCC states that when the components of the SFRS are along a set of orthogonal axis, only independent analyses on the principal axis of the structure are required. It is interesting that rectangular symmetric buildings will satisfy these conditions and they will not require the application of orthogonal loading; this is a difference with ASCE 7-10 because in this standard orthogonal loading has to be always applied unless the structure corresponds to SDC A or B.

Also, the NBCC specifies that for the case where the SFRS does not coincide with a set of orthogonal axis and where $I_E F_a Sa(0.2) < 0.35$, it is permitted to run independent analysis along any two orthogonal directions. Finally, for the case where SFRS does not coincide with a set of orthogonal axis and where $I_E F_a Sa(0.2) > 0.35$, the 30% rule needs to be applied.

In the case of the Eurocode 8 (Section 4.3.3.5.1) it is specified that orthogonal effects can be included in three different ways; however, it is not stated if these different procedures can be applied to all the analysis techniques (ELF, RSA, LRHA, NLRHA) or only to some of them. The first one of these techniques states that the element forces can be estimated by "the square root of the sum of the squared values of the action effect due to each principal component". The second method proposed by the Eurocode 8 consists in applying the 30% rule, and the last method, which is specified for non-linear response history analysis, states that the simultaneous loading of the two record components is used to account for orthogonal effects.

The New Zealand provisions (Council of Standards New Zealand, 2004) defines the direction of loading based on the ductility of the structure which can be classified as ductile, nominally ductile, and brittle structures. For ductile structures and seismic force resisting systems oriented along orthogonal axis, it is only required to apply the load independently in each direction, and no combination of orthogonal effects is needed. Also, for the case of ductile structures not having a seismic force resisting system oriented along orthogonal axis the seismic loads need to be applied separately (no simultaneous loading) but in different orientations to produce the worst effect. Also, the NZS states that for the case of nominally ductile and brittle structures that have seismic force resisting systems oriented along orthogonal axis, the effects of orthogonal loading can be accounted using the 30% rule, and for the case of nominal ductile or brittle structures with seismic force resisting systems not oriented in perpendicular directions, the seismic loads have to be applied in several orientations to produce the worst scenario.

5.4.2 Specific methods to account for orthogonal effects in LRHA procedures when using real records

From the documentation discussed above, three alternatives to define orthogonal loading are analyzed next for the specific case of LRHA:

First Alternative

The first alternative considers applying 100% of the lateral load along each of the principal directions separately, and then getting design forces from the SRSS of the element forces corresponding to each analysis. This technique is effective when doing a modal response spectrum analysis, and it can be considered to be equally effective for the case of LRHA. A drawback of this technique is that it eliminates the sign of the element forces when doing the SRSS. This is considered a serious disadvantage because one of the benefits of doing a LRHA is

to keep track of the appropriate sign of the element forces at any stage of the analysis. Also, and as a clarification, the "100% of the lateral load" is defined for each earthquake component as the product of the original record times the corresponding scale factor from a ground motion scaling approach as the ones given in Chapter 3, times the scale factor from the scaling of element forces (see Section 5.3.1). The first of these scale factors may or may not be the same in each principal direction depending on the assumptions of the designer, and the second factor will most likely be different for each record component because both the base shear from the individual record components and the base shear obtained with ELF procedures are period dependent, and the periods in each principal direction will most likely be different.

An example is presented next to show the how the "100% of the load" was defined for each component of each record used in the building analyzed by Charney et al. (2010b), the details of which are described for Building 2 of Appendix A. The ground motions used for the analysis of this building are those presented in Table 2-6. The scale factors for each ground motion are the same for both horizontal components because those factors were obtained using the method suggested by Charney (2010a). The resulting factors from the scaling of ground motions can be found in Table B- 1. Also, the fundamental periods of the building in both principal directions as well as the base shears are shown in Table 5-3 where it can be noticed that both directions have the same design base shear due to the fact that both fundamental periods are higher than *CuTa*.

Table 5-3 Period and Base shear from ELF for Building 2 of Appendix A

Direction of loading	Period (sec)	Base shear from ELF (kips)
X axis	2.87	1124.5
Y axis	2.60	1124.5

Note *CuTa* = 2.22 sec

The resulting base shears from independently applying each component of each scaled record along the X and Y directions of the building (see Figure A- 2 for directions X and Y of this building) are shown in the column 2 (Col 2) of Table 5-4. Also, Table 5-4 shows the appropriate scale factors for adjusting, when necessary, the base shears multiplied by I_e/R to a

minimum base shear that has been taken as 85% of the base shear given by the ELF procedure as it was recommended in the last paragraph of Section 5.3.1.

Table 5-4 Procedure for getting the desing base shear using LRHA

Col 1	Col 2	Col 3	Col 4	Col 5
Component	Base shear from analysis using scaled ground motions	Col 2 *I_e/R	Scale factor from adjusting shear force	Design base shear
	(kips)	(kips)	(kips)	(kips)
X direction				
A00-X	3510	438.76	2.18	956
A90-X	1592	199.01	4.80	956
B00-X	3015	376.83	2.54	956
B90-X	2928	365.95	2.61	956
C00-X	3134	391.69	2.44	956
C90-X	3226	403.30	2.37	956
Y direction				
A00-Y	3577	447.11	2.14	956
A90-Y	1394	174.23	5.49	956
B00-Y	3132	391.44	2.44	956
B90-Y	3463	432.87	2.21	956
C00-Y	2417	302.16	3.16	956
C90-Y	5084	635.52	1.50	956
Note: 0.85V = 956 kips				

It is interesting to notice in Table 5-4 the high variation of the values in the third column, which correspond to the design base shears in each direction if no scaling were done to 85% of the ELF base shear. These base shears range from 199.01 kips to 438.76 kips in the X direction, and from 174.23 kips to 635.52 kips in the Y direction. It could be expected a small degree of variability of those base shears since these results come from records already scaled to satisfy the requirements of Chapter 16 of ASCE 7, with exception of the scaling to 85% of the ELF base shear. However, the variability in these base shears can be due to taking the average of the spectral measures (SRSS or geomean spectrum) in the scaling of ground motion procedure in ASCE 7-10, because it implies that the spectral measure of some records might be above the design spectrum in some cases and below in other cases.

Finally, it is required to establish the combination of the record components necessary for the application of the first alternative, and those combinations are shown in Table 5-5. The components along the X and Y directions have to be applied separately, and then the SRSS of the results from the loading of each component needs to be done to obtain design element forces.

Table 5-5 Combinations for orthogonal loading using First Alternative

Combination	Component along X direction*	Component along Y direction*
1	A00-X	A90-Y
2	- A90-X	A00-Y
3	- A00-X	- A90-Y
4	A90-X	- A00-Y
5	B00-X	B90-Y
6	- B90-X	B00-Y
7	- B00-X	- B90-Y
8	B90-X	- B00-Y
9	C00-X	C90-Y
10	- C90-X	C00-Y
11	- C00-X	- C90-Y
12	C90-X	- C00-Y

*The components along each direction have to be applied separately, and then the results correspond to the SRSS of the individual responses

Second Alternative

The second alternative for applying orthogonal effects using LRHA considers the application in one of the principal directions of the building of 100% of the load scaled to 85% of the ELF base shear, if necessary, and 30% of the same load in the other direction. The advantage of this technique is that it will keep the signs of the element forces. The combination of the record components when using this alternative is described in Table 5-6.

Table 5-6 Combinations for orthogonal loading using Second Alternative

Combination	Component along X direction*	Component along Y direction*
1	A00-X	0.3 A90-Y
2	A00-X	- 0.3 A90-Y
3	- A00-X	0.3 A90-Y
4	- A00-X	- 0.3 A90-Y
5	A90-X	0.3 A00-Y
6	A90-X	- 0.3 A00-Y
7	- A90-X	0.3 A00-Y
8	- A90-X	- 0.3 A00-Y
9	B00-X	0.3 B90-Y
10	B00-X	- 0.3 B90-Y
11	- B00-X	0.3 B90-Y
12	- B00-X	- 0.3 B90-Y
13	B90-X	0.3 B00-Y
14	B90-X	- 0.3 B00-Y
15	- B90-X	0.3 B00-Y
16	- B90-X	- 0.3 B00-Y
17	C00-X	0.3 C90-Y
18	C00-X	- 0.3 C90-Y
19	- C00-X	0.3 C90-Y
20	- C00-X	- 0.3 C90-Y
21	C90-X	0.3 C00-Y
22	C90-X	- 0.3 C00-Y
23	- C90-X	0.3 C00-Y
24	- C90-X	- 0.3 C00-Y

*The components along each direction have to be applied separately, and then added or they could also be applied simultaneously because superposition is allowed in LRHA.

Third Alternative

The last alternative for including orthogonal effects in LRHA is to use both components of the ground motion simultaneously. When using this procedure, the record components applied in each direction have to be scaled individually to satisfy the requirements of ASCE 7. This procedure intends to resemble what structures feel in actual earthquakes, and it is not

considered to be overconservative. Also, if using this alternative, the structural elements located at the corners of the building (such as columns or shear walls) will experience simultaneous loading in two directions, which is a desired and realistic effect.

Because this alternative has a higher level of resemblance with the nature of actual ground motions than the other two alternatives, the third alternative it is considered the most appropriate procedure (within the options studied) to account for orthogonal loading in linear response history analysis.

5.4.3 Considerations for orthogonal loading when using artificial records

Additional considerations need to be taken into account for the case of using artificial records which as defined in pg. 8 are those records generated so that their response spectrum matches a defined target spectrum. For this case, it will still be possible to apply the three alternatives described in the previous section. Also, the selected acceleration histories in both orthogonal directions need to be statistically independent, and the use of the same component for both directions will not be allowed because it assumes that the most critical responses in both directions will occur at the same time which is a possible but unlikely case.

Having discussed different alternatives for orthogonal loading using LRHA, these are the recommendations for future editions of ASCE 7-10:

Recommendations for orthogonal loading in LRHA: The requirements for orthogonal loading in LRHA will be the same than those given in Section 12.5.2 of the current ASCE 7-10 for structures in SDC B; however, for SDC C, and in addition to the minimum requirements of SDC B, it will be satisfied that both components of the ground motion have to applied simultaneously. The record components applied in each direction have to be scaled individually to satisfy the requirements of ASCE 7.

Additionally, for the case of structures classified with SDC D through F then the requirements will be the same as given in Section 12.5.4 of ASCE 7-10 but considering as minimum the new requirements for SDC C as stated above.

5.5 Explicit definition of load combinations

This section has been included to clarify the fact that for the particular case of LRHA the earthquake load *E* in Section 2.3 and Section 12.4.2 of ASCE 7-10 consists in the envelope (if considering less than seven records) or the average (if considering seven or more records) of the

results obtained when applying all ground motions used in the analysis, and therefore this is the load *E* that will be combined with other types of load as given in Section 2.3 of ASCE 7-10. Then, the designer needs to be aware that the earthquake load *E* is not the load corresponding to a particular earthquake but instead it is the envelope of all the analyzed ground motions.

5.6 Combination of the results

Any appropriate measure to combine the response parameters (i.e. base shear, interstory drift, element forces) from each ground motion in LRHA has to be thought in the context of retaining the signs of the member forces coming from each individual analysis. According to Section 16.1.4 of ASCE 7-10, the response parameters will correspond to the envelope values from all the responses if the analysis includes less than seven earthquakes, or to the average values if the analysis includes more than seven earthquakes. A different criterion is used in ASCE 4-98, which states in its Section 3.2.2.1 that the average of the responses can be used regardless of the number of earthquakes used in the analysis. These procedures in ASCE 7-10 and ASCE 4-98 have an undesired effect of not including exactly the sign and the values of the element forces from each individual analysis.

An alternative to include the element forces coming from the analysis of each individual record consists in considering the earthquake load *E,* defined in section 12.4.2 of ASCE 7-10, as the load coming from an individual earthquake, instead of considering *E* as the combination (i.e. average or envelope) from the responses of all the records. However, this procedure would increase significantly the number of load cases corresponding to the load combinations that include the seismic load *E* in section 2.3.2 of ASCE 7-10. Due to this complexity, this document will still recommend the use of the envelope of the responses when the number of records is less than seven, and the average of the responses when the number of records is equal or more than seven. Nevertheless, more research is encouraged in this topic.

5.7 Solution techniques of LRHA and damping assumptions

Linear response history analysis can be performed using modal analysis or using direct integration, and for the case of modal analysis the modal shapes and periods can be obtained using Eigen vectors or using Ritz vectors. Different response parameters can result for each of these techniques; therefore, it is necessary to described some of the characteristics of these techniques including their assumptions for the modeling of the damping.

The technique using Eigen Vectors obtains the vibration periods by solving the equation:

$$K\phi = \omega^2 M\phi \qquad \textbf{Eq. 5-3}$$

where K is the stiffness matrix

M is the mass matrix

ω is the frequency of vibration of the system

ϕ is the mode shape corresponding to the frequency of vibration ω

The number of solutions for ω in Eq. 5- 2 is equal to the number of mass (dynamic) degrees of freedom of the system and each value of ω will define a particular period of vibration T (T=2π/ω) and a particular Eigen vector shape ϕ. When using a modal analysis with Eigen Vectors as the solution technique for LRHA then the damping in each mode could be specified as a fraction of the critical damping, and the same damping could be applied to all the vibration modes. Values of damping (as ratio of the critical damping) were found as 0.05 for ASCE 7-10 (as specified in the maps defining the seismic hazard in Chapter 22), NBCC (Section 4.1.8.2), EC8 (Section 3.2.2.2), and NZS (Section 6.4.6); therefore, a damping ration of 0.05 is considered convenient for LRHA using modal analysis with Eigen Vectors.

Ritz vectors may also be used to perform a modal analysis in LRHA; in this case the first mode of vibration is obtained using a rational distribution of lateral static forces and corresponding displacements; such distribution of static forces could be taken as the one given for the equivalent lateral force (ELF) procedures. Then, the remaining modal shapes are obtained by mathematical procedures so that each modal shape is orthogonal to all the other ones (Wilson, 2004). Additionally, this technique can also be implemented with a constant damping ratio which could be assigned as 0.05 to be consistent with the modal analysis with Eigen vectors.

The response given when using Eigen vectors or Ritz vectors might not be the same when specifying the same number of modes because the modal shapes might differ. For instance, it was seen in the analysis of a twelve history building (Charney et al., 2010b) that the vibration periods with higher mass participation factor appear earlier when using Ritz vectors than when using Eigen vectors. Therefore, if required to get 90% of the mass for a modal linear response

history analysis, a fewer number of modes will be necessary when using Ritz vectors than when using Eigen vectors.

When using the direct integration approach, the damping is often given by a mass and stiffness proportional model (Rayleigh damping), which yields different damping values in each mode. The equation defining the damping matrix C is:

$$C = \alpha M + \beta K \qquad \textbf{Eq. 5- 4}$$

where α is the mass proportional coefficient

β is the stiffness proportional coefficient

M is the mass matrix

K is the stiffness matrix

The coefficients α and β are given by:

$$\begin{Bmatrix} \alpha \\ \beta \end{Bmatrix} = 2\frac{\omega_m \omega_n}{\omega_n^2 - \omega_m^2}\begin{bmatrix} \omega_n & -\omega_m \\ -1/\omega_n & 1/\omega_m \end{bmatrix}\begin{bmatrix} \xi_m \\ \xi_n \end{bmatrix} \qquad \textbf{Eq. 5- 5}$$

where ω_n is the circular frequency of the selected nth period or any other circular frequency

ω_m is the circular frequency of the selected mth period or any other circular frequency

ξ_n is damping ratio for the circular frequency ω_n

ξ_m is damping ratio for the circular frequency ω_m

It should be noticed from the definition of ω_n and ω_m that these frequencies do not need to be actual structural frequencies. This way, the equation defining the damping ratio at a particular mode i is given by:

$$\xi_i = \frac{1}{2\omega_i}\alpha + \frac{\omega_i}{2}\beta \qquad \textbf{Eq. 5- 6}$$

where ω_i is the circular frequency of the i^{th} period.

ASCE 7-05 does not provide information about how to choose appropriate values for ω_n, ω_m, ζ_n, and ζ_m; however there are recommendations in FEMA750 (FEMA, 2009) and in the

New Zealand Standard NZS 1170.5 (Council of Standards New Zealand, 2004). FEMA750 specifies in the commentary to ASCE 7-05 that two of the lowest frequencies such as the first one and the third one could be used in the analysis. Also, the NZS states that a maximum of 5 percent of critical damping can be used in the first two translational modes, and that no more than 40% damping is allowed at the period T_{90} where T_{90} is the period of the highest mode in the same direction required to achieve 90% of the total mass.

A problem associated with the use of direct integration with Rayleigh damping is that it can yield excessive values of damping at higher modes; this fact will be illustrated by calculating the curve Circular frequency vs. Damping ratio for three different assignments of damping ratios to the vibration periods of Building 2 (see Appendix A for description of Building 2). The two assignations of damping ratios were:.

Case 1: Damping ratio equal to 0.05 at the first and in the fourth periods.

Case 2: Damping ratio equal to 0.05 at $0.2T$ and $1.5T$ where T is the average of the two fundamental translational periods of the system.

These combinations were chosen so that it provides the same damping ratio in the first two modes of the same type (the first two modes that corresponding to translation in the X direction or in the Y direction) in the first case, and it uses the limits of the period range of interest for the scaling of ground motions procedure according to ASCE 7-10 in the second case. The vibration periods to be used in the calculations are shown in Table 5-7, and the calculation of the coefficients α and β for the two combinations is presented in Table 5-8. Also, the curves circular frequency vs. damping ratio for the two cases are shown in Figure 5-28, and the corresponding damping ratios for the first twelve periods of vibration in each case are shown in Table 5-9.

Table 5-7 First four vibration periods and corresponding circular frequencies of Building 2

Vibration mode	Period (sec)	Circular Frequency (rad/sec)	Predominant direction
1	2.870	2.189	X direction
2	2.601	2.416	Y direction
3	1.572	3.997	Torsion
4	1.151	5.459	X direction

Table 5-8 Calculation of coefficients α and β of Rayleigh Damping

Parameter	Damping 0.05 at 1st and 4th period	Damping 0.05 at 0.2*T* and 1.5*T*
Period T_n* (sec)	2.870	$0.2T = 0.548$
Period T_m* (sec)	1.151	$1.5T = 4.110$
Circular frequency ω_n (rad/sec)	2.189	11.466
Circular frequency ω_m (rad/sec)	5.459	1.529
Damping ratio ζ_n	0.050	0.050
Damping ratio ζ_m	0.050	0.050
Coefficient α	0.156	0.135
Coefficient β	0.013	0.008

*The parameters *Tn* and *Tm* represent the fundamental periods of the nth and of the mth vibration mode.

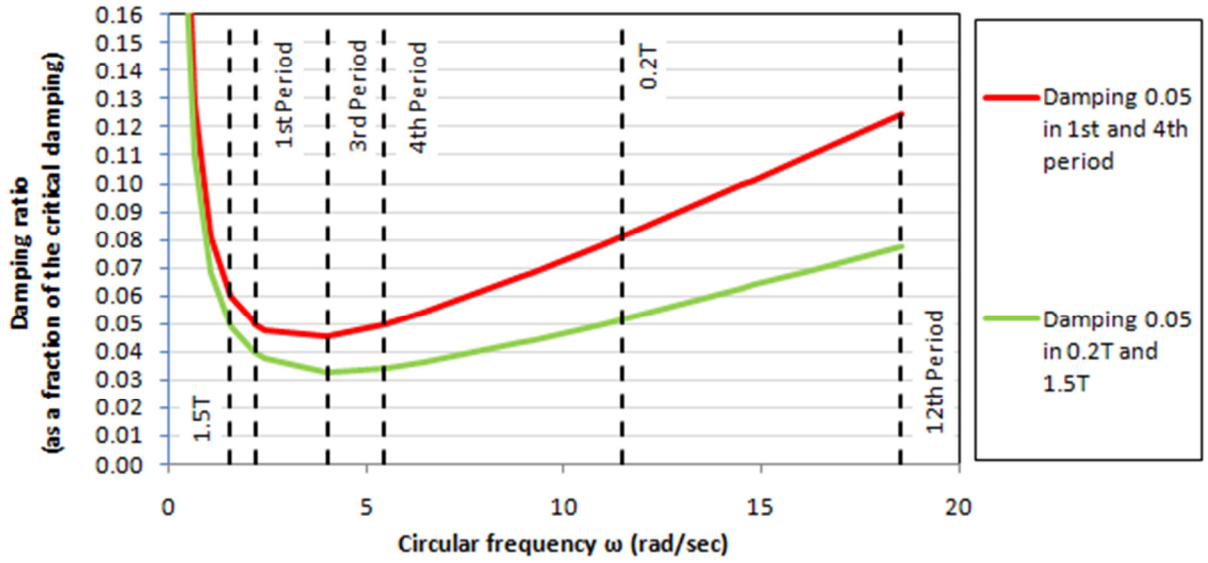

Figure 5-28 Damping ratio at different circular frequencies using Rayleigh Damping for two different cases

Table 5-9 Damping ratios for the first twelve periods of Building 2 when using Rayleigh Damping

Number of period	Period (sec)	Circular frequency ω (rad/sec)	Damping ratios (as a fraction of critical damping)	
			Damping 0.05 at 1st and 4th period	Damping 0.05 at 0.2T and 1.5T
1	2.870	2.189	0.050	0.040
2	2.601	2.415	0.048	0.038
3	1.572	3.996	0.045	0.033
4	1.151	5.459	0.050	0.034
5	0.975	6.441	0.054	0.036
6	0.705	8.911	0.067	0.043
7	0.682	9.213	0.068	0.044
8	0.573	10.968	0.078	0.050
9	0.434	14.487	0.100	0.063
10	0.425	14.777	0.101	0.064
11	0.387	16.252	0.110	0.069
12	0.339	18.546	0.125	0.078

12 modes were chosen in Table 5-9 because at that period the mass participation in the two translational directions X and Y reaches 81% in both directions, and that percentage remains almost constant until the 117th period in the X direction and until the 111th period in the Y direction. The period at which 90% of the mass is reached was not chosen, because that corresponds to the 118th vibration mode in the X direction and to the 112 mode in the Y direction due to issues associated with the modeling of the basement as described in Section 5.10 of this document

It can be seen in Figure 5-28 that the damping ratios for the twelve modes corresponding to damping 0.05 at 0.2*T* and 1.5*T* are smaller than the damping ratios obtained from the other combination. For instance, the damping ratios in the first and third mode when using 5% damping at 0.2*T* and 1.5*T* were 0.040 and 0.033 (see Table 5-9), respectively, while the same values when using the other combination were 0.05, and 0.045, respectively. Therefore, the highest response parameters in a linear response history analysis will be obtained when using Rayleigh damping equal to 0.05 at 0.2*T* and 1.5*T*. Also, it can be noticed in Table 5-9 that the highest damping ratios at the 12th vibration mode are 0.125, and 0.078 for the two cases

analyzed, and these values are below the maximum recommended damping ratio of 0.4 given for T_{90} according to the New Zealand Standard NZS 1170.5 (2004).

Having discussed different solution techniques and their assumptions for damping, then the following recommendations are presented for linear response history analysis procedures.

Recommendations for the analysis technique and damping assumptions for LRHA: For the case of using modal analysis with Eigen vectors or Ritz vectors then a constant damping ratio of 0.05 (as a fraction of the critical damping) should be used. When using direct integration with Rayleigh Damping in structures modeled in three dimensions (3D) a damping ratio of 0.05 could be used in the first and second or in the first and third translational modes moving in the same direction. Additionally, for the case of structures modeled in 3D none of the first two translational periods or the fundamental rotational period will have a damping ratio higher than 0.05. Finally, defining T_{90} as the period at which is reached 90% of the modal mass in both translational directions, the damping ratio at that period T_{90} will not exceed than 0.2 (20%). Otherwise, the designer will have to change the frequencies and/or the corresponding damping ratios of the Rayleigh Damping model such that the limit of 20% damping at T_{90} will be satisfied.

A value of 20% has been chosen as a limit for the damping ratio at T_{90} considering that 10% of damping is already high and 40%, as given by the NZS, is considered to be too high. This way, a limit in the damping ratio of 0.2 (20%) is reasonable although research needs to be done to set up this limit based on more detailed analyses. These recommended provisions for the case of using direct integration with Rayleigh damping in structures modeled in 3D are based on the opinion of the author; however, more research is needed to set up a criteria based on a detailed analysis using Rayleigh Damping in structures modeled in 3D under linear and non-linear response history analysis.

5.8 Number of modes required when doing LRHA with modal analysis

The number of modes required for modal analysis when doing LRHA is not specified directly in ASCE 7-10; however it is reasonable to use the provision given for modal analysis when doing RSA which state that "The analysis shall include a sufficient number of modes to obtain a combined modal mass participation of at least 90 percent of the actual mass in each of the orthogonal horizontal directions of response considered by the model". The same provisions were found in the NBCC (commentary of Section 4.1.8.12), NZS (Section 6.3.3), EC8 (Section

4.3.3.3.1, CHS (Section 6.3.3), and MXS (Section 9.1); therefore, the recommendation for the number of modes when doing modal linear response history analysis could be:

Recommendation for the number of modes required for modal LRHA: Use the same provisions given for RSA in Section 12.9.1 of ASCE 7-10.

5.9 P-Delta effects

The description of a P-Delta analysis when doing linear response history analysis (LRHA) is not addressed in American standard ASCE 7-10 (2010). An option to include P-Delta effects in a linear response history analysis could be the calculation of the stability coefficient θ defined in Eq. 12.8-16 of ASCE 7-10; however, this formula would be difficult to apply because the interstory drift Δ and the interstory shear at a particular story V_x, as defined in Eq. 12.8-16 of ASCE 7-10, need to be computed for the same loading which indicates that for the case of linear response history analysis the stability coefficient θ would need to be computed for each time step. Due to the inconvenience of calculating θ many times, and considering that P-Delta effects a in response spectrum analysis are calculated by static procedures according to ASCE 7-10, it seems convenient to evaluate the P-Delta effects in a linear response history analysis using the provisions given in Section 12.8.7 of ASCE 7-10 which correspond to a static procedure.

Also, even if available software, i.e. SAP2000 (Computer and Structures Inc, 2009), have the capabilities of doing a LRHA including P-Delta effects, it is arguable the appropriateness of this procedure because the inclusion of P-Delta effects in a response history analysis would be more appropriate for a nonlinear (NLRHA) case instead of linear case (LRHA). This is the case because the inclusion of P-Delta effects in a nonlinear response history analysis can produce residual displacements in a structure after the earthquake stops, which is a behavior that the analyst would like to identify. However, when doing a linear response history analysis, it is not possible to recover this behavior because the structure will always return to its original configuration (no residual displacements) after the earthquake stops. This way, the analyst might not have an appropriate indicator of the sensitivity of the structure to P-Delta effects. Nevertheless, an example is presented in this section to calculate the ratios of lateral displacements including and excluding P-Delta effects using the software SAP2000 (Computer and Structures Inc, 2009). The building to be analyzed is the Building 2 described in Appendix A, and the acceleration histories to be used are the record components of the records B and C corresponding to Table 2-6. Direct integration with Rayleigh damping was the technique used in

the analysis, and a damping ratio of 0.05 was used in the first and third vibration modes. The ratios of the lateral displacements including P-Delta effects (gravity load plus lateral load) to the lateral displacements excluding P-delta effects (lateral load only) are presented in Table 5-10 for the record components B00, B90, C00 and C90 applied in the X direction, and in Table 5-11 for the same record components applied in the Y direction. The displacements were taken at the center of mass of each floor.

From Table 5-10 and Table 5-11 it can be seen the ratios of displacements including and excluding P-Delta effects are very close to 1.0 which indicates that for this case in particular, P-Delta effects might not be critical; however, this conclusion need to be checked with the calculation of the stability coefficient θ (formula 12.8-16 of ASCE 7-10) using the static procedure specified in Section 12.8.7 of ASCE 7-10. Also, it can be noticed in Table 5-10 and Table 5-11 that some of the ratios are less than 1.00, and it indicates that the displacements without including P-Delta effects can be higher than when including P-Delta effects. A possible reason for this behavior is that the inclusion of P-Delta effects in the analysis increases the periods of vibration of the building, and therefore, it can yield smaller displacements than when not including P-Delta effects.

Table 5-10 Ratio of lateral displacements including P-delta effects to lateral displacements not including P-Delta effects for record components applied in the X direction

Level	B00-X	B90-X	C00-X	C90-X
1	1.001	1.000	1.001	1.000
2	1.001	1.000	1.001	1.001
3	1.000	0.999	1.001	1.001
4	1.000	0.999	1.001	1.001
5	1.005	1.004	0.995	0.997
6	1.008	1.007	1.009	0.995
7	1.009	0.993	1.010	0.993
8	1.010	0.991	1.012	0.992
9	1.003	0.998	0.998	1.002
10	0.999	0.999	1.001	0.999
11	0.998	0.998	1.003	0.998
12	0.996	0.997	1.003	0.998

Table 5-11 Ratio of lateral displacements including P-delta effects to lateral displacements not including P-Delta effects for record components applied in the Y direction

Level	B00-Y	B90-Y	C00-Y	C90-Y
1	1.000	1.000	1.001	1.000
2	0.998	0.998	1.003	1.002
3	0.997	0.998	0.997	1.002
4	0.997	0.997	0.995	1.000
5	0.997	1.003	0.995	0.998
6	1.001	1.004	0.995	0.997
7	1.005	1.005	0.995	0.997
8	1.004	1.004	1.004	0.998
9	1.002	1.002	1.002	0.999
10	1.001	1.001	0.999	0.999
11	1.001	1.001	0.998	0.999
12	0.998	1.002	0.997	0.999

The recommendation of this document for calculating P-Delta effects in a linear response history analysis consists in applying the static procedure given in section 12.9.6 of ASCE 7-10. However, more research is needed in this topic; particularly, research is needed for providing a dynamic method to estimate the P-Delta effects in linear response history analysis.

Recommendation for P-Delta effects in LRHA: Use the same provisions for response spectrum analysis given in Section 12.9.6 of ASCE 7-10.

5.10 Modeling of the basement

It is common in buildings to have one, two, or more levels of basement. The assumptions in the mathematical model about the loading, meshing, and node restrictions in the basement walls can have a very strong influence in the results, and particularly in the base shear for any level below the ground. Hereafter, it will be used the nomenclature ground level, basement level, shear force at ground level, and shear force at the basement as given in Figure 5-29 which shows the bottom part of a perimeter frame of a building.

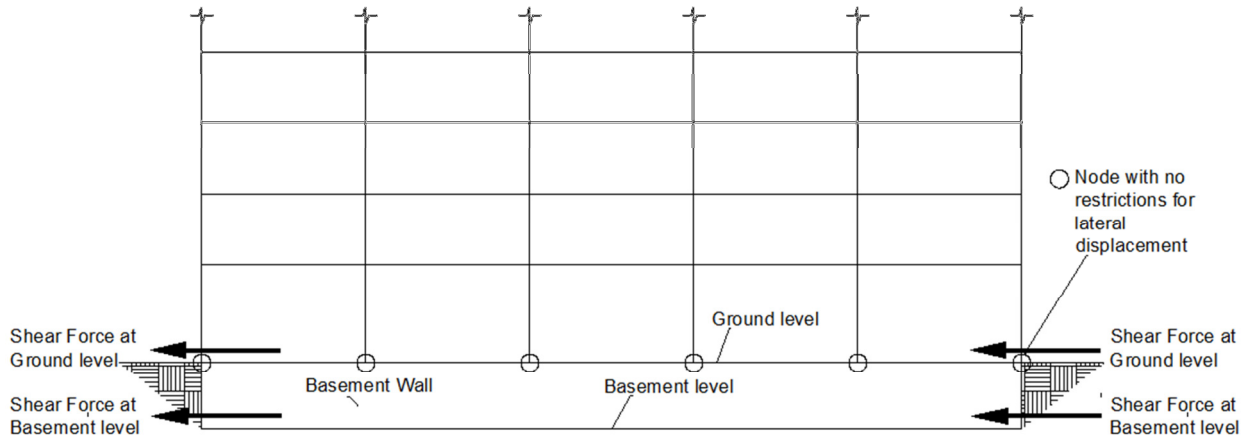

Figure 5-29 Nomenclature for ground level, basement level, shear force at ground level and shear force at the basement level

One of the issues associated with the modeling of the basement arises particularly in buildings with one basement level and with no restrictions in the lateral displacement of the perimeter nodes at ground level (see Figure 5-29). Buildings can be modeled with this assumption of ”allowing” the lateral displacements of the perimeter nodes assuming that the basement walls and the usual thick slab at ground level would provide enough stiffness so that the basement walls and the slab at ground level would not be excited under lateral loads. However, this is not always the case as it was noted in the building analyzed by Charney et al. (2010b) where the ground level was excited in both lateral directions at very low periods. The inclusion of those higher modes in the analysis can yield a considerable increase in the shear force at the basement level although the shear force at ground level and at any other upper story will not change significantly. The increase in the shear force is due to two effects; first, the mass participation factor of those higher modes can be considerably large (10% for the building analyzed by Charney et al.) because of the heavy mass associated with the slab at the ground level and with the mass coming from the basement walls. Also, the shear force could be considerably amplified when doing a LRHA because of the effects associated with the scaling of the ground motions. This issue occurs because the spectral ordinates of the scaled earthquakes at those low periods where the slab at ground level is excited might be considerably above the design spectrum predicted by that site.

The issue regarding the increase in the base shear for the building analyzed by Charney et al. (2010b), which is defined as Building 2 in Appendix A, is explored in detail in this section, and some of the variables of interest are:

R0: Ratio between the shear forces at Level 0 (basement level) using n modes to the shear forces at the same level using 18 modes.

R1: Ratio between the shear forces at Level 1 (ground level) using n modes to the shear forces at the same level using 18 modes.

R: Ratio between the shear forces at Level 0 to the shear forces at Level 1 for different number of modes.

Modal linear response history analyses were run with different number of modes using 5% damping, and the values obtained with 18 modes are used as reference since it is the number of modes required to reach 90% of the mass if the supports of the building were located at ground level instead of at basement level. The ground motions used in the analysis were the records A and C of Table 2-6, and the record 810 of the NGA database (PEER, 1999) which was denoted as record B. The horizontal components of the records A, B, and C are denoted as A00 and A90, B00 and B90, and C00 and C90, respectively, and those record components were applied in the two orthogonal directions X and Y of Building 2 (see Figure A- 2 for orientation of axis X and Y).

The ratio R0 when analyzing the building with different number of modes is presented in Table 5-12 for the record components A00, A90, C00, and C90 as specified in Table 2-6, and the record components B00 and B90 correspond to the record 810 of the NGA database (PEER, 1999). As it can be seen in Table 5-12 the ratio R0 changes drastically when the number of modes goes from 117 to 118 for load in the X direction, and from 111 to 112 modes for load in the Y direction. This happens because modes number 112 and 118 are the modes that excite the ground floor of the building in the Y and X direction, respectively. This fact can also be seen in Table 5-13, which shows the vibration periods and the sudden increase in the mass participation factor in the planar X direction (SumUX), in the planar Y direction (SumUY), and in the rotation about the vertical axis (SumRZ) at the modes 118, 112, and 193, respectively.

Table 5-12 Ratio R0 for different number of modes and for each component of the earthquakes A, B, and C

Earthquake component	Number of modes								
	18	**50**	**111**	**112**	**117**	**118**	**192**	**193**	**200**
A00-X	1.00	1.01	1.01	1.01	1.01	1.70	1.70	1.70	1.70
A90-X	1.00	0.97	0.98	0.98	0.99	3.46	3.48	3.48	3.48
B00-X	1.00	1.03	1.02	1.02	1.01	1.86	1.88	1.88	1.88
B90-X	1.00	1.03	1.02	1.02	1.01	2.72	2.73	2.73	2.73
C00-X	1.00	1.00	1.00	1.00	1.00	1.12	1.12	1.12	1.12
C90-X	1.00	1.00	1.00	1.00	1.00	1.23	1.23	1.23	1.23
A00-Y	1.00	1.01	1.11	1.91	1.93	1.93	1.93	1.93	1.93
A90-Y	1.00	0.99	1.62	3.88	3.92	3.92	3.92	3.92	3.92
B00-Y	1.00	0.99	1.28	3.16	3.19	3.19	3.19	3.19	3.19
B90-Y	1.00	0.96	1.29	3.11	3.15	3.15	3.16	3.16	3.16
C00-Y	1.00	0.95	0.96	1.84	1.86	1.86	1.86	1.86	1.86
C90-Y	1.00	1.00	1.03	1.14	1.14	1.14	1.14	1.14	1.14

Table 5-13 Mass Participation factors of the most important modes regarding the increase in base shear

Mode	Period (sec)	SumUX (%)	SumUY (%)	SumRZ (%)
18	0.277	81.56	81.92	75.46
50	0.145	82.55	82.60	78.66
100	0.072	82.68	82.72	79.36
111	0.067	82.68	86.70	79.36
112	0.067	82.68	97.16	79.36
117	0.061	82.90	97.35	79.37
118	0.057	97.65	97.35	79.71
150	0.047	97.74	97.37	79.73
192	0.040	97.75	97.38	80.03
193	0.040	97.75	97.38	91.18
200	0.038	97.75	97.40	91.76

When the ratio R1 is analyzed in Table 5-14 it can be seen that there is no variation of the shear force at ground level when the number of modes is increased. Therefore, it was concluded that any variation with the number of modes of the shear forces at basement level do not affect the forces in any element above that level.

Table 5-14 Ratio R1 for different number of modes and for each component of the earthquakes A, B, and C

Earthquake component	Number of modes								
	18	**50**	**111**	**112**	**117**	**118**	**192**	**193**	**200**
C00-X	1.00	1.00	1.00	1.00	1.00	1.00	1.00	1.00	1.00
A00-X	1.00	1.01	1.01	1.01	1.01	1.01	1.01	1.01	1.01
B00-X	1.00	1.03	1.02	1.02	1.02	1.03	1.03	1.03	1.03
A90-X	1.00	0.97	0.98	0.98	0.98	0.99	0.99	0.99	0.99
B90-X	1.00	1.03	1.02	1.02	1.02	1.03	1.03	1.03	1.03
C90-X	1.00	1.00	1.00	1.00	1.00	1.00	1.00	1.00	1.00
A00-Y	1.00	1.01	1.01	1.01	1.01	1.01	1.01	1.01	1.01
A90-Y	1.00	0.99	0.98	1.00	1.00	1.00	1.00	1.00	1.00
B00-Y	1.00	0.98	0.99	0.98	0.98	0.98	0.98	0.98	0.98
B90-Y	1.00	0.96	0.96	0.97	0.97	0.97	0.97	0.97	0.97
C00-Y	1.00	0.95	0.95	0.96	0.96	0.96	0.96	0.96	0.96
C90-Y	1.00	1.00	1.00	1.00	1.00	1.00	1.00	1.00	1.00

The factor of major interest is R because it shows the ratio of the shear forces at Level 0 to those at Level 1; Table 5-15 shows that the value of R can be as high as 3.93 which means that the shear forces at Level 0 are about 4 times bigger than those at Level 1 for high modes. This result is consider unexpected because it is not reasonable that the excitement of the ground level (Level 1) with has only 16.9% of the mass of the building (Charney et al., 2010b) would cause an increase of such magnitude in the base shear.

Table 5-15 Ratio R for different number of modes and for each component of the earthquakes A, B, and C

Earthquake component	Number of modes								
	18	**50**	**111**	**112**	**117**	**118**	**192**	**193**	**200**
A00-X	1.00	1.00	1.00	1.00	1.00	1.67	1.67	1.67	1.67
A90-X	1.00	1.00	1.00	1.00	1.01	3.51	3.53	3.53	3.53
B00-X	1.01	1.01	1.01	1.01	1.00	1.82	1.83	1.83	1.83
B90-X	1.01	1.01	1.01	1.01	0.99	2.66	2.67	2.67	2.67
C00-X	1.00	1.00	1.00	1.00	1.00	1.12	1.12	1.12	1.12
C90-X	1.00	1.00	1.00	1.00	1.00	1.23	1.23	1.23	1.23
A00-Y	1.00	1.00	1.10	1.89	1.90	1.90	1.90	1.90	1.91
A90-Y	1.00	1.00	1.65	3.89	3.93	3.93	3.93	3.93	3.93
B00-Y	1.01	1.01	1.31	3.25	3.28	3.28	3.28	3.28	3.28
B90-Y	1.01	1.01	1.35	3.25	3.29	3.29	3.29	3.29	3.29
C00-Y	1.00	1.00	1.02	1.93	1.94	1.94	1.95	1.95	1.95
C90-Y	1.00	1.00	1.03	1.14	1.14	1.14	1.14	1.14	1.14

This issue was explored then by using direct integration instead of a modal analysis; the damping in this case was defined using a mass and stiffness proportional model with damping equal to 0.05 at the 2nd and 10th periods of the structure. The results of the ratio R are shown in Table 5-16.

Table 5-16 Ratio R for each component of the earthquakes A, B, and C using direc integration

Earthquake component	Shear force Level 0 (kips)	Shear force Level 1 (kips)	Ratio R
A00-X	5131	3846	1.33
A90-X	3562	1790	1.99
B00-X	11862	6100	1.94
B90-X	11337	4402	2.58
C00-X	3260	2608	1.25
C90-X	3910	2557	1.53
A00-Y	5441	3966	1.37
A90-Y	4810	1614	2.98
B00-Y	11678	4531	2.58
B90-Y	11306	4403	2.57
C00-Y	4681	1966	2.38
C90-Y	4985	4364	1.14

From studying Table 5-15 and Table 5-16 it can be concluded that the increase in the ratio R is significant; particularly for the earthquake component A90-Y the factor R is equal to 2.98. As it was mentioned before this is due to the significant mass participation factor of the modes that excite the slab at ground level, and because of the high spectral ordinates at those higher periods resulting from the scaling of ground motions.

Some considerations are explained next for the case of buildings having more than one basement level. First, the fundamental period of the building might not be significantly affected by the number of basement levels if the structural system above grade is considerable more flexible than the structural system below grade. Also, as well as for buildings with only one basement level, for buildings with several basement levels, an increase in the base shear at all levels below grade is expected when the nodes of the perimeter basement walls are not restrained laterally at any level. Additionally, the more the basement levels there are, the more the mass is

accumulated under ground level, and the higher mass participation factor of the modes could excite the basement levels.

The restraint of the lateral displacements in the nodes of the basement walls at ground level could be a reasonable assumption; however, the not restraining of these displacements could also be a reasonable assumption; therefore, the designer has the responsibility of using the mathematical model that adjust best to the real behavior of the building analyzed. A suggestion for design purposes is to analyze the building under both assumptions and study the sensitivity of the response (i.e. base shear in the basement walls). Other variables that will influence the results are the supporting conditions of the nodes below ground level, the meshing of the basement walls, and the number of basement levels. Another variable of interest, which is applied only for the case with no restraining of the nodes at basement level, is the mass participation factor of the modes exciting the basement level. It is expected that for higher values of the mass participation factor of these modes, the difference in the models restraining or not restraining the displacements will be bigger.

Further research is encouraged to study these variables and provide more guidance for design purposes. A preliminary recommendation for the modeling of the basement in buildings can be given as follows:

Recommendation for modeling of the basement:

Basement levels should be included in the mathematical model of the building, and their modeling will reassemble as possible, the real behavior expected for the analyzed building.

5.11 Calculation of drifts for structures modeled with semirigid diaphragms

An aspect that requires attention is the calculation of drifts using semirigid diaphragms, and it refers to the calculation of the displacement of the center of mass when such point does not coincide with the location of a node within the grid used to model the floor.

The displacement of the center of mass when such a point is not modeled specifically in the analytical model can be calculated based on the displacement and rotation of a close node P as shown in Figure 5-30.

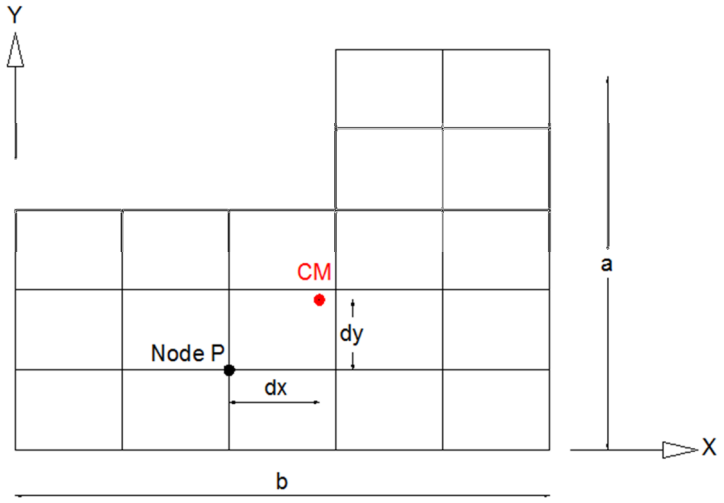

Figure 5-30 Calculation of the displacement of the center of mass CM based on the displacements of a close node P

The formulas required for that calculation are shown below, and they were used for the calculation of the drifts in the building analyzed by Charney et al. (2010b).

$$CM_X = P_X - \theta_P dy \qquad \textbf{Eq. 5- 7}$$

$$CM_Y = P_Y + \theta_P dx \qquad \textbf{Eq. 5- 8}$$

where CM_X is the displacement of the center of mass in the X direction

CM_Y is the displacement of the center of mass in the Y direction

P_X is the displacement of the node P in the X direction

P_Y is the displacement of the node P in the Y direction

θ_P is the rotation of the node P about the vertical axis

dx is the distance, measured in the X direction, between the node P and the center of mass

dy is the distance, measured in the Y direction, between the node P and the center of mass

5.12 Parameter to control damage in nonstructural components

The parameter in ASCE 7-10 that controls the damage in the non-structural components of a building is the interstory drift; however, a better measure of this damage can be given by the "Drift Damage Index", or DDI, suggested by Charney (1990). The drift damage index is defined

as an index "numerically equal to the shear strain occurring within rectangular regions of the structure defined as drift damageable zones" (Charney, 1990). The drift damageable zones, as shown in Figure 5-31, are located at the corners of the building, and they are rectangular regions with zero stiffness that are bounded by floor diaphragms and real or fictitious column lines. The DDI is calculated in each drift damageable zone as the ratio of the shear strain under lateral load to the allowable shear strain, and the latter depends on damageability thresholds of the protected nonstructural (or structural) components and on the level of damage acceptable to the owner of the building (Charney, 1990). The DDI could be automatically computed if using finite element analysis. It is encouraged to further research the potential implementation of this parameter as a measure of damage in non-structural components. The method is applicable for the cases of equivalent lateral force method, response spectrum analysis, and linear response history analysis.

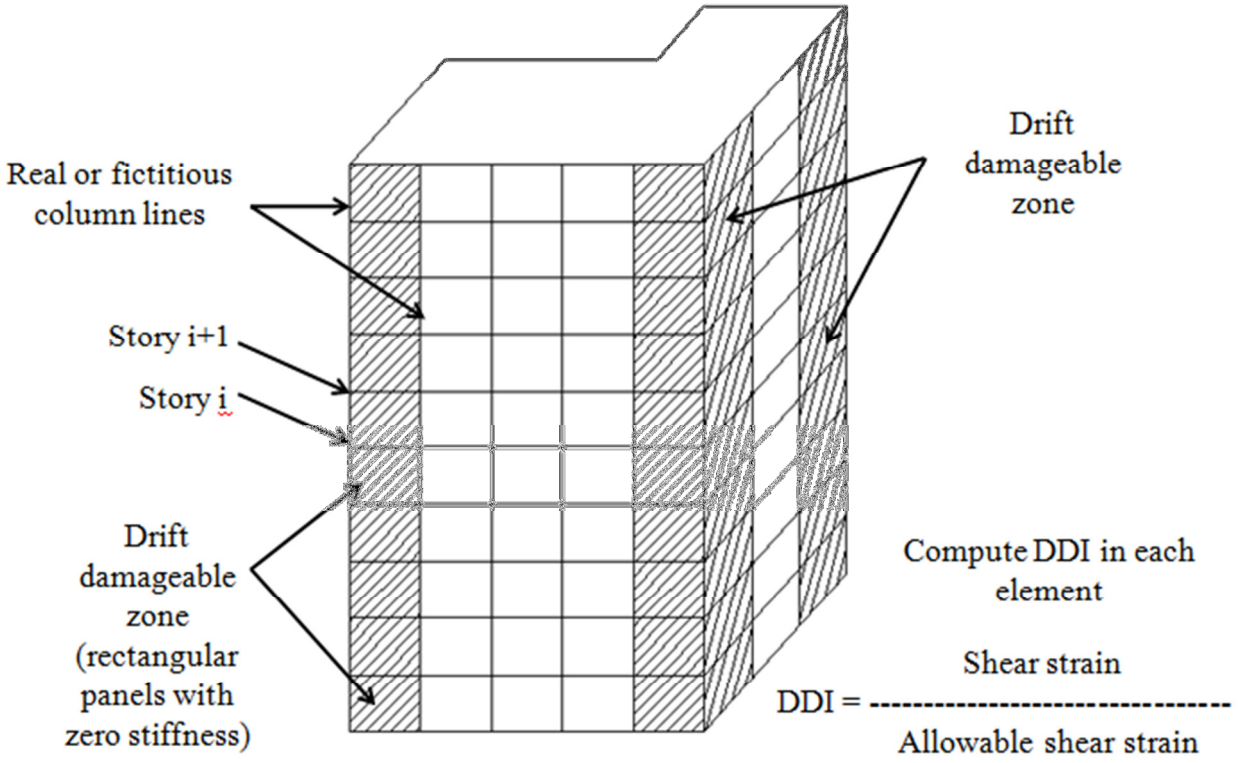

Figure 5-31 Characteristics of the model for the calculation of the Drift Damage Index (DDI)

Chapter 6. SUMMARY AND CONCLUSIONS

6.1 Research summary

This document analyzed the variables required to perform linear response history analysis (LRHA) according to the current provisions of the American standard ASCE 7-10, and it also suggested, when required, the modification or inclusion of new variables. This way, the objectives of identifying and analyzing the variables required to perform LRHA was accomplished.

The first of the variables analyzed was the selection of ground motions, and it is suggested the inclusion of new requirements based on the guidelines for the selection of ground motions of different seismic codes and related literature. Also, the characteristics of spectral matched acceleration histories with three different techniques that can create these records have been explored in detail: a routine developed by Martin Chapman, the computer software SIMQKE-I and the stochastic seismograms generated by the USGS; the analysis of these tools served as the basis to establish a preliminary criteria for the selection of spectral matched acceleration histories. Also, the variables that influence the scaling of ground motions have been analyzed and the discussion of these variables together with a review of the scaling methodologies used by different seismic codes have been used to establish a suggested new proposal for the selection and scaling of earthquake records. Additionally, guidelines for the selection and scaling of ground motions when using spectral matched records have been addressed.

Another variable analyzed was the assumption used in modeling the flexibility of the diaphragm, and it was studied by performing linear response history analyses in buildings modeled with the mass of the floor concentrated at the center of mass (rigid diaphragms), and also by modeling buildings with the mass distributed uniformly along each floor (semirigid diaphragms). Accidental torsion using linear response history analysis was also studied by analyzing the provisions in different seismic codes, by studying the improvements of static procedures to predict dynamic torsional effects, and by studying dynamic procedures to implement torsional effects. Attention was also given to variables that influence linear response history analysis such as the orientation of ground motion axis, the use of the vertical component

of ground motions, the scaling of element forces and displacements, orthogonal loading, solution techniques as modal analysis and direct integration, P-Delta effects, modeling of the basement, and calculation of drifts. The analysis of all the variables mentioned above has been summarized in suggested provisions for the section of linear response history analysis in future editions of ASCE 7. These provisions are presented in the Appendix D, and it accomplishes the principal objective of this thesis.

6.2 Assumptions and Limitations of the Study

Some of the assumptions and limitations of this study are as follows:

- Differences in the treatment of near-fault and far-field records were not explored in detail.
- Provisions for simulated ground motions that are not spectral matched were not studied in this document.
- Analysis of spectral matched acceleration histories was done only with three types of software and in only two buildings.
- Only two sets of ground motions and only one scaling technique were used to study the differences when using the SRSS or the geomean as the spectral measure of an earthquake.
- The differences in response for buildings modeled with rigid and semirigid diaphragms were studied in four buildings only.
- Three procedures that use static forces to account for dynamic torsional effects were described; however, only one of them (method from De la Llera and Chopra) was compared with dynamic torsional effects.
- The suggested procedure to include accidental torsion in semirigid diaphragms by displacing a percentage of the mass of the floor over one of the edges of a building was explored only in one symmetric building.
- Only two methods were explored for the calculation of the torsional spectrum.
- Equivalence between response history analysis using rotational records and its corresponding torsional spectrum was not analyzed.
- Simultaneous loading with translational and rotational records was not studied.

- The inclusion in the analysis of the vertical component of a record as well as the treatment of P-Delta effects in linear response history analysis was not studied in detail.
- Issues related with the modeling of the basement were studied for one case only.

6.3 Conclusions

6.3.1 Use of spectral matched acceleration histories

The tool developed by Martin Chapman and the computer software SIMQKE-I provided spectral matched ground motions that when used in a linear response history analysis predicted interstory drifts and interstory shears that are equivalent to those predicted by a modal response spectrum analysis, when using the same target spectrum. Additionally, the use of the stochastic seismograms generated by the USGS deaggregation models is discouraged as a tool to generate spectral matched acceleration histories because they can be generated only for some specific fundamental periods, and also because the shape of the spectrum from those stochastic seismograms might not have the shape expected of actual or code spectra.

6.3.2 Selection and scaling of ground motions

A new method for selection and scaling of ground motions considering the refinement and the addition of several variables missed in the current ASCE 7-10 has been suggested. The new methodology considers the selection and scaling of ground motions as a unique process, and it applies only to structures modeled in three dimensions (3D). Modeling in two dimensions (2D) has not been allowed for applying LRHA. Also, the suggested method considers different limits of the period range of interest than those of the current provisions in ASCE 7-10, and it yields a unique set of scale factors for the same suit of ground motions. Moreover, the limits of the scale factors that modify the selected earthquake records have been set up as 1/3 and 3.

6.3.3 Diaphragm flexibility

It was noticed no difference in the interstory drift when using rigid or semirigid diaphragms in the four buildings analyzed with linear response history analysis. However, it was not analyzed member forces, which can be significantly affected by the assumptions in the diaphragm flexibility, particularly for the case of stiff wall type systems,

6.3.4 Accidental Torsion

From the review of the provision for accidental torsion in different seismic codes, it was considered convenient to suggest for future editions of ASCE 7 the requirement of the New Zealand Standard NZS 1170.5 describing that for the cases where the lateral load is not parallel to the principal axis of the structure, the point of application of the lateral load will be over the ellipse with center coinciding with the center of mass of the floor and with semiaxis equal to the design eccentricities along the principal axis of the structure. Furthermore, from the literature reviewed it was noticed that the parameter Ω, defined as the ratio between the uncoupled translational and rotational fundamental periods of the building, is a factor that needs to be included in provisions for accidental torsion. Also, it was concluded in the analysis of four buildings that when displacing the center of mass to model accidental torsion, the fundamental periods do not change significantly; however, the mass participation factor corresponding to those periods can have important changes.

In addition, it was concluded that accidental torsion using linear response history analysis could be easily implemented in buildings modeled with masses concentrated at the center of mass (rigid diaphragms); however, difficulties can arise when applying accidental torsion to buildings modeled with mass uniformly distributed along the floor (rigid or semirigid diaphragms). For the latter case, a procedure where a fraction of the mass of the diaphragms is moved towards one of the edges of the building to artificially create accidental torsion was suggested, and this method yielded comparable interstory shears to those obtained from an analysis including accidental torsion using rigid diaphragms.

The interstory shears using static and dynamic procedures to account for torsional effects were compared, and it was concluded that the results from both techniques were similar for the external frames parallel to the direction of loading. Also, from analyzing the rotational record obtained from the difference of two parallel translational acceleration histories, it was concluded that the resulting rotational record is statistically independent from the translational records. Torsional response spectrum was obtained with two different techniques; however, the use of these rotational spectra needs to be explored.

6.3.5 Orientation of ground motion axis

It was concluded for the three records analyzed that the maximum spectral acceleration, velocity or displacement did occur when the components of the original record were rotated a

particular angle denominated “critical angle”. The generated acceleration history for each record component after rotating the critical angle was determined, and called the “critical acceleration history”. However, it was also noticed that the interstory shears for the critical acceleration history can be less than the interstory shears calculated with the original record components due to the influence of vibration modes other than the first one. Therefore, a linear response history analysis should include the response from the original components of the record analyzed as well as the response from its critical acceleration history.

6.3.6 Use of the vertical component of ground motion

It has been identified in the Eurocode 8 (British Standards, 2004) and in the New Zealand Standard NZS 1170.5 (Council of Standards New Zealand, 2004) the structural elements sensitive to the vertical component of ground motions, and it provides a starting point to include or add other structural elements sensitive to vertical movement in future editions of ASCE 7. The use of the vertical component of ground motion was not studied in detail and it is recommended further research in this topic.

6.3.7 Scaling of design parameters

It was concluded that element forces and interstory drifts need to be scaled identically as it is done for the case of response spectrum analysis. In order to achieve this purpose, the current scaling of element forces of Section 16.1.4 of ASCE 7-10 has been modified; however, the provisions of ASCE 7-10 for the scaling of interstory drifts has been unchanged.

6.3.8 Orthogonal loading

After reviewing the guidelines provided in different seismic codes, three alternatives to include orthogonal loading when using linear response history analysis are studied; the first suggests the application of the square root of the sum of the squares (SRSS) of the maximum responses in each direction, another alternative suggest the application of the 30% rule, and the last alternative suggest the simultaneous use of the two record components, where each one of them is scaled according to the requirements of ASCE 7-10. This last alternative is considered to be the most appropriate for linear response history analysis because it represents more realistically what actually happens in real earthquakes, and also because it provides a margin of safety for the resisting elements (i.e columns, shear walls) located at the corners of the building.

6.3.9 Damping and Solution techniques

When doing modal linear response history analysis the required number of modes for the analysis will be given by Section of ASCE 7-10 which corresponds to the provision of modal response spectrum analysis. Also, for modal analysis the damping ratio for all vibration modes will be equal to 0.05.

For the case of direct integration several options were given to select the periods and their damping ratios to define the mass proportional and stiffness proportional coefficient of Rayleigh damping.

6.3.10 P-Delta effects

When applying linear response history analyses to a building including and excluding P-Delta effects, only minor difference in the lateral displacements was found; however, this was only a particular case, and more research is needed in this topic. As an alternative, it is suggested to approximate the P-Delta effects in linear response history analysis using the static procedure for the inclusion of P-Delta effects described in Section 12.8.7 of ASCE 7-10.

6.3.11 Modeling of the basement

A case study is presented to show issues associated with the modeling of the basement.

6.3.12 Damage in nonstructural components

The "Drift Damage Index" has been introduced as an alternative to interstory drift to evaluate the damage in non-structural components.

6.4 Recommendations for future research

Criteria for the selection of ground motions

- Appropriate procedures to define the seismic hazard of a site need to be explored.
- The differences in the requirements for the selection of ground motions for near fault and far field earthquakes need to be studied.
- The appropriateness of the requirement of statistical independence between the record components needs to be explored in detail.
- Additional procedures that generate spectral matched acceleration histories can be explored.

- Studies are required to analyze the minimum duration of spectral matched acceleration histories, as well as the effects of significantly long spectral matched acceleration histories.
- Additional studies regarding the equivalence of techniques that generate spectral matched acceleration histories can be analyzed using non-linear analysis in single and multiple degree of freedom systems.
- An acceptability criterion for simulated non-spectral matched acceleration histories needs to be studied.

Scaling procedure of ground motions

- The appropriateness of using the SRSS or the geomean as the spectral measure of an earthquake needs to be explored in more detailed.
- An analytical study of appropriate limits for the scale factors in the scaling of ground motions procedure needs to be done.
- Additional studies are required to study the advantages and disadvantages of the new selection and scaling procedure provided in section 3.4 of this document.
- It is recommended to create appropriate software so that the suggested method for selecting and scaling of ground motions could be connected directly to an earthquake database and then analyze random combinations of ground motions and respective scale factors.
- Procedures for the scaling of ground motions including weighted contributions of the mass participation factors of different modes needs to be investigated.
- Studies are required to establish an appropriate level of discretization of the periods for the calculation of any response spectrum requested in seismic code procedures.

Modeling of Buildings with rigid and semirigid diaphragms

- The differences in response for buildings modeled with rigid and semirigid diaphragms needs to be studied in buildings with dual systems, because in those systems, the forces transmitted through the diaphragms are significant and difference response could be expected for rigid and for semirigid diaphragms.

- The procedure suggested for including torsional effects in buildings modeled with semirigid diaphragms by displacing a percentage of the mass of the floor over one of the edges of a building needs to be explored in several symmetric and non-symmetric buildings.

Rotational spectra and rotational records

- New techniques to generate rotational spectrum need to be explored.
- The equivalence between response history analysis using rotational records and its respective rotational spectrum needs to be studies.
- The response of buildings under simultaneous translational and rotational records needs to be studied.

Vertical component of ground motion

- The effects of doing linear response history analysis including and excluding the vertical component of a record need to be explored in detail. Also, a study describing the type of elements of a structure more sensitive to vertical accelerations is needed.
- The appropriateness of applying the response modification coefficient R and the deflection amplification factor C_d, as defined in ASCE 7-10, to the vertical accelerations and displacements, respectively, needs further research

Scaling of design parameters

- The appropriateness of using 85% of the ELF base shear as the reference value for scaling the base shear from LRHA needs to be explored.

Combination of results

- Studies are required to address the issue of losing the sign in the element forces from LRHA when using the envelope or the average of the response from all the selected records.

Damping

- A more careful study of the implications and recommendations for use of Rayleigh Damping in linear response history analysis is recommended.

P-Delta effects

- More research about procedures to account for P-Delta effects in linear response history analyses using dynamic approaches is encouraged.

Modeling of basement

- A detailed study of the modeling of the basement in buildings with different structural systems and with different number of basement levels is needed.

Other requirements

- The minimum number of periods for the calculation of any spectrum required by ASCE 7 needs to be investigated.

REFERENCES

Administracion Publica del Distrito Federal (2004). "Normas tecnicas complementarias para diseno por sismo." Gaceta Oficial del Distrito Federal, Mexico.

ASCE (2000). "Seismic Analysis of Safety-Related Nuclear Structures and Commentary ASCE 4-98." American Society of Civil Engineers, Reston, VA.

ASCE/SEI (2003). "Minimum design loads for buildings and other structures." American Society of Civil Engineers, Reston, VA.

ASCE/SEI (2006). "Minimum design loads for buildings and other structures." American Society of Civil Engineers, Reston, VA.

ASCE/SEI (2010). "Minimum design loads for buildings and other structures ASCE/SEI 7-10." *ASCE7-10*, American Society of Civil Engineers, Reston, VA.

ATC (2008). *Quantification of Building Seismic Perfomance Factors ATC-63 Project Report - 90% Draft*, Federal Emergency Management Agency (FEMA).

Atik, and Abrahamson (2010). "An Improved Method for Nonstationary Spectral Matching." *Earthquake Spectra*, 26(3), 601-617.

Baker, and Cornell (2005). "A vector-valued ground motion intensity measure consisting of spectral acceleration and epsilon." *Earthquake Engineering and Structural Dynamics*, 34, 1193-1217.

Baker, and Cornell (2006). "Which spectral acceleration are you using?" *Earthquake Spectra*, 22(Compendex), 293-312.

Beyer, and Bommer (2007). "Selection and scaling of real accelerograms for bi-directional loading: A review of current practice and code provisions." *Journal of Earthquake Engineering*, 11(SUPPL. 1), 13-45.

Bommer, and Acevedo (2004). "The use of real earthquake accelerograms as input to dynamic analysis." *Journal of Earthquake Engineering*, 8(1 supp 1), 43 - 91.

Boore (2000). "SMSIM - Fortran programs for simulating ground motions from earthquakes: Version 2.0 - A revision of OFR 96-80-A." U.S. Geological Survey, Menlo Park, CA.

Bradley (2010). Personal Communication. August 12, 2010.

British Standards (2004). "Eurocode 8: Design of structures for earthquake resistance." *Part 1: General rules, seismic actions and rules for buildings*, European Committee for Standardization, Brussels.

California Department of Conservation's Strong Motion Instrumentation Program (CSMIP), and USGS National Strong Motion Program (NSMP) (2007). "Center for Engineering Strong Motion Data."

Canadian Commission on Building and Fire Codes (2005). *National Building Code of Canada 2005*, National Research Council of Canada 2005, Ottawa.

Canadian Commission on Building and Fire Codes (2006). *User's Guide - NBC2005 Structural Commentaries (Part 4 of Division B)*, National Research Council of Canada 2006, Ottawa.

Carballo, and Cornell "Input to nonlinear structural analysis: Modification of available accelerograms for different source and site characteristics." *Proc., 6th U.S. National Conference on Earthquake Engineering*.

Chapman (2010a). Personal Communication. January 29, 2010a.

Chapman (2010b). Personal Communication. July 27, 2010b.

Charney (1990). "Wind drift serviceability limit state design of multistory buildings." *Journal of Wind Engineering and Industrial Aerodynamics*, 36(Part 1), 203-212.

Charney (1995, 2003). "NONLIN." Federal Emergency Management Agency Training Center, Advanced Structural Concepts Emmitsburg MD, Blacksburg VA.

Charney (2009). Personal Communication. December 01, 2009.

Charney (2010a). *Seismic Loads Guide to the seismic load provisions of ASCE7-05*, American Society of Civil Engineers, Reston VA.

Charney (2010c). Personal Communication. November 14, 2010c.

Charney, and Syed (2004, 2010). "EQTools." Virginia Polytechnic Institute & State University, Blacksburg, VA.

Charney, Tola, and Atlayan (2010b). "Structural Analysis." *NEHRP Recommended Provisions: Design Examples*, B. S. S. Council, ed., To be published.

Chopra (2007). *Dynamics of Structures - Theory and applications to Earthquake Engineering*, Pearson Prentice Hall, Upper Saddle River, NJ.

Computer and Structures Inc (2009). "SAP2000 Static and dynamic finite analysis of structures."

COSMOS (2007). "COSMOS Virtual Data Center." <http://db.cosmos-eq.org/scripts/earthquakes.plx>. (03/25/2010, 2010).

Council of Standards New Zealand (2004). "NZS 1170.5 Structural Design Actions, Part 5: Earthquake actions - New Zealand." Standards New Zealand, Wellington, New Zealand.

Council of Standards New Zealand (2004b). "NZS 1170.5 Supplement 1:2004 Structural Design Actions, Part 5: Earthquake actions - New Zealand - Commentary ", Standards New Zealand, Wellington, New Zealand.

De la Llera, and Chopra (1994a). "Accidental and natural torsion in earthquake response and design of buildings." University of California at Berkeley - College of Engineering, Berkeley, CA.

De la Llera, and Chopra (1994b). "Accidental torsion in buildings due to base rotational excitation." *Earthquake Engineering and Structural Dynamics*, 23(9), 1003-1021.

Dimova, and Alashki (2003). "Seismic design of symmetric structures for accidental torsion." *Bulletin of Earthquake Engineering*, 1(2), 303-320.

Escobar, Mendoza, and Gomez (2004). "Diseno simplificado por torsion sismica estatica." *Revista de Ingenieria Sismica*, Sociedad Mexicana de Ingenieria Sismica, A.C., Distrito Federal, Mexico, 77-107.

Fahjan, and Ozdemir (2008). "Scaling of earthquake accelerograms for non-linear dynamic analyses to match the earthquake design spectra." *14th World Conference on Earthquake Engineering*Beijing, China.

FEMA (1997). "NEHRP Recommended seismic provisions for new buildings and other structures (FEMA 302)." Building Seismic Safety Council, Washington, D.C.

FEMA (2009). "NEHRP Recommended seismic provisions for new buildings and other structures (FEMA P-750)." Building Seismic Safety Council, Washington, D.C.

Gasparine, and Vanmarcke (001976). "SIMQKE A program for artificial motion generation." Department of Civil Engineering Massachusetts Institute of Technology, Cambridge, Massachusetts.

Ghayamghamian, Nouri, Igel, and Tobita (2009). "The effect of torsional ground motion on structural response: Code recommendation for accidental eccentricity." *Bulletin of the Seismological Society of America*, 99(2 B), 1261-1270.

Goel, and Chopra (1993). "Seismic code analysis of buildings without locating centers of rigidity." *Journal of structural engineering New York, N.Y.*, 119(10), 3039-3055.

Gomes, Santos, and Oliveira (2006). "Design spectrum-compatible time histories for numerical analysis: Generation, correction and selection." *Journal of Earthquake Engineering*, 10(Compendex), 843-865.

Hadjian, A. H. (1981). "On the correlation of the components of strong ground motion. II." *Bulletin of the Seismological Society of America* 71(Copyright 1982, IEE): 1323-1331.

Hanks, and Kanamori (1979). "A moment magnitude scale." *Journal of Geophysical Research*, 84(B5), 2348-2350.

Harmsen (2010a). Personal Communication. June 23, 2010a.

Harmsen (2010b). Personal Communication. August 23, 2010b.

Hart, and Wilson (1989). "Simplified Earthquake Analysis of Buildings Including Site Effects."Report No.UCB/SEMM-89/23, Department of Civil Engineering, University of California, Berkeley.

Howell David C. (2007). *Statistical Methods for Psychology*, Thomson Wadsworth.

Huang, Whittaker, Kennedy, and Mayes (2009). "Assessment of Base-Isolated Nuclear

Structures for Design and Beyond-Design Basis Earthquake Shaking."MCEER-09-0008, University of Buffalo, State University of New York, Buffalo, NY.

Humar, Yavari, and Saatcioglu (2003). "Design for forces induced by seismic torsion." *Canadian Journal of Civil Engineering*, 30, 328-337.

Idriss, and Sun (1992). "User's Manual for SHAKE91, a computer program for conducting equivalent linear seismic response analyses of horizontally layered soil deposits, Program modified based on the original SHAKE program published in December 1972 by Schnabel, Lysmer & Seed "Report, Center for Geotechnical Modeling, Department of Civil & Environmental Engineering, University of California, Davis.

Instittuto Nacional de Normalizacion (1996). "Norma Chilena NCh 433.Of96 - Diseno sismico de edificios." Instittuto Nacional de Normalizacion - INN, Santiago - Chile.

Kendall, and Ord (1990). *Time Series*, Oxford University Press, New York NY.

Krawinkler Helmut (2000). "State of the Art Report on Systems Performance of Steel Moment Frames Subject to Earthquake Ground Shaking, FEMA-355C." S. J. Venture, ed.

Lee, and Finn (1978). "DESRA-2, Dynamic effective stress of soil deposits with energy transmitting boundary including assesment of liquefaction potential."Soil Mechanics Series No. 38, University of British Columbia, Vancouver.

Leyendecker, Hunt, Frankel, and Rukstales (2000). "Development of Maximum Considered Earthquake Ground Motion Maps." *Earthquake Spectra*, 16(1), 21-40.

Lin, C. W. (1980). "Time history input deveopment for the seismic analysis of piping systems." *Journal of Pressure Vessel Technology*, Transactions of the ASME 102: 212-218.

Lin, Chopra, and De la Llera (2001). "Accidental Torsion in Buildings: Analysis versus Earthquake Motions." *Journal of Structural Engineering*, 127(5), 475-481.

Madsen (2008). "Time Series Analysis." Chapman & Hall/CRC, Boca Raton FL.

Naeim, Alimoradi, and Pezeshk (2004). "Selection and scaling of ground motion time histories for structural design using genetic algorithms." *Earthquake Spectra*, 20(2), 413-426.

Newmark, and Rosenblueth (1971). *Fundamentals of Earthquake Engineering*, Prentice-Hall Inc., Englewood Cliffs, NJ.

NISEE Pacific Earthquake Engineering Research (PEER) Center (2007). "The Earthquake Engineering Online Archive." <http://nisee.berkeley.edu/elibrary/>. (07/31/2010, 2010).

Ordoñez (2008). "SHAKE2000 A computer program for the 1-D analysis of geotechnical earthquake engineering problems User's Manual." Gustavo A. Ordonez.

Ordoñez (2008). "ShakEdit A pre and post processor for SHAKE and SHAKE91."

Parametric Technology Corporation (2007). "Mathcad 14.0 M011."

PEER (1999). "Pacific Earthquake Engineering Research Center: NGA Database." <http://peer.berkeley.edu/nga/>. (01/18, 2010).

Pollock (1999). "A Handbook of Time-Series Analysis, Signal Processing and Dynamics." Academic Press, London UK.

Santamarina, and Fratta (2005). *Discrete signals and inverse problems An Introduction for Engineers and Scientists*, John Wiley & Sons Ltd., Chinchester, England.

Schnabel, Lysmer, and Seed (1972). "SHAKE A computer program for earthquake response analysis of horizontally layered sites."Report No. UCB/EERC-72/12, Earthquake Engineering Research Center, University of California, Berkeley.

Shome, and Cornell "Normalization and Scaling Accelerograms for Nonlinear Structural Analysis." *Proc., 6th U.S. National Conference on Earthquake Engineering*.

Silva, and Lee (1987). "WES RASCAL Code for synthesizing earthquake ground motions." *State-of-the-art for assessing earthquake hazards in the United States* Report No.24 Miscellanous Paper S-73-1, US Army Engineer Waterways Experiment Station, Vicksburg, Mississippi.

Somerville, Anderson, Sun, Punyamurthula, and Smith (1998). "Generation of ground motion time histories for Performance-Based Seismic Engineering." *Proc., 6th U.S. National Conference on Earthquake Engineering*.

Spudich Paul, Steck Lee K., Hellweg Margaret, Fletcher Jon B., and Baker Lawrence M. (1994). "Transient stresses at Parkfield, California, produced by the M 7.4 Landers earthquake of June 28, 1992: implications for the time-dependence of fault friction." *Annali di Geofisica*, XXXVII(6).

Stewart, Chiou, Bray, Graves, Somerville, and Abrahamson (2001). "Ground motion evaluation procedures for performance-based design." P. E. E. R. Center, ed., University of California at Berkeley, Berkeley CA.

Tso, and Hsu (1978). "Torsional spectrum for earthquake motions." *Earthquake Engineering and Structural Dynamics*, 6(Compendex), 375-382.

U.S. Geological Survey (2006). "Notes on the processing of digitally recorded data." <http://nsmp.wr.usgs.gov/processing.html>. (11/17, 2010).

U.S. Geological Survey (2009a). "2008 Interactive Deaggregations." <http://eqint.cr.usgs.gov/deaggint/2008/index.php>. (03/25, 2010).

U.S. Geological Survey (2009b). "Seismic Hazard Curves, Response Parameters, and Design Parameters." U.S. Geological Survey.

Vanmarcke, Cornell, Gasparini, and Hou (1976, 1990). "SIMQKE-I Simulation of Earthquake Ground Motions." Department of Civil Engineering Massachusetts Institute of Technology, Cambridge, Massachusetts.

Vanmarcke, and Gasparini (1976). "SIMQKE A program for artificial motion generation." Department of Civil Engineering Massachusetts Institute of Technology, Cambridge, Massachusetts.

Willford, Whittaker, Klemencic, and Wood (2008). "Recommendations for the Seismic Design of High-rise Buildings." Council on Tall Buildings and Urban Habitat.

Wilson (2004). *Static & Dynamic Analysis of Structures*, Computers and Structures, Inc., Berkeley, CA.

Wilson, Suharwardy, and Habibullah (1995). "A Clarification of the Orthogonal Effects in a Three-Dimensional Seismic Analysis." *Earthquake Spectra*, 11(4), 659-666.

APPENDIXES

APPENDIX A: Description of analyzed buildings

APPENDIX B: Examples of application of scaling methods

APPENDIX C: Periods and translational and rotational masses of buildings analyzed with rigid diaphragms

APPENDIX D: Proposal of code language for linear response history analysis in ASCE7

APPENDIX E: Abbreviation List

Appendix A. Description of analyzed buildings

Building 1: Symmetric 8 story concrete building with moment resisting frames in both directions

Building 2: Nonsymmetrical 12 story steel building with perimeter moment frames and setbacks at levels 5 and 9

Building 3: Symmetric 8 story concrete building with dual system (shear walls and moment resisting frames) in the short direction and moment resisting frames in the Y direction

Building 4: Symmetric 9 story steel building with perimeter moment frames

Building 1: 8 story concrete building with Moment Resisting Frames

Parameter	Value	Units	Observation
Geometric description			
Number of stories	8		
Material	Concrete		f'c = 5ksi
Dimension in the long direction:	150	ft	5 bays equally spaced at 30 ft.
Dimension in the short direction:	80	ft	2 exterior bays of 30 ft. and an interior bay of 20 ft.
Height of the building	106	ft	
Height First floor	15	ft	
Height other floors	13	ft	Also a parapet of 6 ft.
Columns	28 x 28	in	Through all the building
Beams	20 x 30	in	Through all the building
Joists E-W	8 x 24	in	
Slab thickness	5	in	
Other modeling parameters			
Support conditions at base	Fixed		
Rigid end zone factor	0.5		
Shear area reduction factor for cracking	0.4		
Moment of inertia reduction factor for cracking	0.5		
Type of structural system	SMRF		N-S and E-W directions
Dead loads (DL) including superimposed dead loads			
Structural system	136.89	psf	All floors
Ceiling and Mechanical	15	psf	Levels 2 trough 8
Ceiling and Mechanical	20	psf	Roof level
Fixed partitions	10	psf	Levels 2 trough 8
Exterior cladding	35	psf	Excludes parapet
Parapet	60	psf	
Roofing	12	psf	
Total Dead Load	18983	kips	
Live loads			
Roof	20	psf	
Other floors	50	psf	

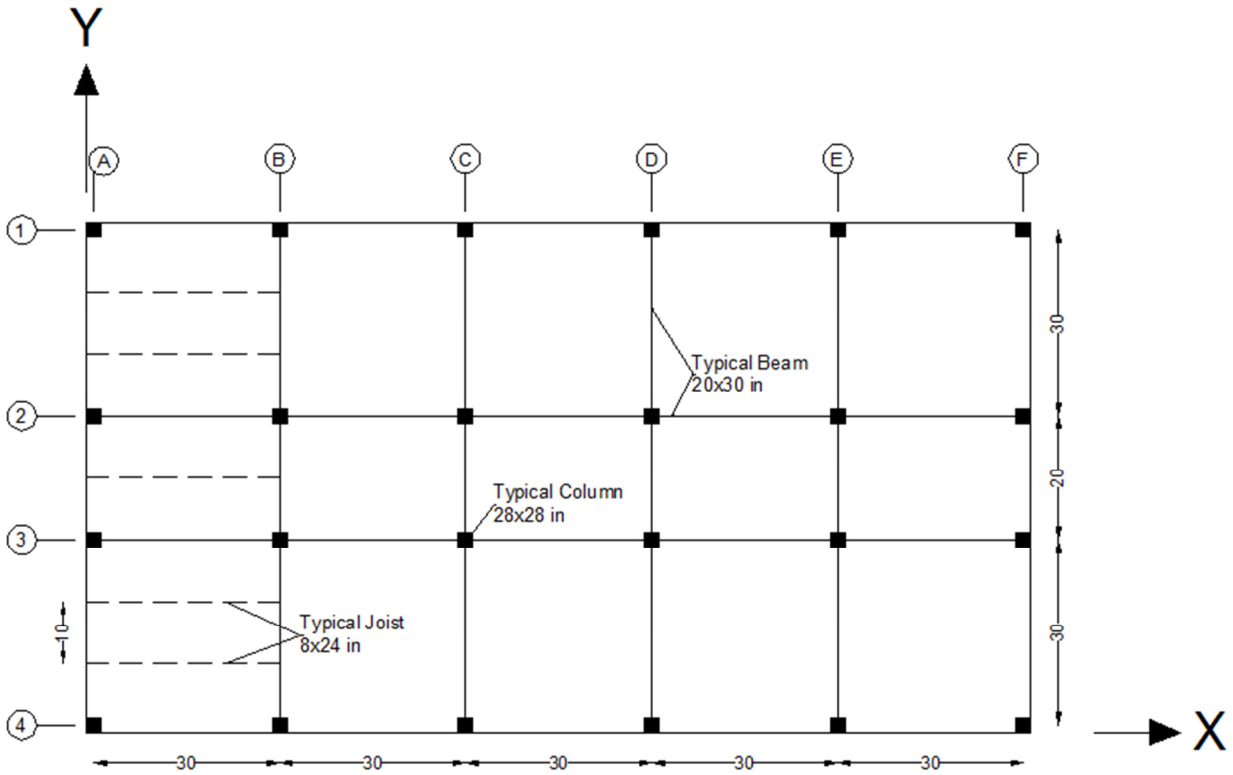

Figure A- 1 Plan view of Building 1 at all levels

Building 2: 12 story steel building with perimeter moment frames

Parameter	Value	Units	Observation
Geometric description			
Number of stories	12		
Material	Steel		fy = 50ksi
Dimension in the long direction:	210	ft	7 bays equally spaced at 30 ft.
Dimension in the short direction:	175	ft	7 bays equally spaced at 25 ft.
Height of the building	155.5	ft	
Height First floor	18	ft	
Height other floors	12.5	ft	
Basement			
Height basement	18	ft	
Thickness walls basement	1	ft	
Columns	Variable	in	
Beams	Variable	in	
Slab Thickness			
Levels G,5,9	6	in	Average value
Other Levels	4	in	
Other modeling parameters			
Support conditions at base			
Columns part of the SMRF	Fixed		
Columns not part of the SMRF	Pinned		
Type of structural system	SMRF		Located only at the perimeter
Dead loads (DL) including superimposed dead loads			
Refer to Table 4.1-1 of Charney et al. (2010)			
Total Dead Load (without including slab at ground level and basement)	30392	kips	
Live loads			
Roof	20	psf	
Other floors	20	psf	

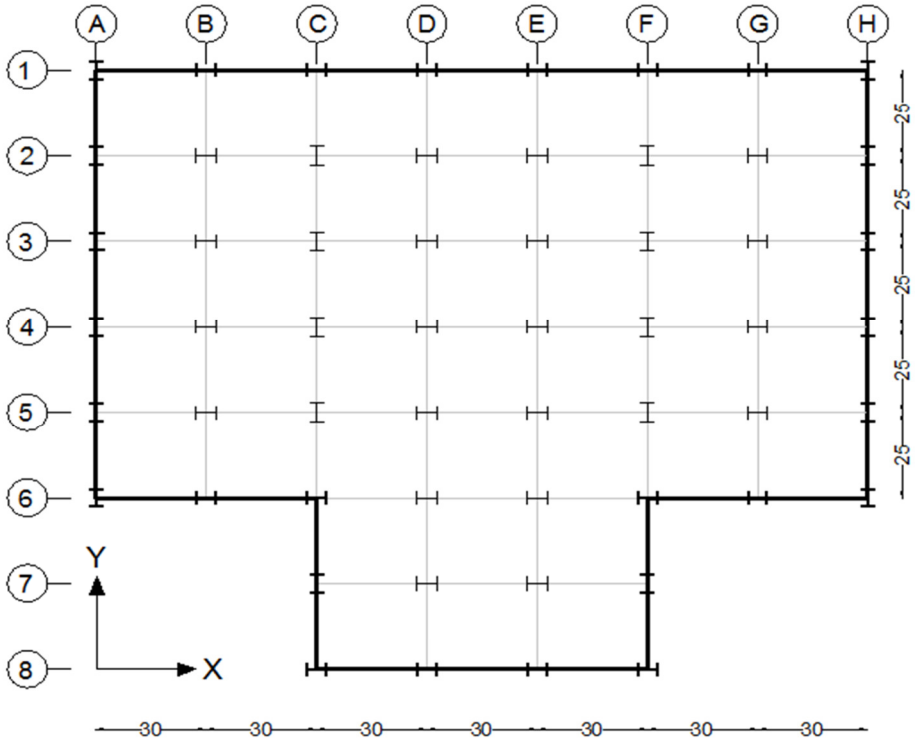

Figure A- 2 Plan view of Building 2 for Levels G, 2, 3, 4*

*Only the thick lines represent SMRF.

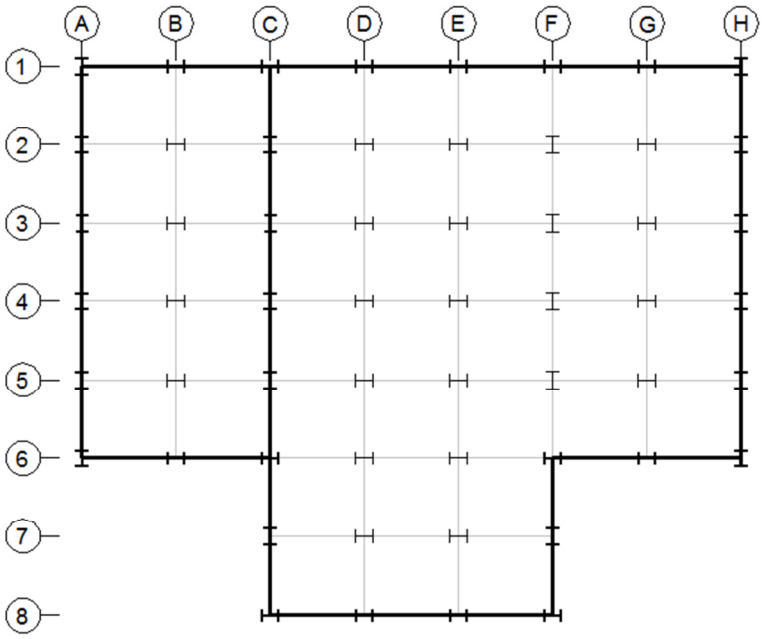

Figure A- 3 Plan view of Building 2 for Level 5

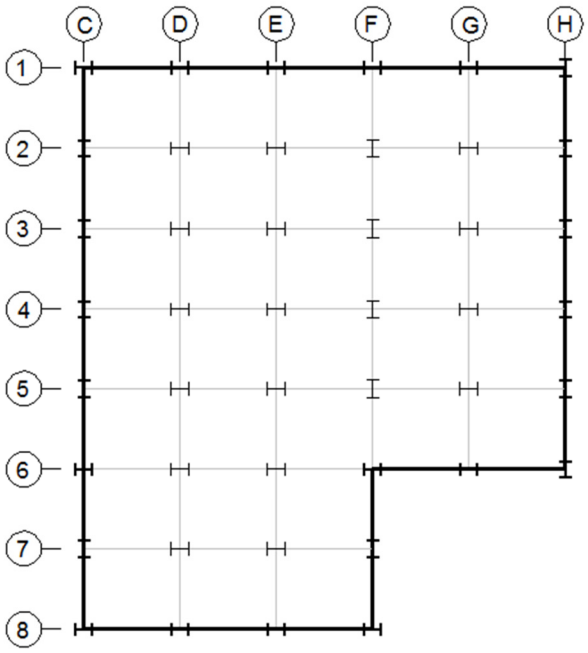

Figure A- 4 Plan view of Building 2 for Levels 6, 7, 8

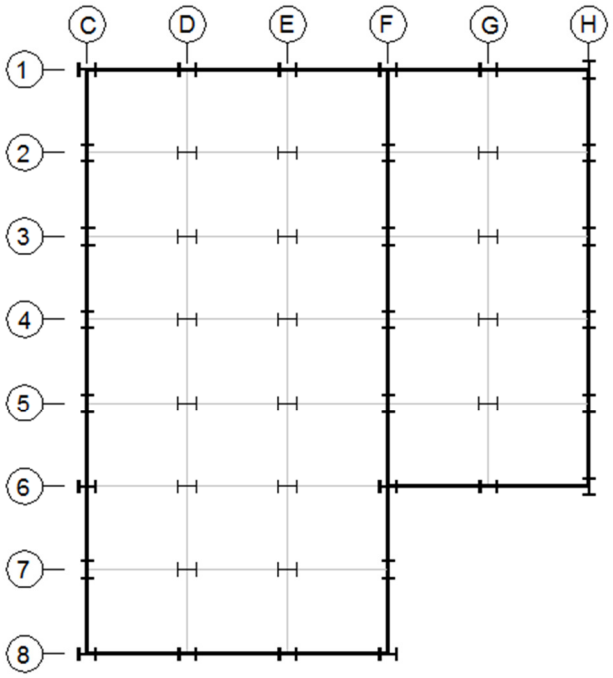

Figure A- 5 Plan view of Building 2 for Level 9

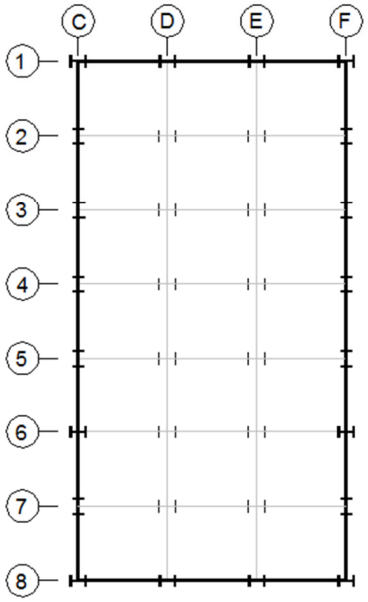

Figure A- 6 Plan view of Building 2 for Levels 10, 11, 12, Roof

Building 3: 8 story concrete building with shear walls

Parameter	Value	Units	Observation
Geometric description			
Number of stories	8		
Material	Concrete		f'c = 5ksi
Dimension in the long direction:	150	ft	5 bays equally spaced at 30 ft.
Dimension in the short direction:	80	ft	2 exterior bays of 30 ft. and an interior bay of 20 ft.
Height of the building	106	ft	
Height First floor	15	ft	
Height other floors	13	ft	Also a parapet of 6 ft.
Columns	28 x 28	in	Through all the building
Beams	20 x 30	in	Through all the building
Joists E-W	8 x 24	in	
Slab thickness	5	in	
Other modeling parameters			
Support conditions at base	Fixed		
Rigid end zone factor	0.5		
Shear area reduction factor for cracking	0.4		
Moment of inertia reduction factor for cracking	0.5		
Type of structural system	Y direction: Dual system X direction: Moment Frame		
Dead loads (DL) including superimposed dead loads			
Structural system	155	psf	All floors
Ceiling and Mechanical	15	psf	Levels 2 trough 8
Ceiling and Mechanical	20	psf	Roof level
Fixed partitions	10	psf	Levels 2 trough 8
Exterior cladding	35	psf	Excludes parapet
Parapet	60	psf	
Roofing	12	psf	
Total Dead Load	20891	kips	

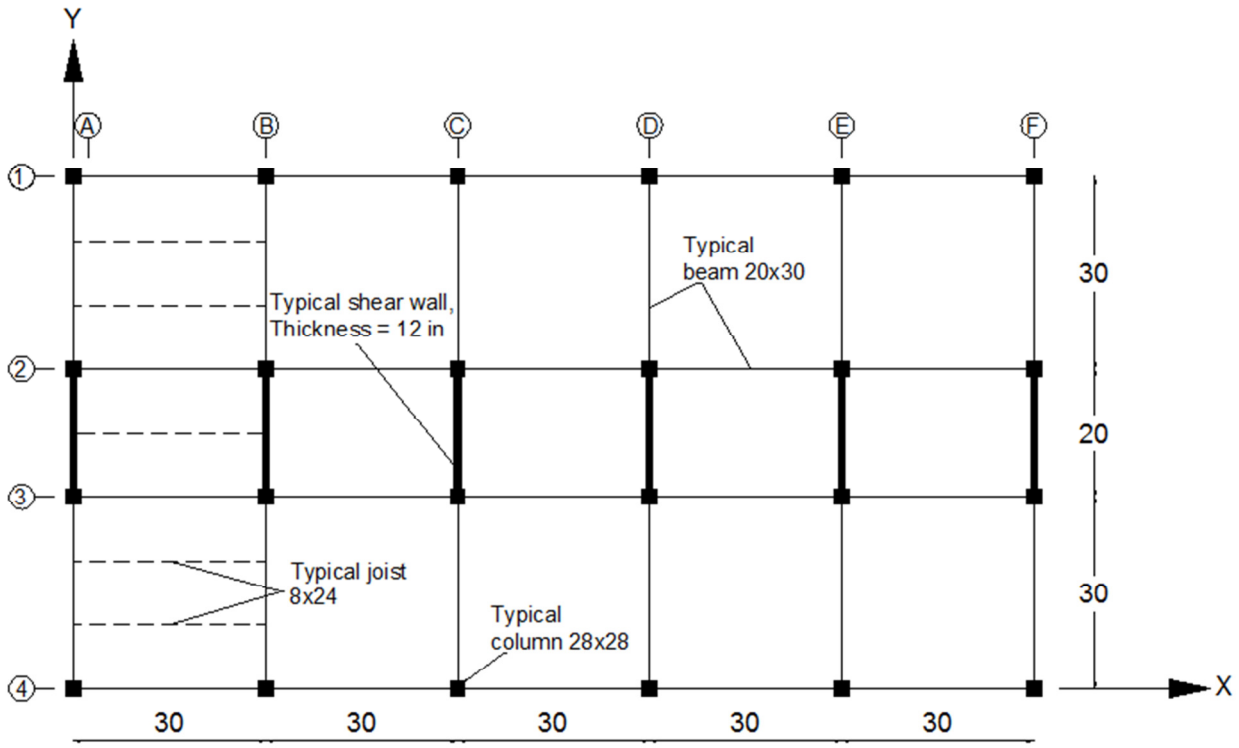

Figure A- 7 Plan view of Building 3 at all levels

Notes on Building 3:

Building 3 has very similar characteristics than those of Building 1, and it only differs in the structural system resisting lateral load in the Y direction, the dead load of the structural system, and therefore the total dead load.

Building 4: 9 story steel building with perimeter moment frames

Parameter	Value	Units	Observation
Geometric description			
Number of stories	9		
Material	Steel		fy = 50ksi
Dimension in the long direction:	150	ft	5 bays equally spaced at 30 ft.
Dimension in the short direction:	80	ft	2 exterior bays of 30 ft. and an interior bay of 20 ft.
Height of the building	122	ft	(without including the basement)
Height Basement	12		
Height First floor	18	ft	
Height other floors	13	ft	Also a parapet of 6 ft.
Columns	As shown in Table below		
Beams			
Joists E-W			
Slab thickness	5.5		3 in metal deck and 2.5 in of concrete
Other modeling parameters			
Support conditions at base	Fixed		All columns
Type of structural system	Perimeter Moment Frames		Both directions
Dead loads (DL) including superimposed dead loads			
Structural system	66	psf	All floors
Ceiling and Mechanical	10	psf	All levels
Fixed partitions	10	psf	Levels 2 trough 8
Exterior cladding	25	psf	Excludes parapet
Parapet	3.5	ft	
Roofing	7	psf	
Total Dead Load	20079	kips	

Story/Floor	Perimeter moment resisting frames			Gravity frames	
	Columns		Girder	Columns	Beams
	Exterior	Interior			
-1/1	W14x370	W14x500	W36x150	W14x193	W18x35
1/2	W14x370	W14x500	W36x150	W14x193	W16x26
2/3	W14x370, W14x370	W14x500, W14x455	W36x150	W14x193, W14x145	W16x26
3/4	W14x370	W14x455	W33x141	W14x145	W16x26
4/5	W14x370, W14x283	W14x455, W14X370	W33x141	W14x145, W14x109	W16x26
5/6	W14x283	W14X370	W33x141	W14x109	W16x26
6/7	W14x283, W14x257	W14X370, W14X283	W33x130	W14x109, W14x82	W16x26
7/8	W14x257	W14X283	W27x102	W14x82	W16x26
8/9	W14x257, W14x233	W14X283, W14X257	W27x94	W14x82, W14x48	W16x26
Roof	W14x233	W14X257	W24x62	W14x48	W14x22

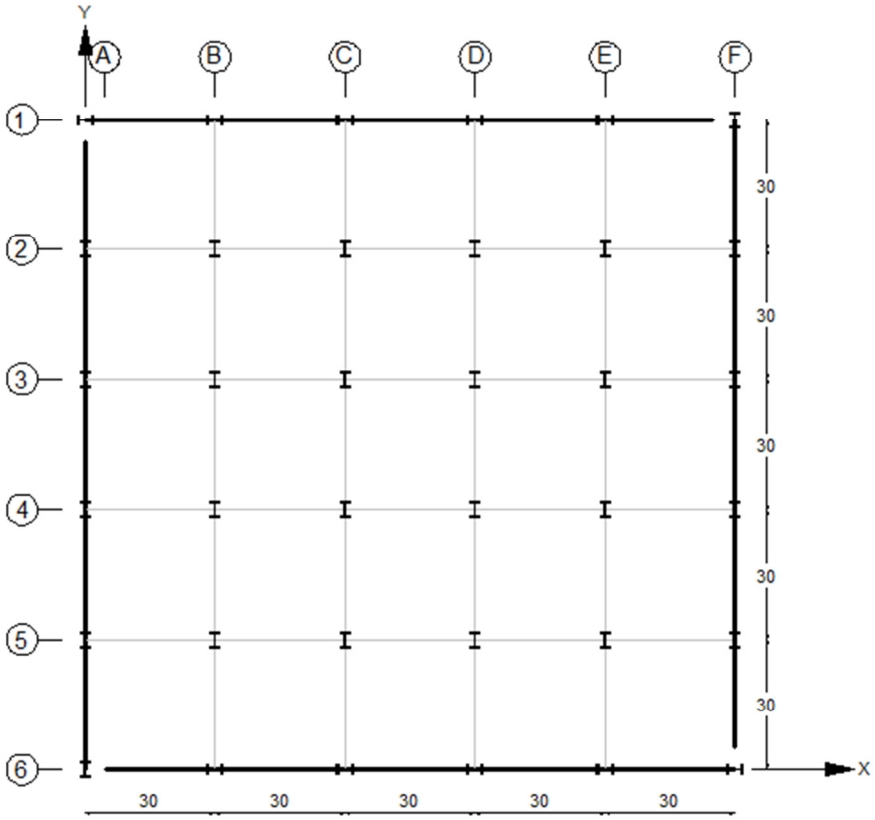

Figure A- 8 Plan view of Building 4

Notes on Building 4:

The loads for Building 4 as well as the geometry were taken from the 9th story building for Los Angeles which is part of the buildings from the SAC Project (Krawinkler Helmut, 002000)..

Appendix B. Examples of application of scaling methods

Example 1: Scaling of three ground motions using the method developed by Finley A. Charney (2010a)

Example 2: Scaling of seven ground motions using the method developed by Finley A. Charney (2010a)

Example 3: Scaling of three ground motions using the New Zealand Standard NZS 1170.5 (2004b)

Example 4: Selection and scaling of ground motions using the new suggested method in Section 3.4

Example 1

Scaling of three ground motions using the method developed by Finley A. Charney (2010a)

This section describes a step by step procedure for the scaling of ground motions using the method developed by Charney (2010a) which was explained in Section 3.1.2 of this document. The ground motions to be scaled as well as the target spectrum correspond to the ones used by Charney et al. (2010b) in the analysis of a twelve story building. The parameters that define the target spectrum, the corresponding plot of the target spectrum, and the set of records used in the analysis are shown in Table 2-5, Figure 2-4, and Table 2-6, respectively, and the horizontal components A00 and A90, B00 and B90, C00 and C90, of Table 2-6 are denoted as A1 and A2, B1 and B2, and C1 and C2, respectively. Furthermore, the periods of vibration used for this scaling example corresponds also to the building analyzed by Charney et al. (2010b), and the details of such building, denoted Building 2, can be found in the Appendix A.

The steps to apply this scaling technique are described below.

Step 1: Calculation of 5% damped spectrum for each component and their SRSS

Figure B- 1, Figure B- 2, and Figure B- 3 show these spectra for the earthquakes A, B, and C, respectively.

Step 2: Determine the period of vibration in each direction analyzed

The building analyzed by Charney et al. (2010b) has different periods in both principal direction, and those periods are T=2.87 sec and T=2.60 sec for the X and Y directions (see Figure A- 2).

Having two different periods in each direction can possibly yield different scale factors in each direction because the range of periods, as defined in the next step, would be different for the two principal directions; therefore, an average of these two values can be used for scaling procedures. Then, T = (2.87+2.60)/2 = 2.74 sec.

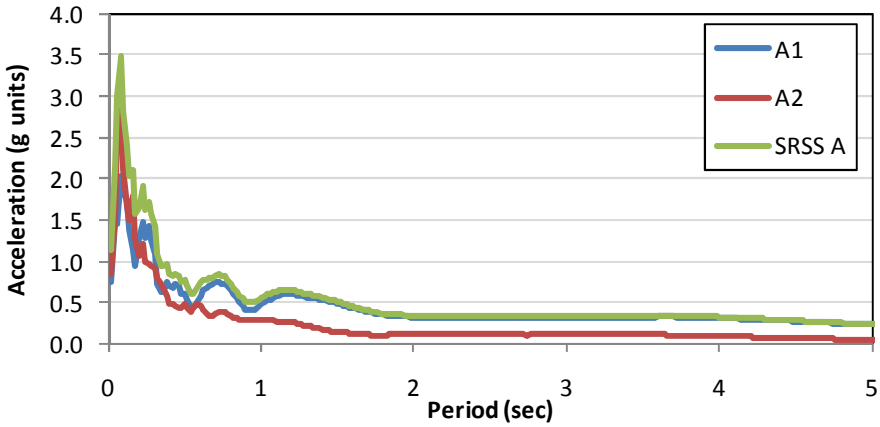

Figure B- 1 Original Spectra and SRSS of horizontal components of Record A

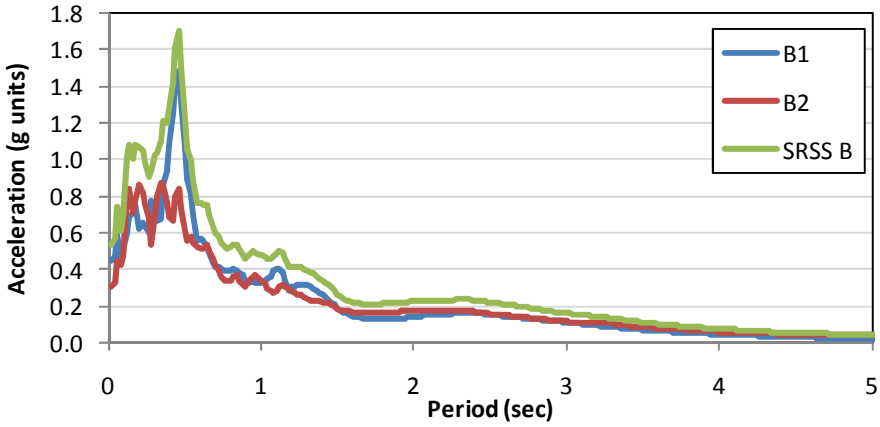

Figure B- 2 Original Spectra and SRSS of horizontal components of Record B

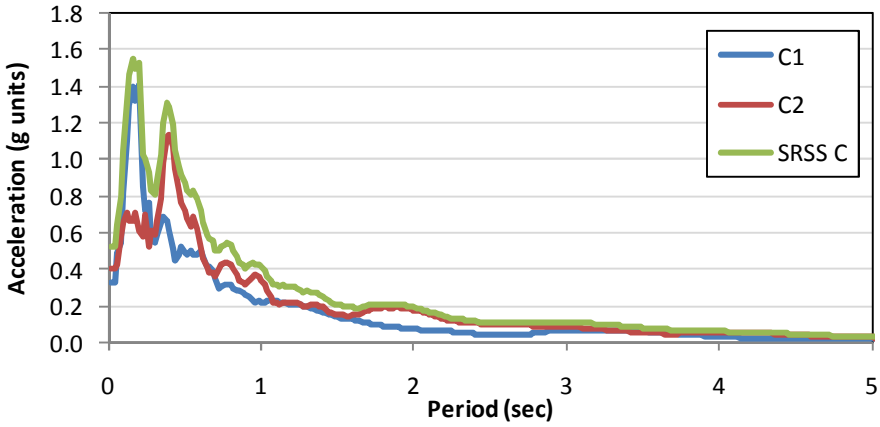

Figure B- 3 Original Spectra and SRSS of horizontal components of Record C

Step 3: Calculation of the period range of interest

The lower and upper limits of the period range of interest are given are defined by 0.2*T* and 1.5*T*, respectively, where *T* is fundamental period of vibration in the direction analyzed. Then, these limits are equal to:

Lower limit = 0.2*2.74 = 0.548 sec.

Upper limit = 1.5*2.74 = 4.110 sec.

Step 4: Calculation of the Fundamental Period Scale Factor *FPS*

This step calculates the fundamental period scale factor as explained in Section 3.1.2. This factor is calculated as the ratio of the spectral ordinate of the design spectrum at the period *T*, and the spectral ordinate of the SRSS spectrum of the i^{th} earthquake at the same period. The calculations are shown in Table B- 1.

Table B- 1 Calculation of the Fundamental Period Scale Factor using the scaling ground motion method suggested by Charney

Earthquake	Spectral ordinate of the SRSS spectra at *T*=2.72 sec (g units)	Target spectral ordinate at *T*=2.74 sec from design spectrum (g units)	Fundamental Period Scale Factor (*FPS*)
A	0.335	0.136	0.406
B	0.191	0.136	0.712
C	0.104	0.136	1.308

Step 5: Calculate the average SRSS spectrum from the individual SRSS spectra already scaled by the factor *FPS*

The next step is to calculate the average SRSS spectrum from the individual SRSS spectra of each record already scaled by the factor *FPS*. This way, the average scaled SRSS spectrum is given by:

$$Average \quad scaled \quad SRSS = \frac{SRSS_A FPS_A + SRSS_B FPS_B + SRSS_C FPS_C}{3} \quad \textbf{Eq. B- 1}$$

where $SRSS_A$ is the SRSS spectrum from the earthquake A

$SRSS_B$ is the SRSS spectrum from the earthquake B

$SRSS_C$ is the SRSS spectrum from the earthquake A

FPS_A is the Fundamental period scale factor of earthquake A

FPS_B is the Fundamental period scale factor of earthquake B

FPS_C is the Fundamental period scale factor of earthquake C

The plot of the average scaled SRSS is shown in Figure B- 4 together with the target spectrum.

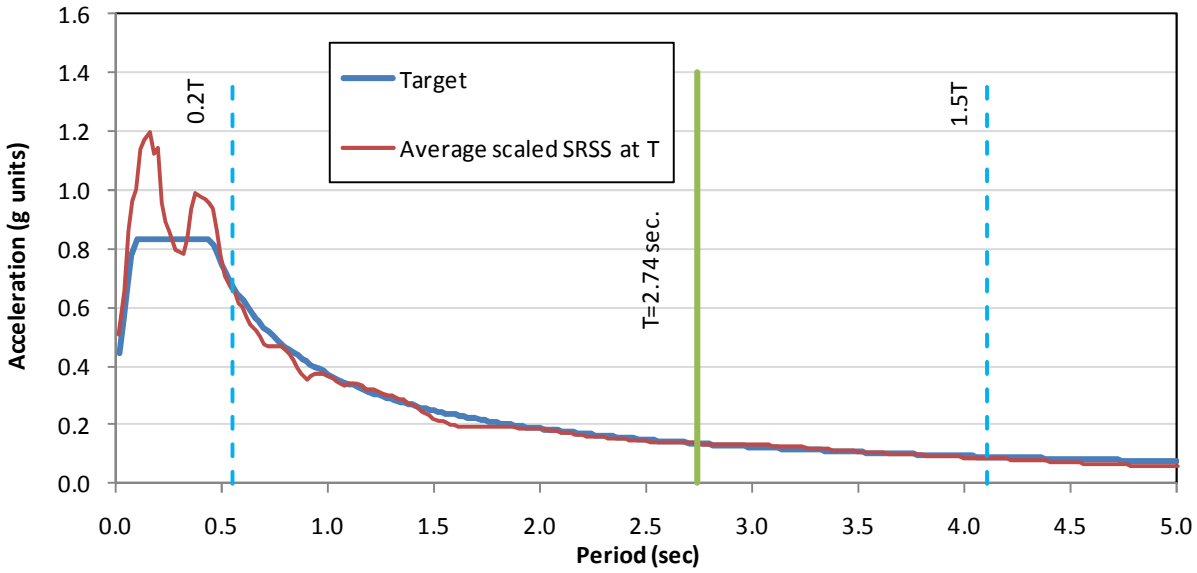

Figure B- 4 Average scaled SRSS spectrum and Target spectrum, for the scaling ground motion method suggested by Charney

Step 6: Calculate the Set Scale factor *SS*

From Figure B- 4 it can be noticed that the average scaled SRSS spectrum is below the target spectrum in many periods within the period range of interest which is defined by the vertical lines at $0.2T$ = 0.548 sec and at $1.5T$ = 4.11 sec. The next step is to calculate the set scale factor, denoted *SS*, such that the average scaled SRSS spectra multiplied by the factor *SS* yields a spectrum whit ordinates above the target spectrum at any period within the limits $0.2T$ and $1.5T$.

The factor *SS* can be obtained by calculating the maximum ratio between the ordinates of the target spectrum and the ordinates of average scaled SRSS spectrum (Eq. B-1) within the period range of interest. Such factor *SS* was calculated as 1.184, and the plot of the target spectrum and the average scaled SRSS spectrum modified by the factor *SS* is shown in Figure B-5 where it can be seen that all the ordinates of the average scaled SRSS spectrum modified by *SS* are now above the target spectrum in the period range of interest.

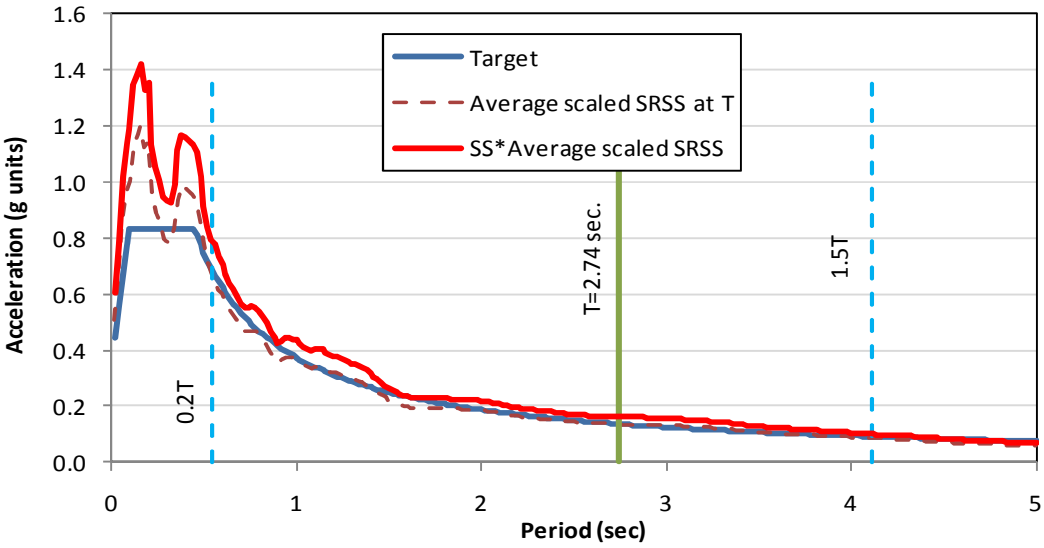

Figure B- 5 Average scaled SRSS spectrum modified by the factor *SS* and Target spectrum, for the scaling ground motion method suggested by Charney

Step 7: Calculation of final scale factors as the product of the factors *FPS* and *SS*

The last step is to calculate the final scale factors which are given by the product of the record scale factor *FPS*, and the set family factor, *SS*. The results are shown in Table B- 2.

Table B- 2 Final scale factors using the method suggested by Finley A. Charney

Record	Factor *FPS*	Factor *SS*	Final scale Factor
A	0.406	1.184	0.481
B	0.712	1.184	0.843
C	1.308	1.184	1.548

These results were calculated using a routine developed in the software Mathcad (Parametric Technology Corporation, 2007), and they were compared with the values calculated

using the software EQTools (Charney and Syed, 2004, 2010). Both procedures use the piecewise exact method to calculate the spectra. The scale factors obtained using EQTools for the records A, B, and C were 0.477, 0.839, and 1.522, respectively, and it can be seen that the results of both procedures yield very similar results.

Example 2

Scaling of seven ground motions using the method developed by Finley A. Charney (2010a)

The method suggested by Charney (2010a) was also applied to the scaling of a set of seven records that were selected from the NGA database (PEER, 1999) considering the following target conditions:

Magnitude:	6.0 – 8.0
Fault Mechanism:	Reverse (Type 2) or Reverse Oblique (Type 3)
Distance from epicenter:	19 km. – 100 km.
Soil Type:	Class C

Table B- 3 lists the selected earthquakes with their characteristics of magnitude, source mechanism, and distance from hypocenter, and all of them were recorded in soil type C. Additionally, a source mechanism type 2 and type 3 indicates a reverse mechanism and a reverse oblique mechanism, respectively.

Table B- 3 Set of seven earthquakes for an example of scaling ground motions using the method suggested by Finley A. Charney

Record	NGA Number	Earthquake name	Station name	Magnitude	Source Mechanism	Distance from Epicenter (km)
A	14	Kern County	Santa Barbara Courthouse	7.36	2	88.39
B	125	Friuli, Italy-01	Tolmezzo	6.50	2	20.23
C	139	Tabas, Iran	Dayhook	7.35	2	20.63
D	802	Loma Prieta	Saratoga - Aloha Ave	6.93	3	27.23
E	827	Cape Mendocino	Fortuna - Fortuna Blvd	7.01	2	29.55
F	1504	Chi-Chi, Taiwan	TCU067	7.62	3	28.70
G	1529	Chi-Chi, Taiwan	TCU102	7.62	3	45.56

The target spectrum is the same spectrum used in the Example 1, and its information is described in Table 2-5 and Figure 2-4. Also, this scaling example is intended to be applied in the design of a structure with an arbitrary fundamental period of vibration equal to T=2 sec which

represents the average of the fundamental periods of vibration in the two principal directions of such structure.

The methodology used in this example is the same as the one described in the Example 1; however, the scale factors were obtained using two independent procedures; the first of them consisted in a small program using the software Mathcad (Parametric Technology Corporation, 2007), and the second one consisted in the use of the software EQTools (Charney and Syed, 2004, 2010). The first of these procedures uses the central difference method as the technique to calculate the spectra while the second procedure uses the piecewise exact method. The resulting scaling factors using the first and second procedures are shown respectively in Table B- 4 and Table B- 5, where *FPS* is the Fundamental Period Scale factor and *SS* is the Set Scale factor (see Section 3.1.2 and Example 1 for definition of these factors).

Table B- 4 Scale factors using a routine developed in the software Mathcad

Record	*FPS*	*SS*	Scale Factor
A	1.188	1.193	1.417
B	2.185	1.193	2.607
C	0.965	1.193	1.151
D	0.575	1.193	0.686
E	0.996	1.193	1.188
F	0.325	1.193	0.388
G	0.276	1.193	0.329

Table B- 5 Scale Factors using the software EQTools

Record	*FPS*	*SS*	Scale Factor
A	1.191	1.181	1.407
B	2.188	1.181	2.584
C	0.968	1.181	1.143
D	0.576	1.181	0.680
E	0.994	1.181	1.174
F	0.324	1.181	0.383
G	0.276	1.181	0.326

From the tables above it can be seen that the scale factors are very similar for both procedures with a maximum difference of 1.33% in the results of Table B- 4 compared to those in Table B- 5. The differences in the described two procedures are due to the technique used to calculate the spectra and the number of points in which the period range of interest is divided.

Example 3
Scaling of three ground motions using the New Zealand Standard NZS 1170.5 (2004)

This section describes a step by step procedure for the scaling of ground motions as given by Section 5.5 of the New Zealand Standard NZS 1170.5 (Council of Standards New Zealand, 2004). The parameters that define the target spectrum, the corresponding plot of the target spectrum, and the set of records used in the analysis are shown in Table 2-5, Figure 2-4, and Table 2-6, respectively, and they correspond to the same target and ground motions used in the Example 1 of this Appendix. Also, as explained in the first paragraph of the Example 1, the horizontal components of the three earthquakes of Table 2-6 are denoted A1 and A2, B1 and B2, and C1, and C2 in correspondence with the components A00 and A90, B00 and B90, and C00 and C90, respectively. Moreover, the periods of vibration used in this example corresponds to the building analyzed by Charney et al. (2010b), and they are specified in the Step 2 of Example 1.

The NZS requires seven steps to apply its scaling procedure, and the third step includes 8 sub-steps. The application of this procedure is describe below.

Step 1: Calculation of the target spectrum

This step refers to the calculation of the target spectrum according to the NZS; however, for this example the target spectrum is already given by Table 2-5 and Figure 2-4, and it is based on the ASCE 7-05 provisions.

Step 2: Calculation of 5% damped spectrum for each component

The NZS states to "Calculate the 5% damped spectrum, $SA_{component}$, of each component of each ground motion record within the family of records being considered", and the plot of these spectra for the records A, B, and C is shown in Figure B- 1, Figure B- 2, and Figure B- 3, respectively.

Step 3: Determine the principal component and associated record scale factor

The third step requires to "Determine the principal component, $SA_{principal}$, and associated record scale factor for each direction in which the records are to be applied by:" This calculation is done with eight separate steps as described below.

i) "Determining the structure orientation relative to the direction selected."

For simplicity this example does not consider different angles of attack of the ground motions; however, this step should be analyzed carefully, especially for structures where the seismic hazard is defined by near field earthquakes because in this case the realistic orientation of the structure relative to the fault and the directivity effects play an important role in the response of the structure.

ii) **"Determine the largest translational period, T_1, of the response mode in the direction of interest."**

The fundamental period of vibration to be used in this example is T_1 = 2.74 sec due to observations done in Step 2 of Example 1.

iii) "Calculate the period range of interest, T_{range} , as being between T_{min} and T_{max} where $T_{min} = 0.4T_1$ and $T_{max} = 1.3T_1$ and where T_1 is the largest translational period in the direction being considered but not less than 0.4 sec."

The range of periods $0.4T_1$ and $1.3T_1$ can vary according to the fundamental periods in each direction. The Section C6.4.3 of the commentary to the NZS (Council of Standards New Zealand, 2004b) states that the lower limit could be obtained using the smaller of the two fundamental periods while the upper limit could be obtained using the bigger of the fundamental periods. However, for this exercise the upper and lower limit will be calculated using the average value of T_1 as calculated in the previous step. This way, the limits of the period range of interest are given by:

Lower limit = 0.4*2.74 = 1.096 sec.

Upper limit = 1.3*2.74 = 3.562 sec.

iv) "Select records that have a seismological signature (i.e. magnitude, source characteristics (including fault mechanism) and source to site distance) the same as (or reasonable consistent with) the signature of the site."

The selected ground motions used by Charney et al. (2010b) were chosen so that the appropriate combination of the spectra of those ground motions (according to ASCE 7-05) would be reasonably similar to the target spectrum, especially in the region that includes the periods of interest; however, they do not come from a detailed seismic hazard analysis using magnitude, fault distance or source mechanism appropriate for the site of interest because the focus of Charney et al. was the scaling procedure itself.

v) "Determine the record scale factor, k_1, for each of the horizontal ground motion components where k_1 = scale value which minimizes in a least mean square sense the function $\log(k_1 SA_{component}/SA_{target})$ over the period range of interest.
In each case the periods used to determine k_1 are to be selected so that each period is within 10% of the preceding one, except that an increment not greater than 1 second may be used for periods greater than 5 seconds."

The periods for this example were generated so that the difference between two adjacent periods would be 5% within the period range of interest; 26 periods were generated at this stage, and the values are shown in Table B- 6. It can be noticed in this Table that the first and last periods of Table B- 6 correspond to the lower and upper limit of the period range of interest as calculated in the in the sub-step iii).

Table B- 6 Periods used for the calculation of factor k_1 using the scaling of ground motion procedure given by the New Zealand Standard

Period	Difference in two adjacent periods	Period	Difference in two adjacent periods
(sec)	(%)	(sec)	(%)
1.096		2.067	5.00
1.151	5.00	2.170	5.00
1.208	5.00	2.279	5.00
1.269	5.00	2.392	5.00
1.332	5.00	2.512	5.00
1.399	5.00	2.638	5.00
1.469	5.00	2.770	5.00
1.542	5.00	2.908	5.00
1.619	5.00	3.053	5.00
1.700	5.00	3.206	5.00
1.785	5.00	3.366	5.00
1.875	5.00	3.535	5.00
1.968	5.00	3.562	0.77

The value of k_1 for each record was obtained by developing a curve k vs. F(k) for each ground motion where k was an arbitrary scale factor and F(k) was the function given by:

$$F(k) = \sum_{i=1}^{n} \left[log\left(\frac{k_i * SA_{component_i}}{SA_{target_i}} \right) \right]^2 \qquad \textbf{Eq. B- 2}$$

The value of k was varied between 0.33 and 3.0 with increments of 0.01, and this was done because the limits of the factor k_1, as stated by the NZS, are 0.33 and 3.0; then, k_1 was taken as the value of k that minimized the function F(k). Also, the function F(k), denoted hereafter F, was evaluated only at periods within the range of interest ($0.4T_1$ to $1.3T_1$).

The plots of the function F(k), denoted hereafter F, against different values of k are shown in Figure B- 6, Figure B- 7, and Figure B- 8 for the horizontal components of the records A, B, and C, respectively. Also, Table B- 7 sumarizes the scale factors k that minimized the function F for each component of each earthquake. It should be noticed that this sub-step calculates a different factor k_1 for each component of an earthquake; however, the factor k_1 has to

be unique for both components, and the calculation such factor k_1 for each record is stated in the substep viii).

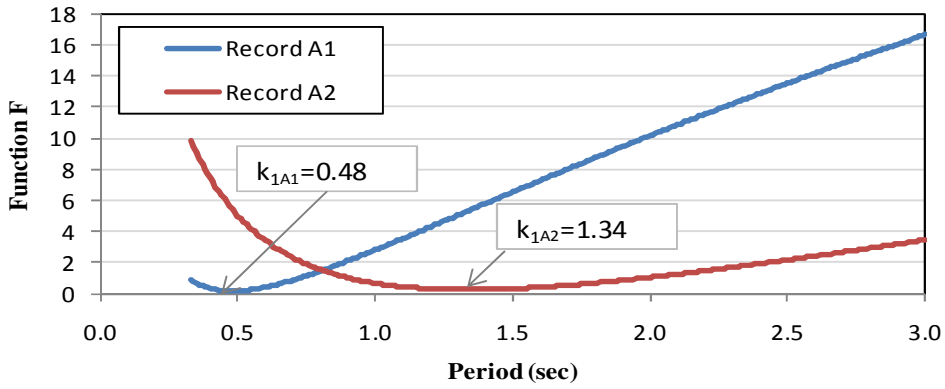

Figure B- 6 Calculation of factor k_1 for horizontal components of Earthquake A

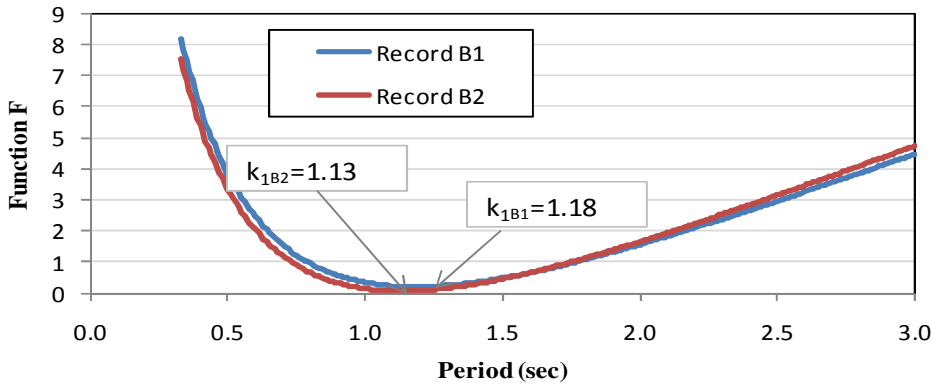

Figure B- 7 Calculation of factor k_1 for horizontal components of Earthquake B

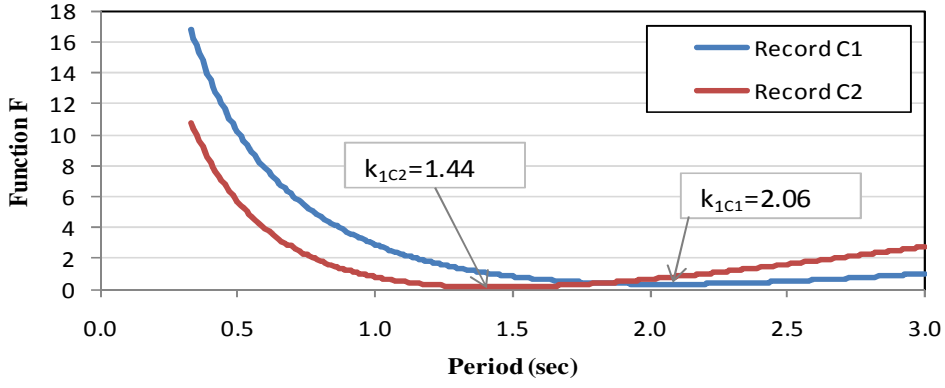

Figure B- 8 Calculation of factor k_1 for horizontal components of Earthquake C

Table B- 7 Factor k_1 for each earthquake component within the period range of interest

Earthquake component	Factor k_1
A1	0.48
A2	1.34
B1	1.18
B2	1.13
C1	2.06
C2	1.44

vi) "Verify that the amplitude of the selected records is sufficiently similar by confirming that $0.33<k_1<3.0$. Reject records that do not satisfy this criteria."

As shown in Table B- 7, all the record components have a k_1 factor within the allowable limits.

vii) "Verify that the record selected is of reasonable fit to the targt spectra. This can be demonstrated by it satisfying the requirement that D_1, being the root mean square difference between the logs of the scaled primary component and the target spectra over the period range of interest, is less than log(1.5). Reject records that are not of reasonable fit."

The formula to calculate D_1 is specified in Section C5.5.2 of the NZS, and it specifies that the range of interest for the calculation of D_1 is between $0.4T$ and $1.5T$. An equivalent formula to calculate D_1 is given by:

$$D_1 = \sqrt{\frac{\sum_{0.4T_1}^{1.5T_1}\left[log\left(\frac{k_1 * SA_{component}}{SA_{target}}\right)\right]^2 * \Delta T}{(1.5-0.4)*T_1}} \qquad \textbf{Eq. B- 3}$$

where D_1= Factor used to compare the fitness between the target spectrum and the spectrum from the each component of each record

T_1= Fundamental period of vibration of the structure in the direction analyzed.

ΔT = Period step between two adjacent periods.

The values of D_1 for each component of ground motion are shown in Table B- 8, and it can be seen that all the values selected are less than log(1.5) which is equal to 0.176. Therefore, the records selected are appropriate.

Table B- 8 Parameter D_1 for each earthquake component

Earthquake component	D_1
A1	0.107
A2	0.107
B1	0.105
B2	0.062
C1	0.112
C2	0.084

viii) "Nominate the principal component as being the record component with the smaller k_1 value and assign this value to k_1 as the record scale factor for this target period T. The other component of the record is considered to be the secondary component."

The record scale factor k_1 was obtained using the infrmation of Table B- 7, and the results are shown in Table B- 9 where it is also identified the principal component of each record.

Table B- 9 Record scale factor k_1 for each earthquake

Earthquake	Principal component	Factor k_1
A	A1	0.48
B	B2	1.13
C	C2	1.44

Although the calculation of the record scale factor k_1 seems to be straight forward, a doubt arises about the identification of the principal component of each record based on the smaller k_1 value of its individual components. The doubt arises because it is the opinion of the author that the principal component is such that it reflects the component with less modification (either amplification or reduction) from its original shape. Then, if that is the case, the fact of

chosing the component with smaller k_1 would not guarantee the selection of the component with smaller modification from the original record. For instance, if the scale factor k_1 of the two components of a record are equal to 0.2 and 1.2 then the designer would choose as the principal component the one associated with the factor 0.2. However, it should be noticed that a scale factor of 0.2 indicates a de-amplification of the original record equal to 1/0.2 = 5 times, while the other component would be only amplified 1.2 times. Then it should be more reasonable to choose the component with the factor 1.2 as the principal component. This way, a better procedure to identify the principal component would consist in calculating an "effective modification factor" of the record which would be equal to 1 if k_1 is bigger than 1, and $1/k_1$ for k_1 less than 1; then, the component with the lowest effective modification factor would be assigned as the principal component.

Nevertheless, for this example it was followed the NZS regulations, and the principal component was defined as the one with the lowest value of k_1 with the results shown in Table B-9.

Step 4: Determine the record scale factor k_2

The NZS uses the following code language for the calculation of k_2:

"Determine the record family factor, k_2, which is required to ensure that for every period in the period range of interest, the principal component of at least one record spectrum scaled by its record scaled factor k_1, exceeds the target spectrum.

The record family scale factor k_2, is the maximum value of the ratio $SA_{target}/max(SA_{principal})$ but at least 1.0 over the period range of interest for the direction under consideration and $max(SA_{principal})$ is the maximum principal component of each record within the family at each period considered."

The procedure to calculate the scale factor k_2 includes two steps; first, an individual factor k_2 is calculated for each record so that their scaled principal component (from Table B- 9) would be above the target spectrum within the period range of interest ($0.4T_1$ to $1.3T_1$). Then, the family factor k_2 is calculated as the smallest of the individual factors k_2 for the principal component of each record.

The individual factors k_2 are shown in Table B- 10, and the spectrum of the principal components already multipplied by their own k_1, and modified additionally by their individual

factor k_2 is shown in Table B- 9, where it can be seen that each record is above the target spectrum within the period range of interest as it was expected.

Table B- 10 Factor k_2 for individual records

Earthquake	Principal component	Factor k_2 for each earthquake
A	A1	1.231
B	B2	1.239
C	C2	1.443

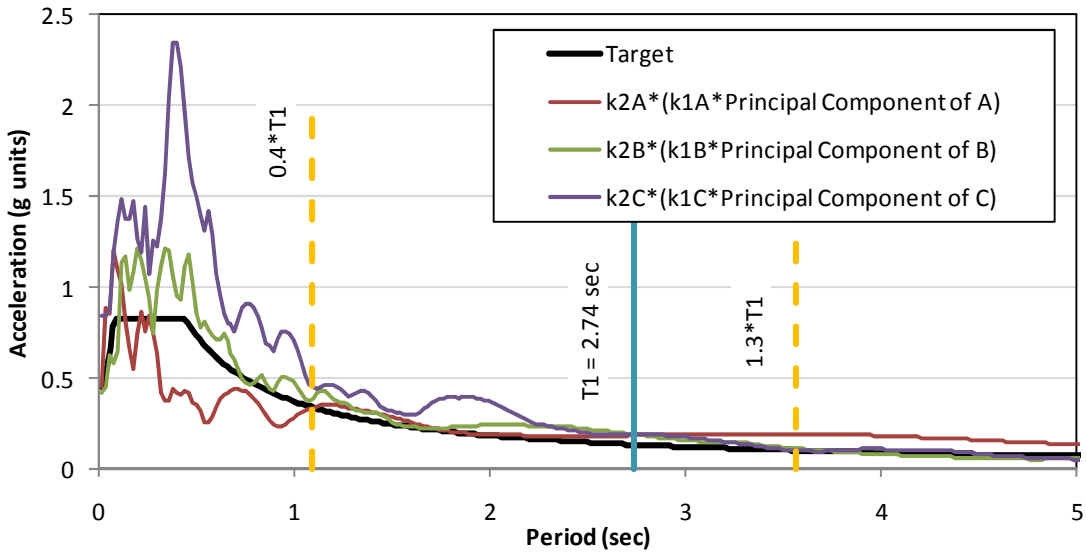

Figure B- 9 Spectra of the principal components of each record multiplied by the record scale factor k_1 and by the individual factor k_2

Then, the family scale factor k_2 is equal to the least of the individual k_2 values of each earthquake shown in Table B- 10. Therefore, the resulting factor k_2 is equal to 1.231 (from the principal component of record A) which is within the allowable limits of k_2 given by the NZS ($1.0 < k_2 < 1.3$). The plot of the principal component of each record multipplied by the record factor k_1 and the family factor k_2 is shown in Figure B- 10 , and although it is hard to distinguish

in the figure, some ordinates of the spectra from the principal components of the records B and C fall below the target spectrum.

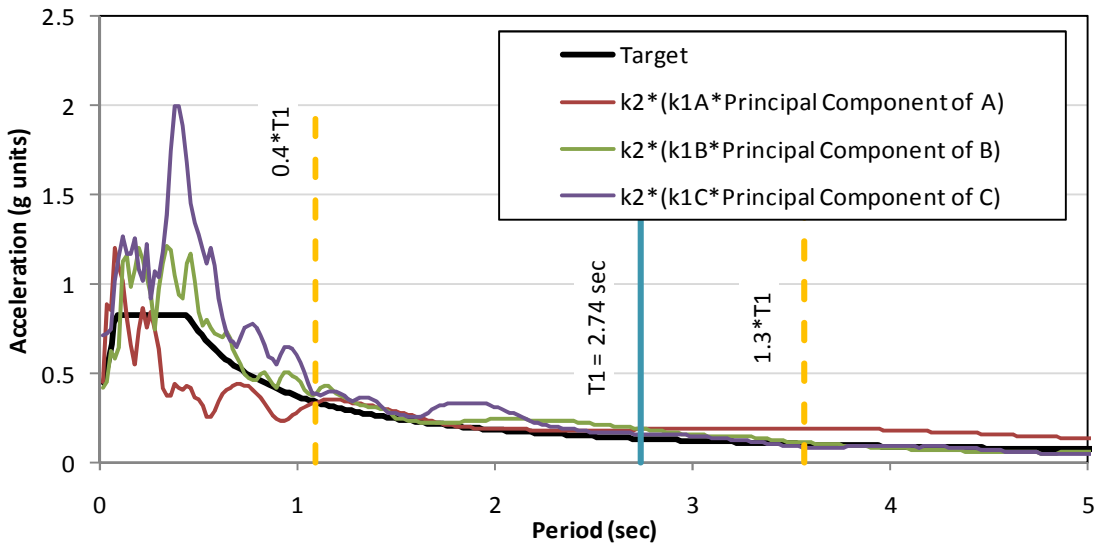

Figure B- 10 Spectra of the principal components of each record multipplied by the record scale factor k_1 and by the set scale factor k_2

Step 5 and Step 6: Confirmation of the principal and secondary components selected

The NZS states that the initial selection of the principal and secondary components in the sub-step viii is confirmed if the factor k_2 is within 1.0 and 1.3; otherwise, the NZS provides procedures to redefine the principal and secondary components of each earthquake. For this example in particular, the value of k_2 is equal to 1.231, and therefore the principal components of Table B- 9 are confirmed.

Step 7: Repeat the steps 3 through 6 for other directions of interest

For simplicity, this step is not performed in this example

Having performed all these seven steps, the resulting scale factors for each record are shown in Table B- 11

Table B- 11 Final Scale Factors for Example 3 using the scaling of ground motion procedure of the New Zealand Standard

Earthquake	k_1	k_2	Final Scale Factor k_1*k_2
A	0.480	1.231	0.591
B	1.130	1.231	1.391
C	1.440	1.231	1.773

Example 4
Selection and scaling of ground motions using the new suggested method in Section 3.4

An example is developed next to show the steps for the selection and scaling of ground motions for LRHA based on the new suggested method described in Section 3.4.2. This example is intended to be applied to the 12th story building analyzed by Charney et al. (2010b) (see Building 2 of Appendix A for details).

Step 1: Calculation of the fundamental period of vibration of the structure

The two translational periods of the building, T_x and T_y, are 2.87 sec and 2.60 sec, respectively, and an average value of T= 2.74 seconds can be used for following calculations.

Step 2: Definition of the seismic hazard

The next step is the definition of the seismic hazard for the site of interest, and it will be given by the appropriate pair Magnitude-Fault distance (abbreviated hereafter as M-D) predicted by the USGS deaggregation model (U.S. Geological Survey, 2009a) for a specific location, probability of exceedance, and fundamental period. The location for this example is given by the coordinates of Latitude = 37.365 and Longitude -121.9, which are the same coordinates of the building analyzed by Charney et al. (2010b). The probability of exceedance for the deaggregation model was chosen as 2% in 50 years in order to have a measure of the maximum considered earthquake (MCE). Also, the scenarios governing at different periods are given in Table B- 12, and it can be noticed that for a structure with fundamental period T equal to T=2.74 sec the seismic hazard is given by a seismic event with magnitude and fault distance equal to 8.01 and 20.8 km, respectively.

Step 3: Selection of ground motions from a database

Now that the pair M-D that controls the scenario is known, ground motions with similar characteristics can be found in the NGA Database (PEER, 1999). The number of earthquakes desired for analysis is chosen as three, and according Table 3-2 the corresponding number of

earthquakes needed with similar parameters M-D-SM-ST is equal to five so that the best three of them are selected for analysis. Table B- 13 shows the selected five earthquakes.

Table B- 12 Scenario that controls the seismic hazard for a location with Latitude = 37.365 and Longitude = -121.9, for a probability of exceedance of 2% in 50 years.

Period (sec)	Frequency (Hz)	Modal Distance (km)	Modal Magnitude
0	PGA	11.8	6.61
0.1	10	11.8	6.61
0.2	5	11.8	6.61
0.3	3.33	11.8	6.61
0.5	2	11.7	6.61
1	1	11.5	6.96
2	0.5	20.8	8.01
3	0.333	20.8	8.01
4	0.25	20.8	7.99
5	0.2	20.8	8.01

Table B- 13 Pre-selected earthquakes for Example 4 of selection and scaling of ground motions for LRHA

Earthquake	# NGA	Earthquake	Year	Mag.	Distance from Epic	Type of soil	Fault mech.	Max. usable period (sec)	# Points	ΔT (sec)	Duration (sec)
A	15	Kern County	1952	7.36	43.49	C	2	16.00	5416	0.010	54.16
B	139	Tabas, Iran	1978	7.35	20.63	C	2	8.00	1192	0.020	23.84
C	739	Loma Prieta	1989	6.93	26.57	C	3	4.00	7921	0.005	39.61
D	828	Cape Mendocino	1992	7.01	4.51	C	2	14.00	1800	0.020	36.00
E	1596	Chi-Chi, Taiwan	1999	7.62	14.16	C	3	16.00	12000	0.005	60.00

The maximum allowable distance in Table B- 13 was 50 km, and the variability of the earthquake magnitude was ±1.1 although a range of ±0.20 was initially tried, but not enough ground motions with the desired properties were available. Moreover, the source mechanism was arbitrarily assigned as Type 2 or Type 3 which corresponds to Reverse and Reverse Oblique, respectively, and this assumption was necessary because the deaggregation model of the USGS does not provide the type of fault expected. Furthermore, all the earthquakes of Table B- 13 are recorded in soil type C which coincides with the soil conditions of the site of interest.

Step 4: Control of the statistical independence of the horizontal components of the pre-selected earthquakes

Following the ASCE 4-98 provisions, statistic independence between the two horizontal components of the ground motion will be guarantee if the absolute value of the correlation coefficient is less than 0.3. The two planar acceleration histories of each record are denoted as A1 and A2, B1 and B2, C1 and C2, D1, and D2, and E1 and E2, for the earthquakes A, B, C, D, and E, respectively. The correlation coefficient between each pair of components is shown in Table B- 14.

Table B- 14 Correlation coefficients between each pair of components of the pre-selected earthquakes

Earthquakes components	Absolute correlation coefficient
A1 and A2	0.133
B1 and B2	0.060
C1 and C2	0.187
D1 and D2	0.115
E1 and E2	0.105

Step 5: Calculation of the acceleration design spectrum for the location of interest.

The design spectrum for the site of interest is given by Table 2-5 and Figure 2-4.

Step 6: Calculation of the SRSS spectrum of the spectral components of each record

The SRSS spectra of the two components of each earthquake are shown in Figure B- 11.

Step 7: Scaling of the pre-selected records to the fundamental period of vibration using the factor FPS

The SRSS spectra shown in Figure B- 11 have different ordinates at the fundamental period T=2.74 sec. The objective of this step is to scale these spectra so that all of them will have the same ordinate at T, and it will be done by calculating the factor *FPS* for each earthquake as explained in Section 3.4. The resulting factors *FPS* are shown in Table B- 15, and the

modified SRSS spectra already multiplied by their respective factor *FPS* are shown in Figure B-12 where it can be seen that all these spectra have the same ordinate at the period *T*.

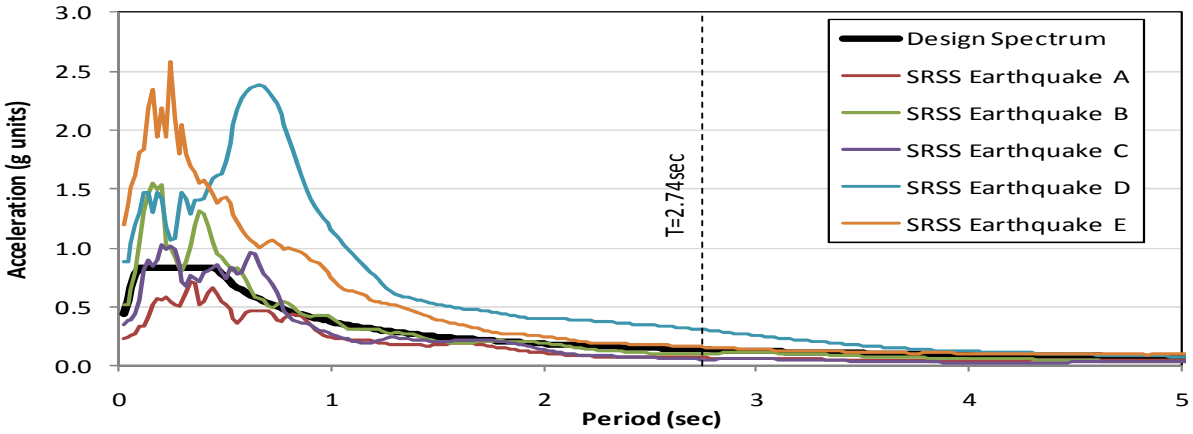

Figure B- 11 SRSS of preselected earthquakes

Table B- 15 Scale Factor *FPS* for the SRSS spectrum of each earthquake

Spectrum	FPS
SRSS Earthquake A	1.980
SRSS Earthquake B	1.310
SRSS Earthquake C	2.520
SRSS Earthquake D	0.450
SRSS Earthquake E	0.850

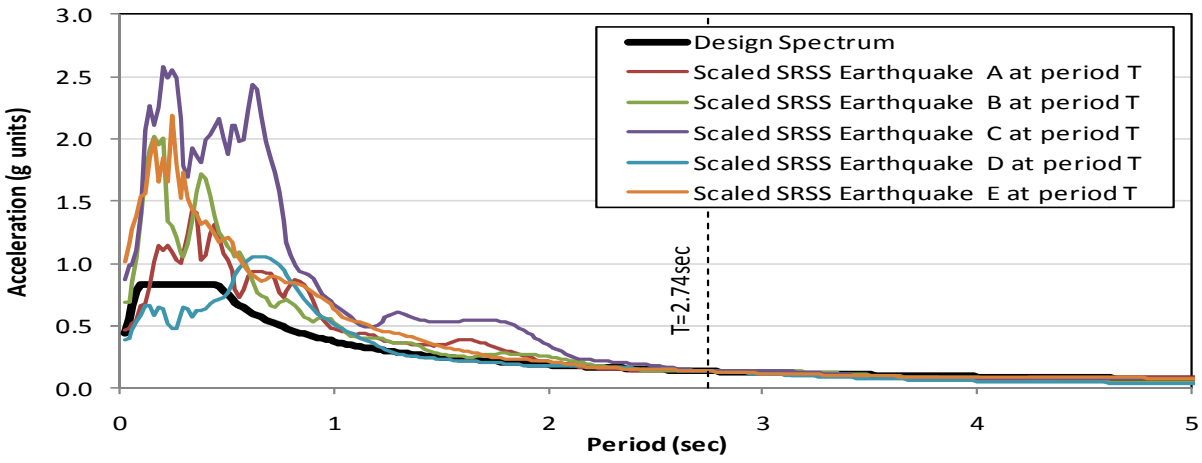

Figure B- 12 Scaled SRSS of preselected earthquakes at the fundamental period of vibration

Step 8: Definition of the period range of interest

Separate calculations are shown below for the definition of the upper and lower periods of the range of interest.

Upper limit

The upper limit of the period range of interest is given directly by the fundamental period of vibration; however, the designer will have to control that the maximum usable period of each earthquake, which is based on the filters for which the record has been gone through, is higher than the fundamental period of vibration of the structure analyzed. The maximum usable period of the selected earthquakes is given by in the NGA documentation (PEER, 1999) by the lowest usable frequency, and those maximum periods for each record are shown in Table B- 16.

Table B- 16 Set maximum usable period based on the maximum usable period given in the NGA database

Earthquake	Lowest usable frequency	Maximum usable period
	(Hz)	(sec)
A	0.063	16.00
B	0.125	8.00
C	0.250	4.00
D	0.070	14.29
E	0.063	16.00
	Set Maximum usable period:	4.00

The set maximum usable period is the lowest of the individual maximum usable periods shown in Table B- 16, and it is equal to 4 sec which is higher than the fundamental period of vibration of the structure T=2.74 sec. Therefore, the records selected are appropriate based on this criterion.

Lower limit

The lower limit of the period range of interest is given by the greatest of:

- The period at which is reached the 90% of the modal mass.

- The period corresponding to the smallest Nyquist frequency of the set of records.
- 0.16
- 0.2 *T* where *T* is the fundamental period of vibration defined in Step 1.
- 4th translational period

The definition of the first two of these parameters is described next:

Period at which 90% of the modal mass is reached

The periods and respective mass participation factors in each translational direction are required in order to obtain the period at which the 90% of the mass is achieved as well as to obtain the 4th translational mode which is required for the definition of the lower limit of the period range of interest. Also, the same information is required to obtain the 2nd translational mode which is required for the definition of the Target Scaled Spectrum as defined in Section 3.4.2.

Table B- 17 and Table B- 18 show the number of mode, the period, and the mass participation factors with predominant contribution to the X and Y directions of the structure (axis X and Y are according Figure A- 2), respectively. Also, based on this information, Table B- 19 shows only the periods at which the 90% of the mass is reached, and the 2nd and 4th translational periods for each direction which are denoted hereafter T_{90}, T_{2Tr}, and T_{4Tr}, respectively. The target spectrum of the new suggested method uses a unique value of these parameters, and therefore T_{90}, T_{2Tr}, and T_{4Tr} are defined as the smaller of the values in each translational direction.

Table B- 17 Mass Participation Factors in modes with predominant contribution to the X direction

Mode	Period (sec)	Mass Participation Factor for translations X, Y and rotation Z			SumUX
		UX	UY	RZ	
1	2.870	0.645	0.000	0.003	0.645
4	1.151	0.109	0.000	0.000	0.757
6	0.705	0.026	0.000	0.027	0.783
118	0.057	0.147	0.000	0.004	0.977

Table B- 18 Mass Participation Factors in modes with predominant contribution to the Y direction

Mode	Period (sec)	Mass Participation Factor for translations X, Y and rotation Z			SumUY
		UX	UY	RZ	
2	2.601	0.000	0.680	0.016	0.681
5	0.975	0.000	0.094	0.018	0.775
8	0.573	0.000	0.019	0.012	0.795
112	0.067	0.000	0.105	0.000	0.972

Table B- 19 Definition of T_{90}, T_{2Tr}, and T_{4Tr}

Direction	T_{90} (sec)	T_{2Tr} (sec)	T_{4Tr} (sec)
X	0.057	1.151	0.057
Y	0.067	0.975	0.067
Value representative of both directions	0.057	0.975	0.057

Period corresponding to the smallest Nyquist frequency of the set of records

Table B- 20 shows the calculation of the period corresponding to the Nyquist frequency of each record which is also the minimum period with energy content in each record. From Table B- 20 it can be seen the minimum period with energy content that is common to all the earthquakes is 0.4 sec, and this value is defined as set minimum period of interest based on this criteria.

Table B- 20 Set minimum period of interest based on the the minimum period with energy content

Earthquake Record	Δt	Sampling Frequency	Nyquist Frequency	Minimum Period with energy content
	(sec)	(Hz)	(Hz)	(sec)
A	0.01	100	50	0.02
B	0.02	50	25	0.04
C	0.005	200	100	0.01
D	0.02	50	25	0.04
E	0.005	200	100	0.01
			Minimum period of interest	0.04 sec

Based on the information of Table B- 19, Table B- 20, Table B- 21 shows the period corresponding to each criterion required to define the lower limit of the period range of interest which is given by the maximum of these individual values. For this case in particular, the lower limit of the period range of interest is governed by 0.2*T*, and it is equal to 0.548 sec.

Table B- 21 Definition of the lower limit of the period range of interest

Criteria	Period (sec)
a) Period at which the 90% of the mass is reached	0.057
b) Period corresponding to the smallest Nyquist frequency of the set of earthquakes	0.040
c) 0.16	0.160
d) 0.2T	0.548
e) Period of the Fourth Translational mode	0.057
Lower limit of the period range of interest:	0.548

This way, the upper and lower limits for this example are given by *T* and 0.2*T*, respectively.

Step 9: Selection of the records that best fit the design spectrum

The pre-selected earthquakes already scaled by the factor *FPS* are now evaluated so that only three of them are selected for analysis based on the best fit of these modified SRSS spectra relative to the design spectrum within the period range of interest.

This example will analyze eight different criteria to select the appropriate three earthquakes for analysis; the first of them consists in obtaining the accumulated squared error between the scaled (by the factor *FPS*) SRSS spectrum and the design spectrum within the period range of interest. The second criterion is very similar to the first one but it measures the accumulated error between the logarithms of the scaled SRSS spectrum and the design spectrum. This criterion was adopted considering that the NZS uses a similar approach. The third, fourth and fifth criteria are very similar to the first criteria, except that three different weighting functions are used to acknowledge the fact that matching of the two spectra at periods closer to

the fundamental period *T* is more important than the matching at periods away from *T*. Also, the sixth, seventh, and eight criteria are very similar to the second criterion except that it uses the same weighting functions of the last three criteria. The described eight criteria, denoted hereafter as CR1, CR2, CR3, CR4, CR5, CR6, CR7 and CR8, are summarized in Table B- 22, and their respective mathematic formulation is shown in equations Eq. B-4 through Eq. B-11. Also, the three weighting functions, Weighting Function 1, Weighting Function 2 and Weighting Function 3 are shown in Figure B- 13.

Table B- 22 List of criteria used for the selection of the three earthquakes whit clower match between the scaled SRSS spectrum and the design spectrum

Criterion	Notation	Definition
1	CR1	Accumulated error of the scaled SRSS spectrum and the design spectrum, using an equal weight for all the periods considered
2	CR2	Accumulated error of the logarithm of the scaled SRSS spectrum and the design spectrum, using an equal weight for all the periods considered.
3	CR3	Accumulated error of the scaled SRSS spectrum and the design spectrum, using the Weighting Function 1
4	CR4	Accumulated error of the scaled SRSS spectrum and the design spectrum, using the Weighting Function 2
5	CR5	Accumulated error of the scaled SRSS spectrum and the design spectrum, using the Weighting Function 3
6	CR6	Accumulated error of the logarithm of the scaled SRSS spectrum and the design spectrum, using the Weighting Function 1
7	CR7	Accumulated error of the logarithm of the scaled SRSS spectrum and the design spectrum, using the Weighting Function 2
8	CR8	Accumulated error of the logarithm of the scaled SRSS spectrum and the design spectrum, using the Weighting Function 3

$$CR1 = \sqrt{\sum_{T=T_{LL}}^{T=T} \left[\left(SRSS_{scTn}\right)_i - \left(\text{Design Spectrum}\right)_i \right]^2} \qquad \textbf{Eq. B- 4}$$

$$CR2 = \sqrt{\sum_{T=T_{LL}}^{T=T} \left[\log\left(\frac{\left(SRSS_{scTn}\right)_i}{\left(\text{Design Spectrum}\right)_i} \right) \right]^2} \qquad \textbf{Eq. B- 5}$$

$$CR3 = \sqrt{\sum_{T=T_{LL}}^{T=T} W1(T_i) * \left[\left(SRSS_{scTn}\right)_i - \left(\text{Design Spectrum}\right)_i \right]^2} \qquad \textbf{Eq. B- 6}$$

$$CR4 = \sqrt{\sum_{T=T_{LL}}^{T=T} W2(T_i) * \left[(SRSS_{scTn})_i - (\text{Design Spectrum})_i \right]^2} \qquad \textbf{Eq. B- 7}$$

$$CR5 = \sqrt{\sum_{T=T_{LL}}^{T=T} W3(T_i) * \left[(SRSS_{scTn})_i - (\text{Design Spectrum})_i \right]^2} \qquad \textbf{Eq. B- 8}$$

$$CR6 = \sqrt{\sum_{T=T_{LL}}^{T=T} W1(T_i) * \left[\log\left(\frac{(SRSS_{scTn})_i}{(\text{Design Spectrum})_i} \right) \right]^2} \qquad \textbf{Eq. B- 9}$$

$$CR7 = \sqrt{\sum_{T=T_{LL}}^{T=T} W2(T_i) * \left[\log\left(\frac{(SRSS_{scTn})_i}{(\text{Design Spectrum})_i} \right) \right]^2} \qquad \textbf{Eq. B- 10}$$

$$CR8 = \sqrt{\sum_{T=T_{LL}}^{T=T} W3(T_i) * \left[\log\left(\frac{(SRSS_{scTn})_i}{(\text{Design Spectrum})_i} \right) \right]^2} \qquad \textbf{Eq. B- 11}$$

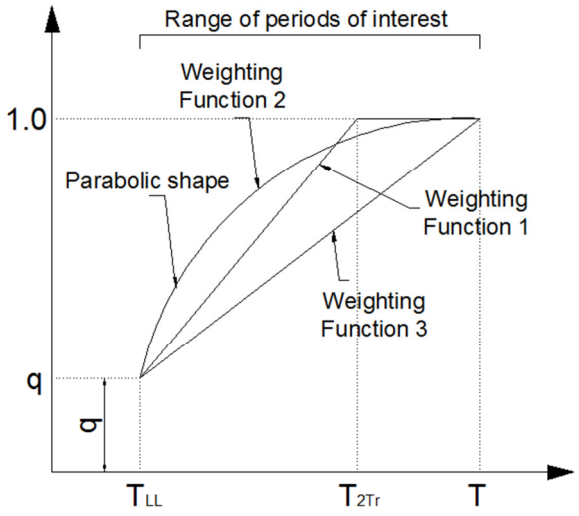

Figure B- 13 Weighting functions used to evaluate the goodness of the fitness between the scaled (by *FPS*) SRSS spectrum and the design spectrum within the period range of interest

As it can be seen from Figure B- 13, the Weighting Function 1 gives a weight of 1 to the periods located between the fundamental period T and T_{2Tr} which is defined as the period corresponding to the second translational mode; then, this weighting function drops with a straight line from the period T_{2Tr} to a specific value q at T_{LL} which is the lower limit of the period

range of interest. The Weighting Function 2 is a parabola with horizontal slope at the fundamental period T and which ordinate at T_{LL} is q. Finally, the Weighting Function 3 is a straight line that goes from 1.0 at the fundamental period T until a value of q at T_{LL}. The equations defining these weighting functions are:

$$W1(T_i) = m(T_i - T_{LL}) + q$$
$$where\ m = \frac{1-q}{T2Tr - T_{LL}} \qquad \textbf{Eq. B- 12}$$

$$W2(T_i) = k(T_i - Tn)^2 + 1$$
$$where\ k = \frac{q-1}{(T_{LL} - Tn)^2} \qquad \textbf{Eq. B- 13}$$

$$W3(T_i) = m(T_i - T_{min}) + q$$
$$where\ m = \frac{1-q}{Tn - T_{LL}} \qquad \textbf{Eq. B- 14}$$

The values of CR1 through CR8 were calculated in order to define the three earthquakes for which these error measures yield smaller values. The values of CR1 and CR2 are independent of the value q, and the results are shown in
Table B- **23** where the three earthquakes for which these two criteria yield the smaller error have been filled with grey color.

Table B- 23 Values given by the error measures CR1 and CR2 for each earthquake

Earthquake	Criterion	
	CR1	**CR2**
A	2.254	2.001
B	1.652	1.503
C	7.695	4.508
D	2.553	1.650
E	2.640	2.127

As it can be seen from Table B- 13, the three earthquakes with smaller values of CR1 and CR2 are the records A, B, and D.

In the case of CR3 through CR8, these error measures are dependent of the value of q, and two different values corresponding to q=0.2 and q=0.3 were tested to analyze the sensitivity of the results. The results are shown in Table B- 24 and Table B- 25, and it can be see that the earthquakes A, B, and D are the ones that yield smaller values, and therefore smaller error, for the majority of the cases. Also, the same conclusion applies for q=0.2 and q=0.3; therefore, the earthquakes selected for analysis are Earthquake A, Earthquake B, and Earthquake D.

Table B- 24 Values given by the error measures CR3 through CR8 considering q=0.2

Earthquake	Criterion					
	CR3	**CR4**	**CR5**	**CR6**	**CR7**	**CR8**
A	1.859	1.468	1.298	1.827	1.519	1.328
B	1.255	1.016	0.916	1.356	1.144	1.012
C	5.415	4.507	4.106	3.994	3.427	3.025
D	1.866	1.456	1.318	1.296	0.994	0.888
E	2.203	1.680	1.482	1.924	1.494	1.299

Table B- 25 Values given by the error measures CR3 through CR8 considering q=0.3

Earthquake	Criterion					
	CR3	**CR4**	**CR5**	**CR6**	**CR7**	**CR8**
A	1.913	1.587	1.453	1.850	1.587	1.429
B	1.311	1.116	1.037	1.375	1.195	1.086
C	5.749	5.017	4.707	4.062	3.580	3.248
D	1.965	1.634	1.528	1.346	1.098	1.015
E	2.262	1.828	1.671	1.951	1.587	1.429

Step 10: Recalculation of the lower limit of the period range of interest if needed

Because the lower limit was governed by 0.2*T*, a recalculation of the period of interest is not necessary.

Step 11: Calculation of the average of the scaled (by *FPS*) SRSS spectra considering the three selected earthquakes

Figure B- 14 shows the average of the scaled (by *FPS*) SRSS spectra for the selected earthquakes.

Step 12: Definition of the new target spectrum

Figure B- 14 shows the new target spectrum calculated as indicated in Section 3.4.2. Also, the same figure shows the design spectrum, which is the current target spectrum given by the scaling procedure of ASCE 7-10. Moreover, it can be noticed that the new target spectrum is defined only within the period range of interest.

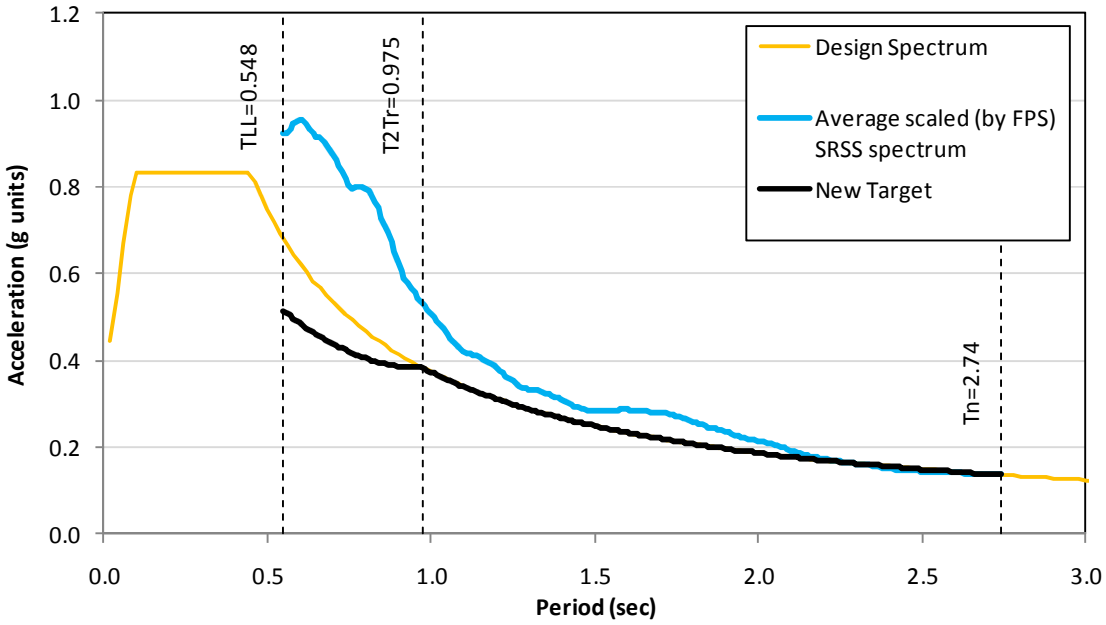

Figure B- 14 Design Spectrum, New Target Spectrum, and average scaled (by *FPS*) SRSS spectrum

Step 13: Calculation of the set scale factor *SS*

The set scale factor modifies the average scaled (by *FPS*) SRSS spectrum so that any point of this last spectrum cannot be below the new target spectrum within the period range of interest. The resulting set scale factor was *SS*=1.038, and the final average scaled SRSS spectrum, which is equal to the product of the factor SS times the average scaled (by FPS) SRSS spectrum, is shown in Figure B- 15.

Step 14: Calculation of final scale factors

The final scale factors are equal to the product of the factor *FPS* of each earthquake times the set scale factor *SS*. The results are shown in Table B- 26.

Step 15: Control of the maximum and minimum allowable limits of the final scale factors

As shown in Table B- 26, the final scale factors are within the limits of 0.33 and 3.0; therefore, those factors are considered appropriate.

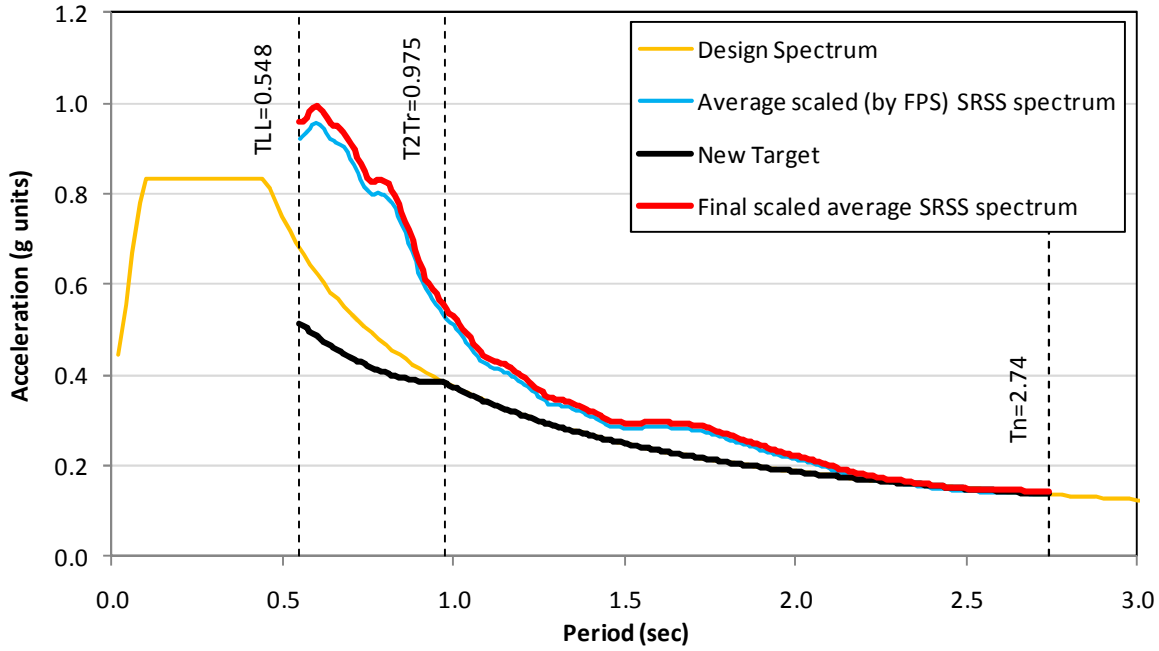

Figure B- 15 Final scale average SRSS spectrum

Table B- 26 Final scale factors for example using the new suggested method for selecting and scaling of earthquakes

Record	Factor *FPS*	Factor *SS*	Final scale Factor
A	1.981	1.038	2.056
B	1.310	1.038	1.360
D	0.445	1.038	0.462

Step 16: Calculation of the average PGA from the selected records

The PGA for each earthquake can be obtained as the maximum value of the geometric mean of the acceleration histories of both horizontal components; these values are directly available from the NGA database (PEER, 2005), and they are shown in Table B- 27. The average PGA is equal to 0.3823g. Also, the PGA given by the design spectrum can be calculated using the formula 11.4-5 of ASCE 7-10 for T=0 which yields in $PGA_{DesignSpectrum} = 0.4S_{DS}$ = 0.4*0.833g = 0.333g. It can be noticed that the average PGA (0.3823g) is bigger than the PGA given by the design spectrum (0.333g); therefore, the requirement of this step is satisfied.

Table B- 27 Scaled PGA from the selected earthquakes

Earthquake	NGA number	PGA (g units)
A	15	0.1728
B	139	0.3505
D	828	0.6236
	Average	0.3823

Appendix C. Periods and translational and rotational masses of buildings analyzed with rigid diaphragms

Table C- 1 Period and translational and rotational mass for Building 1 analyzed with rigid diaphragms

Level	Total Gravity Load each floor (kips)	Translational mass (kips-sec^2/in)	Rotational Mass (in-kips-sec^2)
R	2507	6.488	2250184
8	2351	6.085	2110329
7	2351	6.085	2110329
6	2351	6.085	2110329
5	2351	6.085	2110329
4	2351	6.085	2110329
3	2351	6.085	2110329
2	2368	6.129	2125407
Total	18983	49.128	17037565
Fundamental Period X direction:		1.73	sec
Fundamental Period Y direction:		1.73	sec

Table C- 2 Period and translational and rotational mass for Building 2 analyzed with rigid diaphragms

Level	Total Gravity Load each floor (kips)	Translational mass (kips-sec^2/in)	Rotational* Mass (in-kips-sec^2)
R	1657	4.287	2072000
12	1596	4.130	2017000
11	1596	4.130	2017000
10	1596	4.130	2017000
9	3403	8.807	5309000
8	2331	6.032	3703000
7	2331	6.032	3703000
6	2331	6.032	3703000
5	4320	11.180	9091000
4	3066	7.934	6356000
3	3066	7.934	6356000
2	3097	8.016	6437000
1	6525	16.886	15030000
TOTAL	36912	95.527	67811000
Fundamental Period X direction:		2.94	sec
Fundamental Period Y direction:		2.66	sec

Table C- 3 Period and translational and rotational mass for Building 3 analyzed with rigid diaphragms

Level	Total Load each floor	Translational mass	Rotational Mass
	(kips)	(kips-sec^2/in)	(in-kips-sec^2)
R	2746	7.106	2464213
8	2590	6.702	2324357
7	2590	6.702	2324357
6	2590	6.702	2324357
5	2590	6.702	2324357
4	2590	6.702	2324357
3	2590	6.702	2324357
2	2607	6.746	2339435
Total	20891	54.065	18749791
Fundamental Period X direction:		1.75	sec
Fundamental Period Y direction:		0.65	sec

Table C- 4 Period and translational and rotational mass for Building 4 analyzed with rigid diaphragms

Level	Total Load each floor	Translational mass	Rotational Mass
	(kips)	(kips-sec^2/in)	(in-kips-sec^2)
R	2122	5.493	2966126
9	2240	5.797	3130122
8	2240	5.797	3130122
7	2240	5.797	3130122
6	2240	5.797	3130122
5	2240	5.797	3130122
4	2240	5.797	3130122
3	2240	5.797	3130122
2	2278	5.896	3183296
Total	20079	51.965	28060904
Fundamental Period X direction:		2.16	sec
Fundamental Period Y direction:		2.12	sec

Appendix D. Proposal of code language for linear response history analysis in ASCE7

12.10 LINEAR RESPONSE HISTORY PROCEDURE

Where linear response history procedure is performed the requirements of this section shall be satisfied.

12.10.1 Analysis Requirements

A linear response history analysis shall consist of an analysis of a linear mathematical model of the structure to determine its response, through methods of numerical integration, to suites of ground motion acceleration histories compatible with the design response spectrum for the site. The analysis shall be performed in accordance with the requirements of this section.

12.10.2 Modeling

Mathematical models shall conform to the requirements of Section 12.7, and a 3-D model of the structure must be used.

12.10.3 Ground Motion

12.10.3.1 Requirements for ground motion

A suite of not less than three appropriate ground motions shall be used in the analysis. Ground motion shall conform to the requirements of this section.

Equal criteria will be used for structures modeled in two and in three dimensions.

12.10.3.2 Definition of seismic hazard

Ground motions shall consist of pairs of appropriate horizontal ground motion acceleration components that shall be selected and scaled from individual recorded events. Probabilistic estimates of the seismic hazard at the site may be used to determine the principal contributors to the seismic hazard. Appropriate ground motions shall be selected from events having magnitudes, fault distance, and source mechanisms that are consistent with those that control the maximum considered earthquake. Additionally, the components of each selected ground motion shall be statistically independent.

12.10.3.3 Spectral matched ground motions

Where the required number of recorded ground motion pairs specified in section 12.10.3.1 is not available, the analysis can be done using at least one spectral matched acceleration history having two horizontal components statistically independent.

The selected record shall produce a zero velocity at the end of the earthquake when integrating the acceleration record.

12.10.3.4 Orientation of ground motion axis

As an option, linear response history analysis can be performed using the "critical acceleration history," which is defined as the generated signal after rotation of the original components by a defined "critical angle." The critical angle is defined as the rotation angle of the original record components for which the maximum spectral acceleration is obtained.

In the case of using the critical acceleration history, the maximum response could be defined as the higher value resulting from applying the original components of the ground motion and the critical acceleration history, in the direction of interest. A similar definition could be applied to define the loading of the structure when obtaining interstory drifts is desired. For calculations involving simultaneous loading in the two principal axis of the structure, the use of the original components of the ground motions will be allowed instead of using the critical acceleration history.

12.10.3.5 Fundamental Period for scaling purposes

For scaling purposes the average of the fundamental periods of vibration in each principal direction can be used as the representative fundamental period of the structure T.

12.10.3.6 Period range of interest

The period range of interest for scaling procedures will be defined as follows:

The upper limit of the period range of interest will be given by the fundamental period defined in 12.10.3.5, and it has to be smaller than the maximum usable period of each pre-selected record.

On the other hand, the lower limit of the period range of interest, denoted T_{LL}, is given by the greatest of:

- The minimum usable period of each pre-selected record.
- The period at which is reached the 90% of the modal mass.
- The period corresponding to the smallest Nyquist frequency of the set of records.
- $0.2T$
- 4^{th} translational period.

12.10.3.7 Pre-selection and final selection of records

Ground motions with magnitude and fault distance closer to the target need to be selected from an earthquake database, and the minimum number of records selected from an earthquake database will be

equal to the 1.5 times the number of earthquakes intended for LRHA. This set of ground motions is denoted as the pre-selected earthquakes.

A fundamental period scale factor, denoted *FPS*, will be applied for each pre-selected earthquake so that the spectrum resulting from the square root of the sum of the squares (SRSS) of the spectrum of each component, will have the same ordinate of the design spectrum at the fundamental period of vibration defined in section 12.10.3.5.

Next, at least one error measure will be used to define the best fit within the period range of interest defined in 12.10.3.6 between the scaled (by *FPS*) SRSS spectra of each earthquake and the design spectrum. Then, the pre-selected earthquakes for which the error measures yield smaller values will be assigned as the earthquakes to be used for analysis. The period range of interest will be recalculated, if needed, considering only the characteristics of the selected earthquakes.

12.10.3.8 Definition of the Target Spectrum

The target spectrum is defined for three different scenarios as described next:

Scenario 1: $T_{LL} < T_S < T_{2Tr}$, as shown in Figure 12.10- 1

Scenario 2: $T_{LL} < T_{2T} < T_S$, as shown in Figure 12.10- 2

Scenario 3: $T_S < T_{LL} < T_{2Tr}$, as shown in Figure 12.10- 3

The equations corresponding to each scenario are:

For scenario 1:

$$\begin{cases} k\,S_{DS} & if \quad T_{LL} < T < T_S \\ c\left(T - T_{2Tr}\right)^2 + S_{2Tr} & if \quad T_S \le T < T_{2Tr} \\ \quad where \quad c = \dfrac{kS_{DS} - S_{2Tr}}{\left(T_S - T_{2Tr}\right)^2} & \\ Design \;\; Response \;\; Spectrum & if \quad T_{2Tr} \le T \le Tn \\ (Section \;\; 11.4.5 \; of \;\; ASCE7-10) & \end{cases}$$

For scenario 2:

$$\begin{cases} k\,S_{DS} & if \quad T_{LL} < T < T_{2Tr} \\ Design \quad Response \quad Spectrum & if \quad T_{2Tr} \le T \le Tn \\ (Section\, 11.4.5 \; of \;\; ASCE7-10) & \end{cases}$$

For scenario 3:

$$\begin{cases} c\left(T - T_{2Tr}\right)^2 + S_{2Tr} & if \quad T_{LL} \le T < T_{2Tr} \\ \quad where \quad c = \dfrac{kS_{DS} - S_{2Tr}}{\left(T_{LL} - T_{2Tr}\right)^2} & \\ Design \quad Response \quad Spectrum & if \quad T_{2Tr} \le T \le Tn \\ (Section\, 11.4.5 \; of \;\; ASCE7-10) & \end{cases}$$

where:

k is a constant equal to 0.7

S_{DS} is the design spectral response acceleration parameter at short periods, as defined in section 11.4.4

S_{D1} is the design spectral response acceleration parameter at 1 sec, as defined in section 11.4.4

S_{2Tr} is the ordinate of the design spectrum at the period T_{2Tr}

T_{2Tr} is the least of the second translational period in each principal direction

T_{LL} is the period corresponding to the lower limit of the period range of interest, as defined in section 12.10.3.6

T_S is the ratio between S_{D1} and S_{DS}

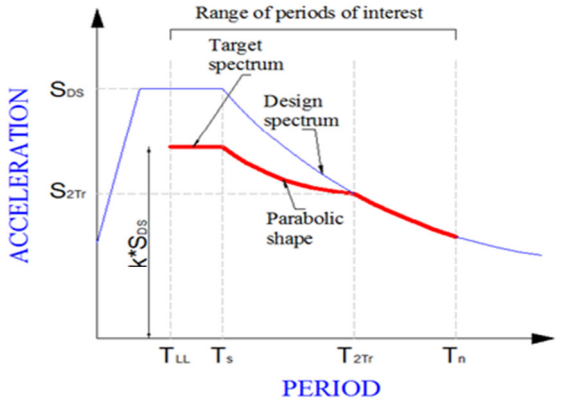

Figure 12.10- 1 Target Period of proposed scaling of ground motion procedure, Scenario 1

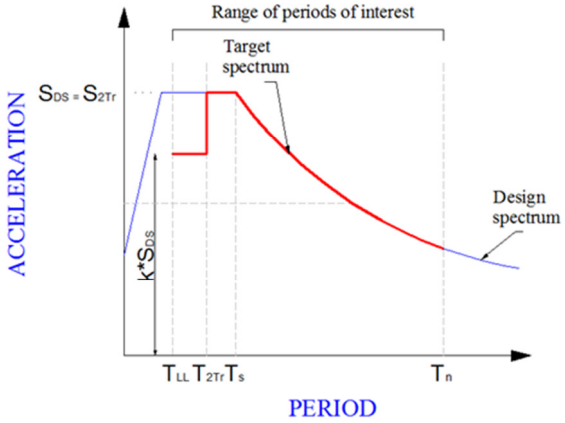

Figure 12.10- 2 Target Period of proposed scaling of ground motion procedure, Scenario 2

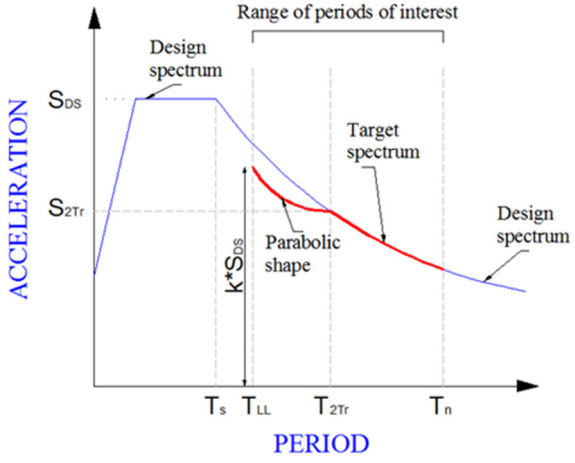

Figure 12.10- 3 Target Period of proposed scaling of ground motion procedure, Scenario 3

12.10.3.9 Scaling of selected records

For each pair of horizontal ground motion components, a square root of the sum of the squares (SRSS) spectrum shall be constructed by taking the SRSS of the 5 percent-damped response spectra for the scaled components (where an identical scale factor is applied to both components of a pair). Each pair of motions shall be scaled such that in the period range of interest, defined in 12.10.3.6 and 12.10.3.7, the average of the SRSS spectra from all horizontal component pairs does not fall below the corresponding ordinate of the target response spectrum specified in Section 12.10.3.8

The requirements of this section will be satisfied by applying two scale factors: *FPS* and *SS* that are calculated as follows. A fundamental period scale factor, denoted *FPS*, will be calculated for each selected earthquake so that its SRSS spectrum will have the same ordinate of the target spectrum of section 12.10.3.8 at the fundamental period of vibration The set scale factor *SS* will be calculated so that the average of the scale (by *FPS*) SRSS spectrum is above the new target spectrum within the period range of interest.

The final scale factors are given by the product of the factor *FPS* for each record by the set scale factor *SS*. The final scale factors need to be between 0.33 and 3.0

12.10.3.10 Other requirements

A set of at least 100 periods per logarithmic scale will be used when calculating any response spectrum required in section 12.10 of this standard.

The average peak ground accelerations (PGA) of the scaled records must be greater than the PGA predicted by the design spectrum for the site of interest.

The ordinate of the average of the scaled SRSS spectrum from each record cannot be greater than 10% of the ordinate of the design spectrum, at the fundamental period *T*.

At sites within 3 miles (5 km) of the active fault that controls the hazard, each pair of components shall be rotated to the fault-normal and fault-parallel directions of the causative fault and shall be scaled so that the average of the fault-normal components is not less than the MCE response spectrum for the period range specified in section 12.10.3.6.

12.10.4 Diaphragm Flexibility

The provisions given in Section 12.3.1 are applicable for the analysis of diaphragm flexibility. .

12.10.5 Response parameters

The value for each force-related design parameter of interest, including support forces, and individual member forces will be divided by the quantity *R/Ie* where *R* is the response modification coefficient defined in Table 12.2-1 and I_e is the importance factor defined in section 11.5.1. The resulting base shear after this modification is denoted as V_t.

Also, the displacements and drift quantities shall be multiplied by the quantity C_d/I_e where C_d is the deflection amplification factor defined in Table 12.2-1

12.10.6 Scaling Design values of combined response

.

12.10.6.1 Scaling of forces

Use the same provisions for response spectrum analysis given in Section 12.9.4.1 of ***ASCE 7-10*** except that V_t is defined as the base shear obtained in Section 12.10.6.

12.10.6.2 Scaling of displacements

Use the same provisions for response spectrum analysis given in Section 12.9.4.1 of ASCE 7-10 except that V_t is defined as the base shear obtained in Section 12.10.6.

12.10.7 Horizontal shear distribution

12.10.7.1 General

The distribution of horizontal shear shall be in accordance with Section 12.8.4 except that amplification of torsion in accordance with Section 12.8.4.3 is not required where accidental torsion effects are included in the dynamic analysis model.

12.10.7.2 Additional considerations when considering accidental torsion

For the cases where the lateral load is not parallel to the principal axis of the structure the point of application of the lateral load to create accidental torsion will be over the ellipse with center coinciding with the center of mass of the floor and with semiaxis equal to the eccentricities 0.05a and 0.05b along the principal axis of the structure, where a and b are the longest dimensions parallel to each principal axis.

The eccentricity in each floor of a structure with more than one story will be applied in the same directions for all the floors of a building. For the case of using rigid diaphragms, the rotational mass from the model without accidental torsion will not need to be changed when displacing the center of mass. Linear masses, if exist, should be considered in the calculation of the rotational moment of inertia of each floor.

The calculation of torsional effects using static moments will be allowed only for the cases where the parameter Ω, which is the ratio of the fundamental translational and rotational period, is greater than 1. For other cases torsional effects will be calculated using dynamic procedures.

12.10.8 Orthogonal loading

The requirements for orthogonal loading in linear response history analysis will be the same as those given in Section 12.5.2 for structures in seismic design category (SDC) B. However, for SDC C, in addition to the minimum requirements of SDC B, it will be satisfied that both components of the ground motion have to be applied simultaneously. The record components applied in each direction have to be scaled individually to satisfy the requirements of section 12.10.3.9.

For the case of structures classified with SDC D through F, the requirements will be the same as given in Section 12.5.4 plus the requirements for SDC C as stated above as a minimum.

12.10.9 Damping and Solution techniques

12.10.9.1 Number of modes for modal linear response history analysis

The required number of modes will be given by Section 12.9.1. For the case of using modal analysis with Eigen vectors or Ritz vectors, a constant damping ratio of 0.05 (as a fraction of the critical damping) should be used.

12.10.9.2 Direct Integration

When using direct integration with Rayleigh Damping in structures modeled in three dimensions (3D), a damping ratio of 0.05 could be used in the 1st and 2nd or in the 1st and 3rd translational modes moving in the same direction. Additionally, the first two translational periods or the fundamental rotational period will have a damping ratio higher than 0.05. Finally, defining T_{90} as the period at which 90% of the modal mass in both translational directions is reached, the damping ratio at that period T_{90} will not exceed 0.2 (20%).

12.10.10 P-Delta effects

Use the same provisions for response spectrum analysis given in Section 12.9.6. Direct modeling of P-Delta effects can also be used.

12.10.11 Modeling of the basement

Basement levels should be included in the mathematical model of the building, and their modeling will reassemble as possible, the real behavior expected for the analyzed building.

COMMENTARY

C12.10.2 The capabilities of current software for structural analysis can create 3-D models of structures with relative not difficulties. Also, and more importantly, the response parameters (i.e. element forces and displacements) are more reliable when using a 3-D model than when using a 2-D model.

C12.10.3.2 Due to the capabilities of commercial structural analysis software and due to an increased accuracy in the results it is required to perform only a three dimensional analysis when applying acceleration histories as the input seismic load.

C12.10.3.2 The requirement for defining the probabilistic estimates of the seismic hazard has been taken from ASCE 4-98 (American Society of Civil Engineers, 2000).

A tolerance of ± 0.25 in the magnitude of the selected earthquakes has been suggested by Stewart et al. (2001).

As given by ASCE 4-98, statistical independence between the components of a ground motion can be considered satisfied if the absolute value of the correlation coefficient does not exceed 0.3.

C12.10.3.3 Equivalent response from a modal response spectrum analysis can be obtained if using one spectrally matched acceleration record (Tola, 2010).

Useful information for the amplitude and duration of simulated ground motions can be found in Table 2.3-1 of ASCE 4-98 which provides suggested values for rise time, strong motion time, and decay time based on a trapezoidal envelope of the artificial record. Additionally, the Eurocode 8 (British Standards, 2004) suggests a minimum of 10 sec for the stationary part of the simulated ground motions.

When using software that generates spectral matched acceleration histories, it is preferred to select software that requires an actual record as the seed to generate the spectral matched acceleration history. This way, the designer can compare the acceleration, velocity, and displacement records, of the generated signal with those from the seed record.

Initial conditions of the earthquake motion have to be considered so that the velocity at the end of record would be zero. For the case of earthquakes selected from the NGA database (PEER, 1999), the initial conditions of the movement are not specified, but for those earthquakes selected from the COSMOS database (COSMOS, 2007), this information is given.

C12.10.3.4 The critical angle can be obtained by constructing the orbit spectrum for the components of a particular record. The software EQTools (Charney and Syed, 2004, 2010) can be used to performed this task. Also, the formulas to obtain the critical acceleration history can be found in Tola (2010).

As shown in Tola (2010), the critical response history will not always provide a higher response than that when using only the original record components, and this occurs due to the influence of vibration modes other than the fundamental mode.

C12.10.3.5 A common fundamental period for both principal directions is required so that the same scale factors are obtained in each principal direction of the structure.

C12.10.3.6 Different limits in the period range of interest have been suggested to replace the values of $0.2T$ and $1.5T$ of ASCE 7-10.

Discussion about controlling the upper limit of the period range of interest with the maximum usable period can be found in Beyer and Bommer (2007).

The maximum and minimum usable period should be available from the database where the ground motions are selected. When the records come from the NGA database (PEER, 1999) then this maximum usable period can be found in the flat file provided in the PEER website.

The criteria to define the lower limit is explained in detail in Tola (2010).

C12.10.3.7 Pre-selected ground motions only satisfy requirements of having similar magnitude and fault distance with those of the target values; however, the similarity of the design spectrum with the spectrum of each earthquake was not accounted in Chapter 16 of ASCE 7-10. This way, a measure error of the records already scaled to the fundamental period of vibration is calculated for each earthquake, and those with the least error are finally selected for analysis.

Error measures can include weighting functions that give more weight to the periods closer to the fundamental period than at periods away from the fundamental period.

C12.10.3.8 The fundamentals to adopt a new target spectrum for scaling purposes instead of the design spectrum of section 11.4.5 are explained in Tola (2010).

C12.10.3.9 The concept and application of the fundamental period scale factor *FPS*, and the set

scale factor *SS* were originally suggested by Charney (2010a). The limits in the scale factors has been taken from the New Zealand Standard NZS 1170.5 (Council of Standards New Zealand, 2004).

C12.10.3.10 The requirement about having a PGA bigger than that predicted PGA for a site spectrum is stated in ASCE 4-98 (ASCE, 2000) and in the Eurocode 8 (British Standards, 2004).

C12.10.4 The modeling of diaphragms with mass distributed over the floor is considered a more realistic model than when concentrating all the mass at the center of mass.

The modeling of diaphragms with mass distributed over the floors could be mandatory for the case of dual systems because in this type of systems there is significant force transmitted through the diaphragms. Studies including linear response history analysis of buildings modeled with the mass concentrated at the center of mass and with the mass distributed over the floor can be found in Tola (2010)

C12.10.5 The same provision of response spectrum analysis will be used for linear response history analysis when obtaining the response parameters.

C12.10.6 The provisions for the scaling of element forces given in ASCE 7-10 have been modified significantly in order to be consistent with the provisions from a response spectrum analysis given in section 12.9.4 of ASCE 7-10. The reasons for this change are explained in Tola (2010).

The provisions for the scaling of drifts given in ASCE 710 are unchanged.

C12.10.7.1 Al the provisions applicable to modal response spectrum analysis are also applicable to linear response history analysis procedures.

C12.10.7.2 The additional statement about the application of accidental torsion when the lateral force is not parallel to the principal axis of the structure is a current requirement of the New Zealand Standard NZS 1170.5 (Council of Standards New Zealand, 2004).

According to De la Llera and Chopra (1994a), the uncoupled fundamental translational and rotational periods required for the calculation of the parameter Ω can be calculated using Rayleigh-Ritz vectors.

For the case of using a mathematical model where the mass is concentrated at the center of mass of the floor the inclusion of accidental torsion can be easily done by displacing the center of mass the design eccentricity 0.05b. On the other hand, for the case of using a mathematical model where the mass is distributed over the floor then the mass of the floor needs to be artificially moved to create accidental torsion. A suggested procedure displacing a fraction of the mass of the building towards one of its edges is explained in Tola (2010).

The application of dynamic procedures to include accidental torsion such as rotational ground motions and torsional spectrum needs further research.

C12.10.8 The procedure specified for SDC C referring to the simultaneous application of the two record components is considered to be the most convenient technique to account for orthogonal loading if comparing with the 30% rule and the SRSS of the components in each direction. This procedure intends to resemble what structures feel in actual earthquakes. Also, if using this alternative, the structural elements located at the corners of the building (such as columns or shear walls) will experience simultaneous loading in two directions, which is a desired and realistic effect. Detailed information can be found in Tola (2010).

C12.10.11 Caution needs to be taken when modeling the basement of buildings. For instance, as shown in Charney et al. (2010b), if the mass participation factor of the mode exciting the grade level is significant then the base shear in the basement walls can increase by a factor of 4.0.

REFERENCES

ASCE (2000). "Seismic Analysis of Safety-Related Nuclear Structures and Commentary ASCE 4-98." American Society of Civil Engineers, Reston, VA.

Beyer, and Bommer (2007). "Selection and scaling of real accelerograms for bi-directional loading: A review of current practice and code provisions." *Journal of Earthquake Engineering*, 11(SUPPL. 1), 13-45.

British Standards (2004). "Eurocode 8: Design of structures for earthquake resistance." *Part 1: General rules, seismic actions and rules for buildings*, European Committee for Standardization, Brussels.

Charney (2010a). *Seismic Loads Guide to the seismic load provisions of ASCE7-05*, American Society of Civil Engineers, Reston VA.

Charney, and Syed (2004, 2010). "EQTools." Virginia Polytechnic Institute & State University, Blacksburg, VA.

Charney, Tola, and Atlayan (2010b). "Structural Analysis." *NEHRP Recommended Provisions: Design Examples*, B. S. S. Council, ed., To be published.

Council of Standards New Zealand (2004). "NZS 1170.5 Structural Design Actions, Part 5: Earthquake actions - New Zealand." Standards New Zealand, Wellington, New Zealand.

De la Llera, and Chopra (1994a). "Accidental and natural torsion in earthquake response and design of buildings." University of California at Berkeley - College of Engineering, Berkeley, CA.

PEER (1999). "Pacific Earthquake Engineering Research Center: NGA Database." <http://peer.berkeley.edu/nga/>. (01/18, 2010).

Stewart, Chiou, Bray, Graves, Somerville, and Abrahamson (2001). "Ground motion evaluation procedures for performance-based design." P. E. E. R. Center, ed., University of California at Berkeley, Berkeley CA.

Tola (2010). "Using Linear Response History Analysis in ASCE7." Master, Virginia Tech, Blacksburg.

Appendix E. Abbreviation List

Abbreviation List

ASCE 4-98	American Standard ASCE 4-98
ASCE 7-05	American Standard ASCE 7-10
ASCE 7-10	American Standard ASCE 7-05
CHS	Chilean Standard
CQC	Complete Quadratic combination
CTBUH	Council of Tall Buildings and Urban Habitat
EC8	Eurocode 8
ELF	Equivalent Lateral force Method
LRHA	Linear Response History Analysis
M-D	Set of parameters Magnitude and Fault distance.
M-D-SM-ST	Set of parameters Magnitude, Fault distance, Source mechanism, and Soil type.
M-D-ST	Set of parameters Magnitude, Fault distance, and Soil type.
MXS	Mexican Standard
NBCC	National Building Code of Canada
NLRHA	Non-linear Response History Analysis
NZS	New Zealand Standard NZS 1170.5
RSA	Response Spectrum analysis
SRSS	Square root of the sum of the squares
USGS	United States Geological Survey